

**ISTANBUL TECHNICAL UNIVERSITY ★ GRADUATE SCHOOL OF
SCIENCE ENGINEERING AND TECHNOLOGY**

**INVESTIGATION OF THE EFFECTS OF *ENTEROBACTER* GROUP OF
MICROORGANISMS ON COLON CANCER**

PhD. THESIS

Dilşad YURDAKUL

Department of Advanced Technologies

Molecular Biology, Genetics and Biotechnology Programme

SEPTEMBER 2013

**ISTANBUL TECHNICAL UNIVERSITY ★ GRADUATE SCHOOL OF
SCIENCE ENGINEERING AND TECHNOLOGY**

**INVESTIGATION OF THE EFFECTS OF *ENTEROBACTER* GROUP OF
MICROORGANISMS ON COLON CANCER**

PhD. THESIS

**Dilşad YURDAKUL
(521072031)**

Department of Advanced Technologies

Molecular Biology, Genetics and Biotechnology Programme

**Thesis Advisor : Prof. Dr. Ayten YAZGAN KARATAŞ
Co-advisor : Prof. Dr. Fikrettin ŞAHİN**

SEPTEMBER 2013

İSTANBUL TEKNİK ÜNİVERSİTESİ ★ FEN BİLİMLERİ ENSTİTÜSÜ

***ENTEROBACTER GRUBU MİKROORGANİZMALARIN KOLON KANSERİ
ÜZERİNE ETKİLERİNİN ARAŞTIRILMASI***

DOKTORA TEZİ

**Dilşad YURDAKUL
(521072031)**

İleri Teknolojiler Anabilim Dalı

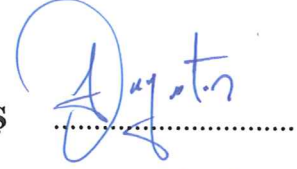
Moleküler Biyoloji, Genetik ve Biyoteknoloji Programı

**Tez Danışmanı: Prof. Dr. Ayten YAZGAN KARATAŞ
Eş Danışman : Prof. Dr. Fikrettin ŞAHİN**

EYLÜL 2013

Dilşad Yurdakul, a **Ph.D.** student of **ITU Graduate School of Science, Engineering and Technology**, student ID **521072031**, successfully defended the thesis entitled “**INVESTIGATION OF THE EFFECTS OF *ENTEROBACTER* GROUP OF MICROORGANISMS ON COLON CANCER**”, which she prepared after fulfilling the requirements specified in the associated legislations, before the jury whose signatures are below.

Thesis Advisor : **Prof. Dr. Ayten YAZGAN KARATAŞ**
Istanbul Technical University




Co-advisor : **Prof. Dr. Fikrettin ŞAHİN**
Yeditepe University



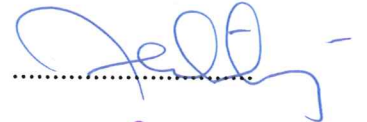
Jury Members : **Prof. Dr. Candan TAMERLER**
The University of Kansas

Prof. Dr. Gamze KÖSE
Yeditepe University

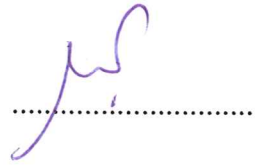


Assoc. Prof. Dr. Nevin KARAGÜLER
Istanbul Technical University

Assoc. Prof. Dr. Fatma Neşe KÖK
Istanbul Technical University



Prof. Dr. Meral BİRBİR
Marmara University



Date of Submission : 22 August 2013

Date of Defense : 27 September 2013

FOREWORD

I would like to thank,

My PhD Advisors; Prof. Dr Fikrettin Şahin and Prof. Dr. Ayten Yazgan Karataş for their excellent support and advices,

Prof. Dr. Candan Tamerler, Prof. Dr. Gamze Köse and Assoc. Prof. Dr. Nevin Karagüler for being in my thesis commitee,

Assoc. Prof. Dr. Dilek Telci, Prof. Dr. Ufuk Hasdemir, Prof. Dr. Necmettin Sökücü, Prof. Dr. Adile Çevikbaş, Assoc. Prof. Dr. Ümran Soyoğul Gürer for their help and support,

Ayşe Burcu Ertan, Özlem Demir, Ali Umman Doğan, Ayca Zeynep İltter, İrem Atay, Merve Seven, Zişan Turan, Ayşegül Doğan, Sadık Kalaycı, Raziye Piranlıoğlu, Nurullah Aydoğdu, Sıdıka Tapşın and Neslihan Durmuş Taşlı for their help,

Ersan Güray, Ülkü Yılmaz, Dilek Sevinç, Mehmet Emir Yalvaç, Ömer Faruk Bayrak, Müge Yazıcı, Fatih Çakar, İsmail Kaşoğlu, Esra Aydemir, Selami Demirci, Aysu Yılmaz, Ahmet Katı, Safa Aydın, Atakan Şurdum Avcı, Başak Kandemir, Seçil Demir, Elif Kon and all my friends in our department for their friendship,

My dear mother Nigar Yurdakul and my dear brother Kürşad Yurdakul for their courage and support...

September 2013

Dilşad YURDAKUL

TABLE OF CONTENTS

	<u>Page</u>
FOREWORD	vii
TABLE OF CONTENTS	ix
ABBREVIATIONS	xi
LIST OF TABLES	xiii
LIST OF FIGURES	xv
SUMMARY	xix
ÖZET	xxi
1. INTRODUCTION	1
1.1 Parts and Histology Of The Colon.....	1
1.2 General Knowledge About Cancer.....	4
1.3 Programmed Cell Death, Apoptosis, Autophagy and Programmed Necrosis....	5
1.4 Programmed Cell Death and Cancer.....	11
1.5 Colorectal Cancer and Molecular Pathways.....	14
1.6 Colitis Associated Colorectal Cancer.....	17
1.7 Bacteria and Cancer.....	19
1.8 <i>Enterobacter</i> Species.....	20
1.9 Purpose of Thesis.....	21
2. METHODS	23
2.1 Isolation of <i>Enterobacter</i> Strains.....	23
2.2 Identification of bacteria by FAME profile analysis.....	23
2.3 Microbial Identification by Metabolic Activities.....	24
2.4 16S rDNA Sequence Analysis.....	26
2.4.1 Genomic DNA isolation.....	26
2.4.2 Agarose gel electrophoresis.....	26
2.4.3 Amplification of 16S rDNA, sequencing and phylogenetic analysis of bacterial strains.....	26
2.5 Isolation of bacterial proteins.....	27
2.6 Cell culture.....	27
2.7 Determination of the optimum protein concentration to apply onto cell lines and examination of cell proliferation.....	27
2.8 Detection of Apoptosis and Cell Viability Assays.....	28
2.9 Detection of CD24.....	29
2.10 Detection of COX-2.....	29
2.11 Determination of NFkB and Bcl2 Expression.....	30
2.12 Statistical Analysis.....	31
3. RESULTS	33
3.1 Identification of bacterial strains.....	33
3.2 Phylogenetic Analysis of the Effective <i>Enterobacter</i> Species.....	36
3.3 MTS Results.....	37

3.4 Apoptosis and Cell Viability Assay Results	64
3.5 CD24 Detection Results	68
3.6 COX2 Detection Results	73
3.7 NFkB and Bcl2 Expression Assay Results.....	73
4.DISCUSSION AND CONCLUSIONS	79
REFERENCES	91
APPENDICES	99
CURRICULUM VITAE	137

ABBREVIATIONS

CNF	:Cytotoxic Necrotizing Factor
LEF	:Lymphoid Enhancer Factor
TSA	:Tryptic Soy Agar
TCF	:T cell factor
IAP	:Inhibitor of Apoptosis Protein
MPT	:Mitochondrial Permeability Transition
MMR	:Mismatch repair
INOS	:Inducible Nitric Oxide Synthase
MALT	:Mucosa Associated Lymphoid Tissue
AIF	:Apoptosis Inducing Factor
SMAC	:Second Mitochondria Derived Activator of Caspase
DIABLO	:Direct IAB Binding Protein with Low Pi
DISC	:Death Inducing Signalling Complex
HtrA	:High Temperature Requirement Protein A
TNF	:Tumor Necrosis Factor
FAME	:Fatty Acid Methyl Ester
NFKB	:Nuclear Factor Kappa B
COX2	:Cyclooxygenase 2
Bcl2	:B cell lymphoma 2
PMSF	:Phenylmethylsulfonyl Fluoride
DMSO	:Dimethyl sulfoxide
FBS	:Fetal Bovine Serum
PSA	:Penicillin Streptomycin Amphotericin
BSA	:Bovine Serum Albumin
EMEM	:Eagle's Minimal Essential Medium
ELISA	:Enzyme Linked Immunosorbent Assay

LIST OF TABLES

	<u>Page</u>
Table 1.1 :Reagents Required For Fatty Acid Isolation.....	24
Table 1.2 :Test Substrates on Gram Negative Card.....	25
Table 2.1 :Apoptosis assay results.	67
Table 3.1 :CD24 Detection results	71
Table 4.1 :Comparison of the results	72

LIST OF FIGURES

	<u>Page</u>
Figure 1.1 :Diagram of the major regions of the colon.....	1
Figure 1.2 :Normal colonic surface epithelium	2
Figure 1.3 :Colonic epithelium stained with haemotoxylin eosin	3
Figure 1.4 :Colonic epithelial.....	3
Figure 2.1 :Pathways of Apoptosis 1	6
Figure 2.2 :Pathways of Apoptosis 2	7
Figure 2.3 :Forms of Cell Death	11
Figure 2.4 :Apoptosis mechanisms during cancer	13
Figure 3.1 :Progression of Colon Cancer.....	14
Figure 3.2 :Molecular Pathogenesis of Colon Cancer	17
Figure 3.3 :Initiation of Sporadic and Colitis-Associated Colon Cancer.....	19
Figure 4.1 :Sequence Analysis of DB7Y strain	33
Figure 4.2 :Sequence Analysis of DE8 strain	34
Figure 4.3 :Sequence Analysis of DE129 strain	34
Figure 4.4 :Sequence Analysis of DE365 strain	35
Figure 4.5 :Sequence Analysis of DE51strain	35
Figure 4.6 :Sequence Analysis of HIA strain	36
Figure 5.1 :Phylogenetic tree of <i>Enterobacter</i> strains	37
Figure 6.1 :Absorbance- Concentration Graphic of CRL1790-3h.....	38
Figure 6.2 :Cell viability-Concentration Graphic of CRL1790-3h.....	38
Figure 6.3 :Absorbance-Concentration Graphic of CRL1790-DB7Y	39
Figure 6.4 :Cell viability-Concentration Graphic of CRL1790-DB7Y	39
Figure 6.5 :Absorbance-Concentration Graphic of CRL1790-DE8	40
Figure 6.6 :Cell viability-Concentration Graphic of CRL1790-DE8	40
Figure 6.7 :Absorbance-Concentration Graphic of CRL1790-DE12	41
Figure 6.8 :Cell viability-Concentration Graphic of CRL1790-DE12	41
Figure 6.9 :Absorbance-Concentration Graphic of CRL1790-DE36	42
Figure 6.10 :Cell viability-Concentration Graphic of CRL1790-DE36	42
Figure 6.11 :Absorbance-Concentration Graphic of CRL1790-DE47	43
Figure 6.12 :Cell viability-Concentration Graphic of CRL1790-DE47	43
Figure 6.13 :Absorbance-Concentration Graphic of CRL1790-DE103	44
Figure 6.14 :Cell viability-Concentration Graphic of CRL1790-DE103	44
Figure 6.15 :Absorbance-Concentration Graphic of CRL1790-DE129	45
Figure 6.16 :Cell viability-Concentration Graphic of CRL1790-DE129	45
Figure 6.17 :Absorbance-Concentration Graphic of CRL1790-DE256	46
Figure 6.18 :Cell viability- Concentration Graphic of CRL1790-DE256	46
Figure 6.19 :Absorbance - Concentration Graphic of CRL1790-DE365	47
Figure 6.20 :Cell viability-Concentration Graphic of CRL1790-DE365	47
Figure 6.21 :Absorbance-Concentration Graphic of CRL1790-huc2.....	48
Figure 6.22 :Cell viability-Concentration Graphic of CRL1790-huc2.....	48

Figure 6.23 :Absorbance-Concentration Graphic of CRL1790-HIA.....	49
Figure 6.24 :Cell viability-Concentration Graphic of CRL1790-HIA.....	49
Figure 6.25 :Absorbance-Concentration Graphic of CRL1790-DE51	50
Figure 6.26 :Cell viability-Concentration Graphic of CRL1790-DE51.....	50
Figure 6.27 :Absorbance-Concentration Graphic of NCM460-3h	51
Figure 6.28 :Cell viability-Concentration Graphic of NCM460-3h.....	51
Figure 6.29 :Absorbance -Concentration Graphic of NCM460-DB7Y	52
Figure 6.30 :Cell viability-Concentration Graphic of NCM460-DB7Y	52
Figure 6.31 :Absorbance-Concentration Graphic of NCM460-DE8	53
Figure 6.32 :Cell viability-Concentration Graphic of NCM460-DE8	53
Figure 6.33 :Absorbance-Concentration Graphic of NCM460-DE12	54
Figure 6.34 :Cell viability-Concentration Graphic of NCM460-DE12	54
Figure 6.35 :Absorbance-Concentration Graphic of NCM460-DE36	55
Figure 6.36 :Cell viability-Concentration Graphic of NCM460-DE36	55
Figure 6.37 :Absorbance-Concentration Graphic of NCM460-DE47	56
Figure 6.38 :Cell viability-Concentration Graphic of NCM460-DE47	56
Figure 6.39 :Absorbance-Concentration Graphic of NCM460-DE103	57
Figure 6.40 :Cell viability-Concentration Graphic of NCM460-DE103	57
Figure 6.41 :Absorbance-Concentration Graphic of NCM460-DE129	58
Figure 6.42 :Cell viability-Concentration Graphic of NCM460-DE129	58
Figure 6.43 :Absorbance-Concentration Graphic of NCM460-DE256	59
Figure 6.44 :Cell viability-Concentration Graphic of NCM460-DE256	59
Figure 6.45 :Absorbance-Concentration Graphic of NCM460-DE365	60
Figure 6.46 :Cell viability-Concentration Graphic of NCM460-DE365	60
Figure 6.47 :Absorbance-Concentration Graphic of NCM460-huc2.....	61
Figure 6.48 :Cell viability-Concentration Graphic of NCM460-huc2.....	61
Figure 6.49 :Absorbance-Concentration Graphic of NCM460-HIA	62
Figure 6.50 :Cell viability-Concentration Graphic of NCM460-HIA	62
Figure 6.51 :Absorbance-Concentration Graphic of NCM460-DE51	63
Figure 6.52 :Cell viability-Concentration Graphic of NCM460-DE51	63
Figure 7.1 :Detection of Apoptosis by Annexin in CRL1790 before bacterial protein application	64
Figure 7.2 :Detection of Apoptosis by Annexin in CRL1790 after DE365 protein application	65
Figure 7.3 :Detection of Apoptosis by Annexin in CRL1790 after DE8 protein application	65
Figure 7.4 :Detection of Apoptosis by Annexin in CRL1790 after HIA protein application	65
Figure 7.5 :Detection of Apoptosis by Annexin in NCM460 before bacterial protein application.....	66
Figure 7.6 :Detection of Apoptosis by Annexin in NCM460 after DB7Y protein application	66
Figure 7.7 :Detection of Apoptosis by Annexin in NCM460 after DE129 protein application	66
Figure 7.8 :Detection of Apoptosis by Annexin in NCM460 after DE51 protein application	67
Figure 8.1 :CD24 Detection in CRL1790 before bacterial protein application	68

Figure 8.2 :Isotype measurement in CRL1790 before bacterial protein application.....	68
Figure 8.3 :CD24 Detection in CRL1790 after DE365 protein application.....	69
Figure 8.4 :Isotype measurement in CRL1790 after DE365 protein application	69
Figure 8.5 :CD24 Detection in CRL1790 after DE8 protein application	69
Figure 8.6 :Isotype measurement in CRL1790 after DE8 protein application.....	70
Figure 8.7 :CD24 Detection in CRL1790 after HIA protein application	70
Figure 8.8 :Isotype measurement in CRL1790 after HIA protein application.....	70
Figure 9.1 :COX2 Determination by Western Blotting	73
Figure 10.1 :Relative Normalized Expression of NFkB on NCM460	74
Figure 10.2 :Relative Normalized Expression of Bcl2 on NCM460	74
Figure 10.3 :Relative Normalized Expression of NFkB on CRL1790	75
Figure 10.4 :Relative Normalized Expression of Bcl2 on CRL1790	75
Figure 11.1 :NFkB Expression on NCM460 after statistical analysis	76
Figure 11.2 :Bcl2 Expression on NCM460 after statistical analysis	76
Figure 11.3 :NFkB Expression on CRL1790 after statistical analysis.....	77
Figure 11.4 :Bcl2 Expression on CRL1790 after statistical analysis.....	77

INVESTIGATION OF THE EFFECTS OF *ENTEROBACTER* GROUP OF MICROORGANISMS ON COLON CANCER

SUMMARY

Many studies have been performed to determine the interaction between some bacterial species and cancer. However, there has been no attempts to demonstrate a possible relationship between *Enterobacter* spp. and colon cancer. Therefore, it is aimed to investigate the effects of *Enterobacter* group of microorganisms on colon cancer in the present study. Determination of the interaction between *Enterobacter* spp. and colon cancer will lead to new approaches to colon cancer initiation and mechanism. Identification of a possible interaction between colon cancer and *Enterobacter* spp. may also be important for development of prophylaxis and new treatment strategies.

Two strains of *Enterobacter* spp. and one strain of *Escherichia coli* were isolated using Sheep Blood Agar from patients who were treated at Istanbul University, Istanbul Faculty of Medicine, Department of General Surgery. Eight strains of *Enterobacter* spp. and one strain of *Morganella morganii* were provided from Marmara University, School of Medicine, Department of Medical Microbiology. One *Enterobacter* spp. strain that was isolated from environmental samples was obtained from Microbial Collection Unit at Yeditepe University, Genetics and Bioengineering Department. Then strains were identified based on FAME profiles, biochemical activities and 16S rDNA sequencing. Bacterial protein from thirteen strains was isolated, protein concentration was determined by Bradford Assay. The optimum protein concentration to apply onto NCM460 (Incell) and CRL1790 (ATCC) cell lines was determined by MTS assay. Cell viability and proliferation was also determined. For statistical analysis Graphpad Software was used. The values were analysed using One way ANOVA test following Dunnett test. Before and after bacterial protein application, CD24 was detected by flow cytometry, apoptosis detection was performed using annexin V. Then, bacterial proteins were isolated from the strains which increase cell viability and proliferation and decrease the apoptosis was applied onto cell lines. RNA was isolated, cDNA was synthesized. NFkB and Bcl2 expression was determined by CFX96 Real Time PCR Detection System. Statistical analysis was performed by One way ANOVA following Tukey test in Graphpad Software. To detect COX-2 on those strains Western Blotting technique was used. Phylogenetic analysis was performed by SDSC Biology Workbench.

Among thirteen bacterial strains tested in this study, six of them were defined as effective either on CRL1790 or NCM460 cell line. All effective strains increased the cell viability and proliferation at their optimum concentrations and decreased apoptosis. Also, they were determined as COX-2 negative. By molecular techniques based on 16S rDNA sequences, fatty acid compositions and metabolic activities, HIA and DE51 were identified as *Escherichia coli* and *Morganella morganii*, respectively. It was found that the remaining four effective strains belonged to the *Enterobacter* genus. Three of them signed as DB7Y, DE129 and DE365 decreased apoptosis by increasing NFκB and Bcl2 expression. Also DE365 increased CD24 level in CRL1790. DE8, which was identified as *Enterobacter aerogenes*, increased CD24 level as well as NFκB expression on CRL1790. However, it did not affect Bcl2 expression. In addition to the increase in NFκB expression, these results indicate that DE8 may follow another pathway for apoptosis reduction. This suggestion was confirmed by drawing the phylogenetic tree of the effective *Enterobacter* strains. When the effective *Enterobacter* strains were examined in a phylogenetic tree, it was observed that DE8 was located far from the others.

Apoptosis inhibition is an important pathogenicity mechanism which enables the bacteria to replicate inside host cells. Some bacteria induce apoptosis but in that case they target immune cells like macrophages and neutrophils because otherwise these cells will kill them. Apoptosis inhibition can be observed in many bacterial strains. Our study was the first to demonstrate apoptosis can be inhibited by *Enterobacter* strains. Apoptosis inhibition is so important for cancer development since apoptosis is a complex process that contains many pathways, at any point along these pathways defects can occur which lead to malignant transformation of the affected cells, tumor metastasis and resistance to anticancer drugs. In the previous studies, it was reported that the proto-oncogene Bcl-2, which inhibits apoptosis encourages tumor progression and reduction of apoptosis is important for carcinogenesis.

In conclusion, the present study, the data indicated that *Enterobacter* strains might promote colon cancer. This is the first study showing that *Enterobacter* spp. may be a clinically important factor for colon cancer initiation and progression. Studies can be extended on animal models in order to develop new strategies for treatment.

ENTEROBACTER GRUBU MİKROORGANİZMALARIN KOLON KANSERİ ÜZERİNE ETKİLERİNİN ARAŞTIRILMASI

ÖZET

Kanser, hücrelerin kontrolsüz olarak çoğaldığı bir hastalıktır. Düzensiz, kontrolsüz çoğalma neticesinde tümör oluşumu görülür. Kolon kanseri, görülme sıklığı açısından dünyada üçüncü sıradadır. Kolon kanserinin oluşumunda genetik yatkınlığın yanısıra yaş, beslenme, fiziksel aktivite eksikliği, fazla kilolu veya obez olma gibi faktörler de etkilidir.

Apoptoz hücre ölümünden sorumlu çok aşamalı bir mekanizmadır. Sadece gelişim esnasında değil yetişkin organizmalarda hücre sayısının kontrolü amacıyla kullanılmaktadır. Hücre büzülmesi, kromatin yoğunlaşması, çekirdek ve hücre parçalanması apoptozun en bilinen özellikleridir. Apoptoz ayrıca hastalık ya da zararlı ajanlar sonucu hücre hasar gördüğü zaman aktifleştirilen bir koruma mekanizmasıdır. Hücre büzülmesi ve piknoz apoptozun erken aşamalarında görülür. Hücre büzülmesi neticesinde hücre boyutu küçülür, sitoplazma yoğunlaşır ve organeller daha sıkı paketlenirler. Kromatin yoğunlaşmasından sonra piknoz oluşur. Apoptotik yapılar fagositik hücreler tarafından yutulmaktadır. Çalışmalar apoptoz azalmasının veya apoptoza karşı gelişen direncin kanserleşmeyle ilgisi olduğunu göstermektedir.

Kolon ve rektum kanserlerinin farklı çeşitleri bulunmaktadır. Bunlar arasında barsaktaki özel hormon üreten hücrelerde başlayan karsinoid tümörler olabileceği gibi, kolon duvarında yer alan Kajal hücrelerinde başlayan tümörler de yer alır. Bu tümörler selim yada habis olabilirler. Sindirim sisteminin herhangi bir bölgesinde görülebilirler fakat kolonda nadir olarak görülürler. Lenfomalar lenf düğümlerinde görülmekle beraber kolonda da başlayabilmektedirler. Sarkomalar nadir olarak kolon ve rektum duvarındaki kan damarları ve bağ dokusundan gelişirler. Kolorektal kanserlerin % 95 inden fazlası adenokarsinomadır.

Kolorektal kanser kolon veya rektum epitelinde bulunur, ilk aşama polip oluşumudur. Daha sonra tümör hücreleri yayılır, epiteli geçerek kaslar, lenf düğümleri, karaciğer ve diğer organlara dağılır. Kalıtsal kolorektal kanser, bazı genlerde mutasyon oluşumuyla başlar. Bu hastalığın oluşumunda en önemli bir başka sebep ise inflamasyondur. Ülseratif kolit ve inflamatuvar barsak hastalığı geçirmiş hastalarda kolon kanseri olma riski yüksektir. Kolitin süresi ve anatomik genişliği riski arttırmaktadır. İnflamasyon, kolit ve kolon kanseri ile neticelenen hücre hasarı oluşturan, oksidatif stres oluşumuna yol açar. İnflamasyon sonucu makrofaj ve diğer lökositlerden tümör başlangıcına yol açabilecek mutasyonlara sebep olan reaktif oksijen ve nitrojen türleri üretilmektedir. Tümör hücrelerinin yayılmaları için gerekli olan taban zarının yıkımını lökositler ve diğer immün hücreleri gerçekleştirmektedir.

Nötrofiller, eozinofiller, dendritik hücreler, mast hücreleri ve lenfositler de epitel kaynaklı tümörlerin oluşumunda aktiflerdir.

Bakteri türleri ve kanser arasındaki ilişkiyi tespit etmek üzere pek çok çalışma yapılmıştır. Fakat *Enterobacter* spp. ve kolon kanseri arasındaki muhtemel ilişkiyi gösterebilecek herhangi bir girişimde bulunulmamıştır. Bu nedenle, bu çalışmada, *Enterobacter* grubu mikroorganizmaların kolon kanseri üzerine etkilerinin araştırılması amaçlanmaktadır. *Enterobacter* spp. ve kolon kanseri arasındaki ilişkinin tespit edilmesi kolon kanseri başlangıcı ve mekanizmasına yönelik yeni yaklaşımlara yol açabilecektir. Ayrıca *Enterobacter* spp. ve kolon kanseri arasında olası bir ilişkinin tanımlanması profilaksi ve yeni tedavi geliştirmek için önem taşımaktadır.

Çalışmamızda İstanbul Üniversitesi, İstanbul Tıp Fakültesi, Genel Cerrahi Anabilim Dalı'nda tedavi gören hastalardan İki *Enterobacter* spp. ve bir *Escherichia coli* suşu Koyun Kanlı Agar kullanılarak izole edilmiştir. Sekiz *Enterobacter* spp. ve bir *Morganella morganii* suşu da Marmara Üniversitesi, Tıp Fakültesi, Tıbbi Mikrobiyoloji Anabilim Dalı'ndan temin edilmiştir. Çevresel örneklerden izole edilmiş olan bir *Enterobacter* spp. suşu ise Yeditepe Üniversitesi, Genetik ve Biyomühendislik Bölümü'ndeki Mikrobiyal Koleksiyon Biriminden elde edilmiştir. Bu suşlar daha sonra, yağ asidi metil ester profilleri, sahip oldukları biyokimyasal aktiviteler ve 16S rDNA dizilemesi ile tanımlanmıştır. Onüç suştan bakteriyel protein izole edilmiş, protein konsantrasyonu Bradford testi ile belirlenmiştir. NCM460 (Incell) ve CRL1790 (ATCC) hücre hatları üzerine uygulanacak en uygun protein konsantrasyonu MTS testi ile saptanmıştır. Hücre canlılığı ve çoğalması da ayrıca tespit edilmiştir. İstatistik analiz için Graphpad Software kullanılmıştır. Değerler 'One way ANOVA' testini takiben Dunnett test ile analiz edilmiştir.

CD24 prematüre lenfositler, epitel ve sinir hücrelerinde üretilen bir yüzey proteindir. CD24' ün pek çok kanser dokusunda ve kolon kanserinde arttığı tespit edilmiştir. Çalışmamızda, bakteri proteini uygulama öncesi ve sonrasında, CD24 flow sitometri ile saptanmıştır. Apoptoz tespiti annexin V kullanılarak yapılmıştır. Apoptotik hücrelerde hücre dışı ortama zar fosfolipid fosfatidilserin çıkışı olur. Annexin, Ca²⁺ varlığında negatif yüklü fosfolipidlere yüksek afinite gösteren bir proteindir, fosfatidilserin'e bağlanır. Annexin V, FITC ile birleştirilmiştir, tespiti flow sitometri ile yapılmaktadır. Erken apoptotik, geç apoptotik, nekrotik veya canlı hücre ayırımı belirleyebilmek için pi kullanılmıştır.

Çalışmamızda daha sonra hücre canlılığı ve çoğalmasını arttırarak, apoptozu düşüren suşlardan bakteriyel proteinler izole edilmiş, hücre hatlarına uygulanmıştır. RNA izole edilmiş, cDNA üretilmiş, NFKB ve Bcl2 ekspresyonu CFX96 Real Time PCR Detection System ile saptanmıştır. NFKB, proliferasyon, apoptoz ve kanserleşmede etkili olan bir proteindir. Bcl2 da pek çok kanser hücresinde artan bir apoptoz düzenleyicisidir. Real-time datalarının istatistiksel analizi Graphpad Software'deki 'One way ANOVA'ı takiben Tukey test ile yapılmıştır.

Cox-2, prostaglandin sentezinde etkili olan bir enzimdir. Bcl2 ekspresyonunu arttırarak apoptozu inhibe eder. Apoptozu düşürüp canlılığı arttıran altı suştan izole

edilen proteinler hücrelere uygulanmış, inkübasyon sonrası hücre lizatları elde edilmiş, Cox-2 saptanması için Western Blotting tekniği kullanılmıştır. Filogenetik analiz SDSC Biology Workbench ile yapılmıştır.

Bu çalışmada test edilen onüç bakteri suşu arasından altısı CRL1790 veya NCM460 hücre hattı üzerinde etkili olarak tanımlanmıştır. Bütün etkili suşlar, en uygun konsantrasyonlarda hücre canlılığı ve çoğalmasını arttırmış, apoptozu düşürmüştür. Ayrıca, örneklerin COX-2 negatif olduğu belirlenmiştir. 16S rDNA dizileri, yağ asidi kompozisyonu ve metabolik aktiviteye dayanan moleküler tekniklerle HIA ve DE51 sırasıyla *Escherichia coli* ve *Morganella morganii* olarak tanımlanmıştır. Geriye kalan dört etkili suşun ise *Enterobacter* cinsine ait olduğu bulunmuştur. DB7Y, DE129 ve DE365 olarak kodlanan üç suşun NFkB ve Bcl2 ekspresyonunu arttırarak apoptozu düşürdüğü saptanmıştır. Ayrıca DE365 CRL1790'de CD24 seviyesini arttırmıştır. *Enterobacter aerogenes* olarak tanımlanan DE8, CRL1790 da NFkB ekspresyonunu arttırırken CD24 seviyesini de arttırmıştır. Fakat, Bcl2 ekspresyonunu etkilememiştir. NFkB ekspresyon artışına ek olarak, bu sonuçlar göstermiştir ki DE8 apoptoz düşmesi için başka bir yolak takip etmektedir. Bu fikir etkili *Enterobacter* suşlarının filogenetik ağaçlarının çizilmesiyle doğrulanmıştır. Etkili olan *Enterobacter* suşları filogenetik ağaçta incelendiği zaman, DE8 in diğerlerinden daha uzakta olduğu gözlenmiştir.

Apoptoz inhibisyonu, bakterilerin konak hücresinde çoğalmalarına olanak sağlayan önemli bir patojenite mekanizmasıdır. Bazı bakteriler apoptozu indükleyebilirler, bu durumda ise bakterilerin hedefi kendilerini fagositozdan koruma amacıyla makrofajlar, nötrofiller gibi immün sistem hücreleri olmaktadır. Apoptozu inhibe eden pek çok bakteri suşu bulunmaktadır. Bizim çalışmamız ise apoptozun *Enterobacter* suşları tarafından inhibe edilebileceğini gösteren ilk çalışmadır. Kanser gelişimi için apoptoz inhibisyonu neden bu kadar önemlidir? Çünkü apoptoz farklı aşamalar içeren kompleks bir olaydır ve bu aşamaların herhangi birisinde olabilecek bir bozukluk kanserleşmeye yol açabilmektedir. Bcl2 nun apoptozu inhibe ederek kanserleşmeyi teşvik ettiği ve apoptoz düşmesinin kanserleşmeye sebep olduğunu gösteren çalışmalar bulunmaktadır.

Sonuç olarak bizim çalışmamızda *Enterobacter* suşlarının kolon kanserine yol açabileceği gösterilmiştir. Bu çalışma, kolon kanseri başlangıcı ve ilerlemesinde *Enterobacter* spp. nin klinik olarak önemli bir faktör olabileceğini gösteren ilk çalışmadır. Tedavi için yeni stratejiler geliştirilmesine yönelik çalışmalar hayvan modelleriyle genişletilebilir.

1. INTRODUCTION

1.1 Parts and Histology of The Colon

The terminal 1-1,5 m of the gastrointestinal tract is called as the colon. As shown in Figure 1.1, it consists of different parts named; Ascending Colon, Transverse Colon, Descending Colon and Sigmoid Colon (Levine and Haggitt, 1989).

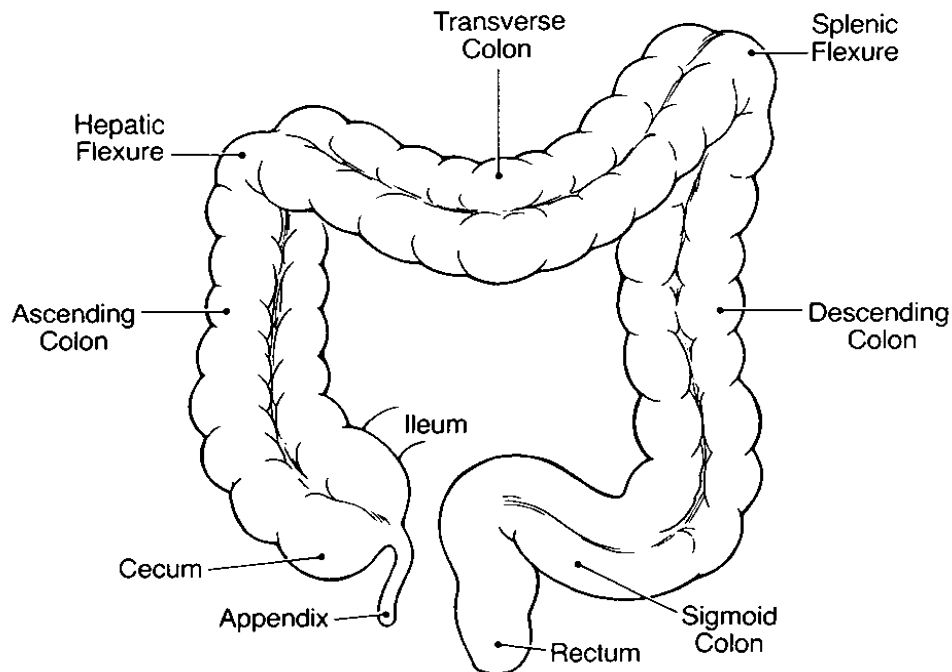


Figure 1.1: Diagram of the major regions of the colon (Levine and Haggitt,1989).

The large intestine, in which water and electrolyte absorption is made, contains the feces. The colonic mucosa is composed of columnar epithelium covering the surface and lining the crypts, also lamina propria and a muscle layer the muscularis mucosae. The surface epithelium which is a protective barrier between the host and the luminal environment, is composed of absorptive and goblet cells. Absorptive cells are active in colonic ion and water transport. Goblet cells synthesize, store and secrete mucous granules. In Figure 1.2, absorptive cells (A) and goblet cells (G) in the normal colonic surface epithelium, the underlying basement membrane complex (small

arrows) , intraepithelial lymphocytes (arrowheads) and nuclear dust in the lamina propria (large arrow) is shown (Levine and Haggitt, 1989).

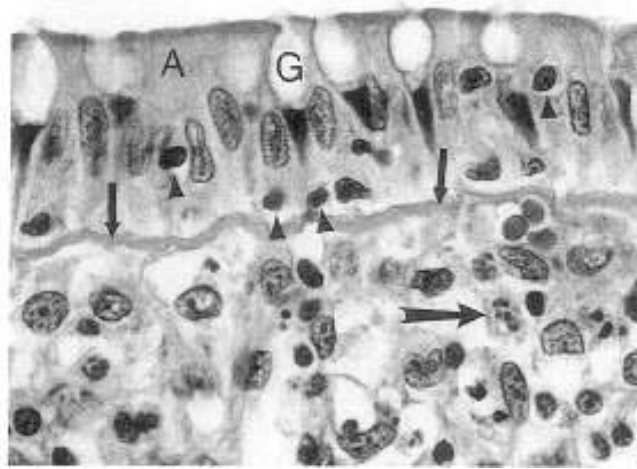


Figure 1.2 : Normal colonic surface epithelium (Levine and Haggitt,1989).

In the crypt epithelium in addition to mature absorptive cells and goblet cells, immature and undifferentiated precursor cells, endocrine and Paneth cells exist. In the endocrine cells hormones within the cytoplasmic secretory granules are observed. Paneth cells are also secretory cells. The lamina propria extends from the subepithelial basement membrane complex to the muscularis mucosae. The cells in the lamina propria are mostly active in host defense. Plasma cells (B cells) exist in lamina propria. T-lymphocytes exist in the lamina propria, colonic epithelium and submucosa. Myeloid cells including eosinophils and mast cells normally exist in the lamina propria. Eosinophils and mast cells may permeate the surface epithelium but neutrophils are not normally present in either the surface or crypt epithelium. Fibroblasts also exist in lamina propria as well as macrophages and neuroendocrine cells. Muscularis mucosae which is a thin layer of muscle, separates the mucosa epithelium and lamina propria from the deeper submucosa. Same as lamina propria the submucosa contains lymphocytes, plasma cells, fibroblasts, macrophages and different from lamina propria it contains fat cells. The external smooth muscles of the colon has 2 layers and neural tissue lies between those 2 layers. The layer of connective tissue between the serosa and muscularis propria constitutes the subserosal tissue (Levine and Haggitt , 1989). Colonic epithelial photo was given in Figure 1.3 and Figure 1.4.

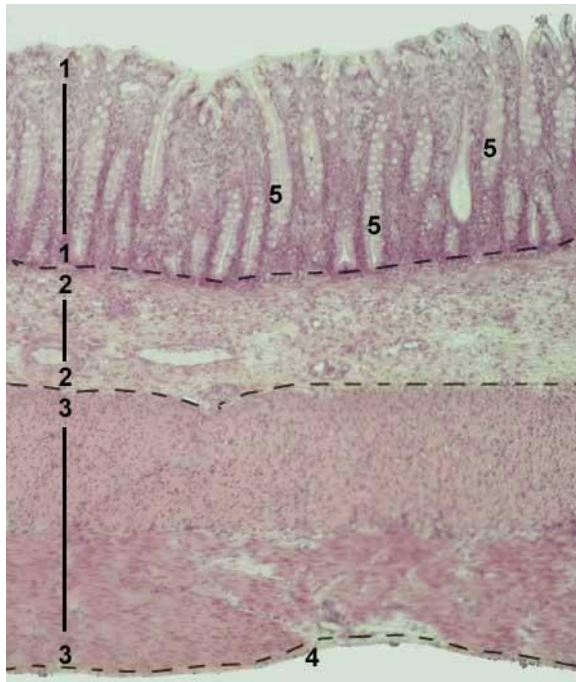


Figure 1.3: Colonic - epithelium stained with haemotoxylin eosin. 1-tunica mucosa, 2- tunica submucosa, 3-tunica muscularis propria, 4- tunica serosa, 5-glands (crypts) in the lamina propria (Url-1).



Figure 1.4: Colonic epithelial (Url-2).

1.2 General Knowledge About Cancer

Cancer is a disease in which cells proliferate without regulation. As a result of unregulated proliferation of cells tumor formation which is defined as growing mass of abnormal cells occurs. If a tumor cell invade the surrounding tissues, it is defined as malignant, if not , the tumor is called as benign. Metastasis is the process in which malignant tumors spread to other locations in the body, forming secondary tumors. If the mechanism for apoptosis which is defined as programmed cell death, is impaired or inactivated, cancer may develop (Snustad and Simmons, 2006; Alberts et al., 2002).

According to the tissue and cell type they arise, cancers can be classified. Carcinomas are cancers that arise from epithelial cells, sarcomas are those that arise from connective tissue or muscle cells. Cancers that are derived from hemopoietic cells and from cells of the nervous system are called as leukemias. According to the structure of the tumor, the location in the body, and the specific cell type these categories can be subdivided. A benign epithelial tumor with a glandular organization is called as an adenoma and the corresponding type of malignant tumor is called as an adenocarcinoma. Because most of the cell proliferation in the body occurs in epithelia, or because epithelial tissues are most frequently exposed to the physical and chemical conditions that cause cancer, about 90% of human cancers are carcinomas. A single cell that has an initial mutation is thought to cause the cancer but in order to make the cell cancerous, additional mutations whose protein products are involved in the control of the cell cycle, must also occur. Tumor progression, that takes many years, includes mutation and natural selection among somatic cells (Alberts et al., 2002; Snustad and Simmons, 2006).

Products of some genes can make a cell cancerous and that can promote cell division is called as oncogen whereas product of a gene is involved in the repression of cell division and appears to prevent the formation of cancer is called as a tumor suppressor gene. Colon cancer is one of the most common cancer types which results from genetic factors such as oncogene overexpression and tumor suppressor gene inactivation (Alberts et al., 2002; Snustad and Simmons, 2006; Rupnarain et al., 2004).

1.3 Programmed Cell Death : Apoptosis, Autophagy and Programmed Necrosis

Apoptosis is a multi-step pathway which is responsible for cell death. It exists not only during development but also in adult multicellular organisms to control cell numbers. Cell shrinkage, chromatin condensation, nuclear and cell fragmentation are the main features of apoptosis (Cotter, 2009). Apoptosis can also exist as a defense mechanism when cells are damaged as a result of disease or noxious agents. Cell shrinkage and pyknosis are observed during early stage of apoptosis. As a result of cell shrinkage, the cell becomes smaller in size, the cytoplasm becomes dense and the organelles become more tightly packed. After the chromatin condensation pyknosis occurs. Apoptotic bodies are engulfed by phagocytic cells. No inflammatory reaction occurs as a result of apoptosis or removal of apoptotic cells because, apoptotic cells do not release their cellular constituents into the surrounding interstitial tissue, they are phagocytized by surrounding cells, the engulfing cells do not produce anti-inflammatory cytokines (Elmore, 2007). Apoptosis mechanisms are summarized on Figure 2.1 and Figure 2.2

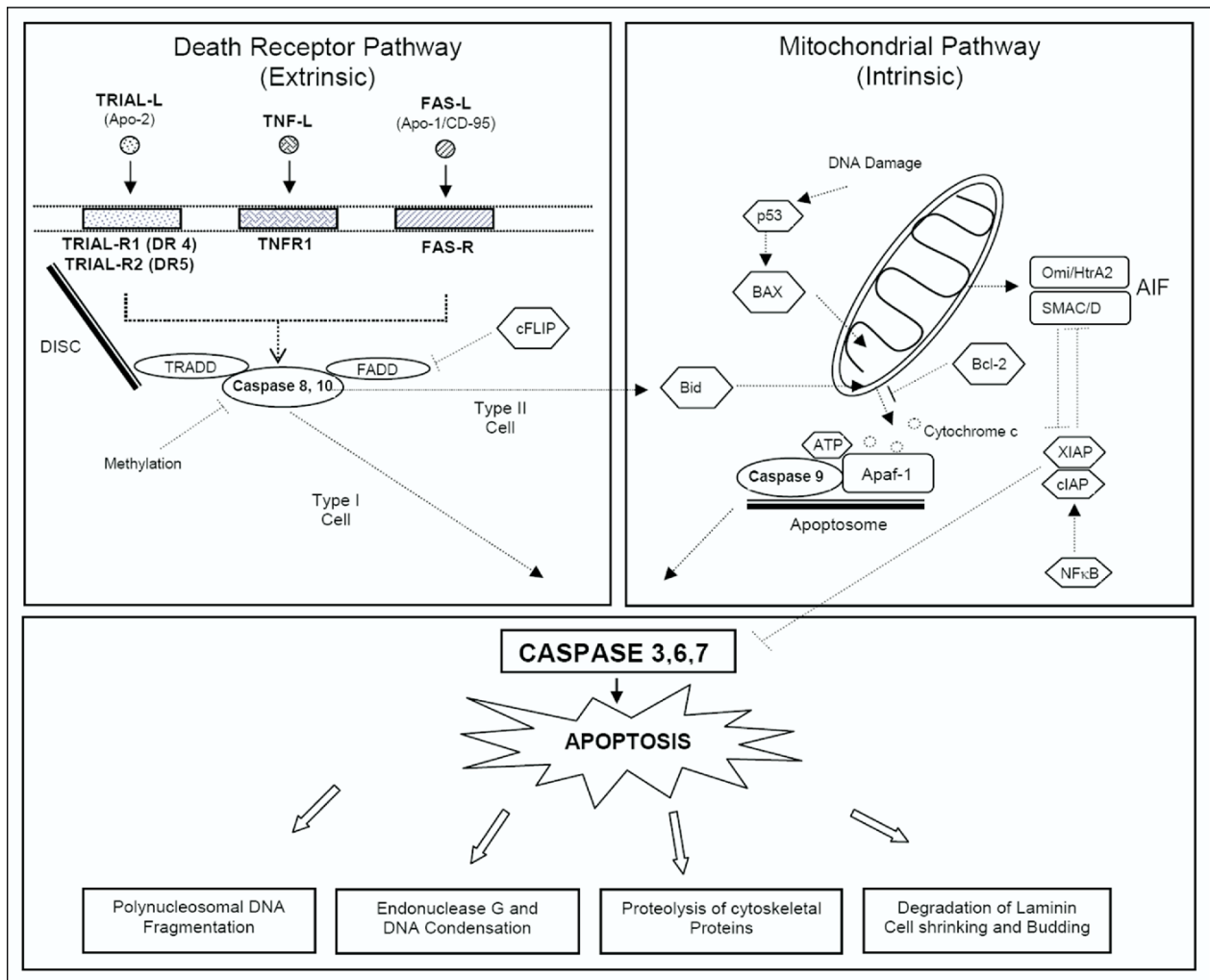


Figure 2.1: Pathways of Apoptosis 1 (Huerta et al, 2006).

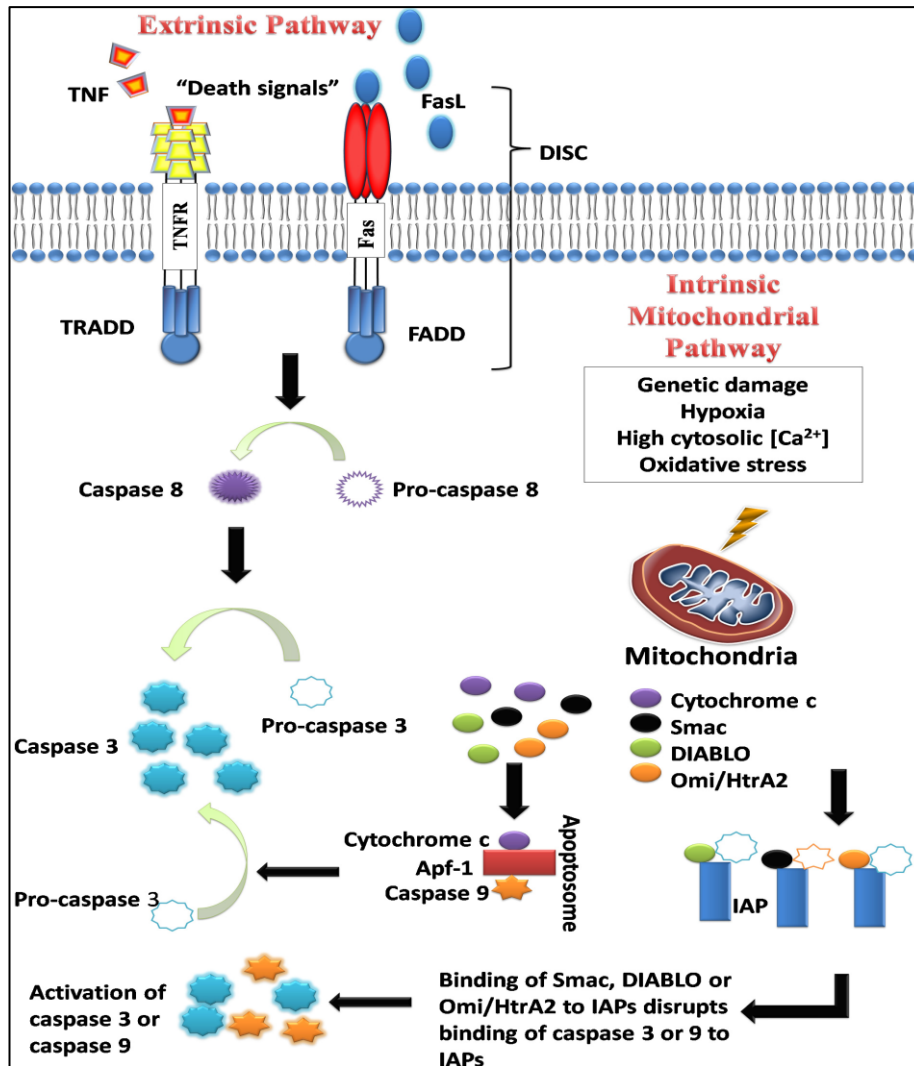


Figure 2.2: Pathways of Apoptosis 2 (Wong, 2011).

There are two main apoptotic pathways; the extrinsic or death receptor pathway, the intrinsic or mitochondrial pathway and an additional pathway which involves T-cell mediated cytotoxicity and perforin-granzyme dependent killing of the cell. In the perforin granzyme pathway, apoptosis is induced by either granzyme A or granzyme B. The extrinsic, intrinsic and granzyme B pathways converge on the same terminal, execution pathway which is initiated by the cleavage of caspase-3. Then DNA fragmentation, degradation of cytoskeletal and nuclear proteins, crosslinking of proteins occur. Apoptotic bodies are formed, ligands for phagocytic cell receptors are expressed and finally they are engulfed by phagocytic cells. The granzyme A pathway activates caspase independent cell death pathway via single stranded DNA damage (Elmore, 2007).

Caspases cleave proteins at aspartic acid residues. Different types of caspases exist such as initiators (caspase-2,-8,-9,-10), effectors (caspase -3,-6,-7) and inflammatory caspases (caspase -1,-4,-5). In addition to those caspase -11 which regulates apoptosis and cytokine maturation during septic shock, caspase -12 that mediates endoplasmic specific apoptosis and cytotoxicity by amyloid- β , caspase-13 which is suggested to be a bovine gene and caspase-14 which is highly expressed in embryonic tissues but not in adult tissues are known. As a result of the expression and activation of tissue transglutaminase in apoptotic cells extensive protein cross linking occurs. DNA breakdown is performed by Ca^{2+} and Mg^{2+} dependent endonucleases. Another important event in apoptotic cell is the movement of the membrane lipid phosphatidylserine from the inner to the outer side of the plasma membrane. This functions as a recognition signal for phagocytic cells to engulf apoptotic cells (Elmore, 2007; Cotter, 2009).

The extrinsic pathway involves transmembrane receptor mediated interactions. Members of the tumor necrosis factor (TNF) receptor family have cysteine rich extracellular domains and death domain. This death domain transmits the death signal from the cell surface to the intracellular signaling pathways. The best characterized ligands and corresponding death receptors are FasL/FasR and

TNF- α /TNFR1. When the death ligand binds to the death receptor, binding site for an adaptor protein is formed and whole ligand-receptor-adaptor protein complex is called as the death inducing signaling complex (DISC). DISC then initiates the assembly and activation of procaspase 8. The activated caspase 8 initiates apoptosis by cleaving other caspases (Elmore, 2007; Wong, 2011).

Cytotoxic T lymphocytes can kill target cells using the extrinsic pathway and FasL/FasR interaction. But also another pathway is used against tumor cells and virus-infected cells in which the transmembrane pore forming molecule perforin is secreted with a subsequent exophytic release of cytoplasmic granules through the pore and into the target cell. These granules possess serine proteases such as granzyme A and granzyme B. Granzyme B cleave proteins at aspartate residues and activate procaspase-10. Mitochondrial pathway and direct activation of caspase-3 are

also utilized by granzyme B. Granzyme A is important in cytotoxic T cell induced apoptosis and activates caspase independent pathway (Elmore, 2007).

The intrinsic pathway is initiated within the cell. Genetic damage, hypoxia, extremely high concentrations of cytosolic Ca^{2+} and oxidative stress are some of the factors that activate the intrinsic mitochondrial pathway. Increase in mitochondrial permeability and the release of proapoptotic molecules such as cytochrome-c into the cytoplasm are the main features. This pathway is regulated by a group of proteins which belongs to the Bcl-2 family. Bcl-2 proteins are divided into 2 groups such as proapoptotic proteins (Bax, Bak, Bad, Bcl-Xs, Bid, Bik, Bim and Hrk) and the antiapoptotic proteins (Bcl-2, Bcl-X_L, Bcl-W, Bfl-1 and Mcl-1). While the antiapoptotic proteins block the mitochondrial release of cytochrome-c, the proapoptotic proteins promote such release. The balance between those two groups of proteins determines whether the apoptosis would be initiated. Other apoptotic factors are apoptosis inducing factor (AIF), second mitochondria-derived activator of caspase (Smac), direct IAP Binding protein with Low pI (DIABLO), and Omi/high temperature requirement protein A (HtrA2). As a result of the release of cytochrome-c to the cytoplasm, a complex which is made up of cytochrome c, Apaf-1 and caspase 9 is formed and this activates caspase 3. Smac/DIABLO or Omi/HtrA2 promotes caspase activation by binding to inhibitor of apoptosis proteins (IAPs) which leads to disruption in the interaction of IAPs with caspase-3 or caspase -9 (Wong, 2011).

In the execution phase of apoptosis, a series of caspases are activated. Caspase 9 is the upstream caspase in the intrinsic pathway whereas caspase 8 in extrinsic pathway. Both pathways converge to caspase 3. Then the inhibitor of the caspase activated deoxyribonuclease which is responsible for nuclear apoptosis is cleaved by caspase 3. Downstream caspases induce cleavage of protein kinases, cytoskeletal proteins, DNA repair proteins and inhibitory subunits of endonucleases family. These also have effects on the cytoskeleton, cell cycle and signaling pathways (Wong, 2011).

There is one more pathway in apoptosis which is not well known and called as the intrinsic endoplasmic reticulum pathway. It is caspase-12 dependent and mitochondria independent. As a result of cellular stresses such as hypoxia, free radicals or glucose starvation the ER is injured and unfolding of proteins, reduced

protein synthesis occurs, then activation of caspases is performed by dissociation of an adaptor protein known as TNF receptor associated factor 2 (TRAF2) from procaspase-12 (Wong,2011).

Autophagy is a catabolic process in which recycling occurs. It can also be accepted as a primary degradation way for long lived proteins. It is observed in many eukaryotic cell types, where organelles and other cell components are degraded by lysosomes. Lysosome is a cellular compartment, which possess hydrolases. These hydrolases can cleave proteins, lipids, nucleic acids, and carbohydrates. Autophagosome formation is the first step in this process. A double membrane vacuole engulfs a portion of the cytoplasm to form this structure. The double membrane is obtained from ribosome-free areas of rough endoplasmic reticulum. Then autophagosomes fuse with lysosomes to form autolysosomes. Digestion of the cellular components lead to amino acids and fatty acids generation which can be used for either protein synthesis or can be used for ATP production after they are oxidized by the mitochondrial electron transport chain in order to survive the cell under starvation conditions. It is a mechanism that is activated as a result of extra- or intracellular stress, and can result in cell survival. Autophagy can also lead to cell death if it is overactivated. Autophagic cell death is caspase independent. In cells grown in presence of caspase inhibitors or in cells that possess defects in apoptosis system, autophagic death is demonstrated. Chromatin condensation, membrane blebbing are also observed in autophagy but there is no DNA fragmentation or apoptotic bodies (Ouyang et al, 2012; Sun and Peng, 2009; Guimaraes and Linden, 2004).

Programmed necrosis occurs as a result of several signaling pathways. The differences of the programmed necrosis from other programmed cell death mechanisms are the lack of caspase and lysosomal involvement. Main features of this process are the swelling of intracellular organelles such as mitochondria, ER and Golgi apparatus and loss of the plasma membrane integrity. As a result of signaling or damage induced lesions, mitochondrial dysfunction, enhanced generation of reactive oxygen species, ATP depletion and proteolysis by calpains and cathepsins are observed. Programmed necrosis is also associated with nuclear degradation (Sun and Peng, 2009).

Mitochondria are not only an energy factory of living cells but also they trigger or amplify the signals that are required for cell death. Cell death by apoptosis is related with mitochondrial membrane permeabilization. In addition to the induction of the permeability transition in the inner mitochondrial membrane, the release of cytochrome c, Smac/Diablo, AIF and endonuclease G may also exist in mitochondria dependent apoptosis. Researches show that mitochondrial permeabilization also occurs in autophagy and necrosis and cells behave against mitochondrial permeability transition (MPT) in a graded manner. Autophagy is activated when MPT occurs only in a few mitochondria, apoptosis is observed when a large number of mitochondria is permeabilized. It can be because of the higher concentration of molecules such as cytochrome c and AIF in the cytoplasm. Necrosis is promoted when all of the mitochondria in the cell are affected (Guimaraes and Linden, 2004). Forms of cell death are shown in Figure 2.3.

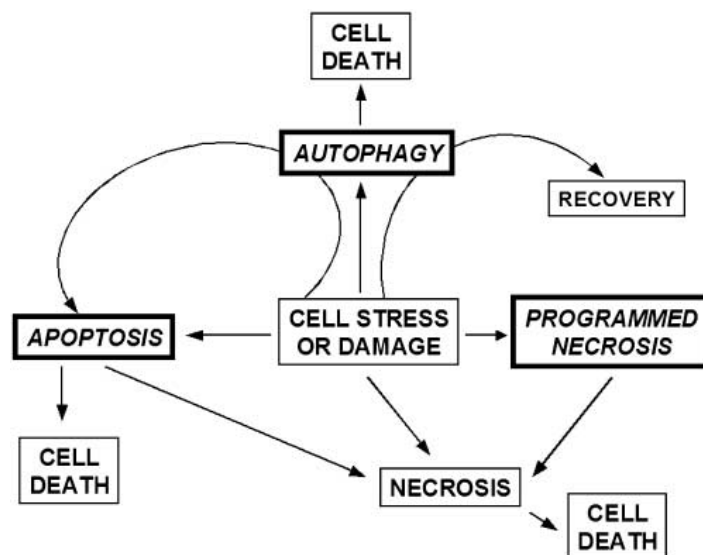


Figure 2.3 : Forms of Cell Death (Guimaraes and Linden, 2004).

1.4 Programmed Cell Death and Cancer

Under extreme conditions it is known that autophagy is effective in cell survival because it provides the energy required by the cells for their minimal functions when nutrients are scarce by degradation of intracellular macromolecules. Thus, in early stages of cancer progression, autophagic activation can play a protective role. By activating proautophagic genes and blocking antiautophagic genes in oncogenesis, autophagy can work as a tumor suppressor. However, autophagy can also take part in

carcinogenesis as a pro-tumor process, by regulating several pathways including Beclin-1, Bcl-2, Class III and I PI3K, mTORC1/C2 and p53. Necrosis was previously accepted as an accidental death but studies proved that it is controlled. Receptor interacting protein (RIP) kinases, poly (ADP-ribose) polymerase-1 (PARP1), NADPH oxidases and calpains are involved in programmed necrosis. When cells are necrosied, integrity of the cell membrane is destroyed, and intracellular materials are released leading to inflammatory responses by immune cells. As a result of the inflammation, tumor growth may be promoted (Ouyang et al, 2012).

Studies showed that apoptosis reduction or resistance is effective in carcinogenesis. The mechanisms for apoptosis evasion and carcinogenesis are ; balance disruption of proapoptotic and antiapoptotic proteins, reduction of caspase function and impairment of death receptor signaling. Bcl2 family of proteins is important in apoptosis regulation. When there is disruption in the balance, dysregulated apoptosis occurs. The p53 protein, coded by gene TP53, located at the short arm of chromosome 17, is the mostly known tumor suppressor protein. It is involved in many processes such as cell cycle regulation, development, differentiation, gene amplification, DNA recombination, chromosomal segregation, cellular senescence and induction of apoptosis. Oncogenic property of this gene occurs as a result of a mutation. Defects in p53 gene are related with more than 50% of human cancers. p53 regulated the expression of BAX in both in vitro and in vivo systems. It also controls the expression of Bcl2 family proteins. The inhibitor of apoptosis proteins (IAPs), which are a group of proteins that regulate apoptosis, cytokinesis and signal transduction, are inhibitors of caspases. Their main feature is the presence of a baculovirus IAP repeat (BIR) protein domain. They inhibit caspase activity by binding their conserved BIR domains to the active sites of caspases and by promoting degradation of active caspases or by keeping the caspases away from their substrates. In many cancers dysregulation in IAP expression is observed. Caspases which are classified in two groups such as the ones related to caspase 1 (caspase-1, -4,-5,-13,-14) that are functional during inflammation by cytokine processing, and the ones that are effective in apoptosis (caspase -2, -3, -6, -7, -8, -9, -10). Apoptosis related caspases are also divided into two groups such as initiator caspases (caspase

-2, -8, -9, -10) that are functional in initiation of apoptosis and effector caspases (caspase -3, -6, -7) that act by cleaving cellular components during apoptosis. Low levels of caspases or defects in caspase function are related with a decrease in apoptosis and carcinogenesis. Death receptors such as TNFR1(DR1), Fas (DR2, CD95, APO-1), DR3(APO-3), DR4 [TNF related apoptosis inducing ligand receptor 1 (TRAIL-1) or APO-2], DR5 (TRAIL-2), DR6, ectodysplasin A receptor (EDAR) and growth factor receptor (NGFR) have a death domain. As a result of a death signal, molecules go to the death domain and a signaling cascade is activated. Abnormalities like down regulation of the receptor, impairment of receptor function, reduced level in death signals all lead to apoptosis reduction (Wong, 2011; Cotter, 2009).

The mechanisms that are effective on apoptosis during cancer is summarized in Figure 2.4.

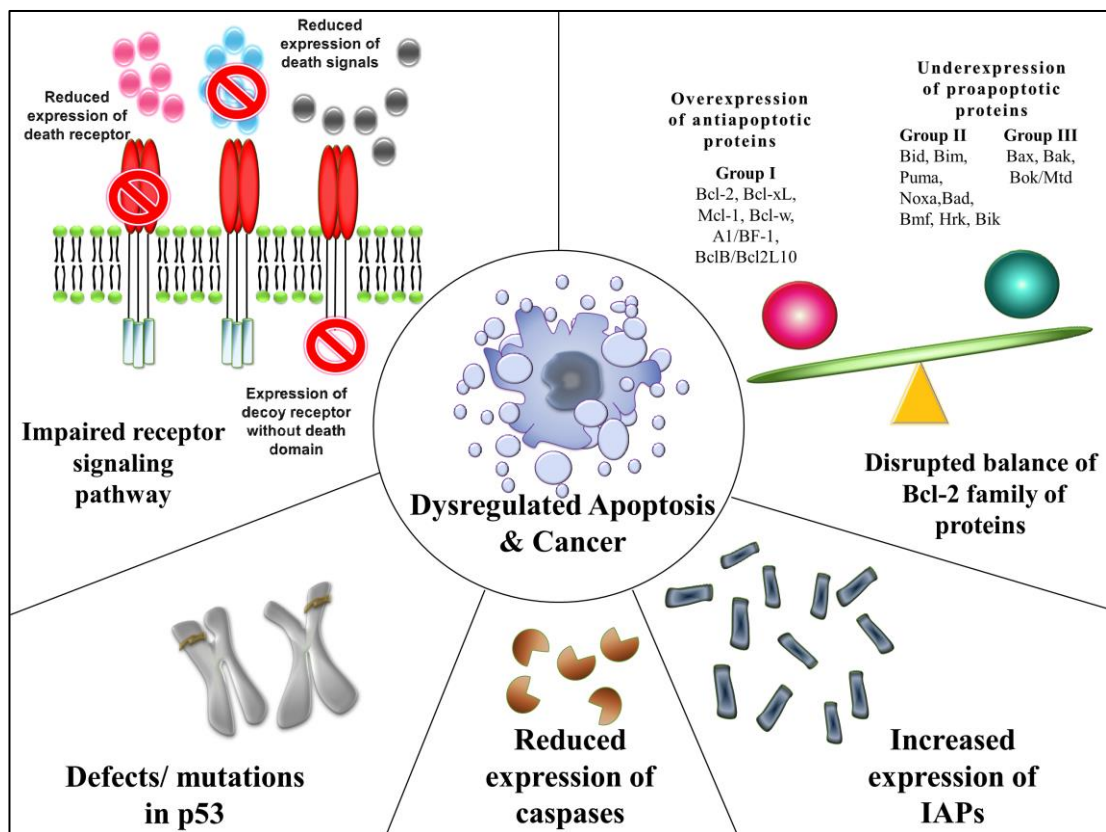


Figure 2.4: Apoptosis mechanisms during cancer (Wong, 2011).

1.5 Colorectal Cancer and Molecular Pathways

Cancer in colon and rectum have different types. Among them are carcinoid tumors which start from specialized hormone-producing cells in the intestine, gastrointestinal stromal tumors that start from specialized cells in the wall of the colon called the interstitial cells of Cajal. These types of tumors are either benign or malignant. They can be found anywhere in the digestive tract, but are unusual in the colon. Lymphomas start in lymph nodes, but they can also start in the colon. Sarcomas are tumors that can start in blood vessels, connective tissue, in the wall of the colon and rectum. Sarcomas are rare in colon and rectum. More than 95 % of colorectal cancers are adenocarcinomas (Url-3). Progression of colon cancer is shown in Figure 3.1.

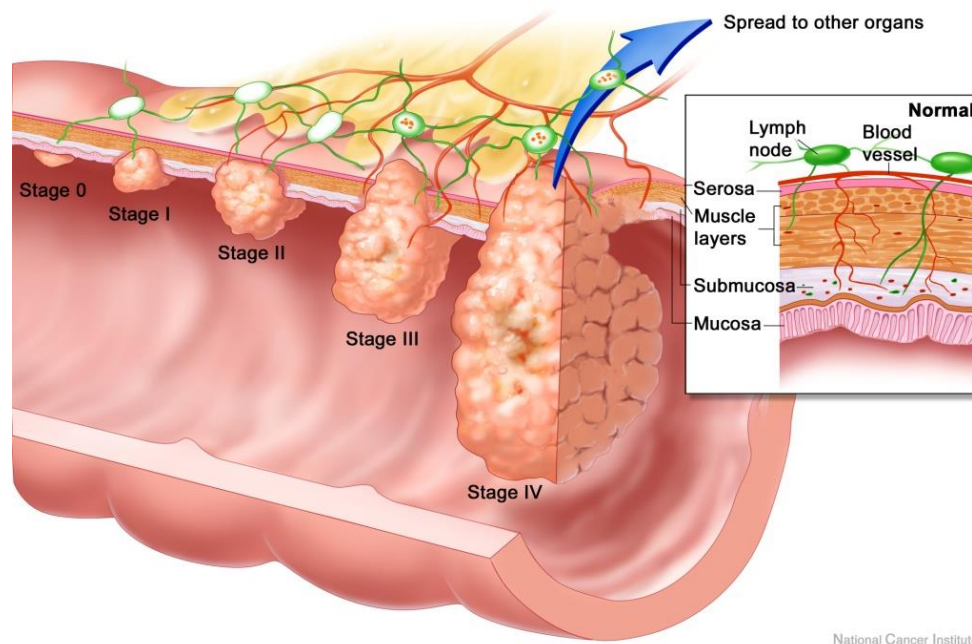


Figure 3.1: Progression of Colon Cancer (Url-4).

Colorectal cancer exists in the epithelium lining the colon and rectum. The first stage is the polyp formation. These polyps are accepted as the precursors of most colorectal cancers. Then tumor cells become invasive, break through the epithelial basal lamina, spread through the muscle and finally metastasize to lymph nodes, liver and other tissues. Hereditary Colorectal Cancer Syndromes result from mutations in genes involved in colorectal carcinogenesis. Approximately 5% of colorectal cancers are in this group. Familial Adenomatous Polyposis is more common. Adenomatous

Polyposis Coli gene is a tumor suppressor gene which is located on chromosome 5q21. It has 15 exons and encodes a 310 kDa protein with multiple functional domains. APC protein regulates epithelial homeostasis and degradation of cytoplasmic β -catenin. Wnt signaling pathway which is an important signal transduction pathway in colon cancer includes APC and β -catenin. APC protein is an inhibitory component in this pathway. Firstly in colon cancer, mutations on chromosome 5 appear. When APC mutation occurs, cytoplasmic β -catenin accumulation is observed and then it binds to the Tcf family of transcription factors. When it binds to β -catenin, activation of TCF4 which stimulates growth of the colonic epithelium when it has β -catenin bound to it, is prevented. Depletion of the gut stem cell population is observed as a result of loss of TCF4, so that loss of the antagonist APC can cause overgrowth by the opposite effect. In another words, in the Wnt pathway, APC binds to β -catenin and induces its degradation. When APC function is lost as a result of mutation or promoter methylation, cytoplasmic β -catenin is accumulated which leads to nuclear translocation, and binding of β -catenin to T-cell factor (TCF) / Lymphoid enhancer factor (LEF) Alteration exists in expression of several genes that affects proliferation, differentiation, migration and apoptosis. APC gene is also important in controlling cell cycle progression, stabilizing microtubules and promoting chromosomal stability. These mutations can be observed both in small benign polyps and malignant tumors. Generally, progression of polyps into lethal cancers requires additional mutations. As a result of the inactivating mutations in APC gene the rate of cell proliferation in the colonic epithelium increases. Abnormal tissues within the intestinal epithelium which contain dysplastic cells that are defined as cells with unusual shapes and enlarged nuclei develop. Then those abnormal tissues grow to form early stage adenomas. Among the few colorectal tumors that lack APC mutation, has a high proportion of activating mutations in β -catenin instead. So, that shows that WNT signaling pathway is one of the major pathways that is critical for cancer. It is especially important for initiation and progression of colorectal cancer. SMAD4 gene mutations are also reported in 30% of colon cancers. If the *K-ras* proto-oncogene is activated in one of these adenomas, that adenoma may grow and develop more fully. The *K-ras* gene codes for a 21kDa protein that is activated by extracellular signals. Because of the impaired GTPase activity which hydrolyses GTP to GDP, the mutated protein is locked in the active form. Mostly activating mutations are found in codons 12 and

13 of exon 1. Multiple cellular pathways that control cellular growth, differentiation, survival, apoptosis, cytoskeleton organization, cell motility, proliferation and inflammation are affected by Ras activation. After the adenoma formation, to induce it to progress further, inactivating mutations in tumor suppressor genes located in the long arm of the chromosome 18 occur. In order to transform this late adenoma into carcinoma *p53* tumor suppressor gene on chromosome 17, should also be inactivated. Those carcinoma cells invade other tissues in presence of additional inactivation mutations in other tumor suppressor genes. *p53* tumor suppressor gene mutations are common in colon cancer but occur late in tumorigenesis. It is suggested that *p53* did not restrict the proliferation of DNA damaged cells, but induce apoptosis in response to mutations of *APC* and *ras* and *p53* is inactivated at a late stage of tumor development (Alberts et al, 2002; Snustad and Simmons, 2006; Rupnarain et al, 2004; Roncucci and Ponz de Leon, 2000; Sohaily et al, 2012).

In MYH-Associated Polyposis (MAP), colorectal adenomatous polyps are formed. This is an autosomal recessive disorder in which bi-allelic mutations occur in the MYH gene, located on chromosome 1p35. MYH gene is a base excision repair gene that targets oxidative DNA damage. In this type of colorectal cancer, APC mutations also exist and in addition to this low frequency of loss of heterozygosity (LOH) is observed. Hereditary Non Polyposis Colorectal Cancer caused by mutations in DNA mismatch repair (MMR) genes which lead to replication errors and high potential for cancer. Chromosomal instability is the most common cause of genomic instability in colorectal cancer. Gain or loss of whole chromosomes or chromosomal regions is observed in this pathway. Imbalance in chromosome number, chromosomal genomic amplifications and a high frequency of loss of heterozygosity exists. Another pathway in colorectal cancer is the microsatellite instability pathway. Microsatellites are short repeat nucleotide sequences which spread over the whole genome and because of their repetitive manner, they cause errors in replication. During replication DNA mismatch repair system (MMR) normally recognizes and repairs base-pair mismatches but as a result of the microsatellite instability mismatch repair system becomes unable to correct the errors. In CpG Island Methylator Phenotype pathway, DNA methylation and as a result of this gene silencing occurs in tumor suppressor genes. In humans, epigenetic changes are caused by DNA methylation or

histone modifications. DNA methylation usually occurs at the 5'-CG-3' (CpG) dinucleotide (Sohaily et al, 2012).

Differences between sporadic colon cancer and colitis associated colon cancer is shown in Figure 3.2 below.

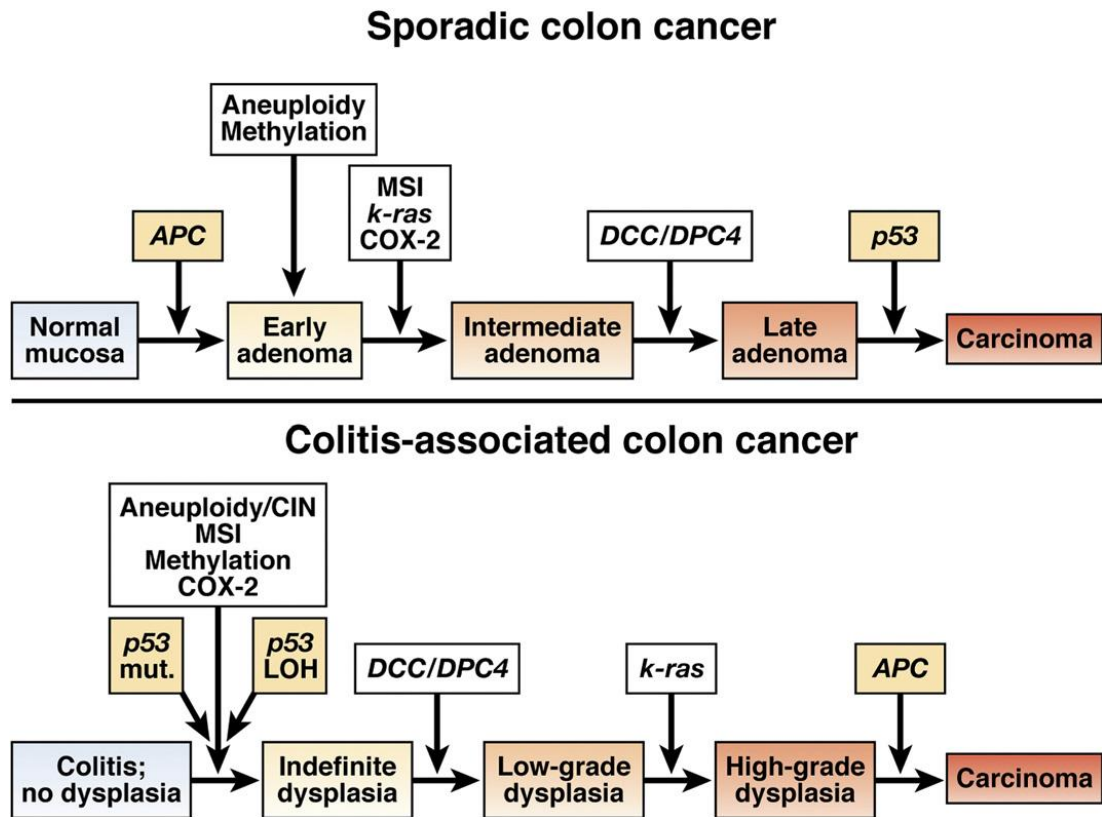


Figure 3.2 : Molecular Pathogenesis of Colon Cancer (Ullman and Itzkowitz, 2011).

1.6 Colitis Associated Colorectal Cancer

Researches demonstrated that patients with ulcerative colitis and Crohn’s disease have high risk for colorectal cancer. Duration and anatomic extent of colitis increases the risk. Chromosome instability, microsatellite instability and DNA hypermethylation which lead to sporadic colorectal cancer, are also observed in colitis associated colorectal cancer. In inflamed colonic mucosa, unlike the normal colon mucosa, these genetic alterations occur before any histologic evidence of dysplasia or cancer (Ullman and Itzkowitz, 2011). The dysplastic precursor in sporadic colon cancer is an adenoma which is a discrete focus of neoplasia that can be removed by endoscopic polypectomy whereas in Inflammatory Bowel Disease dysplasia is polypoid or flat, localized, diffuse or multifocal and the most important

point is that once it is found the entire colon is at high risk of neoplasia, therefore surgical removal of the entire colon and rectum is required for treatment (Itzkowitz and Yio, 2004).

It is found in the studies that colitis associated colorectal cancer occurs at a younger age than the general population. The molecular alterations that exist in Sporadic Colorectal Cancer can also be observed in Colitis Associated Colorectal Cancer. It is reported in studies that the frequency of chromosomal instability and microsatellite instability is roughly the same as in Sporadic Colorectal Cancer. However, it is also reported that differences exist in timing and frequency of these alterations (Itzkowitz and Yio, 2004; Willenbacher et al, 1999). APC mutation (loss of function) which is a common event and occurs at an early step in sporadic colon cancer, is a less frequent event and occurs late in colitis associated colon cancer. In colitis, p53 mutations occur at an early stage even before dysplasia. Also most of the p53 mutations were observed in inflamed mucosa derived from ulcerative colitis patients without cancer, which makes us think that chronic inflammation itself might induce these mutations. Allelic deletion of p53 exists in almost 50%-85% of colitis associated colon cancer. Methylation is also important in development and progression of colitis associated cancer. Methylation of CpG islands in several genes is observed in colitis patients. Inflammation also acts on colon carcinogenesis by oxidative stress production which causes cellular damage that leads to colitis and colon cancer. As a result of inflammation, reactive oxygen and nitrogen species are produced by macrophages and other leukocytes, which causes mutations that result in tumor initiation. The mismatch repair system is inactivated by hydrogen peroxide. Leukocytes and other types of immune cells that compose the tumor inflammatory microenvironment are responsible from the breakage of the basement membrane which is required for the invasion and migration of tumor cells. Neutrophils, eosinophils, dendritic cells, mast cells and lymphocytes are also functional in epithelial-originated tumors. Angiogenesis, which is an important process in tumor progression, is also found related to chronic inflammation (Itzkowitz and Yio, 2004; Ullman and Itzkowitz, 2011; Lu et al, 2006). Initiation of Sporadic Colon Cancer and Colitis Associated Colon Cancer is shown in Figure 3.3.

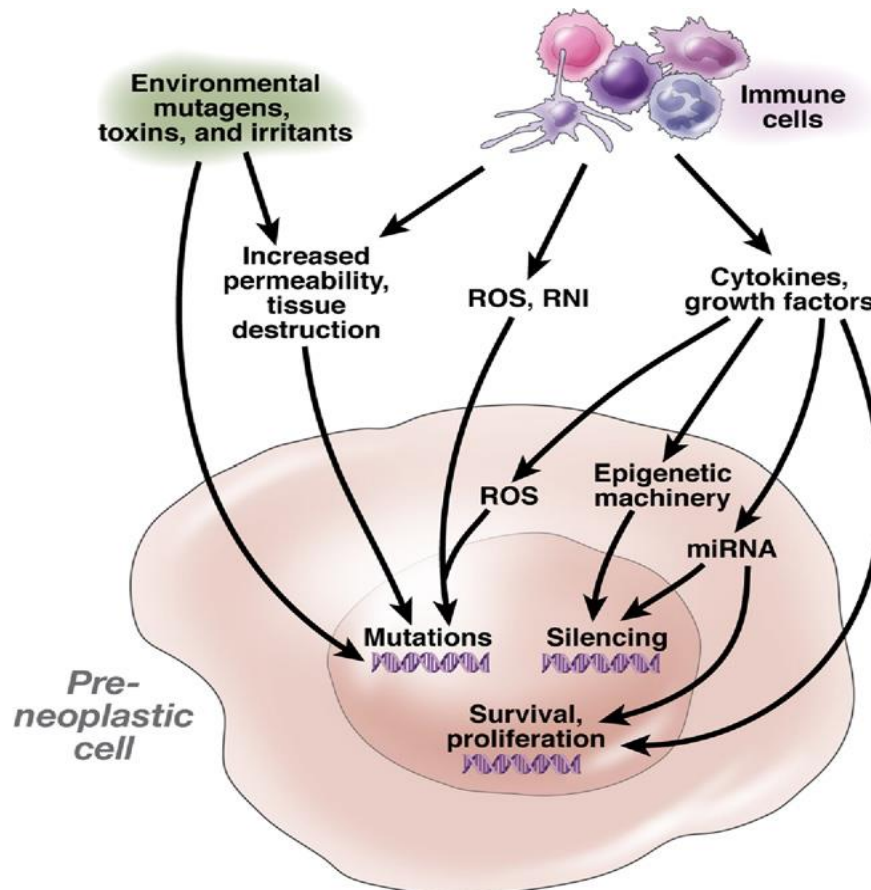


Figure 3.3: Initiation of Sporadic and Colitis- Associated Colon Cancer

(Terzic et al, 2010).

1.7 Bacteria and Cancer

Environmental factors, such as meat, saturated fat, low physical activity, obesity, smoking and alcohol beverages are also reported as the causes that increase the colorectal cancer risk. In the previous studies, a strong relationship between inflammatory diseases and colon cancer has also been reported. It was shown that patients with ulcerative colitis, Crohn's disease and inflammatory bowel diseases had increased risk for colorectal cancer (Roncucci and Ponz de Leon, 2000).

Recently, different studies have been performed to clarify the relationship between bacteria and cancer. *Helicobacter pylori* is well known to be associated with gastric cancer and *Salmonella typhi*, *Echerichia coli* and *Chlamydia pneumoniae* are the organisms that are associated with gall bladder, colon and lung cancer, respectively. *Streptococcus bovis* is defined as a low grade pathogen that is involved in bacteremia and endocarditis. Existence of a relationship between *Streptococcus bovis* and colon cancer was also determined (Mager, 2006; Biarc et al, 2004). It was shown that

Bartonella spp., *Lawsonia intracellularis* and *Citrobacter rodentium* infections can induce cellular proliferation which can be reversed by antibiotic treatment (Lax and Thomas, 2002). Small intestinal lymphomas and ocular lymphomas were found to be linked to *Campylobacter jejuni* and *Chlamydia psittaci* infections, respectively. In each case, it was shown that antibiotic treatment could eradicate the disease at an early stage (Lax, 2005). In animal models, it was found that *Citrobacter freundii* developed colonic hyperplasia and when exogenous mutagens were applied, malignancy occurred more rapidly than the uninfected ones (Parsonnet, 1995). *Enterococcus faecalis*, another intestinal commensal, developed colitis and tumors in IL-10 knockout mice (Huycke and Gaskins, 2004).

Studies also showed that several bacterial toxins interfere with cellular signalling mechanisms in a way that is characteristic of tumour promoters, they can disrupt cellular signalling to perturb the regulation of cell growth or to induce inflammation. Proliferation, apoptosis and differentiation processes are affected by those toxins. Some of those, directly damage DNA by enzymatic attack, these are the toxins that mimic carcinogens and tumour promoters. *Pasteurella multocida* toxin that acts as a mitogen and *Escherichia coli* cytotoxic necrotizing factor (CNF) which activates all members of the Rho family of small GTPases can be given as an example. In this way, signalling components that are downstream of Rho such as COX2 which is involved in different stages of tumour development including inhibition of apoptosis, is stimulated. Bacterial products can also affect DNA repair mechanisms. *Bacteroides fragilis* toxin is another one that leads to cell proliferation. According to the studies on mice it was also reported that *Citrobacter rodentium* infection caused a colonic hyperplastic disease that could lead to colonic cancer (Lax, 2005; Lax and Thomas, 2002).

1.8 *Enterobacter* species

Enterobacter strains are gram negative, opportunistic and increasingly important nosocomial pathogens. They are a member of the family *Enterobacteriaceae*. *Enterobacter aerogenes* and *Enterobacter cloacae* are the most frequently encountered human pathogens among this genus. As a gram negative organism they possess endotoxin. In some *Enterobacter* species, Shiga-like toxin production has also been observed. The great resistance to disinfectants and antimicrobial agents

make these pathogens available to cause nasocomial infections (Sanders and Sanders, 1997; Bilgehan, 2000).

1.9 Purpose of Thesis

Many studies have been performed to determine the interaction between bacteria and cancer. However, there has been no attempts to demonstrate a possible relationship between *Enterobacter* spp. and colon cancer. Therefore, in the present study, it was aimed to investigate the effects of *Enterobacter* group of microorganisms on colon cancer. Determination of the interaction between strains of *Enterobacter* spp. and colon cancer will lead to new approaches to colon cancer initiation and mechanism. Identification of a possible interaction between colon cancer and strains of *Enterobacter* spp. may also be for development of prophylaxis and new treatment strategies.

2. METHODS

2.1 Isolation of *Enterobacter* strains

Total thirteen bacterial strains were used in this study. Two strains of *Enterobacter* spp. and one strain of *Escherichia coli* were isolated using Sheep Blood Agar from patients who were treated at Istanbul University, Istanbul Faculty of Medicine, Department of General Surgery. Eight strains of *Enterobacter* spp. and one strain of *Morganella morganii* were provided from Marmara University, School of Medicine, Department of Medical Microbiology. In addition, an environmental strain of *Enterobacter* spp. was obtained from Microbial Collection Unit at Yeditepe University, Genetics and Bioengineering Department.

2.2 Identification of Bacteria by FAME profile analysis

Bacterial strains were identified by FAME profile analysis. Fatty acids exist in lipids in biological membranes including phospholipids, glycolipids and/or lipopolysaccharides. Fluidity, integrity and permeability of the membrane and the activities of membrane-bound enzymes are the properties that are influenced by fatty acids. Fatty acids differ in phylogenetically different microorganisms, mainly in the concentration and composition such as chain length, double-bound positions and substitutions. But in closely related organisms they are found similar, and under standardized conditions they remain constant. MIDI (Microbial Identification System) is a system that identifies and classifies microorganisms according to their fatty acid profiles. In order to isolate the fatty acids a single colony of the microorganism to be tested was inoculated by streaking on TSA (Tryptic Soy Agar) and was incubated about 24h at 37 °C. After the incubation period, the microorganism was harvested from the third and the fourth quadrant and transferred to a sterile 13mm x 100 mm screw cap glass tube. Using a four stepped procedure fatty acids were isolated and then fatty acid methyl esters were gained. Stock reagents to isolate the fatty acids were prepared according to Table 1. Then 1 ml

Saponification Reagent was added , after vortexing for 5-10 sec it was incubated at 100 °C for 5 min. Again vortexing was done for 5-10 sec. and was incubated at 100 °C for 25 min. After the incubation cooling was done. Methylation was performed by adding 2 ml Methylation Reagent and vortexing for 5-10 sec, and then it was incubated at 80 °C for 10 min. Rapidly cooling was done after the incubation. For extraction, 1.25 ml Extraction Solvent was added and incubated for 10 min at rotator. Then bottom phase was removed and top phase was saved. For purification, base wash was done and finally 2/3 top phase was transferred to GC vials. Using a fused-silica capillary column (25m by 0.2mm) with cross-linked 5% phenylmethyl silicone, gas chromatography was performed. Calibration standard mix, that contains nC9-nC20 saturated, 2 and 3 hydroxy fatty acids, were used to identify the peaks and to check the column performance. Identification of the fatty acids were performed by equivalent chain length data. Identity of the unknown strain was determined by comparing the FAME profiles, to those that exist in the standard libraries in the MIS software package (Şahin, 2001; Buyer, 2002; Agilent-Sherlock MIS Operating Manual, 2005).

Table 1.1: Reagents required for fatty acid isolation.

REAGENT	CONTENT	
1.Saponification Reagent	Sodium hydroxide	45g
	Methanol	150 ml
	Deionized distilled water	150 ml
2.Methylation Reagent	6.00N Hydrochloric Acid	325 ml
	Methanol	275ml
3.Extraction Solvent	Hexane	200ml
	Methyl tert-butyl ether	200 ml
4.Base Wash	Sodium hydroxide	10.8 g
	Deionized distilled water	900 ml

2.3 Microbial Identification by Metabolic Activities

VITEK2 (Biomérieux) is an automatic system which makes identification and antimicrobial susceptibility testing in a few hours according to metabolic changes (Perez-Vazquez et al, 2001). With colorimetric reagent cards, hardware and software systems, it becomes a useful instrument for microbial identification. Reagent cards used, have wells that contain different substrates, which can measure metabolic activities including acidification, alkalization, enzyme hydrolysis and growth in

presence of inhibitory substances. From 24 h pure bacterial cultures, bacterial suspensions which were prepared in sterile saline according to Mac Farland Turbidity Range 0.50 - 0.63 for Gram Negatives, were measured by a turbidity meter and then were transferred to appropriate card of the system. Test substrates on Gram Negative card were shown in Table 1.2. After incubation for maximum 10 hours, results were obtained (Jin et al, 2011; Pincus, H.D).

Table 1.2: Test substrates on Gram Negative card (Pincus, D).

Test	Mnemonic
Ala-Phe-Pro-Arylamidase	APPA
Adonitol	ADO
L-Pyrrolydonyl-Arylamidase	PyrA
L-Arabitol	IARL
D-Cellobiose	dCEL
Beta-galactosidase	BGAL
H ₂ S Production	H ₂ S
Beta-N-acetyl-glucosaminidase	BNAG
Glutamyl Arylamidase pNA	AGLTp
D-glucose	dGLU
Gamma-glutamyl-transferase	GGT
Fermentation / Glucose	OFF
Beta-glucosidase	BGLU
D-maltose	dMAL
D-mannitol	dMAN
D-mannose	dMNE
Beta-xylosidase	BXYL
Beta-alanine arylamidase pNA	BAlap
L-Proline Arylamidase	ProA
Lipase	LIP
Palatinose	PLE
Tyrosine Arylamidase	TyrA
Urease	URE
D-sorbitol	dSOR
Saccharose/ Sucrose	SAC
D-tagatose	dTAG
D-trehalose	dTRE
Citrate (sodium)	CIT
Malonate	MNT
5-Keto-d-gluconate	5KG
L-lactate alkalisation	ILATk
Alpha-glucosidase	AGLU
Succinate alkalisation	SUCT
Beta-N-acetyl galactosaminidase	NAGA
Alpha-galactosidase	AGAL
Phosphatase	PHOS
Glycine Arylamidase	GlyA
Ornithine Decarboxylase	ODC
Lysine Decarboxylase	LDC
Decarboxylase Base	ODEC
L-Histidine assimilation	IHISa
Coumarate	CMT
Beta-glucuronidase	BGUR
O/129 Resistance (comp. Vibrio)	O129R
Glu-Gly-Arg-Arylamidase	GGAA
L-Malate assimilation	IMLTa
ELLMAN	ELLM
L-lactate assimilation	ILATa

2.4 16 S rDNA Sequence Analysis

To confirm the FAME profile analysis and biochemical test results, the bacterial strains that were found as effective in the study, were also identified using 16 S rDNA sequence analysis. In this technique first genomic DNA was isolated from the bacterial strains and was controlled by agarose gel electrophoresis, then 16S rRNA coding region was amplified by PCR. After purification of the PCR products, sequencing was performed and the results were evaluated using databases (Weisburg et al, 1991).

2.4.1 Genomic DNA isolation

Bacterial Genomic DNA was isolated using QiAcube System. First bacteria was inoculated onto agar medium (Sheep Blood Agar or LB Agar) After incubation for 24h, bacteria was collected and washed using PBS then was centrifugated, the supernatant was removed and the pellet was run according to the QiAcube Bacterial Pellet Protocol.

2.4.2 Agarose gel electrophoresis

1% (w/v) Agarose gel was prepared using TBE Buffer. Electrophoresis was carried out at 100 V for 20 minutes.

2.4.3 Amplification of 16S rDNA sequencing and phylogenetic analysis of bacterial strains

16S rDNA was amplified using universal primers (27F: AGAGTTTGATCCTGGCTCAG, 1492R: ACGGCTACCTTGTTACGACTT) (Weisburg et al, 1991). PCR mix was prepared and PCR was carried out. After PCR, samples were controlled in 1% agarose gel and then were purified using Roche PCR purification kit. Using these purified samples sequencing was performed at REFGEN. Sequence results were evaluated by the help of databases. For phylogenetic analysis SDSC Biology Workbench was used (Higgins et al, 1992; Thompson et al, 1994; Felsenstein, 1989).

2.5 Isolation of bacterial proteins

In order to minimize the chance to lose the enzymatic activity, bacterial protein was isolated using Easylyse bacterial protein extraction solution. For this purpose, first bacteria was grown in Brain Heart Broth, after 24h bacterial pellet was frozen at -20° C. Then pellet was resuspended in a solution containing 1 M MgCl₂, Lysis buffer and enzyme mix and was incubated for 5 minutes at room temperature. After centrifugation steps finally the clear supernatant was transferred to a new tube and protease inhibitor cocktail was added to the sample. Protein concentration was determined by Bradford Assay. This assay was performed in 96 well plates. Protein standards that were ranging from 0,1-1.5 mg/ml were prepared using BSA. 250 µl of the Bradford Reagent was transferred onto each well being used. 5 µl of protein standards, 5 µl of water as blank and 5 µl of bacterial protein samples were added onto separate wells. After 10 min. of incubation at room temperature absorbance at 590 nm. was measured using an ELISA plate reader. According to the absorbance values of BSA the standard curve graph was prepared and the bacterial protein concentration was calculated.

2.6 Cell culture

NCM 460 and CRL1790 cell lines that were provided from Incell and ATCC, respectively were used in this study. NCM cell lines were cultured in M3 base medium A that was supplemented with 10% FBS and CRL1790 cell line was cultured in EMEM including 10% FBS and 1% PSA. Cell lines were incubated at 37°C in a humidified environment with 5% CO₂.

2.7 Determination of the optimum protein concentration to apply onto cell lines and examination of cell proliferation

To determine the optimum protein concentration to apply onto the epithelial cell lines and examine the cell proliferation, MTS assay was performed. MTS is a tetrazolium compound which is bio-reduced by cells into a formazan product. Using dehydrogenase enzymes, metabolically active cells produced NADPH or NADH which performed this conversion (Berridge and Tan, 1993; Cory et al, 1991; Riss and Moravec, 1992).

Firstly in this test, according to the growth properties of cell lines 8000- 22000 cells were seeded on 96 well plates. Bacterial proteins at concentrations ranging from 2µg- 15µg were applied onto cell lines. After incubation for 72h, the medium containing the bacterial proteins was removed and fresh medium containing MTS was added and incubated for 1-4 hours. Absorbance at 490 nm was measured using ELISA Reader. The quantity of formazan product was directly proportional to the number of living cells in culture (Berridge and Tan, 1993; Cory et al, 1991; Riss and Moravec, 1992). Same procedure was applied for negative control (NC) which contained only growth medium and for positive control (PC) which contained DMSO. All the experiment was repeated four times. The concentration which had the highest cell viability was determined as optimum. Using the Cell viability – Concentration graphs, evaluation of the cell proliferation was performed.

2.8 Detection of Apoptosis and Cell Viability Assays

In apoptotic cells, the membrane phospholipid phosphatidylserine exposure occurs to the external cellular environment. Annexin is a Ca^{+2} regulated phospholipid binding and membrane-binding protein. In the presence of physiological concentrations of Ca^{+2} , Annexin V has a high affinity for negatively charged phospholipids and thus it binds to cells with exposed phosphatidylserine. Because Annexin V is conjugated with FITC, detection could be performed using flow cytometry. Pi was used together with annexin to determine if the cells are early apoptotic, late apoptotic, necrotic or viable. Viable cells could not be stained with pi due to the intact membrane but dead and damaged cells could be stained (BD Technical data sheet, Niu and Chen, 2010; Elmore, 2007; Rescher and Gerke, 2004; Dillon et al, 2000).

To detect apoptosis using annexin V, first of all, bacterial proteins at appropriate concentrations were applied onto cell lines that were seeded on 6-well plates. After 3 days of incubation, bacterial proteins were removed, cell lines were washed and trypsinized and then were mixed with annexin antibody and pi. The mixture was incubated for 10 min. Then PBS was added and the mixture was centrifugated. After centrifugation the supernatant was removed, the pellet was resuspended in PBS and was run in flow cytometry. The same steps were also repeated for cell lines without bacterial protein application and also sample without annexin or pi and samples

containing only annexin, and only pi were run as negative and as controls, respectively.

2.9 Detection of CD24

CD24, a molecular marker of malignant tumors, was detected by flow cytometry in CRL1790 and NCM460 cell lines before and after bacterial protein application. In order to do this, first of all cell lines were seeded in 6 well plates in appropriate medium that was previously described. Then the total bacterial proteins at the optimum concentration were applied onto the cell lines and were incubated for 3 days. After this, the proteins were removed, cell lines were washed and trypsinized and were mixed in PBS with conjugated CD24 antibody. Samples were incubated at +4°C for 1 hour. After the incubation PBS was added to the tubes and they were centrifugated at 1000 rpm for 5 min. The supernatant was removed and then PBS was added onto the pellet. Finally pi was added and after 5 min. of incubation CD24 and pi was measured by flow cytometry. Same procedure was applied for Isotype which was used to measure background signal. To calculate CD24 level, Isotype values were extracted from the CD24 values (Sagiv et al, 2006; Han and Nair, 1995; Lim, 2005).

2.10 Detection of COX-2

COX-2 is an enzyme that acts in prostaglandin synthesis. It inhibits apoptosis by increasing Bcl2 expression through the mitogen activated protein kinase or phosphoinositide 3-kinase-AKT signaling pathways (Terzic et al, 2010).

The samples which increased CD24 level and at the same time decreased apoptosis in CRL1790 cell lines and for NCM 460 cell lines again the samples that apoptosis reduction occurred were included in this assay. To detect COX-2, Western Blotting technique was used. Bacterial protein was applied onto cell lines that were seeded on 6-well plates. Also samples from both of the cell lines without bacterial protein application were tested. After 3 days of incubation, cells were washed with DPBS . Then whole cell lysate was obtained by addition of complete RIPA buffer which contains protease inhibitor cocktail, PMSF and sodium orthovanadate. Cell lysates were collected using a cell scraper. Then samples were sonicated on ice with a probe sonicator and were stored at - 80°C. Same procedure was also applied for cell lines

without bacterial protein application. To determine the protein concentration Protein Content Assay was performed. Protein samples were diluted in distilled water. Bradford assay was done using Biorad Protein reagent. Protein concentration was calculated using the standard curve graph which was prepared according to the absorbance values of BSA. SDS-PAGE was performed using Bio-Rad Mini-Protean Tetra Cell Electrophoresis System. MiniProtean TGX Gel (Precast) was used. After mixing with 2X Laemmli buffer at 1:1 volume ratio, 30 µg protein samples were boiled at 95°C for 5 minutes. Protein samples and protein marker was loaded to the wells. To compare, a COX-2 positive control; cell lysate from a macrophage cell, Raw 264.7 which was induced with LPS, was also loaded. Electrophoresis was carried out at 200V constant voltage until the dye front reaches the line near the bottom edge of the gel cassette. After the proteins are separated, they were transferred from the gel to nitrocellulose membrane by Trans- Blot Turbo System. Then to check the transfer, Poncaeu staining was performed. Blocking was done for 1 hour in 5% (w/v) non-fat dry milk in TBS-Tween, pH 7.4. After blocking membrane was incubated overnight with primary antibody against COX-2 (1:1000 dilution). Then the membrane was washed 3 times with TBS Tween and incubated with antimouse Horseradish Peroxidase conjugated secondary antibody (1:15000 dilution) for 2 hours. After the incubation, membrane was washed 3 times with TBS Tween and was incubated in PBS for 10 min. Immunodetection of membrane was performed using ECL-Thermo kit, chemiluminescent signal was detected via Biorad Chemiluminescence imaging system.

2.11 Determination of NFκB and Bcl2 Expression

NFκB is a protein involved in many cellular processes including cell proliferation, apoptosis and tumorigenesis. Bcl2 is one of the key regulators of apoptosis which is over-expressed in many cancer types (Ouyang et al, 2012).

To determine NFκB and Bcl2 Expression, firstly RNA was isolated from cell lines before and after bacterial protein application. Same as COX-2 detection assay, CRL1790 without bacterial protein application, CRL1790 after DE8, DE365 and HIA applications, NCM460 without bacterial protein application, and after DE129, DE51 and DB7Y applications were included in this assay. Bacterial protein was applied onto cell lines that were seeded on 6-well plates. After 3 days of incubation,

RNA isolation was performed using Roche Total RNA Isolation kit and Ambion RNA isolation kit. RNA concentration was determined by nanodrop measurement. Then according to the RNA concentration cDNA was synthesized using Fermentas Revertaid First Strand cDNA Synthesis Kit. Real Time PCR was performed using primers for Bcl2 and NFkB. PCR mix was prepared with Takara SYBR Premix Ex Taq II (Tli RNaseH Plus) β -actin was used as reference and for normalization. All samples and reference were tested in triplicate with CFX96 Real-Time PCR Detection System. Results were evaluated using Biorad Software.

2.12 Statistical Analysis

For statistical analysis, Graphpad Software was used. In MTS assay, the values were analysed by One way ANOVA test following Dunnett test. Using the Dunnett test, the mean of the absorbance values from the wells that contain different concentrations of bacterial proteins were compared with the mean of the negative control wells which contained only growth medium. Statistical analysis of real-time pcr results were performed by One way ANOVA following Tukey test. Using the Tukey test, data of the samples without bacterial protein application and with different bacterial protein applications were all compared to each other.

In both tests, threshold significance level was set as 0,05. During the evaluation, p value lower than 0,001 ($p < 0,001$) was accepted as 'Extremely significant' and defined as '***'. p value between 0,001 to 0,01 (p: 0,001-0,01) was accepted as 'Very significant' and defined as '**'. p value between 0,01 to 0,05 ($p: 0,01-0,05$) was accepted as 'Significant' and defined as '*'. p value higher than 0,05 ($p > 0,05$) was accepted as 'Not significant' and defined as 'ns'.

3. RESULTS

3.1 Identification of bacterial strains

Thirteen bacterial strains used in the present study were identified by FAME profile analysis and biochemical tests. To confirm the results, six bacterial strains that were defined as effective because of the apoptosis reduction, were also identified by 16S rDNA sequencing. As a result of these tests, it was determined that eleven bacteria belong to *Enterobacter* species whereas two of them were identified as *Echerichia coli* and *Morganella morganii*. The documents including our FAME profile analysis and biochemical test results were given in Appendix Part. 16S rDNA sequencing analysis results, which were obtained by matching in **Ribosomal Database Project**, were given below.

In Figure 4.1, sequence matching of DB7Y was shown. As it can be observed from the figure, DB7Y belonged to the *Enterobacter* genus.

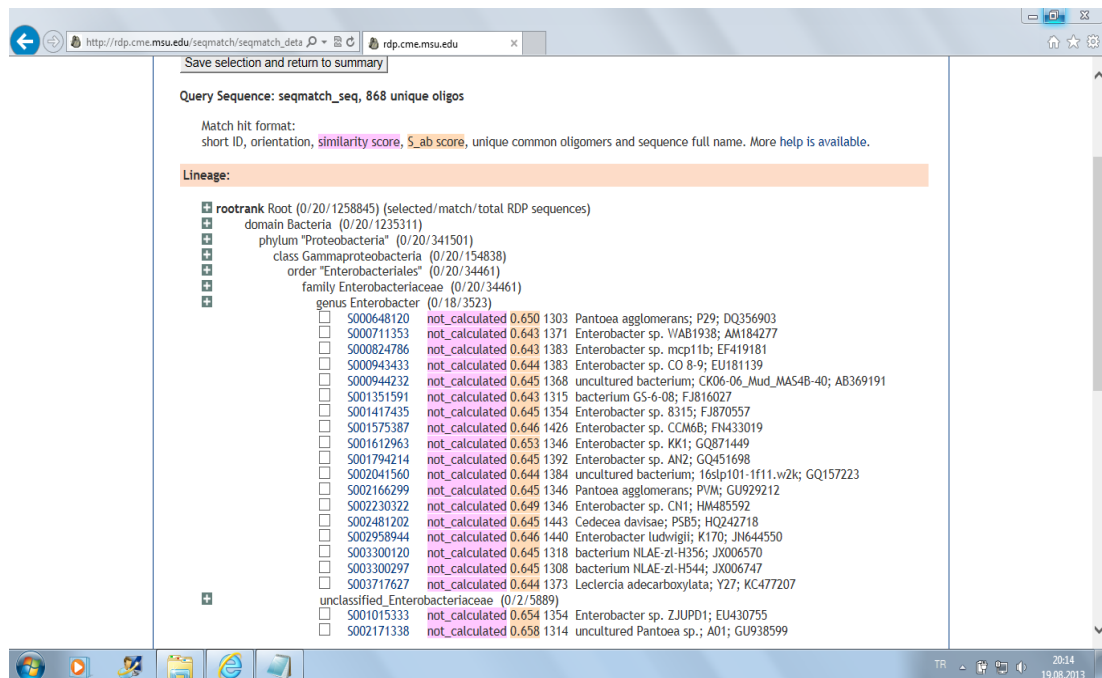


Figure 4.1: Sequence Analysis of DB7Y strain.

In Figure 4.2, the matching results of DE8 were given. When the similarity results were evaluated it was determined that DE8 was *Enterobacter aerogenes*.

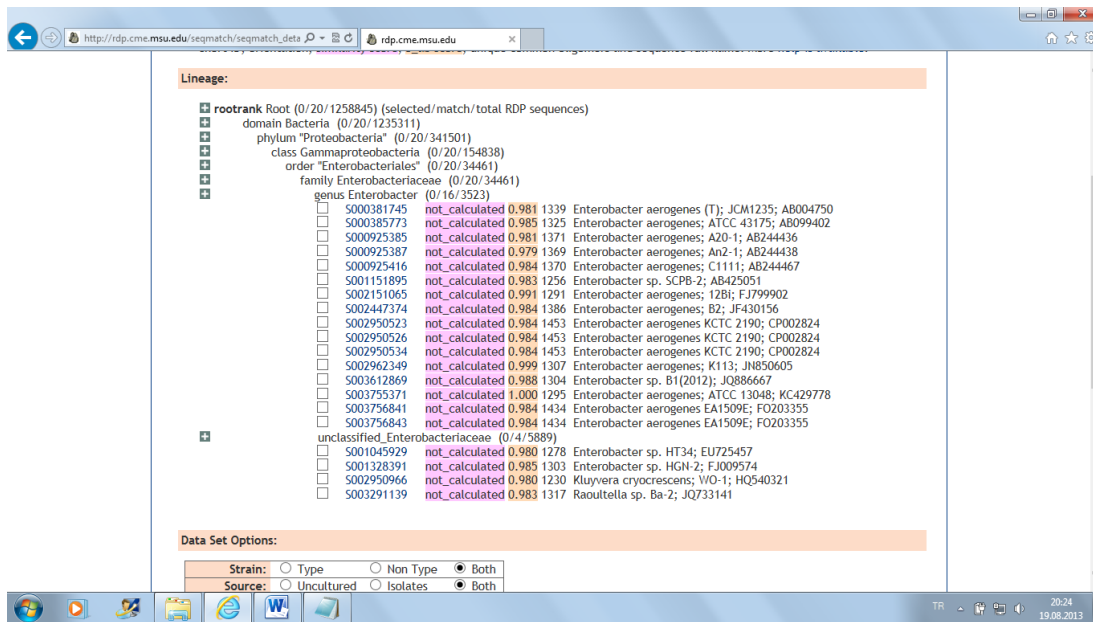


Figure 4.2: Sequence Analysis of DE8 strain.

In Figure 4.3 , the results of DE129 was shown. It was identified as *Enterobacter* spp.

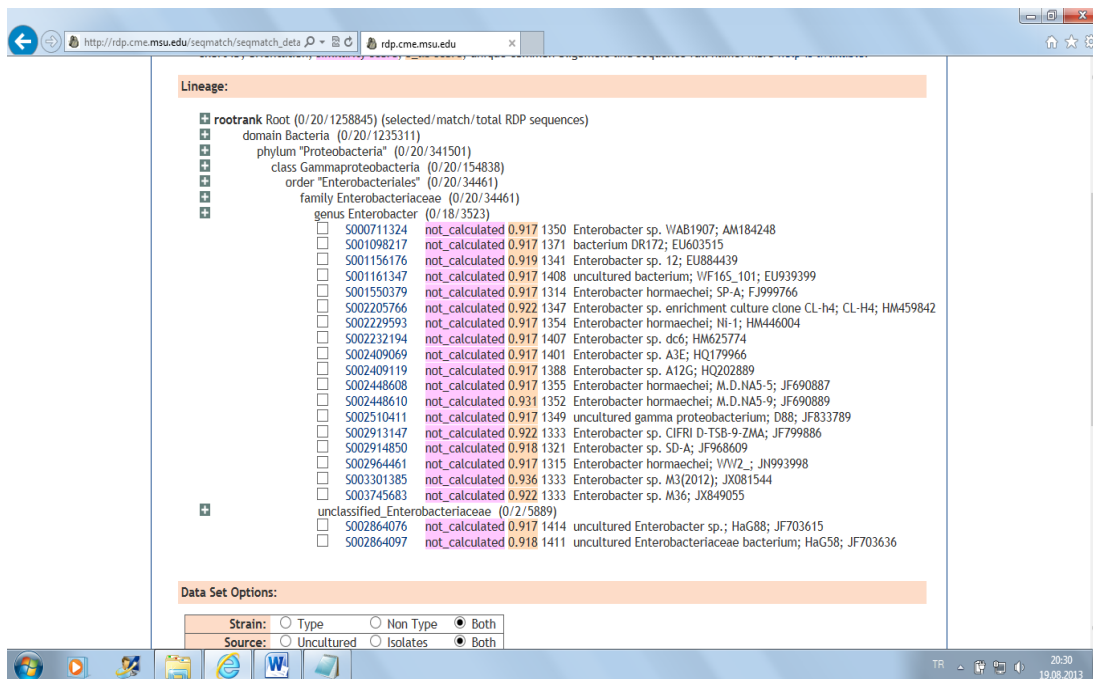


Figure 4.3: Sequence Analysis of DE129 strain.

Figure 4.4 included the results of DE365. It was similar to *Enterobacter aerogenes* but it could also be identified as *Enterobacter* spp.

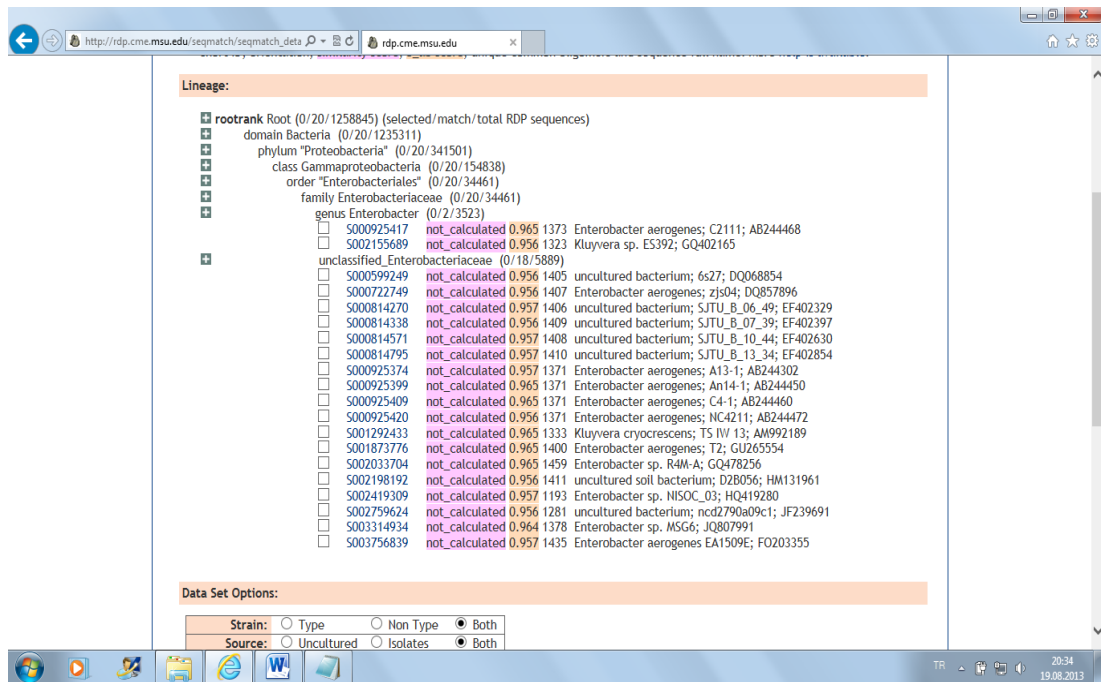


Figure 4.4 : Sequence Analysis of DE365 strain.

Figure 4.5 possessed DE51 results. As it can be observed, DE51 belonged to the *Morganella* genus. It was very similar to *Morganella morganii*.

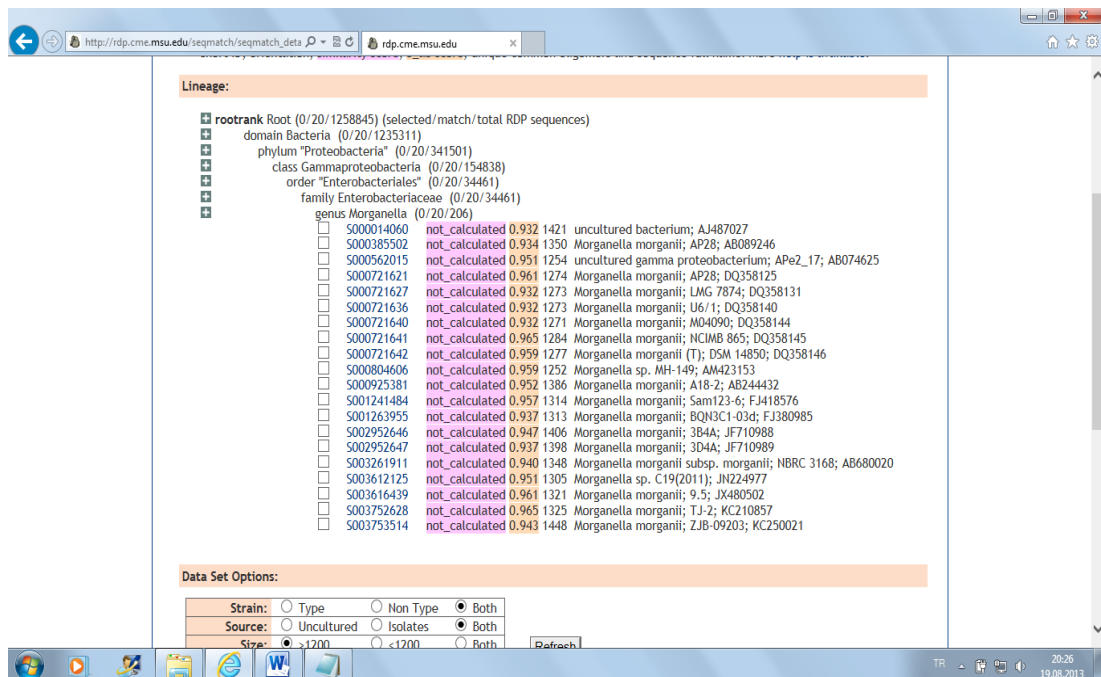


Figure 4.5 : Sequence Analysis of DE51.

In Figure 4.6 results of HIA were given. HIA belonged to the *Escherichia/Shigella* genus. It was found mostly similar to *Escherichia coli*.

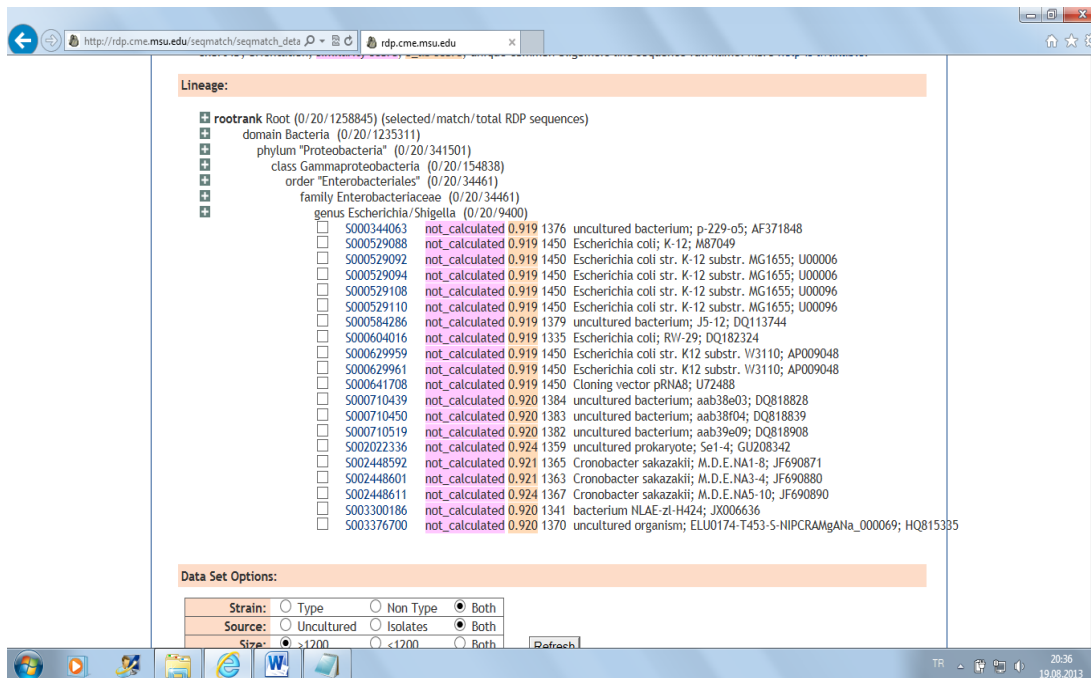


Figure 4.6: Sequence Analysis of HIA strain.

3.2 Phylogenetic Analysis of The Effective *Enterobacter* Species

Figure 5.1 demonstrated the phylogenetic analysis of *Enterobacter* strains. The nearby location of DE365 and DE129 followed by DB7Y, indicated that they were familiar. DE8, which was located far from the other strains, were familiar with *Enterobacter aerogenes* C2111.

PHYLIP rooted tree -Phenogram

[Download a PostScript version of the output](#)

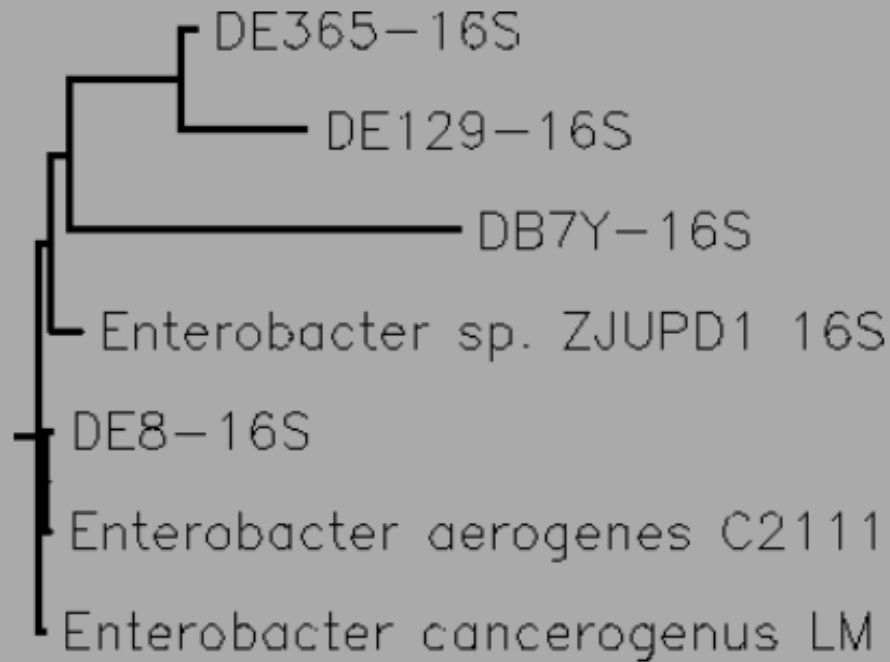


Figure 5.1: Phylogenetic tree of *Enterobacter* strains.

3.3 MTS Results

To determine the optimum bacterial protein concentration onto CRL1790 and NCM460 cell lines, MTS assay was performed. Absorbance-Concentration and Cell Viability-Concentration graphs were prepared. The concentration which had the highest cell viability was determined as optimum.

Cell Proliferation Examination Result (1):

When Cell viability – Concentration graphs were examined, it was observed that all of the bacterial proteins except for DE47 and DE12 increased cell proliferation in CRL1790 cell lines.

According to the test, the optimum concentration for 3h bacterial protein on CRL1790 cell line was determined as 2 µg. Graphs were given in Figure 6.1 and Figure 6.2.

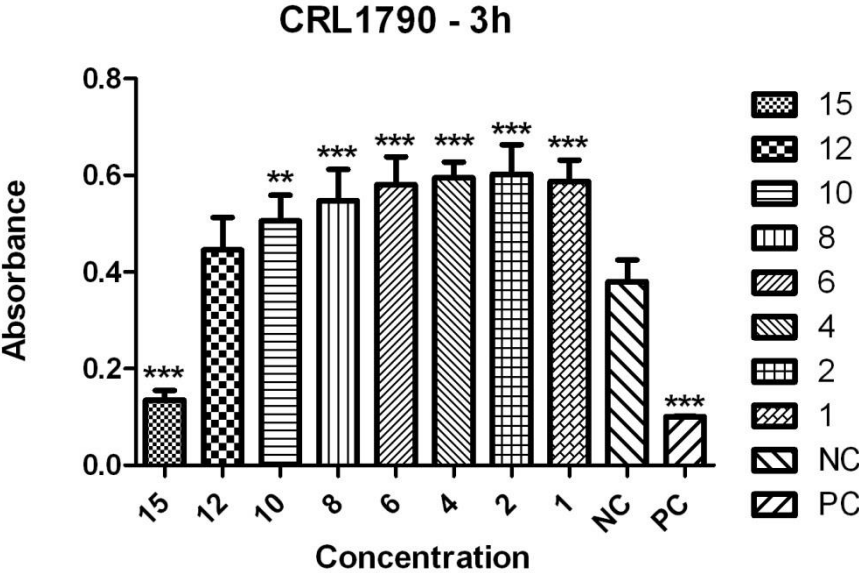


Figure 6.1: Absorbance - Concentration Graphic of CRL1790 cell line-3h.

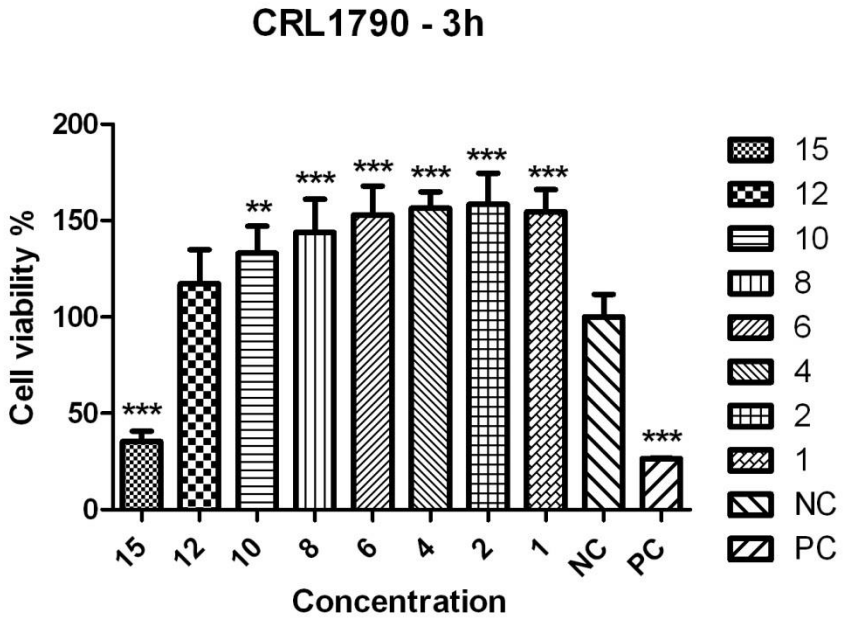


Figure 6.2 : Cell viability - Concentration Graphic of CRL1790 cell line-3h.

The optimum concentration for DB7Y bacterial protein on CRL1790 cell line was determined as 6 μ g in MTS assay. Graphs were given in Figure 6.3 and Figure 6.4.

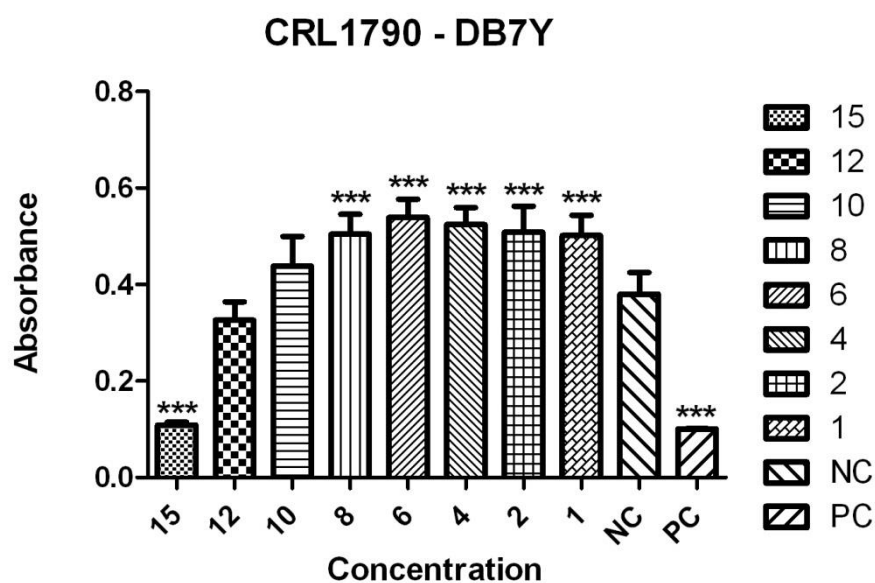


Figure 6.3: Absorbance - Concentration Graphic of CRL1790 cell line -DB7Y.

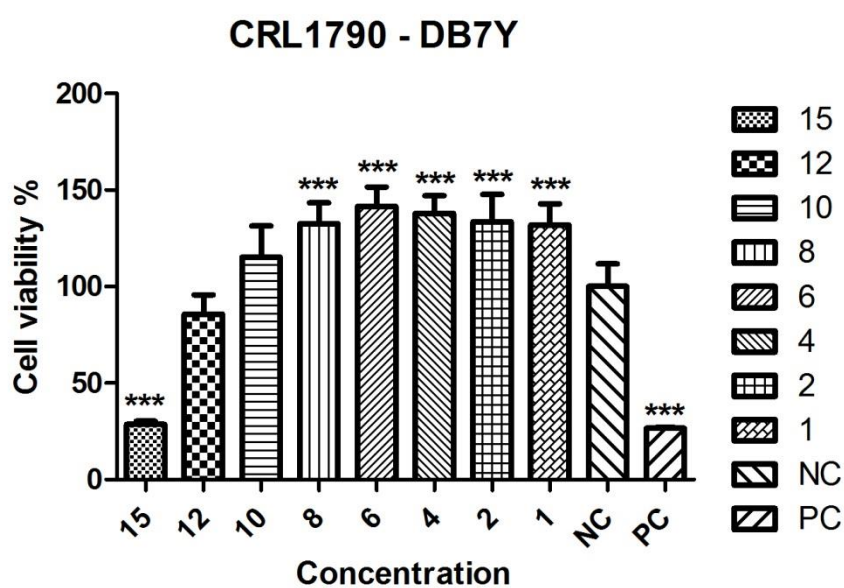


Figure 6.4 : Cell viability - Concentration Graphic of CRL1790 cell line -DB7Y.

The optimum concentration for DE8 bacterial protein on CRL1790 cell line was determined as 8 µg in MTS assay. Graphs were given in Figure 6.5 and Figure 6.6.

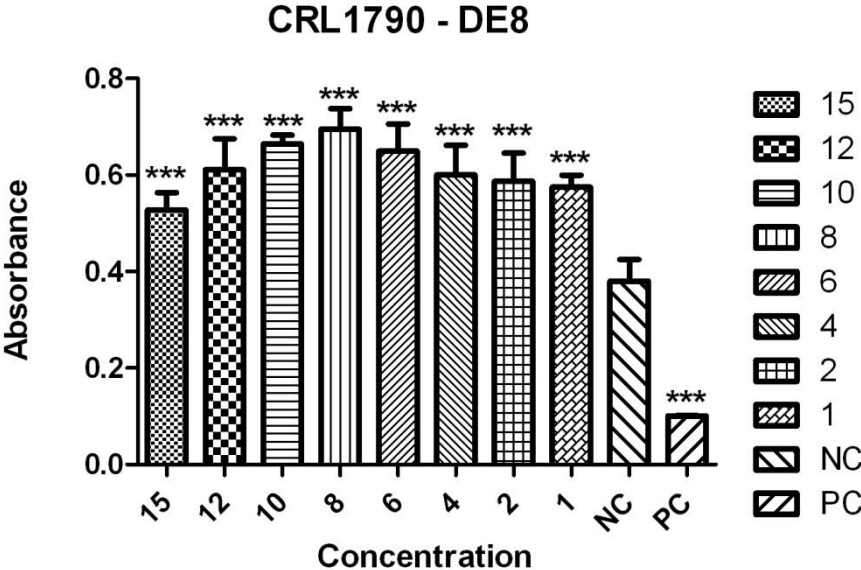


Figure 6.5: Absorbance - Concentration Graphic of CRL1790 cell line -DE8.

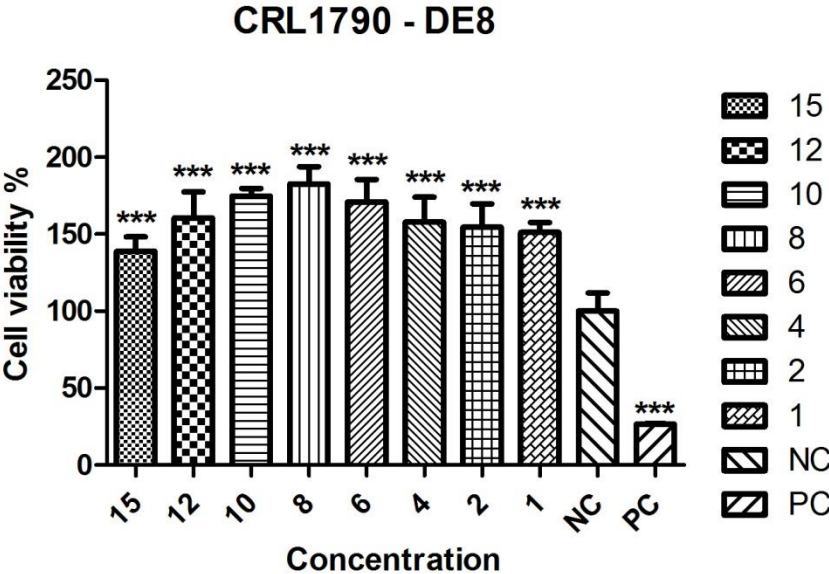


Figure 6.6 : Cell viability - Concentration Graphic of CRL1790 cell line -DE8.

The optimum concentration for DE12 bacterial protein on CRL1790 cell line was determined as 10 µg in MTS assay. Graphs were given in Figure 6.7 and Figure 6.8.

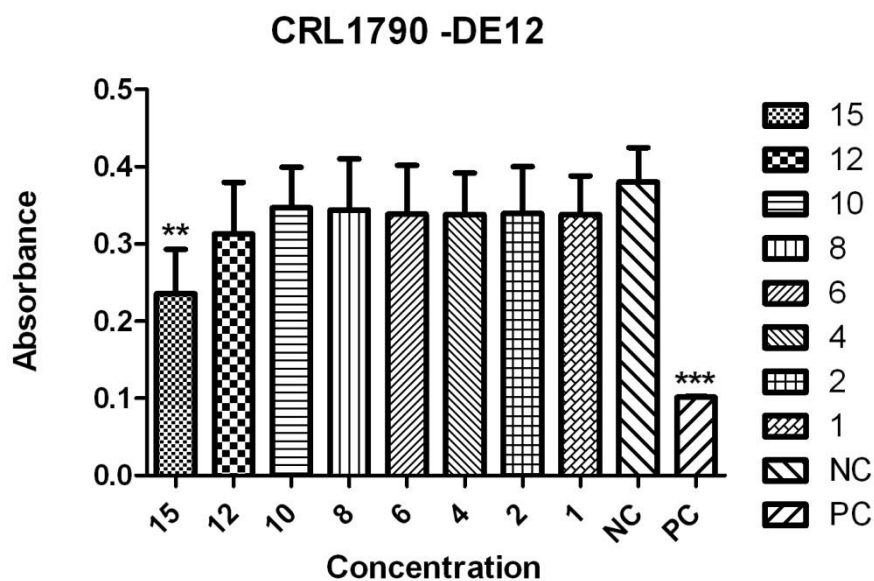


Figure 6.7: Absorbance - Concentration Graphic of CRL1790 cell line -DE12.

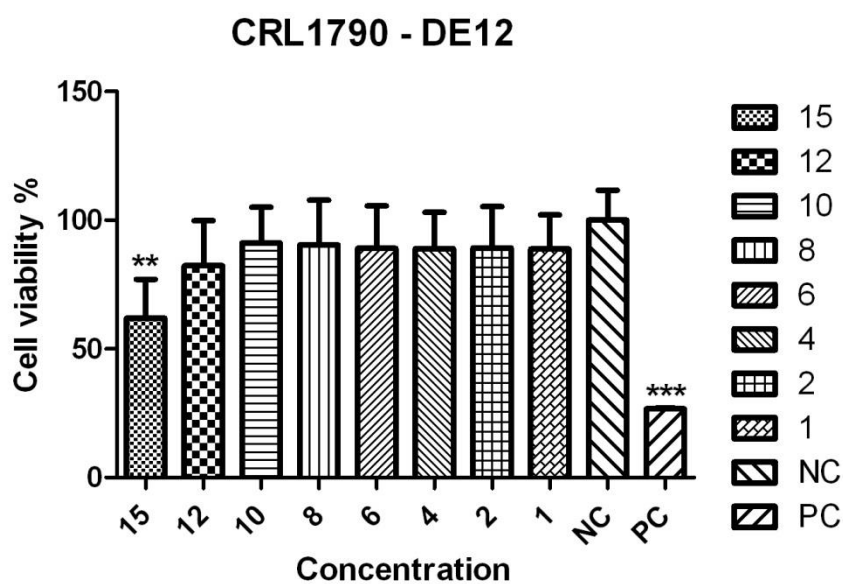


Figure 6.8 : Cell viability - Concentration Graphic of CRL1790 cell line -DE12.

The optimum concentration for DE36 bacterial protein on CRL1790 cell line was determined as 12 µg in MTS assay. Graphs were given in Figure 6.9 and Figure 6.10.

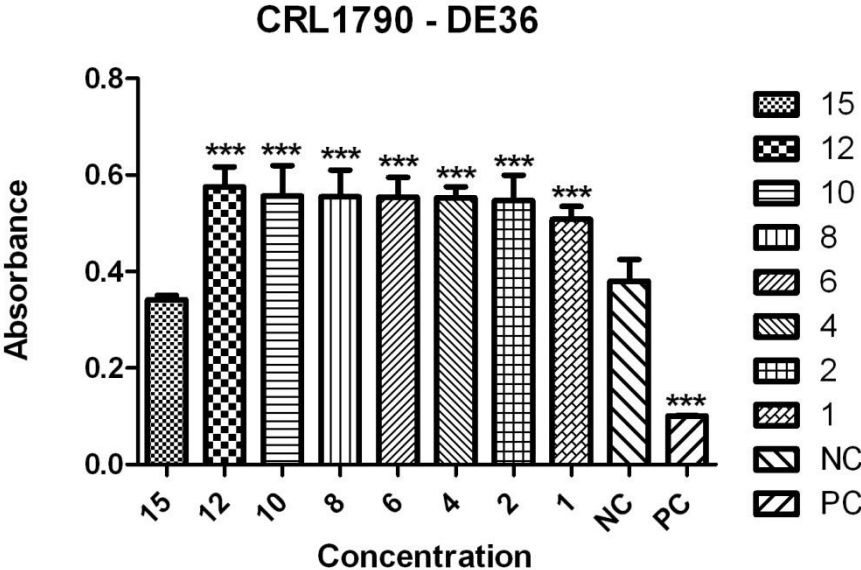


Figure 6.9: Absorbance - Concentration Graphic of CRL1790 cell line -DE36.

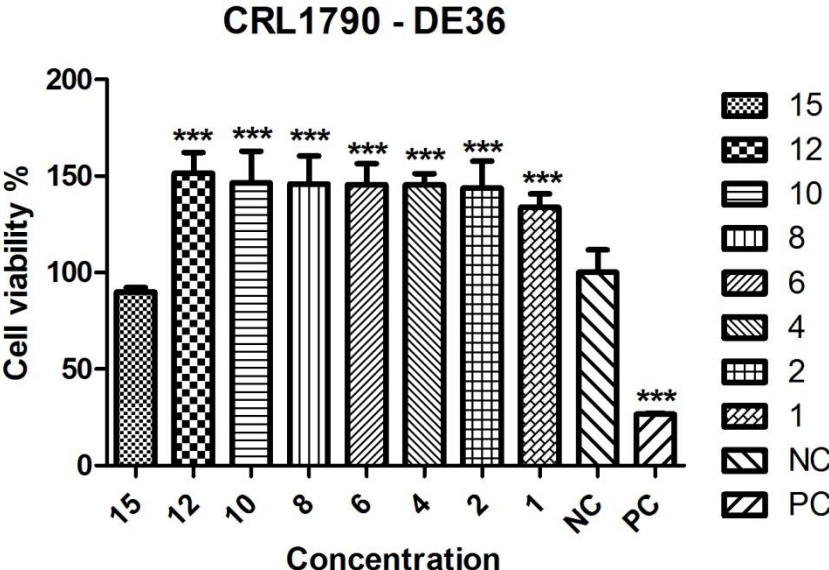


Figure 6.10 : Cell viability - Concentration Graphic of CRL1790 cell line -DE36.

The optimum concentration for DE47 bacterial protein on CRL1790 cell line was determined as 15 μg in MTS assay. Graphs were given in Figure 6.11 and Figure 6.12.

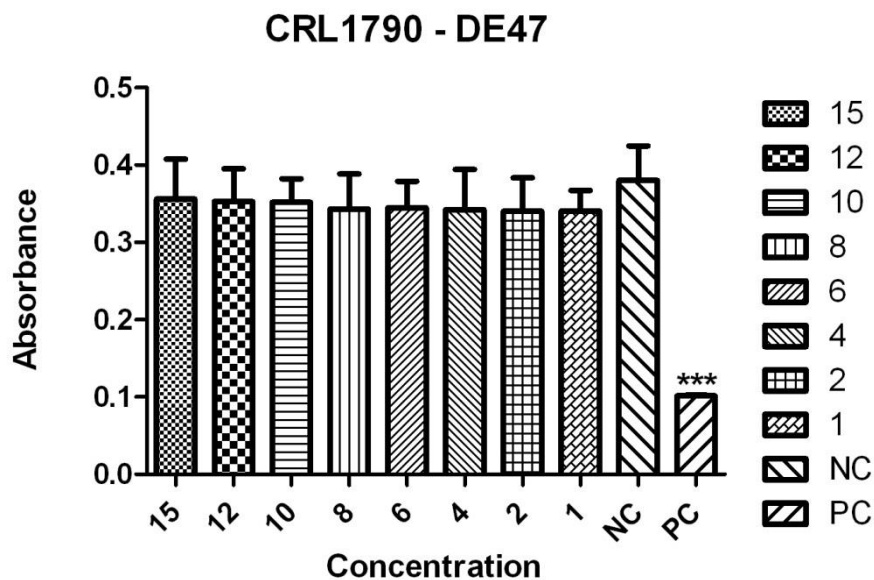


Figure 6.11: Absorbance - Concentration Graphic of CRL1790 cell line -DE47.

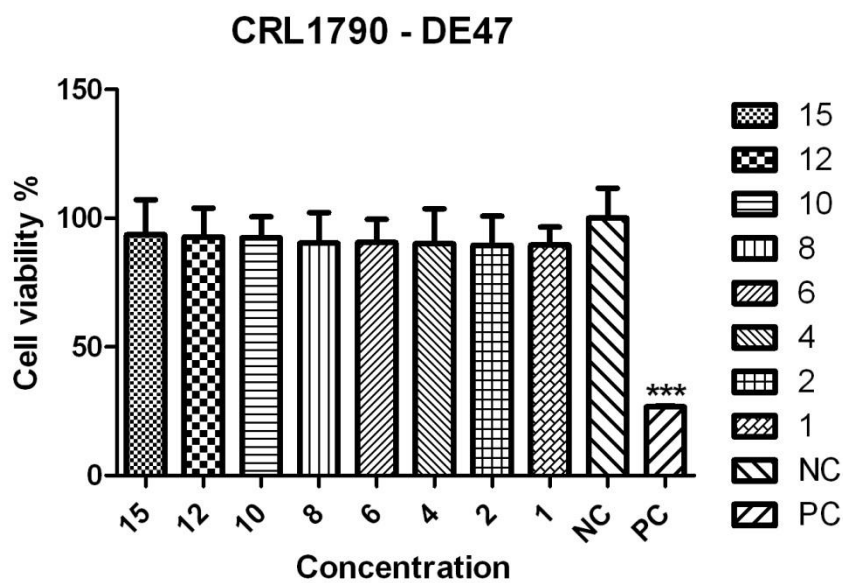


Figure 6.12 : Cell viability - Concentration Graphic of CRL1790 cell line -DE47.

The optimum concentration for DE103 bacterial protein on CRL1790 cell line was determined as 12 µg in MTS assay. Graphs were given in Figure 6.13 and Figure 6.14.

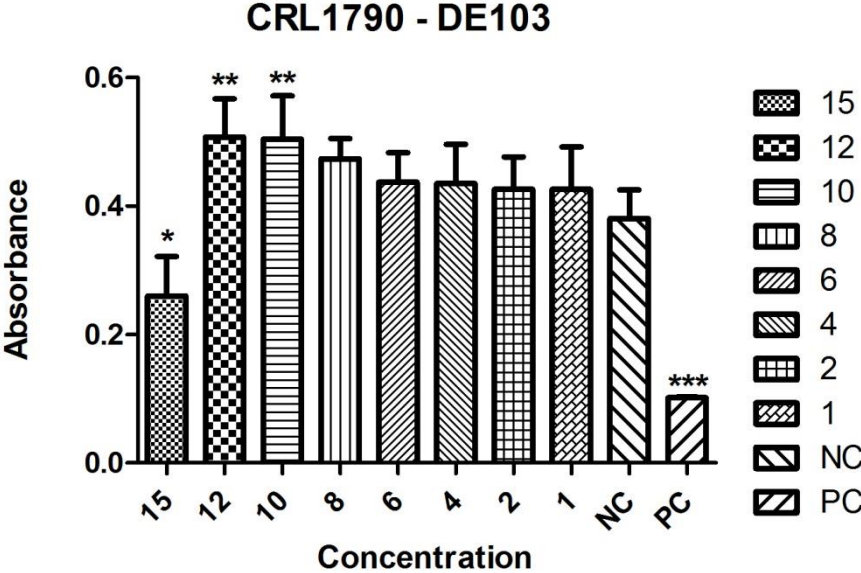


Figure 6.13: Absorbance - Concentration Graphic of CRL1790 cell line -DE103.

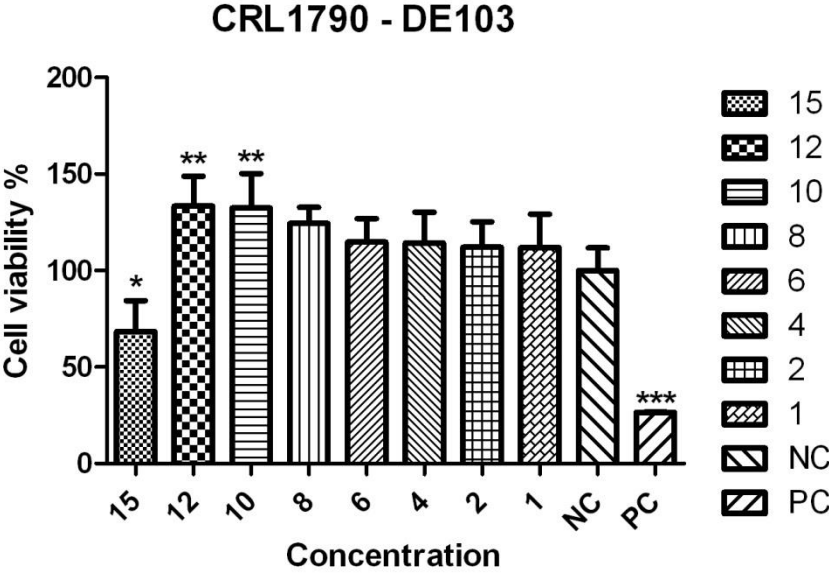


Figure 6.14 : Cell viability - Concentration Graphic of CRL1790 cell line -DE103.

The optimum concentration for DE129 bacterial protein on CRL1790 cell line was determined as 12 μg in MTS assay. Graphs were given in Figure 6.15 and Figure 6.16.

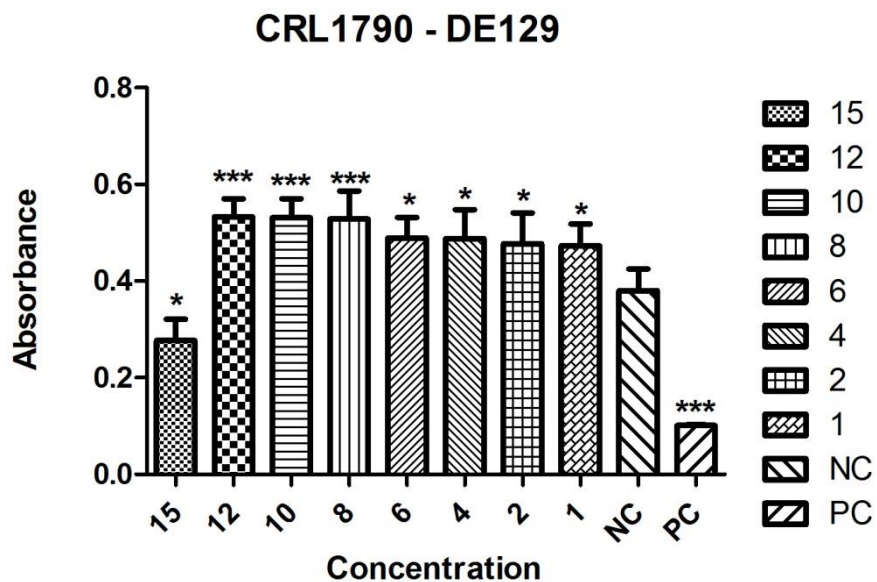


Figure 6.15: Absorbance - Concentration Graphic of CRL1790 cell line -DE129.

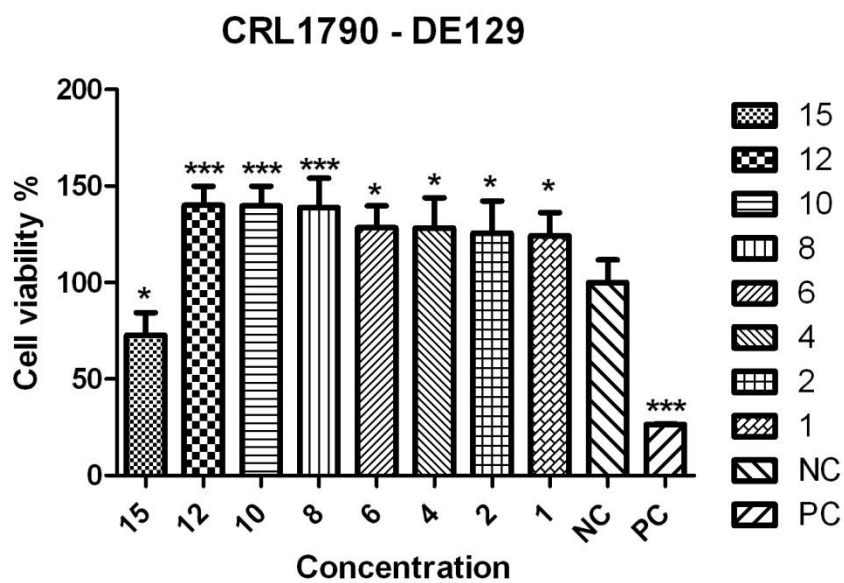


Figure 6.16 : Cell viability - Concentration Graphic of CRL1790 cell line -DE129.

The optimum concentration for DE256 bacterial protein on CRL1790 cell line was determined as 12 µg in MTS assay. Graphs were given in Figure 6.17 and Figure 6.18.

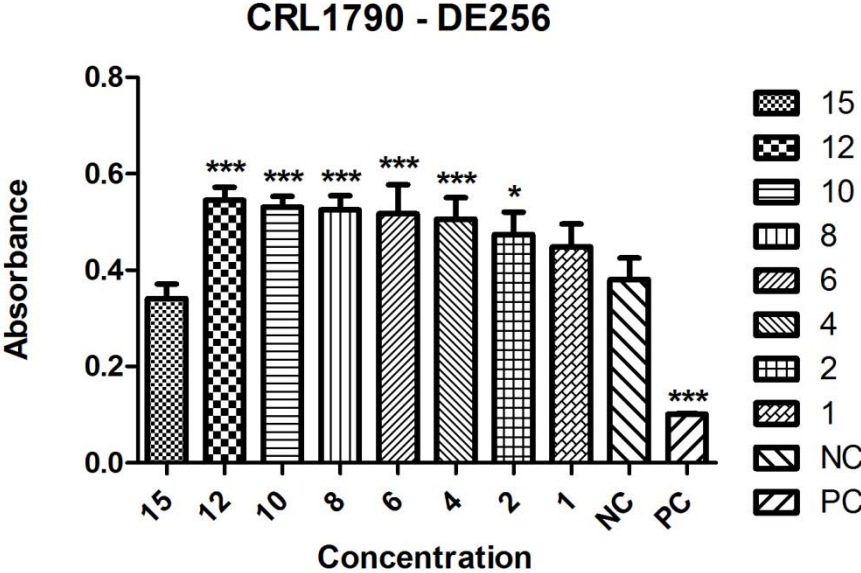


Figure 6.17: Absorbance - Concentration Graphic of CRL1790 cell line -DE256.

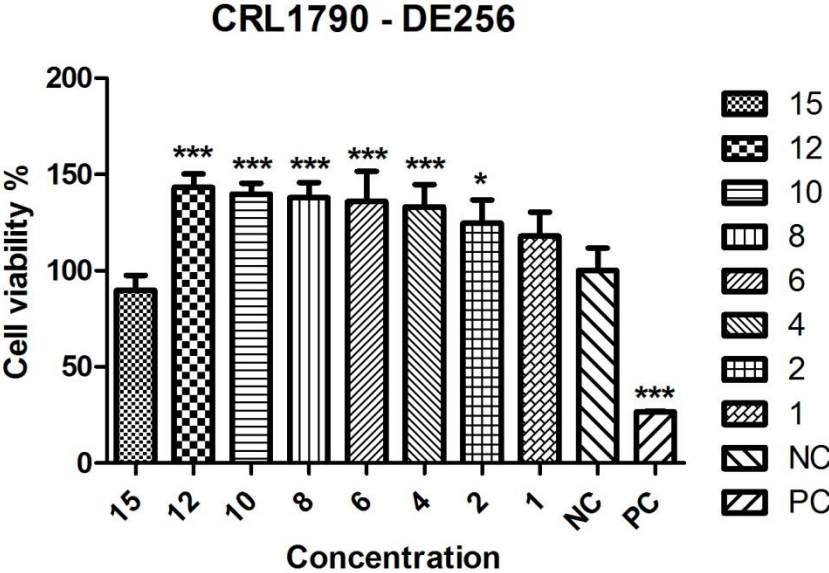


Figure 6.18 : Cell viability - Concentration Graphic of CRL1790 cell line -DE256.

The optimum concentration for DE365 bacterial protein on CRL1790 cell line was determined as 12 μg in MTS assay. Graphs were given in Figure 6.19 and Figure 6.20.

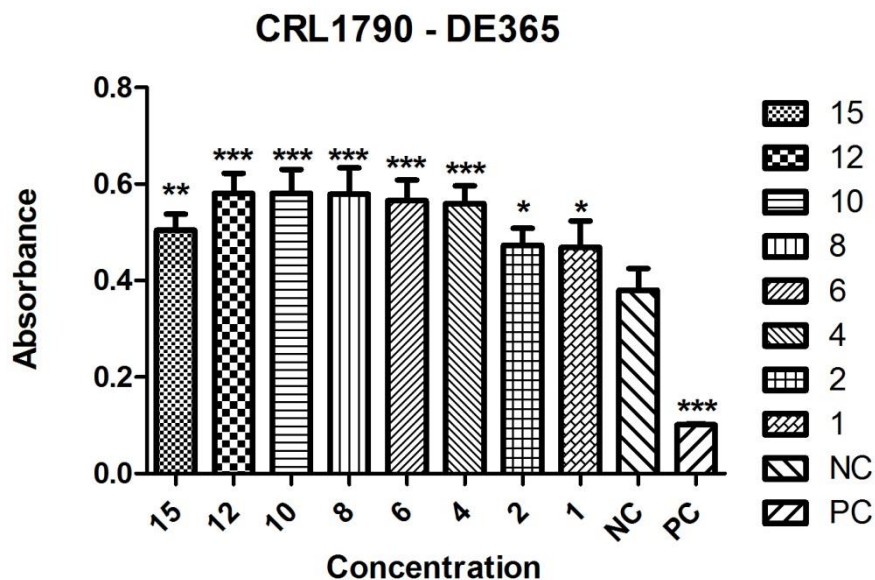


Figure 6.19: Absorbance - Concentration Graphic of CRL1790 cell line -DE365.

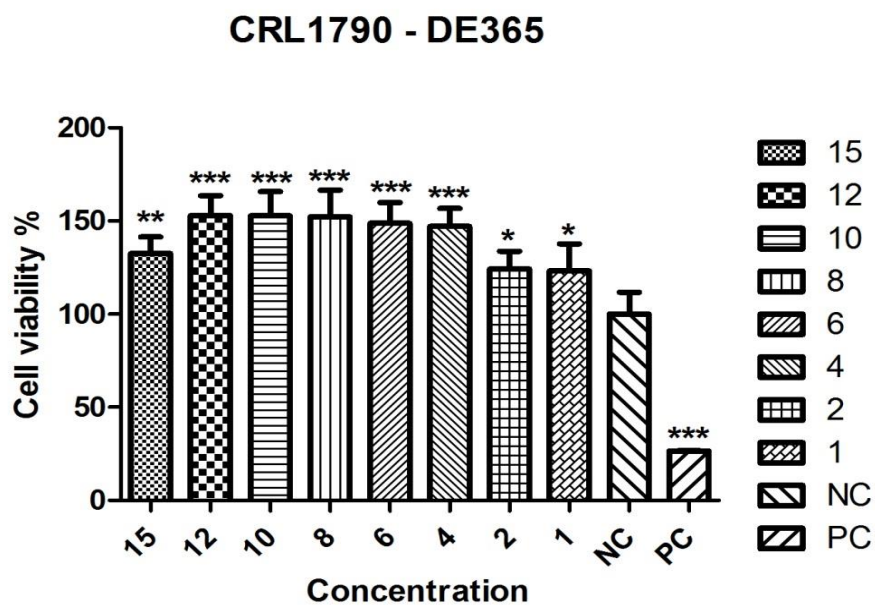


Figure 6.20 : Cell viability - Concentration Graphic of CRL1790 cell line -DE365.

The optimum concentration for huc2 bacterial protein on CRL1790 cell line was determined as 6 µg in MTS assay. Graphs were given in Figure 6.21 and Figure 6.22.

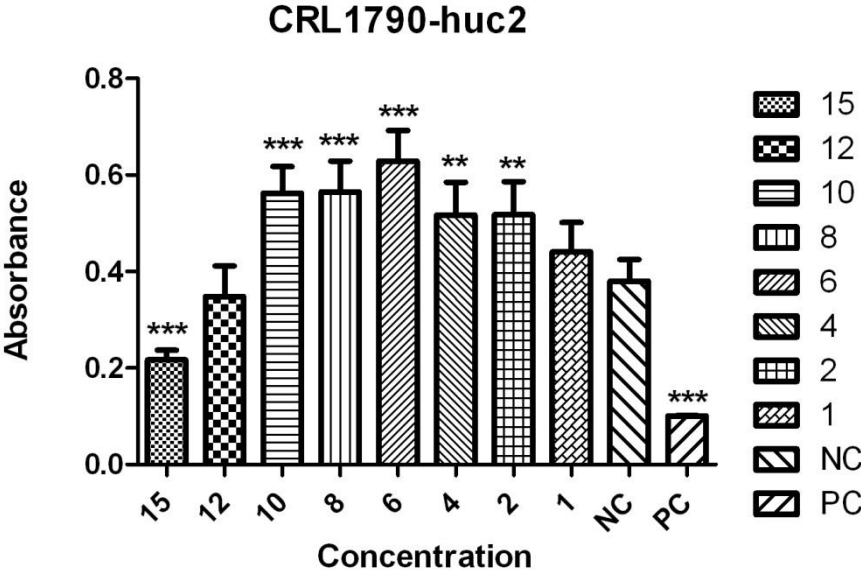


Figure 6.21: Absorbance - Concentration Graphic of CRL1790 cell line -huc2.

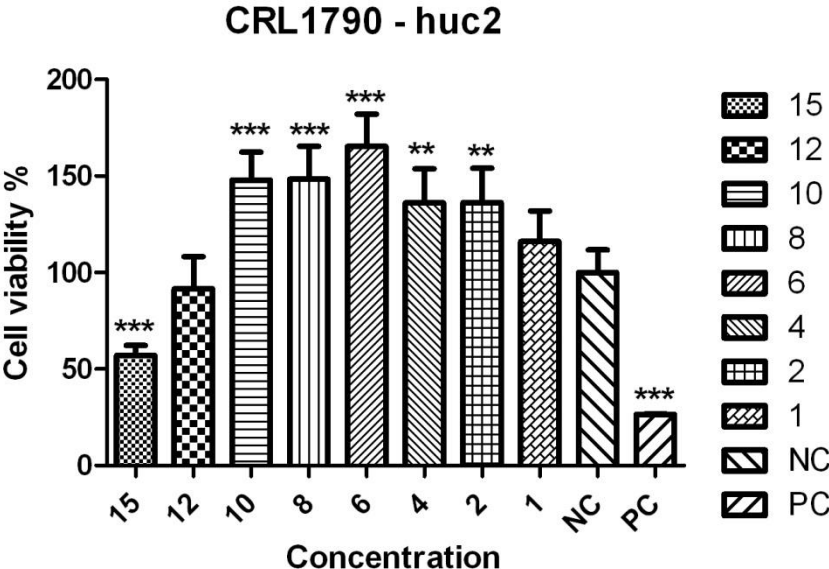


Figure 6.22 : Cell viability - Concentration Graphic of CRL1790 cell line -huc2.

The optimum concentration for HIA bacterial protein on CRL1790 cell line was determined as 2 μ g in MTS assay. Graphs were given in Figure 6.23 and Figure 6.24.

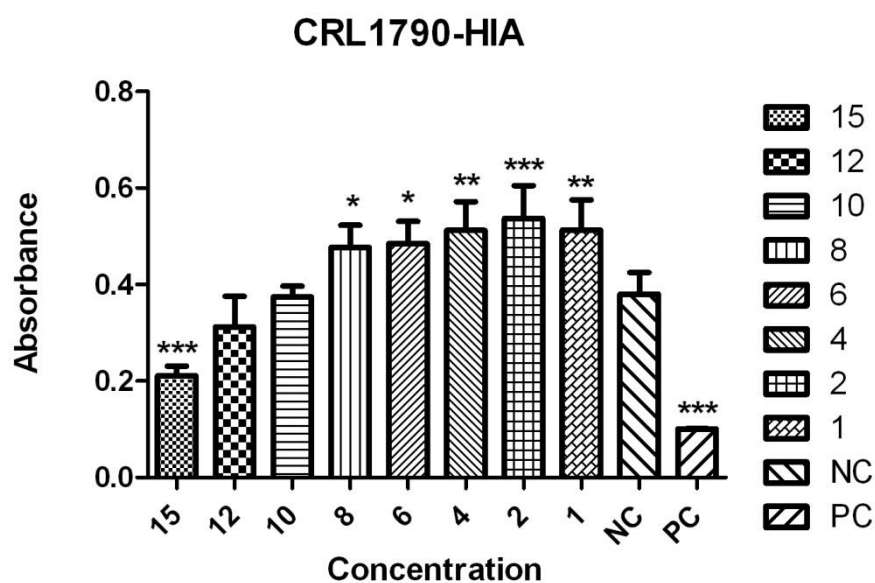


Figure 6.23: Absorbance - Concentration Graphic of CRL1790 cell line -HIA.

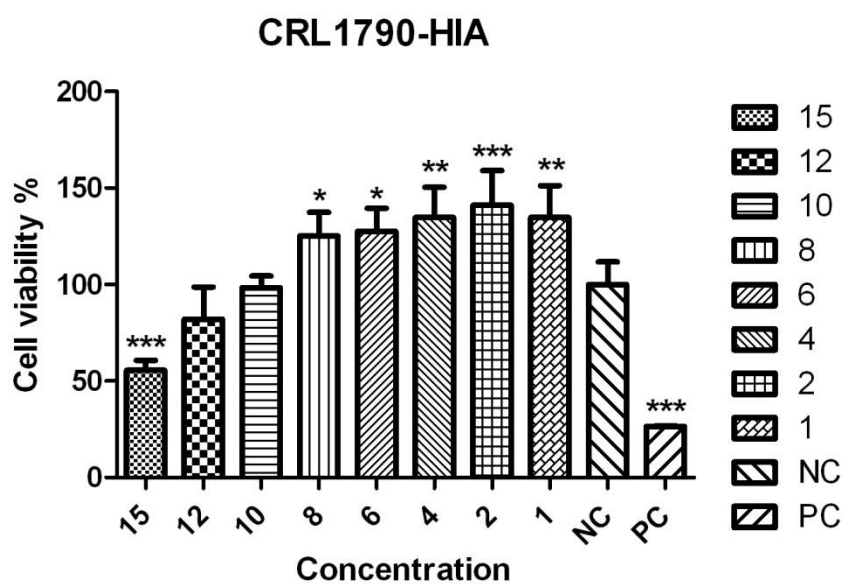


Figure 6.24 : Cell viability - Concentration Graphic of CRL1790 cell line -HIA.

The optimum concentration for DE51 bacterial protein on CRL1790 cell line was determined as 12 µg in MTS assay. Graphs were given in Figure 6.25 and Figure 6.26.

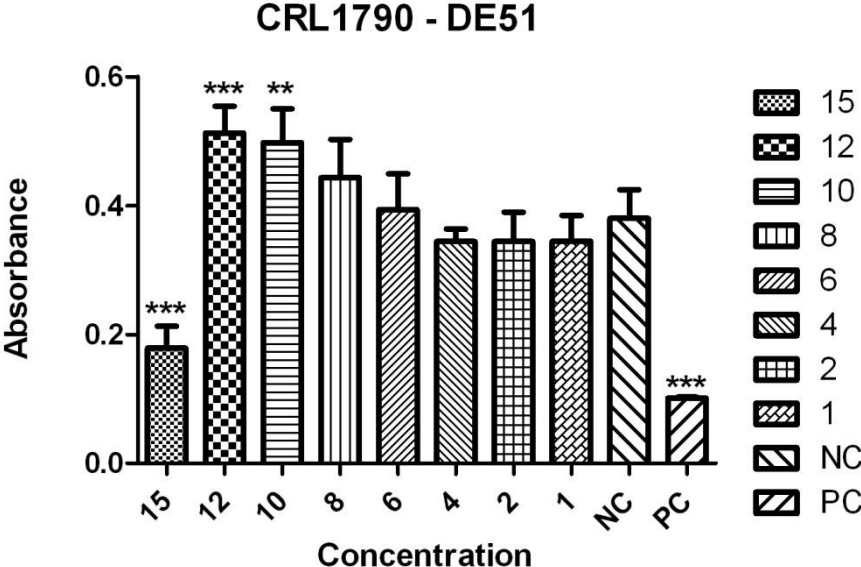


Figure 6.25: Absorbance - Concentration Graphic of CRL1790 cell line -DE51.

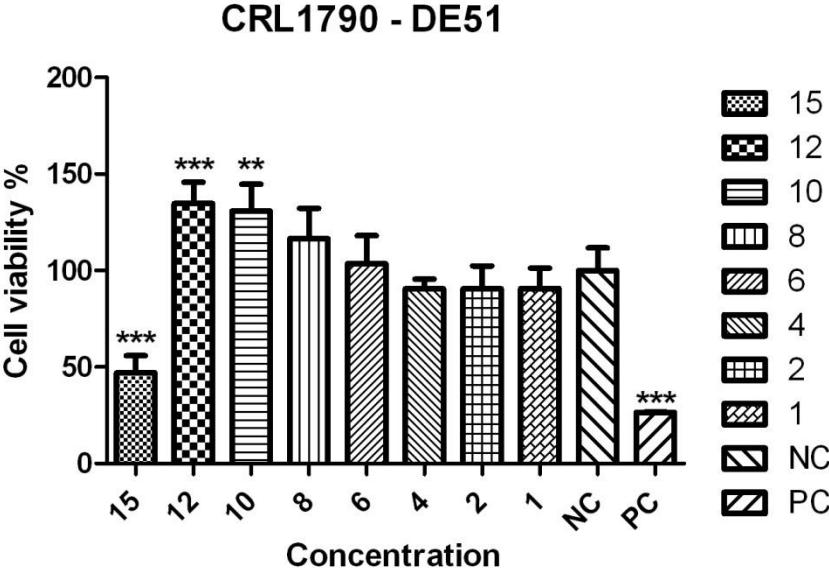


Figure 6.26 : Cell viability - Concentration Graphic of CRL1790 cell line -DE51.

The optimum concentration for 3h bacterial protein on NCM460 cell line was determined as 10 μg in MTS assay. Graphs were given in Figure 6.27 and Figure 6.28.

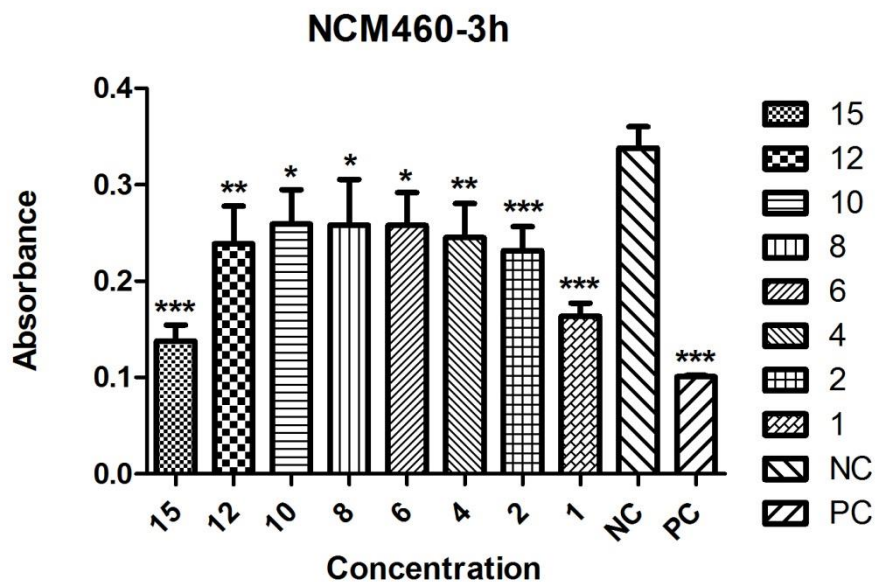


Figure 6.27: Absorbance - Concentration Graphic of NCM460 cell line -3h.

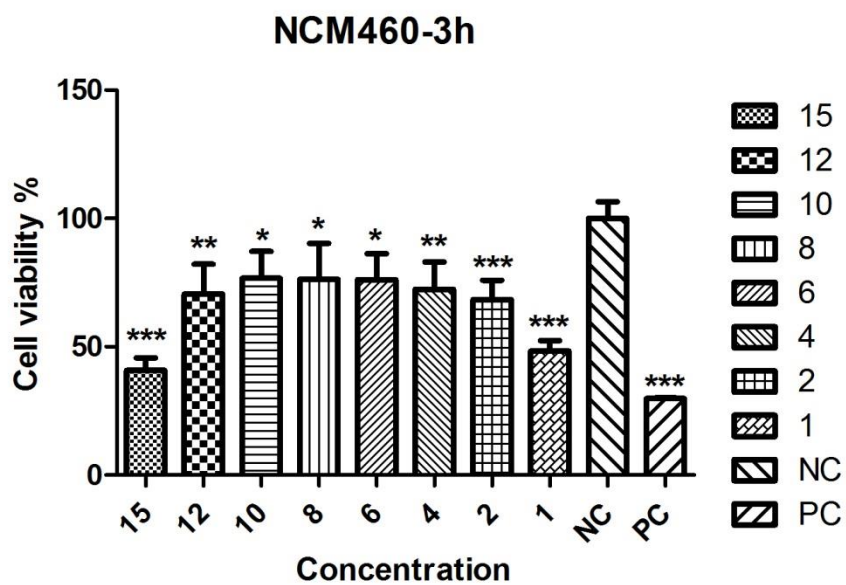


Figure 6.28 : Cell viability - Concentration Graphic of NCM460 cell line -3h.

The optimum concentration for DB7Y bacterial protein on NCM460 cell line was determined as 4 µg in MTS assay. Graphs were given in Figure 6.29 and Figure 6.30.

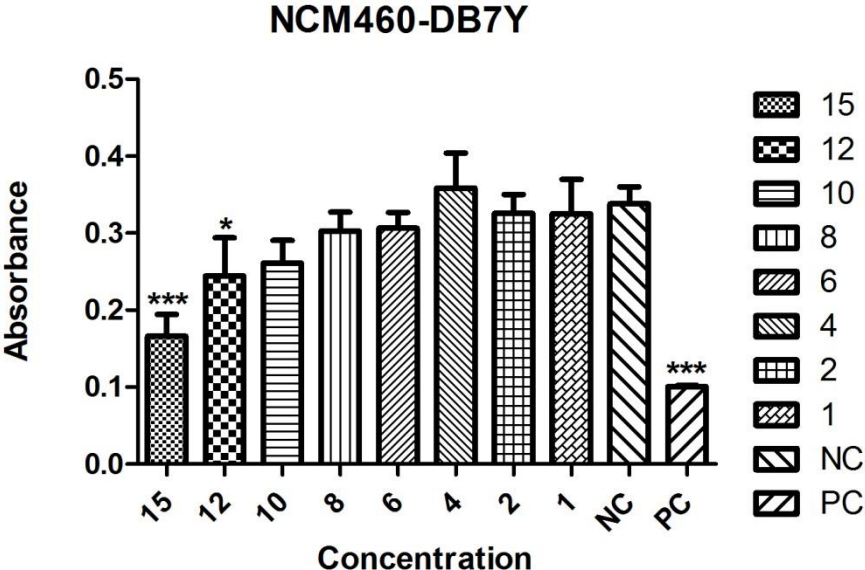


Figure 6.29: Absorbance - Concentration Graphic of NCM460 cell line -DB7Y.

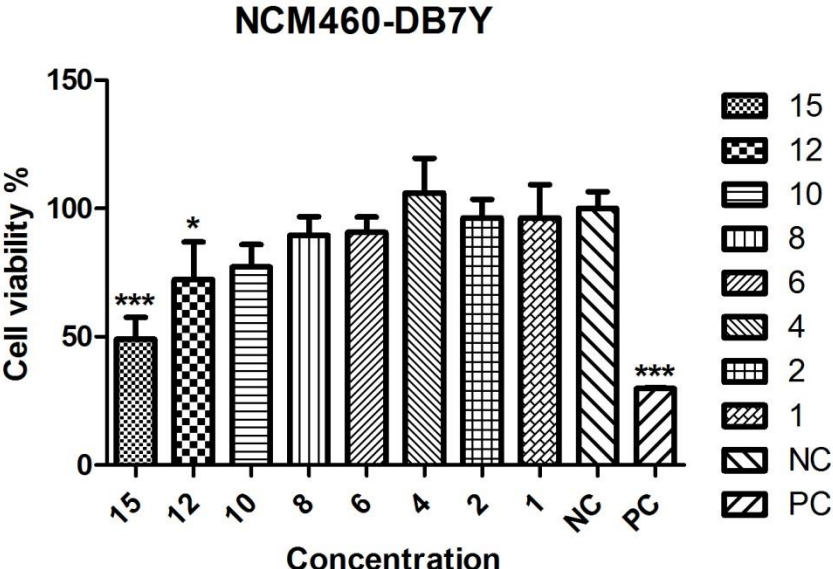


Figure 6.30 : Cell viability - Concentration Graphic of NCM460 cell line -DB7Y.

The optimum concentration for DE8 bacterial protein on NCM460 cell line was determined as 12 μ g in MTS assay. Graphs were given in Figure 6.31 and Figure 6.32.

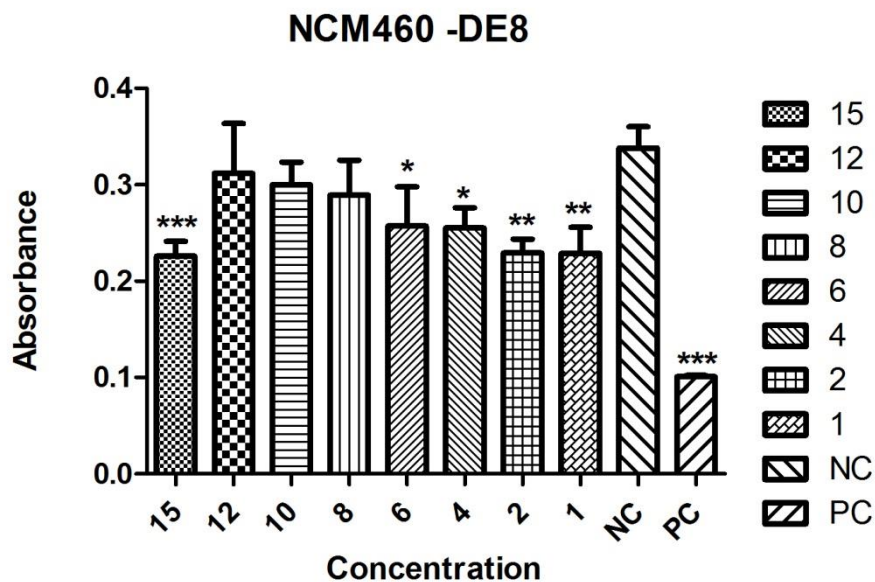


Figure 6.31: Absorbance - Concentration Graphic of NCM460 cell line -DE8.

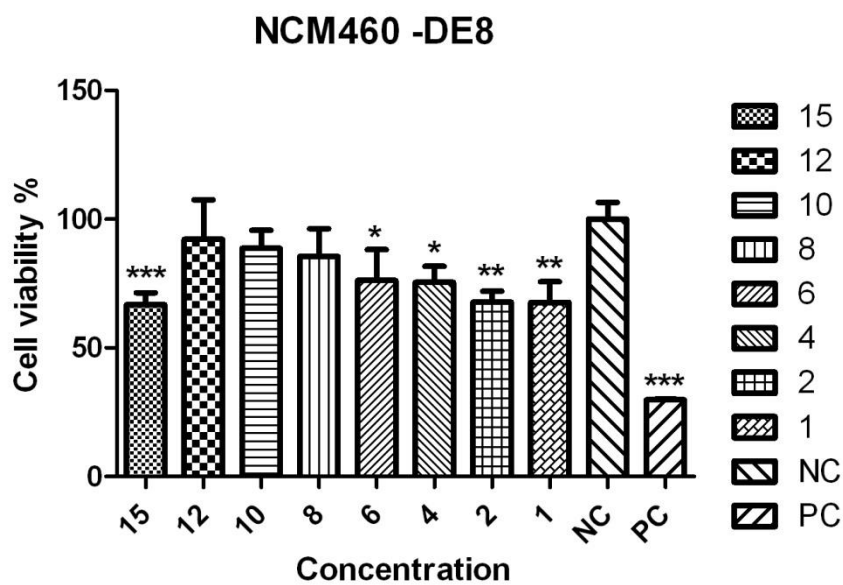


Figure 6.32: Cell viability - Concentration Graphic of NCM460 cell line -DE8.

The optimum concentration for DE12 bacterial protein on NCM460 cell line was determined as 8 µg in MTS assay. Graphs were given in Figure 6.33 and Figure 6.34.

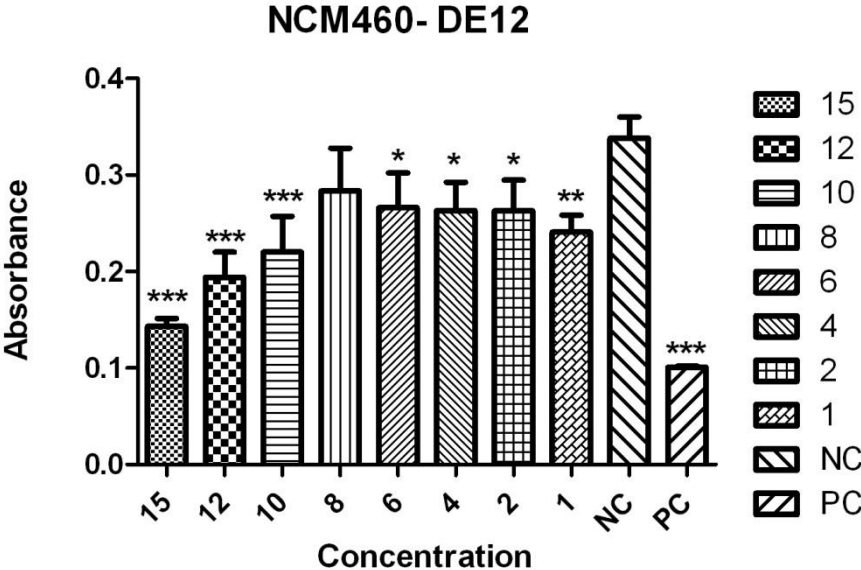


Figure 6.33: Absorbance - Concentration Graphic of NCM460 cell line -DE12.

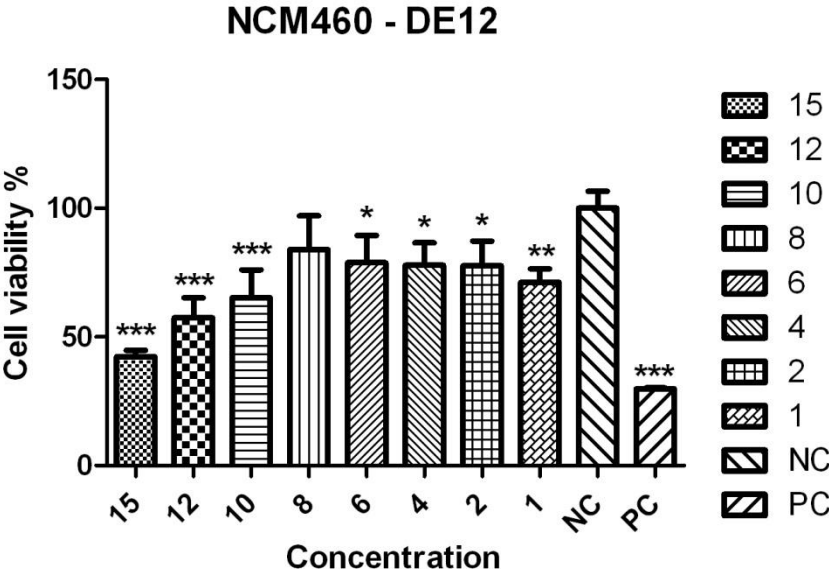


Figure 6.34 : Cell viability - Concentration Graphic of NCM460 cell line -DE12.

The optimum concentration for DE36 bacterial protein on NCM460 cell line was determined as 8 μ g in MTS assay. Graphs were given in Figure 6.35 and Figure 6.36.

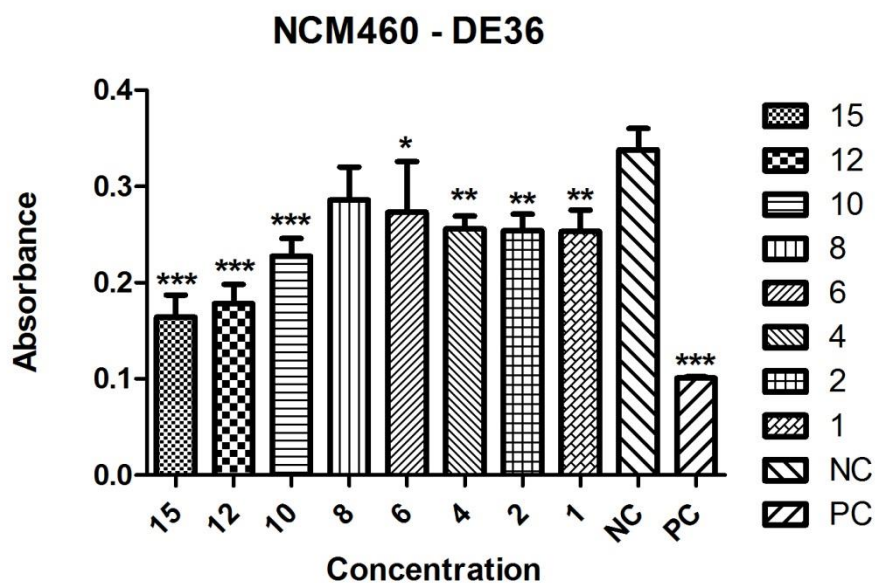


Figure 6.35: Absorbance - Concentration Graphic of NCM460 cell line -DE36.

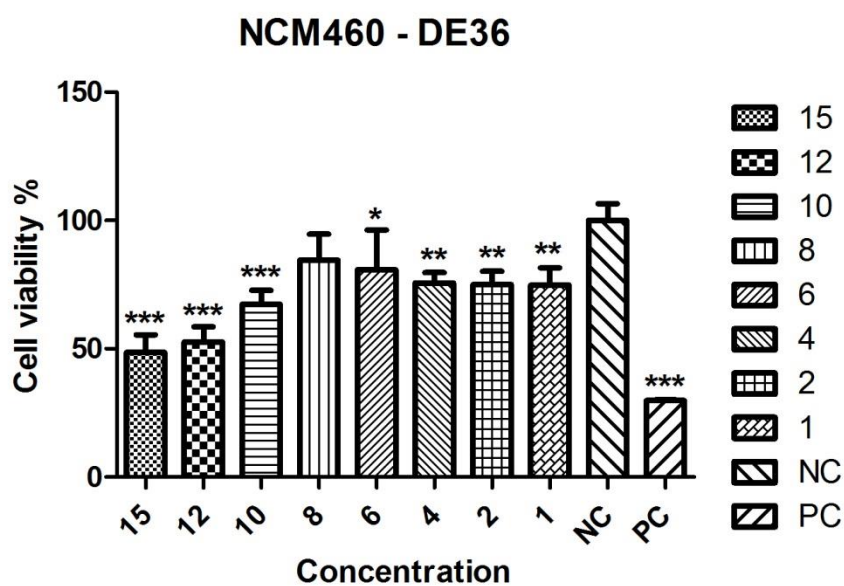


Figure 6.36 : Cell viability - Concentration Graphic of NCM460 cell line -DE36.

The optimum concentration for DE47 bacterial protein on NCM460 cell line was determined as 4 µg in MTS assay. Graphs were given in Figure 6.37 and Figure 6.38.

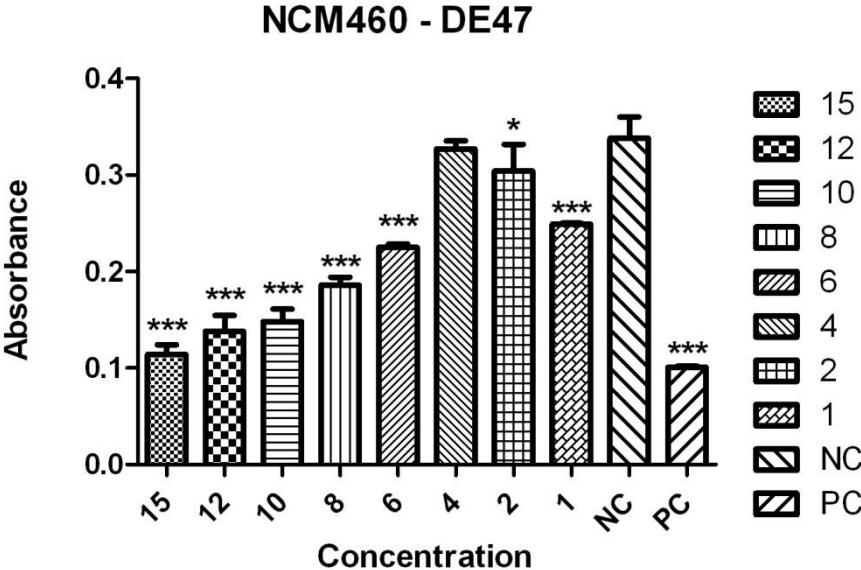


Figure 6.37: Absorbance - Concentration Graphic of NCM460 cell line -DE47.

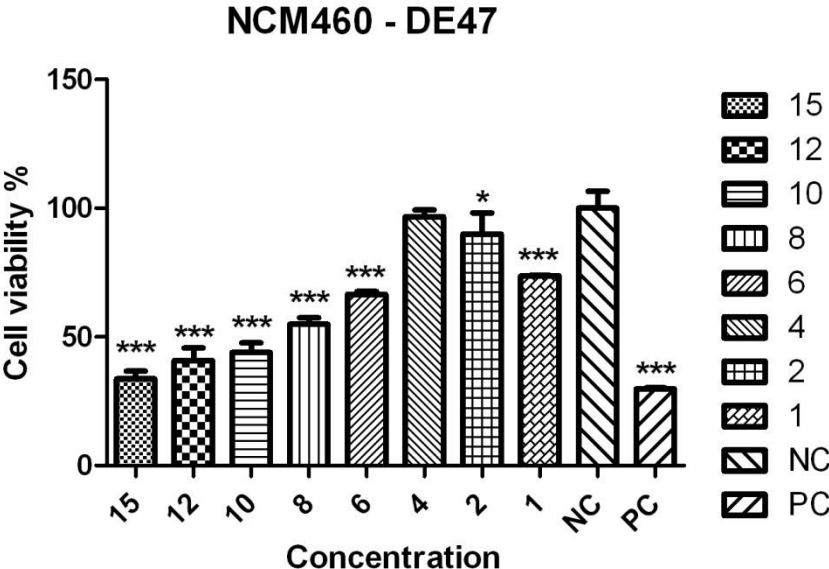


Figure 6.38 : Cell viability - Concentration Graphic of NCM460 cell line -DE47.

The optimum concentration for DE103 bacterial protein on NCM460 cell line was determined as 10 μg in MTS assay. Graphs were given in Figure 6.39 and Figure 6.40.

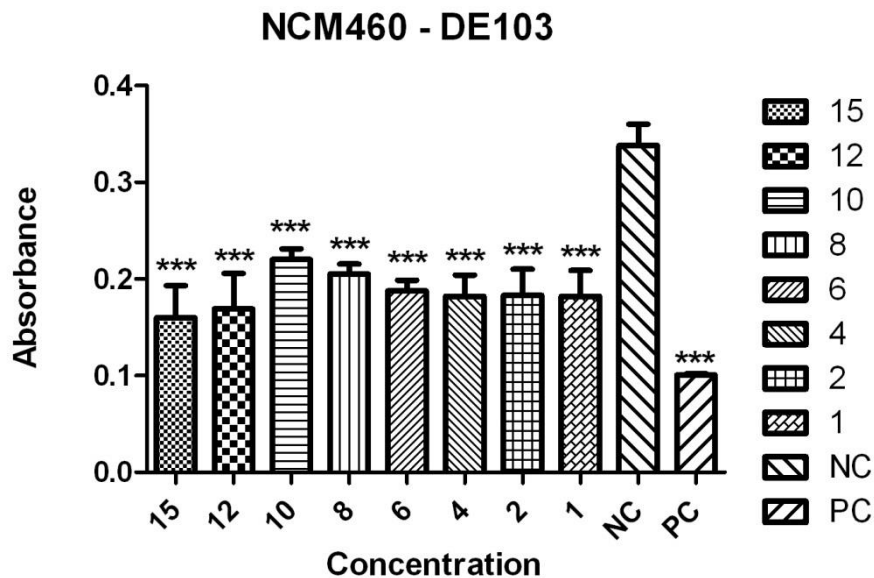


Figure 6.39: Absorbance - Concentration Graphic of NCM460 cell line -DE103.

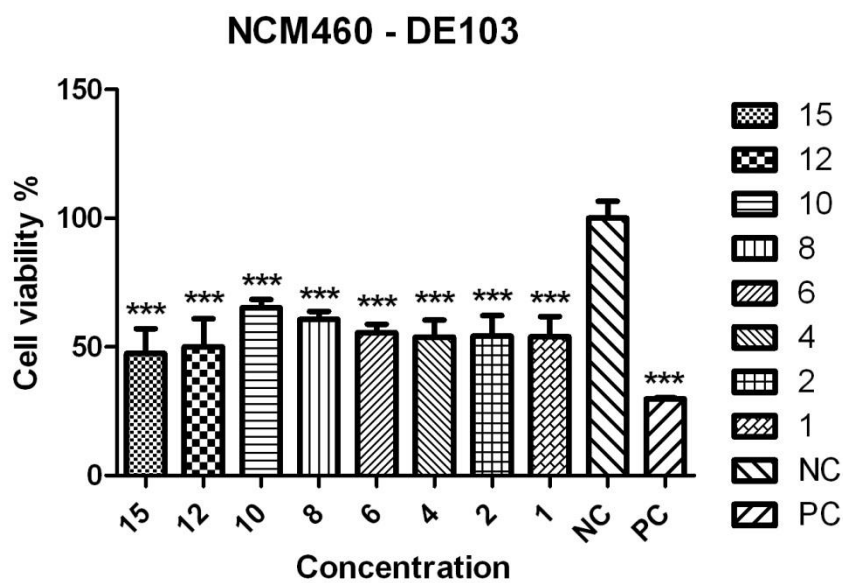


Figure 6.40 : Cell viability - Concentration Graphic of NCM460 cell line -DE103.

The optimum concentration for DE129 bacterial protein on NCM460 cell line was determined as 8 µg in MTS assay. Graphs were given in Figure 6.41 and Figure 6.42.

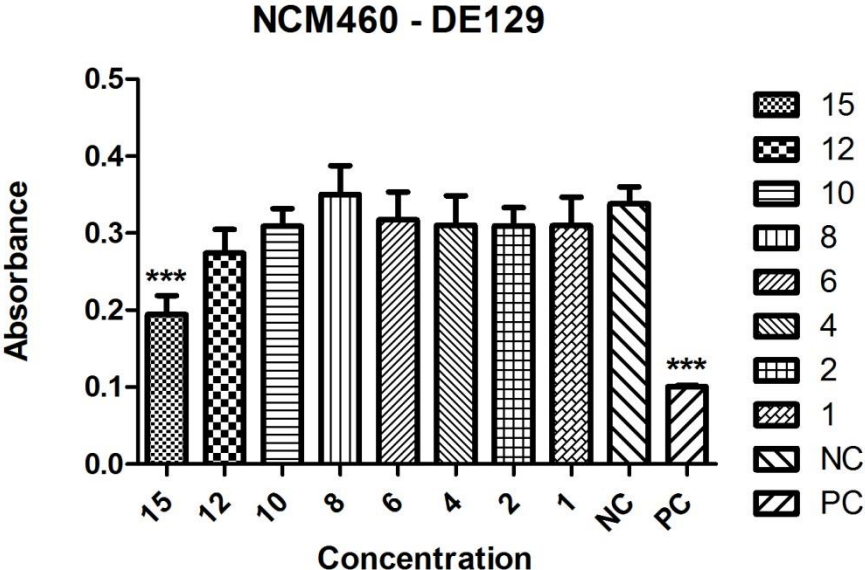


Figure 6.41: Absorbance - Concentration Graphic of NCM460 cell line -DE129.

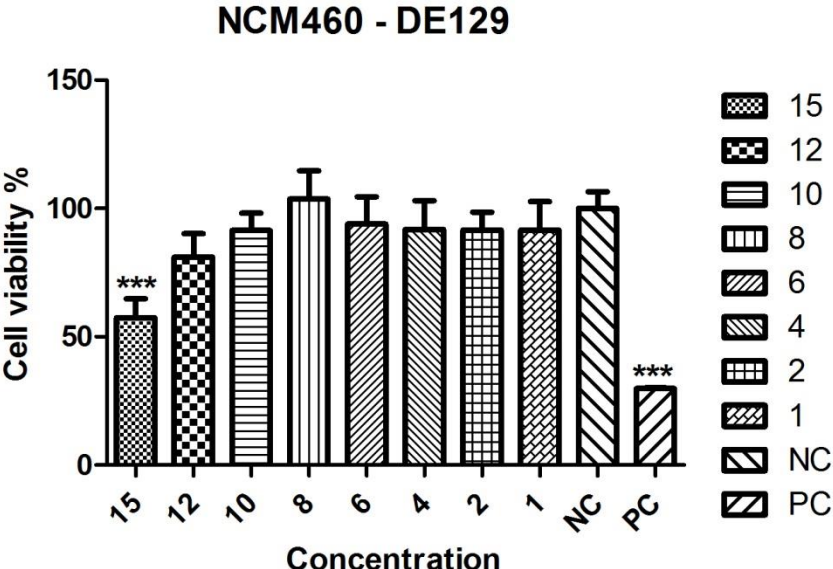


Figure 6.42 : Cell viability - Concentration Graphic of NCM460 cell line -DE129.

The optimum concentration for DE256 bacterial protein on NCM460 cell line was determined as 10 µg in MTS assay. Graphs were given in Figure 6.43 and Figure 6.44.

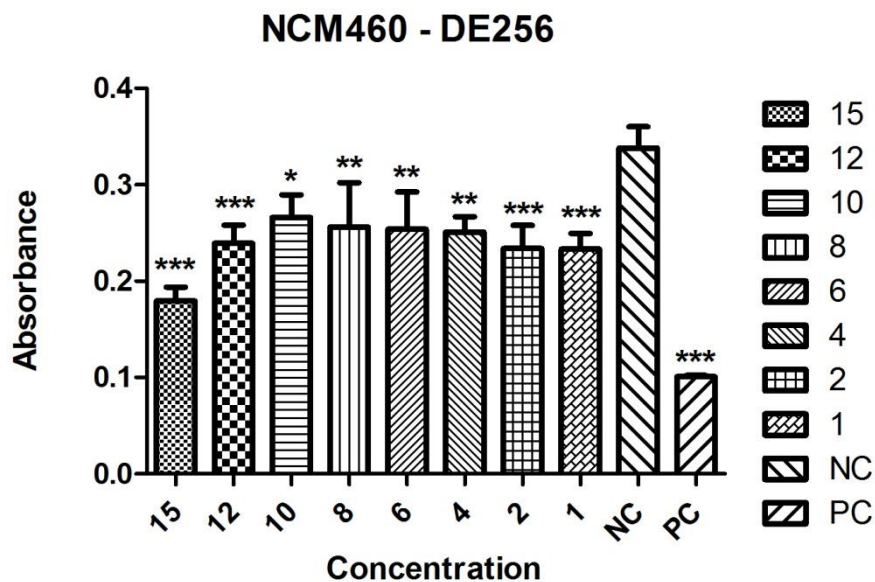


Figure 6.43: Absorbance - Concentration Graphic of NCM460 cell line -DE256.

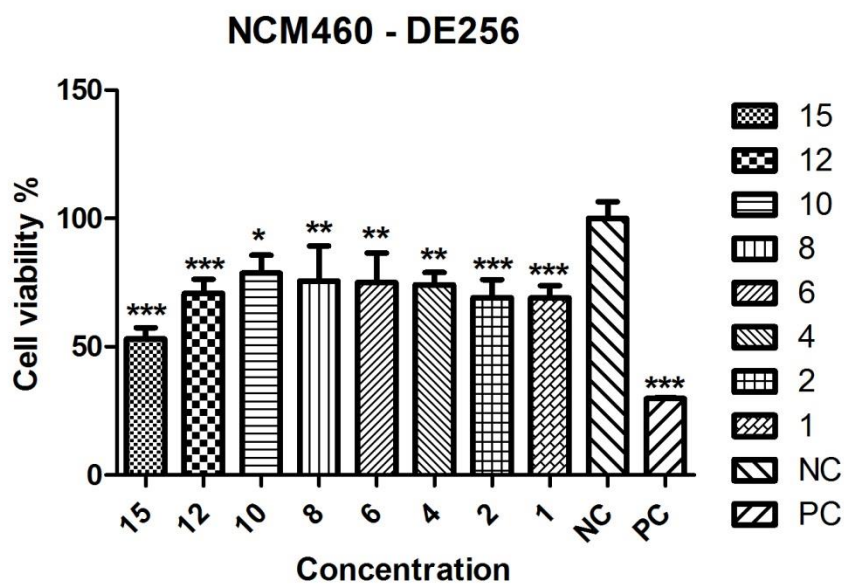


Figure 6.44 : Cell viability - Concentration Graphic of NCM460 cell line -DE256.

The optimum concentration for DE365 bacterial protein on NCM460 cell line was determined as 15 µg in MTS assay. Graphs were given in Figure 6.45 and Figure 6.46.

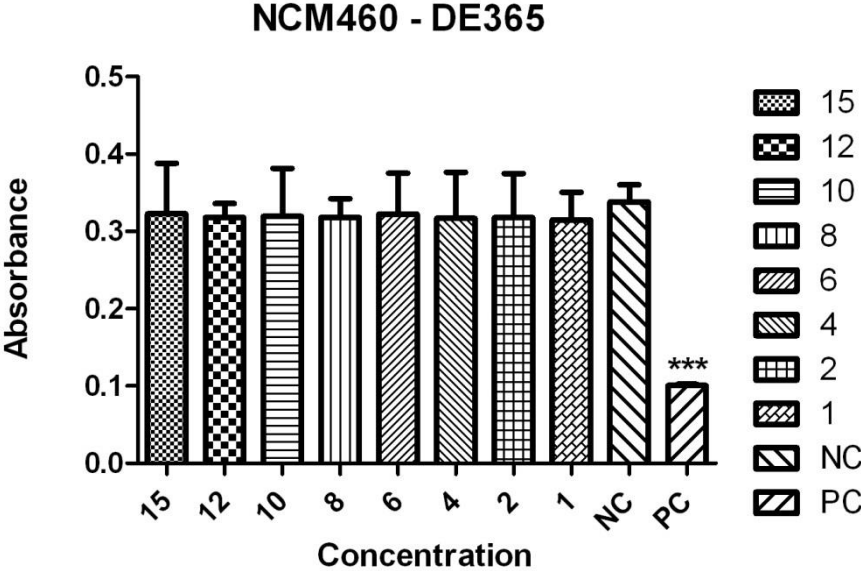


Figure 6.45: Absorbance - Concentration Graphic of NCM460 cell line -DE365.

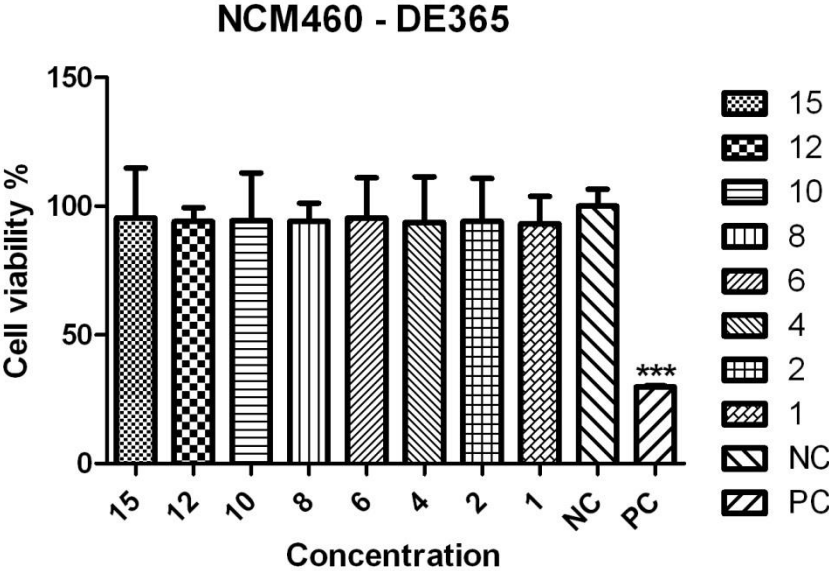


Figure 6.46 : Cell viability - Concentration Graphic of NCM460 cell line -DE365.

The optimum concentration for huc2 bacterial protein on NCM460 cell line was determined as 10 μ g in MTS assay. Graphs were given in Figure 6.47 and Figure 6.48.

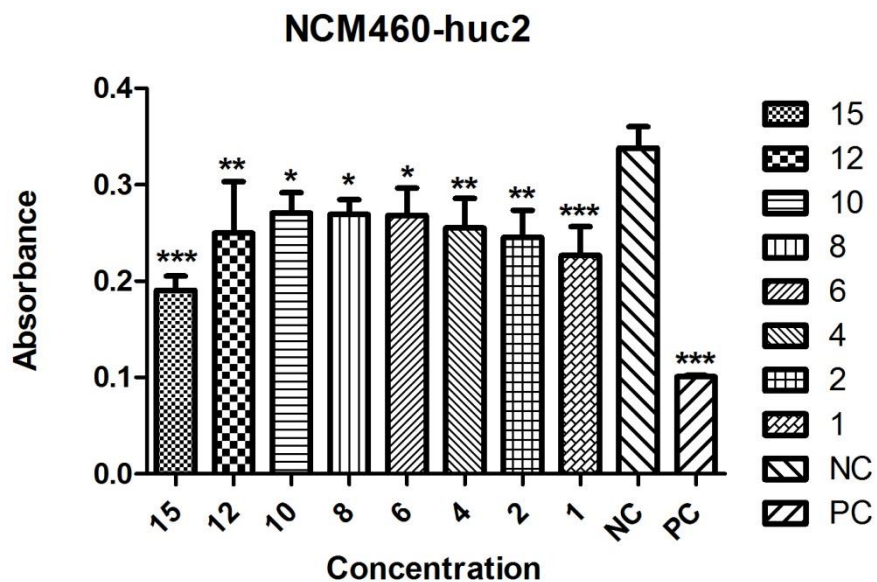


Figure 6.47: Absorbance - Concentration Graphic of NCM460 cell line -huc2.

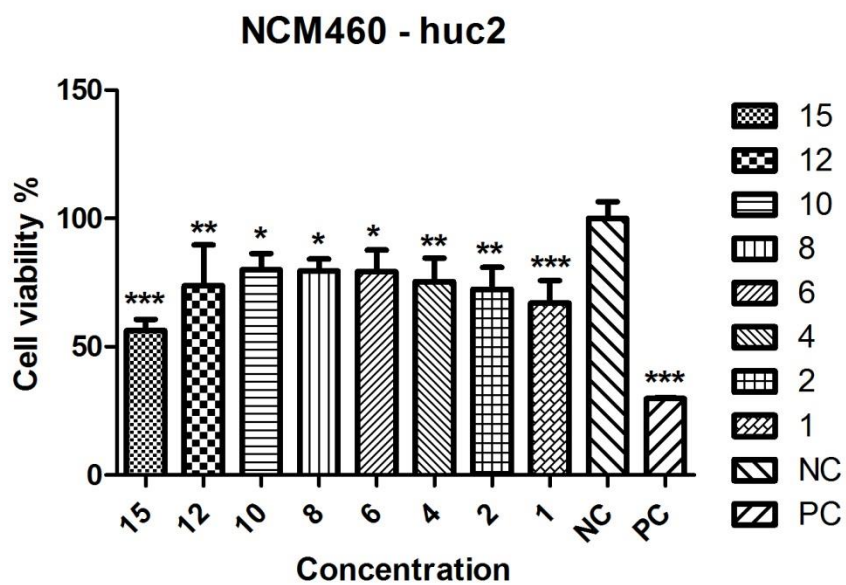


Figure 6.48 : Cell viability - Concentration Graphic of NCM460 cell line -huc2.

The optimum concentration for HIA bacterial protein on NCM460 cell line was determined as 6 µg in MTS assay. Graphs were given in Figure 6.49 and Figure 6.50.

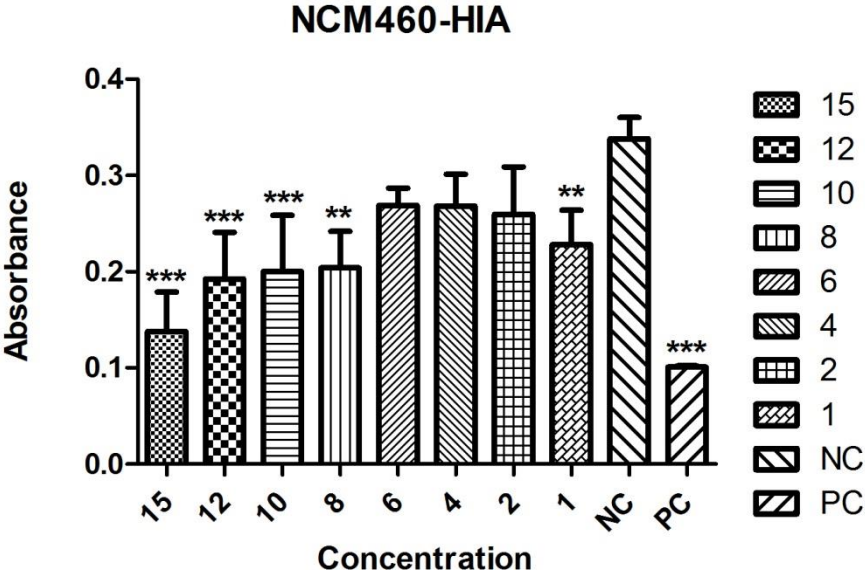


Figure 6.49: Absorbance - Concentration Graphic of NCM460 cell line -HIA.

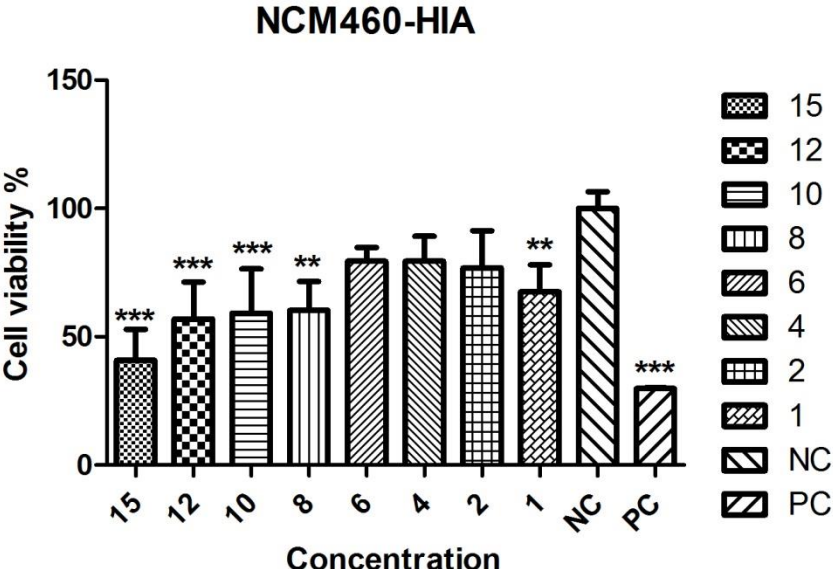


Figure 6.50 : Cell viability - Concentration Graphic of NCM460 cell line -HIA.

The optimum concentration for DE51 bacterial protein on NCM460 cell line was determined as 4 μ g in MTS assay. Graphs were given in Figure 6.51 and Figure 6.52.

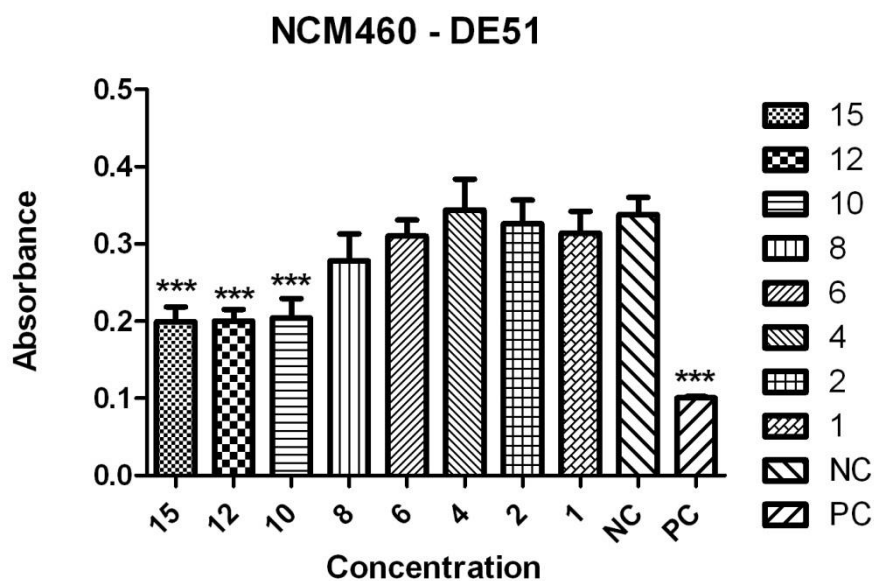


Figure 6.51: Absorbance - Concentration Graphic of NCM460 cell line -DE51.

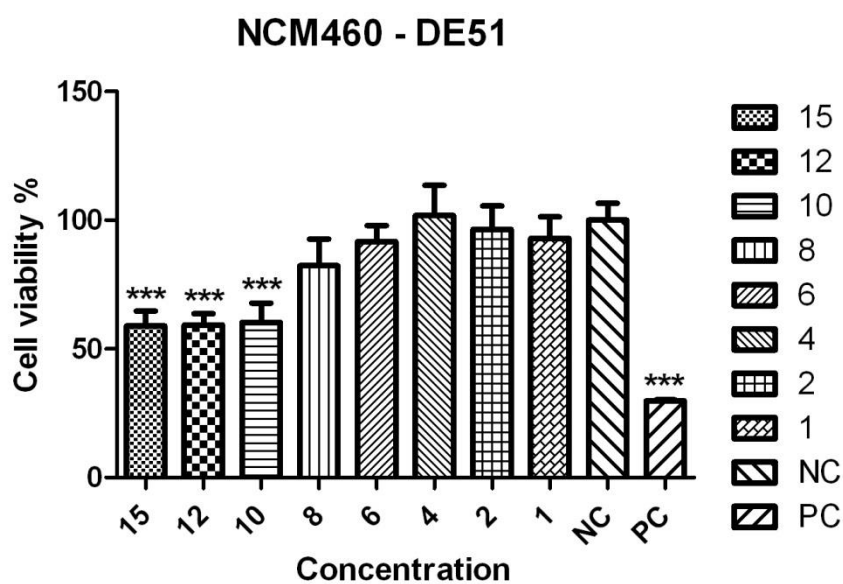


Figure 6.52 : Cell viability - Concentration Graphic of NCM460 cell line -DE51.

Cell Proliferation Examination Result (2):

The samples such as DB7Y, DE129, DE47 and DE51 had the highest cell viability and proliferation in NCM 460 cell lines, which were near to the level of negative control. At optimum concentrations the cell viability % of the samples were found at the level of negative control.

3.4 Apoptosis and Cell Viability Assay Results

The presence of apoptosis was detected by annexin V in the present study. During the evaluation, in Flow cytometry reports, in quadrants the lower left side represents the viable cells which are Annexin V negative and pi negative whereas the upper left side represents the dead cells which are Annexin V negative but pi positive. Upper right side shows the late apoptotic cells or sometimes dead cells which are both Annexin V positive and pi positive. Finally the lower right side shows the early apoptotic cells that are Annexin V positive but pi negative. The results of the apoptosis test were summarized in Table 2.1. Flow cytometry reports of the samples that decreased the apoptosis were given below. Reports of the other samples were shown in Appendix part.

From the Figure 7.1, Annexin in CRL1790 before application was determined as 10.55. In Figures 7.2, 7.3 and 7.4, it was shown that Annexin measurement was, 7.12, 4.37 and 6.56 after DE365, DE8 and HIA application, respectively .

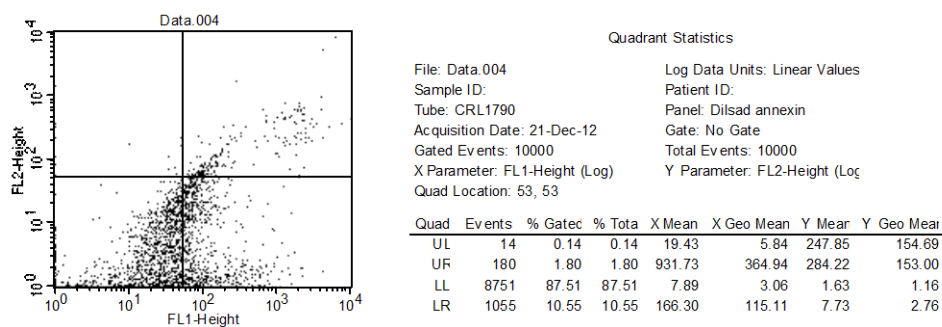
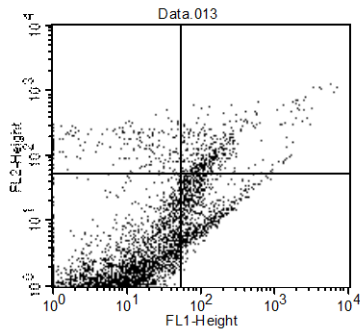


Figure 7.1: Detection of Apoptosis by Annexin in CRL1790 before bacterial protein application.



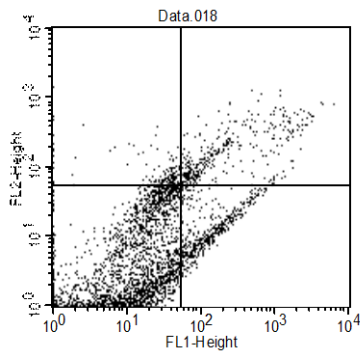
Quadrant Statistics

File: Data.013
Sample ID:
Tube: CRL1790 de365
Acquisition Date: 21-Dec-12
Gated Events: 10000
X Parameter: FL1-Height (Log)
Quad Location: 53, 53

Log Data Units: Linear Values
Patient ID:
Panel: Dilsad annexin
Gate: No Gate
Total Events: 10000
Y Parameter: FL2-Height (Log)

Quad	Events	% Gated	% Tot	X Mean	X Geo Mean	Y Mean	Y Geo Mean
UL	192	1.92	1.92	17.57	9.18	167.89	148.85
UF	396	3.96	3.96	393.91	181.56	180.35	132.62
LL	8700	87.00	87.00	5.96	2.54	1.87	1.27
LR	712	7.12	7.12	112.93	94.60	19.83	15.21

Figure 7.2: Detection of Apoptosis by Annexin in CRL1790 after DE365 protein application.



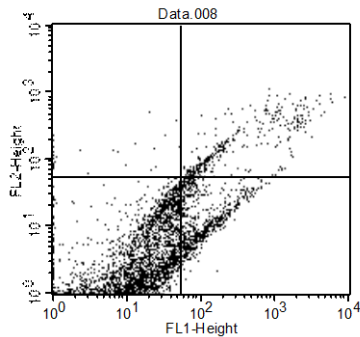
Quadrant Statistics

File: Data.018
Sample ID:
Tube: CRL1790 de8
Acquisition Date: 21-Dec-12
Gated Events: 10000
X Parameter: FL1-Height (Log)
Quad Location: 53, 53

Log Data Units: Linear Values
Patient ID:
Panel: Dilsad annexin
Gate: No Gate
Total Events: 10000
Y Parameter: FL2-Height (Log)

Quad	Events	% Gated	% Tot	X Mean	X Geo Mean	Y Mean	Y Geo Mean
UL	173	1.73	1.73	31.37	22.45	103.32	83.66
UF	369	3.69	3.69	498.34	215.18	219.29	157.64
LL	9021	90.21	90.21	5.59	2.32	2.98	1.40
LR	437	4.37	4.37	157.54	122.65	15.81	12.13

Figure 7.3: Detection of Apoptosis by Annexin in CRL1790 after DE8 protein application.



Quadrant Statistics

File: Data.008
Sample ID:
Tube: CRL1790 HIA
Acquisition Date: 21-Dec-12
Gated Events: 10000
X Parameter: FL1-Height (Log)
Quad Location: 53, 53

Log Data Units: Linear Values
Patient ID:
Panel: Dilsad annexin
Gate: No Gate
Total Events: 10000
Y Parameter: FL2-Height (Log)

Quad	Events	% Gated	% Tot	X Mean	X Geo Mean	Y Mean	Y Geo Mean
UL	30	0.30	0.30	13.15	4.54	141.25	119.85
UF	355	3.55	3.55	703.17	303.43	233.17	163.67
LL	8959	89.59	89.59	6.97	2.68	2.51	1.40
LR	656	6.56	6.56	131.77	105.52	17.81	13.22

Figure 7.4: Detection of Apoptosis by Annexin in CRL1790 after HIA protein application.

In Figure 7.5 it was shown that Annexin in NCM460 before application was 7.40. From the other Figures 7.6, 7.7 and 7.8, Annexin level in NCM460 was determined as 0.32, 6.91 and 5.13 after DB7Y, DE129 and DE51 application, respectively.

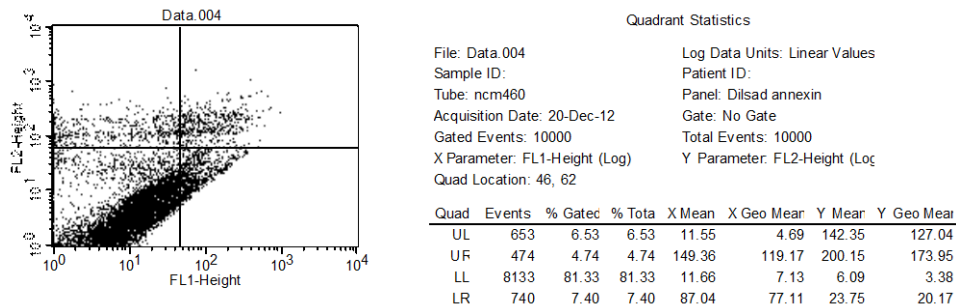


Figure 7.5 : Detection of Apoptosis by Annexin in NCM460 before bacterial protein application.

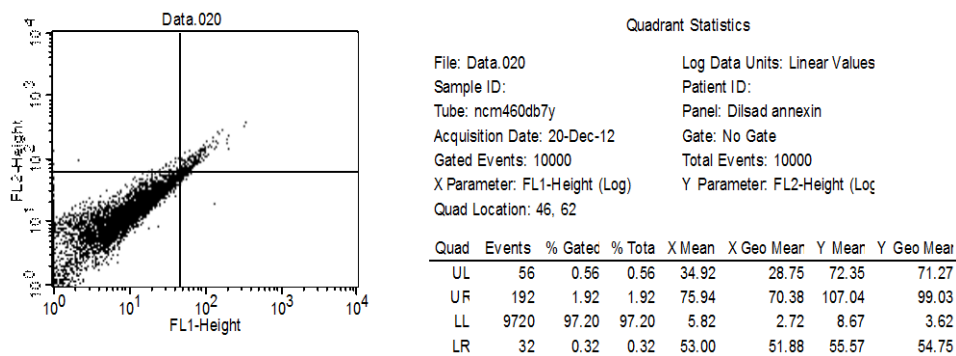


Figure 7.6 : Detection of Apoptosis by Annexin in NCM460 after DB7Y protein application.

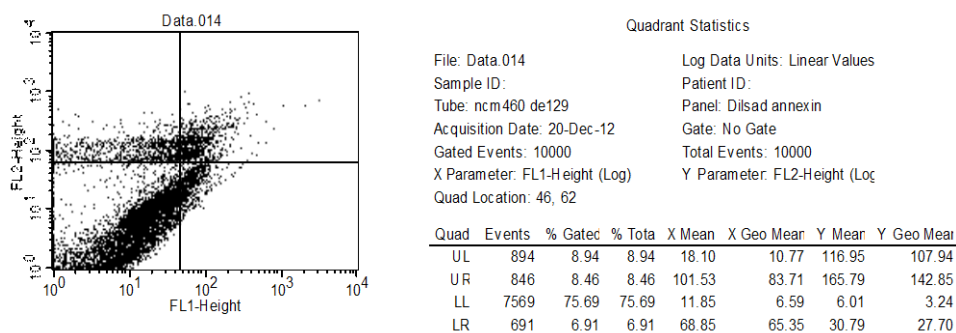


Figure 7.7 : Detection of Apoptosis by Annexin in NCM460 after DE129 protein application.

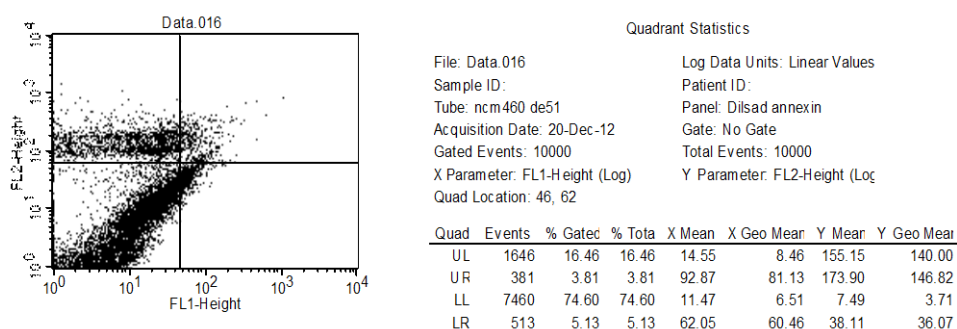


Figure 7.8: Detection of Apoptosis by Annexin in NCM460 after DE51 protein application.

Table 2.1 : Apoptosis assay results.

	CRL1790		NCM460	
	Annexin	Pi	Annexin	Pi
Neg.	10,55	1,8	7,4	4,74
3h	10,84	4,37	7,22	4,97
HIA	6,56	3,55	9,62	8,76
Huc2	11,16	3,51	11,19	8,45
DE129	21,53	9,45	6,91	8,46
DE51	34,48	6,97	5,13	3,81
DE365	7,12	3,98	14,74	7,9
DE8	4,37	3,69	7,68	7,08
DE12	14,88	6,26	11,94	10,48
DE47	10,61	6,59	8,74	9,12
DE36	8,27	4,54	9,33	8,43
DE256	11,8	3,57	7,65	6,88
DE103	14,8	6,03	8,57	5,32
DB7Y	14,23	5,74	0,32	1,92

In this assay, as shown in Table 2.1, annexin values of the cell lines without application of bacterial protein were determined as 10,55 and 7,4 for CRL1790 and NCM460 cell lines, respectively. 3 bacterial strains signed as HIA, DE365 and DE8 decreased the annexin level on CRL1790 cell lines whereas 3 bacterial strains DE129, DE51 and DB7Y decreased annexin on NCM460 cell lines. Even, DB7Y decreased annexin level to 0,32 from 7,4. Pi levels were also low for those samples.

3.5 CD24 Detection Results

CD24 values in this study were measured by flow cytometry. Isotype values were the background signal. In order to calculate the CD24 level, Isotype values for all samples were extracted from the CD24 values. In Table 3.1, all the results of the CD24 Detection assay in the present study were summarized. Flow cytometry reports including the results of the bacterial strains that decreased the apoptosis in the previous test were shown below. The reports of the other bacterial strains tested in the study were given in Appendix part.

As it was shown in Figure 8.1, CD24 was measured as 31.8 in CRL1790 before bacterial protein application. Isotype measurement of the same sample (Figure 8.2) was measured as 23.43.

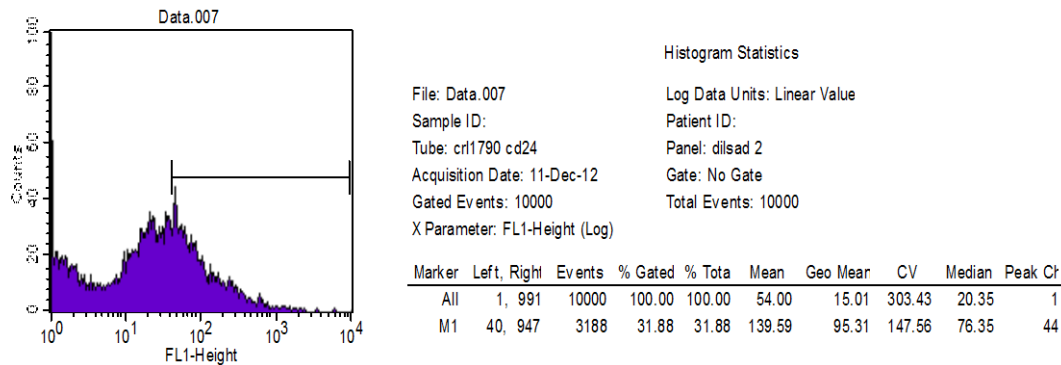


Figure 8.1: CD24 Detection in CRL1790 before bacterial protein application.

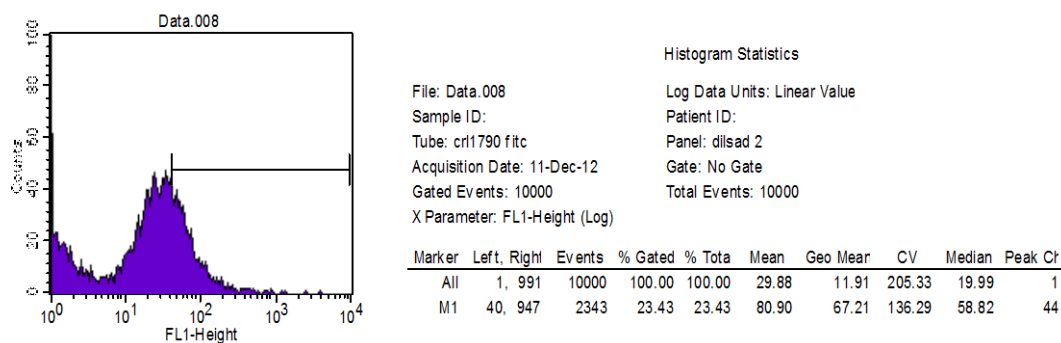


Figure 8.2: Isotype measurement in CRL1790 before bacterial protein application.

From the Figure 8.3 it can be observed that, CD24 was measured as 75.16 in CRL1790 after DE365 protein application. Isotype measurement of the sample, was determined as 16.09 (Figure 8.4).

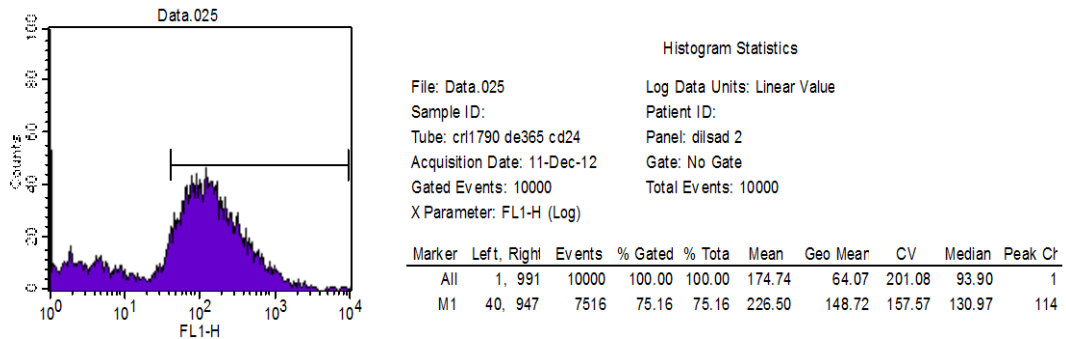


Figure 8.3: CD24 Detection in CRL1790 after DE365 protein application.

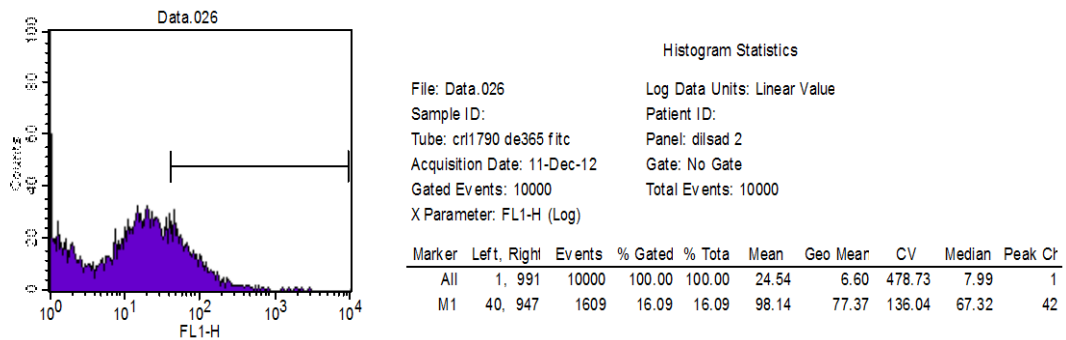


Figure 8.4: Isotype measurement in CRL1790 after DE365 protein application.

According to the Figures 8.5 and 8.6, CD24 was determined as 66,67 and isotype as 37,62 in CRL1790 after DE8 protein application.

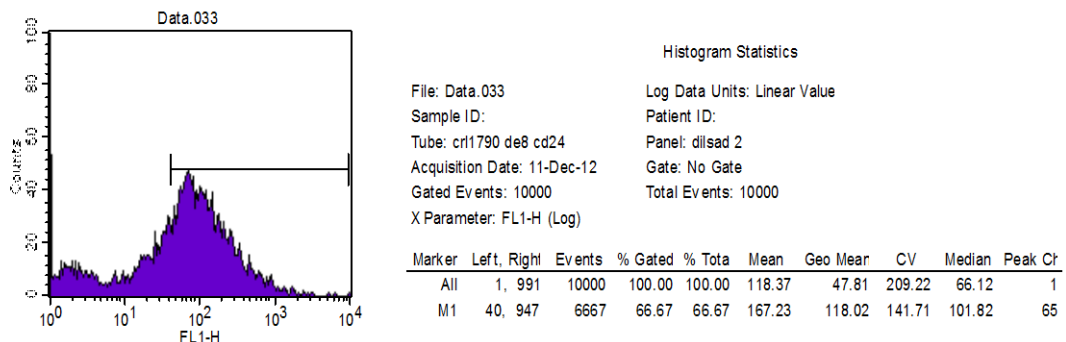
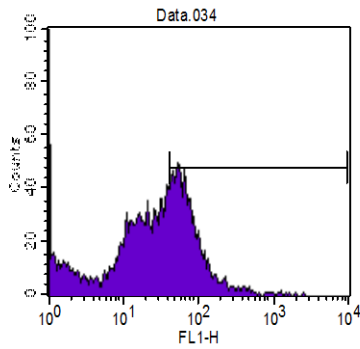


Figure 8.5: CD24 Detection in CRL1790 after DE8 protein application.



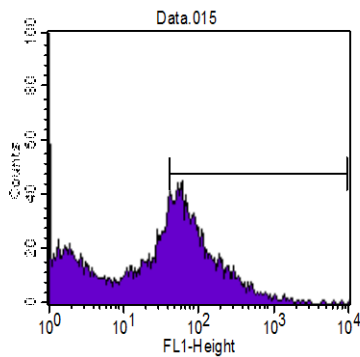
File: Data.034
 Sample ID:
 Tube: cri1790 de8 fitc
 Acquisition Date: 11-Dec-12
 Gated Events: 10000
 X Parameter: FL1-H (Log)

Log Data Units: Linear Value
 Patient ID:
 Panel: dilsad 2
 Gate: No Gate
 Total Events: 10000

Marker	Left, Right	Events	% Gated	% Tota	Mean	Geo Mear	CV	Median	Peak Ct
All	1, 991	10000	100.00	100.00	40.53	18.98	159.68	27.38	1
M1	40, 947	3762	37.62	37.62	82.74	69.79	108.34	62.08	50

Figure 8.6: Isotype measurement in CRL1790 after DE8 protein application.

CD24 was measured as 45,67 (Figure 8.7) and isotype as 27,17 (Figure 8.8) in CRL1790 after HIA protein application.

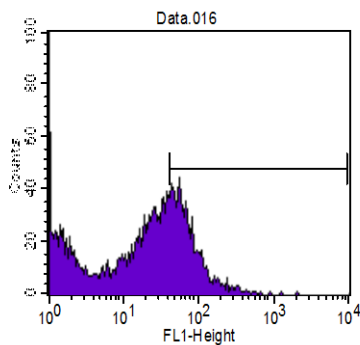


File: Data.015
 Sample ID:
 Tube: cri1790 HIA cd24
 Acquisition Date: 11-Dec-12
 Gated Events: 10000
 X Parameter: FL1-Height (Log)

Log Data Units: Linear Value
 Patient ID:
 Panel: dilsad 2
 Gate: No Gate
 Total Events: 10000

Marker	Left, Right	Events	% Gated	% Tota	Mean	Geo Mear	CV	Median	Peak Ct
All	1, 991	10000	100.00	100.00	74.48	20.25	311.51	34.91	1
M1	40, 947	4567	45.67	45.67	147.09	97.75	199.97	79.15	57

Figure 8.7: CD24 Detection in CRL1790 after HIA protein application.



File: Data.016
 Sample ID:
 Tube: cri1790 HIA fitc
 Acquisition Date: 11-Dec-12
 Gated Events: 10000
 X Parameter: FL1-Height (Log)

Log Data Units: Linear Value
 Patient ID:
 Panel: dilsad 2
 Gate: No Gate
 Total Events: 10000

Marker	Left, Right	Events	% Gated	% Tota	Mean	Geo Mear	CV	Median	Peak Ct
All	1, 991	10000	100.00	100.00	30.85	10.60	355.09	17.94	1
M1	40, 947	2717	27.17	27.17	77.84	67.63	87.69	60.43	53

Figure 8.8: Isotype measurement in CRL1790 after HIA protein application.

Table 3.1: CD24 detection results.

	CRL1790			NCM460		
	CD24	Calculation	ISOTYPE	CD24	Calculation	ISOTYPE
Neg.	31,88	8,45	23,43	31,57	26,71	4,86
3h	55,91	28,09	27,82	16,9	12,12	4,78
HIA	45,67	18,5	27,17	24,49	15,18	9,31
Huc2	69,9	30,59	39,31	26,05	20,17	5,88
DE129	74,61	44,56	30,05	15,6	13,2	2,4
DE51	61,38	23,07	38,31	23,23	17,26	5,97
DE365	75,16	59,07	16,09	20,68	14,75	5,93
DE8	66,67	29,05	37,62	26,67	20,97	5,7
DE12	54,65	12,91	41,74	22,84	16,16	6,68
DE47	88,62	25,73	62,89	29,11	24,23	4,88
DE36	50,97	22,25	28,72	9,02	3,05	5,97
DE256	52,99	21,91	31,08	23,73	19,02	4,71
DE103	62,01	25,35	36,66	23,68	17,46	6,22
DB7Y	56,03	20,09	35,94	27,99	22,76	5,23

According to Table 3.1, it was determined that all of the bacterial strains tested in the present study increased CD24 level on CRL1790 compared with those before application (8.45) The highest level was observed after DE365 application. (59,07) CD24 level was determined as 26,71 on NCM460 cell line before application. But no increase was observed on NCM460 after treatment.

A combination of CD24 and apoptosis detection assay results were given on Table 4.1.

Table 4.1: Comparison of the results.

Application	CRL1790					NCM460				
	CD24 DETECTION			APOPTOSIS		CD24 DETECTION			APOPTOSIS	
	CD24		ISOTYPE	ANNEXIN	PI	CD24		ISOTYPE	ANNEXIN	PI
CRL1790	31,88		23,43	10,55	1,8					
NCM460						31,57		4,86	7,4	4,74
Calculation		8,45					26,71			
3h	55,91	28,09	27,82	10,84	4,37	16,9	12,12	4,78	7,22	4,97
HIA	45,67	18,5	27,17	6,56	3,55	24,49	15,18	9,31	9,62	8,76
Huc2	69,9	30,59	39,31	11,16	3,51	26,05	20,17	5,88	11,19	8,45
DE129	74,61	44,56	30,05	21,53	9,45	15,6	13,2	2,4	6,91	8,46
DE51	61,38	23,07	38,31	34,48	6,97	23,23	17,26	5,97	5,13	3,81
DE365	75,16	59,07	16,09	7,12	3,98	20,68	14,75	5,93	14,74	7,9
DE8	66,67	29,05	37,62	4,37	3,69	26,67	20,97	5,7	7,68	7,08
DE12	54,65	12,91	41,74	14,88	6,26	22,84	16,16	6,68	11,94	10,48
DE47	88,62	25,73	62,89	10,61	6,59	29,11	24,23	4,88	8,74	9,12
DE36	50,97	22,25	28,72	8,27	4,54	9,02	3,05	5,97	9,33	8,43
DE256	52,99	21,91	31,08	11,8	3,57	23,73	19,02	4,71	7,65	6,88
DE103	62,01	25,35	36,66	14,8	6,03	23,68	17,46	6,22	8,57	5,32
DB7Y	56,03	20,09	35,94	14,23	5,74	27,99	22,76	5,23	0,32	1,92

The data showed that in addition to the apoptosis reduction, 3 bacterial strains coded as HIA, DE365 and DE8 increased the CD24 level on CRL1790 cell line. Whereas another group of bacterial strains including DB7Y, DE129 and DE51 decreased apoptosis on NCM 460 cell line. The lowest annexin value was observed after DB7Y application (0,32).

3.6 COX-2 Detection Results

Presence of COX2 was determined by Western Blotting technique. The 6 samples including DB7Y, DE365, DE129, DE8, DE51 and HIA that decreased the apoptosis after annexin test, were included in this assay. Cell lysates were prepared from NCM460 and CRL1790 before and after bacterial protein application. As positive control, Raw 264.7, a cell lysate from a macrophage cell that was induced with LPS, was used. Positive control band was shown in Figure 9.1a. In Figure 9.1b, the transferred proteins to the nitrocellulose membrane after Poncaeu staining can be observed.

As a result, all of the samples tested were determined as COX-2 negative. The experiment was performed twice and same result was obtained.

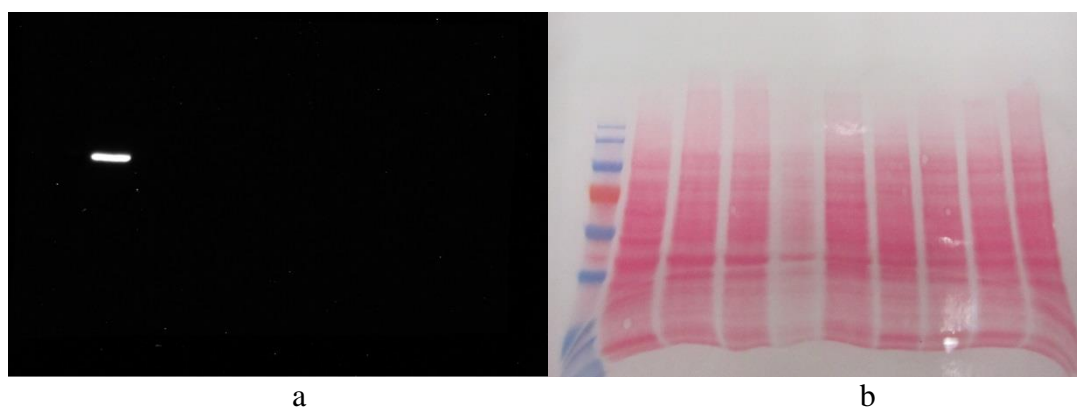


Figure 9.1: COX2 Determination by Western Blotting
a) After incubation with COX2 antibody
b) After Poncaeu staining

3.7 NFkB and Bcl2 Expression Assay Results

Similar to COX-2 detection, the 6 samples including DB7Y, DE365, DE129, DE8, DE51 and HIA that decreased the apoptosis after annexin test, were included in this assay. Real-Time PCR Results were given below.

In Figure 10.1 Relative Normalized Expression of NFkB on NCM 460 cell lines with and without bacterial protein was shown. The blue colored sample which was signed as NCM 460 represented the cell line without application. It was observed from the graph that bacterial protein application increased NFkB expression in NCM460 cell lines. The highest expression of NFkB belonged to DB7Y (yellow

color) followed by DE129 (white color). The least expression belonged to DE51 on NCM460 cell lines.

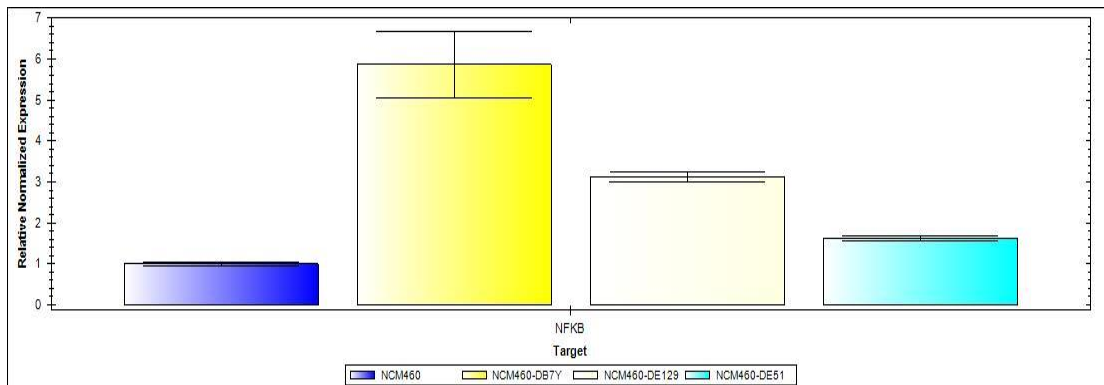


Figure 10.1: Relative Normalized Expression of NFKB on NCM460 cell line.

As shown in Figure 10.2, all bacterial treatment increased the expression of Bcl2. The highest expression was observed after DB7Y treatment (light blue) followed by DE51 (dark blue) and DE129 (pink color) compared with NCM460 before treatment (green).

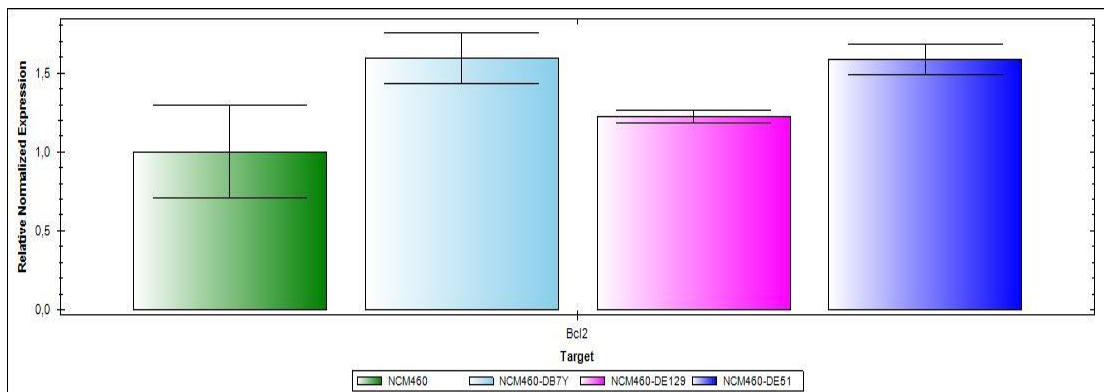


Figure 10.2: Relative Normalized Expression of Bcl2 on NCM 460 cell line.

In Figure 10.3, Relative Normalized Expression of NFKB on CRL1790 cell lines before and after bacterial treatment was shown. The pink colored column represented the result of the CRL1790 cell line before bacterial protein application. As it was observed from the graph, the highest expression belonged to DE365 (yellow) followed by DE8 (blue). There was no increase in NFKB expression after HIA (white) treatment.

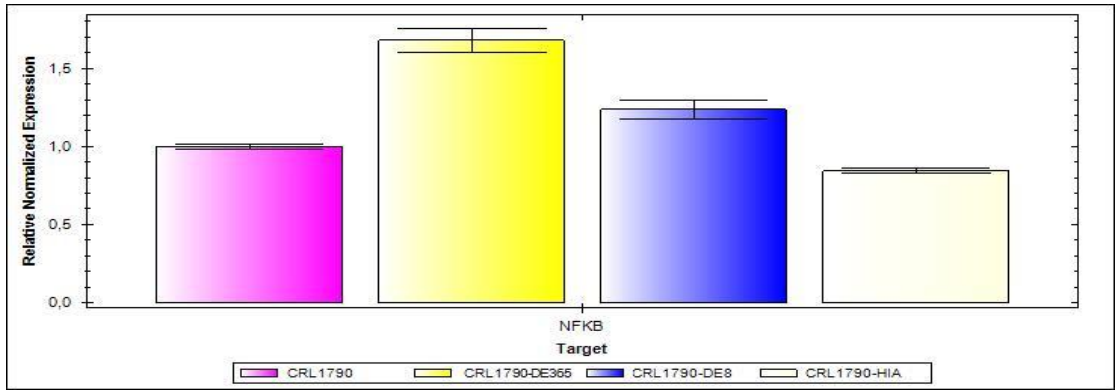


Figure 10.3: Relative Normalized Expression of NFKB on CRL1790 cell line.

In Figure 10.4, Relative Normalized Expression of Bcl2 on CRL1790 cell lines with and without bacterial protein application was shown. According to the graph, only DE365 (pink) treatment increased the Bcl2 expression compared with CRL1790 (green) before treatment. No increase was observed in Bcl2 expression after DE8 (light blue) and HIA (dark blue) treatment.

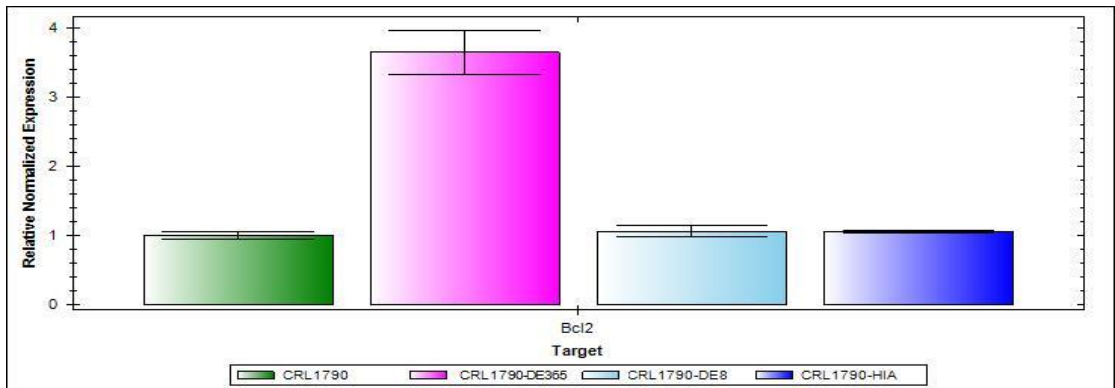


Figure 10.4: Relative Normalized Expression of Bcl2 on CRL1790 cell line.

Statistical Analysis of the NFKB and Bcl2 expression was performed by One way ANOVA following Tukey test in Graphpad Software. Figure 11.1 showed NFKB expression on NCM460 cell line. According to the graph, all bacterial treatment increased the expression. Figure 11.2 showed Bcl2 expression on NCM460 cell line.

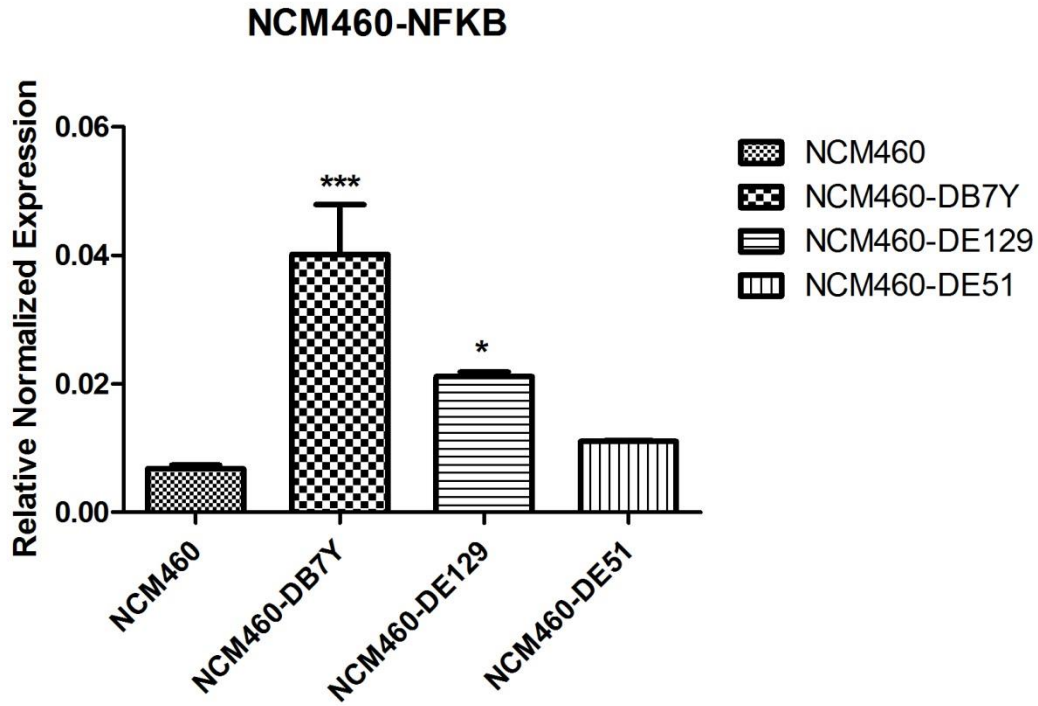


Figure 11.1: NFKB Expression on NCM460 cell line after statistical analysis.

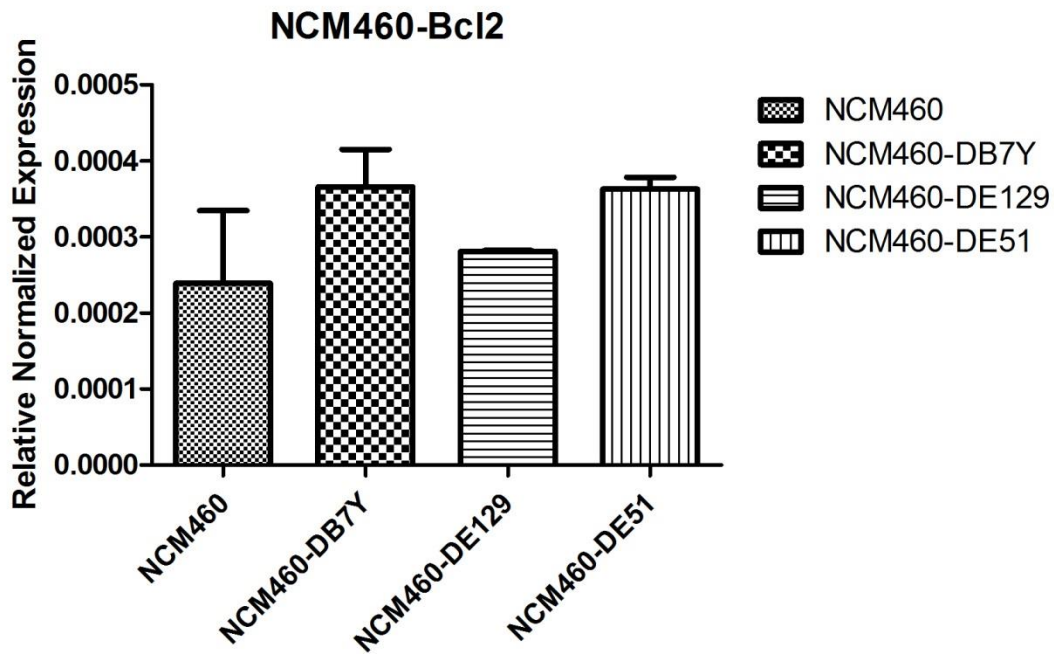


Figure 11.2 : Bcl2 Expression on NCM460 cell line after statistical analysis.

Figure 11.3 showed NFKB expression on CRL1790 cell line. Figure 11.4 showed Bcl2 expression on CRL1790 cell line.

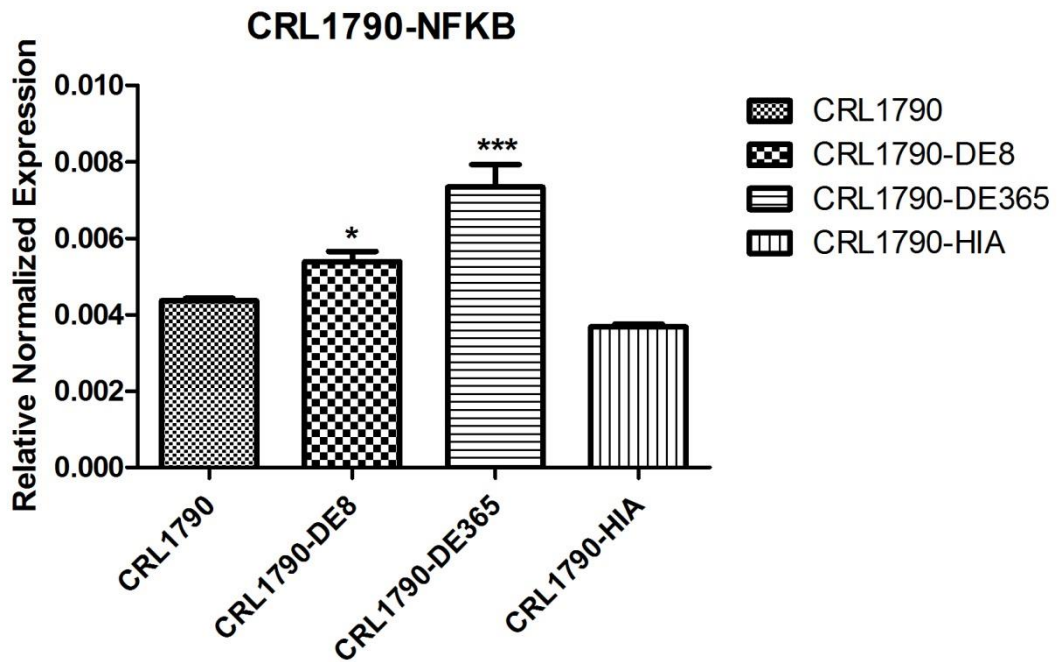


Figure 11.3: NFKB Expression on CRL1790 cell line after statistical analysis.

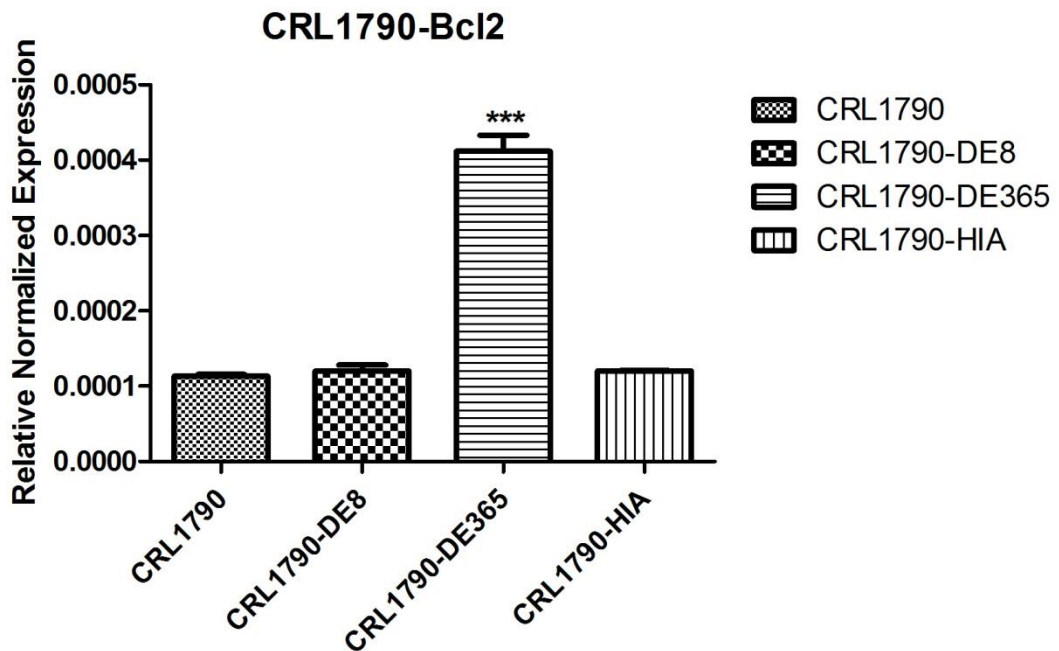


Figure 11.4 : Bcl2 Expression on CRL1790 cell line after statistical analysis.

4. DISCUSSION AND CONCLUSIONS

Cancer is a disease characterized by uncontrolled growth and spread of abnormal cells. Unless the spread is controlled, it can lead to death. If it is detected at an early stage, it is more treatable. Surgery, radiation, chemotherapy, hormones and immunotherapy are the approaches to make the treatment (American Cancer Society, 2011-b).

Colon cancer is the third most common cancer globally. Worldwide 1.2 million cases occurred in 2008 (American Cancer Society, 2011-b). Different factors including, age, diet, genetic diseases, physical inactivity, being overweight or obese are effective in colon carcinogenesis. People, who have had colorectal cancer or have one or more polyps, are in risk group. One of the most important factor that causes colon cancer is the inflammation. People who have chronic inflammatory bowel disease are in risk for colorectal cancer. Sporadic colon cancer and colitis associated colon cancer follow different pathways in tumorigenesis. Apoptotic pathways are also effective in colon carcinogenesis (American Cancer Society, 2011-a; Rupnarain et al, 2004).

Many studies were performed to determine the interaction between bacteria and colon cancer. The gram negative, rod shaped bacteria, *Enterobacter* can be observed in various areas including freshwater, sewage, soil, vegetables, human and animal intestines and the hospital environment. They are nosocomial pathogens that exist in many infections such as urinary tract infections, bacteremia, ventilator-associated pneumonia and meningitis and brain abscess. Infections are mostly caused by *Enterobacter aerogenes* and *Enterobacter cloacae* strains. Antibiotic resistance can be observed among *Enterobacter* strains against ampicillins, cephalosporins (Grimont and Grimont, 2006; Breathnach et al, 2006). Up to now, no study was performed to demonstrate a possible relationship between *Enterobacter* spp. and colon cancer. Therefore, it was aimed to investigate the effects of *Enterobacter* strains on colon cancer in the present study.

In our study, the tumorigenic potential of 11 bacterial strains in the genera of *Enterobacter*, 1 *Escherichia coli* and 1 *Morganella morganii* strain were investigated. Our approach first of all was to isolate the bacterial proteins and apply them onto healthy colonic epithelial cell lines. After incubation, cell viability and proliferation, presence of apoptosis, and level of tumor markers such as CD24, COX-2, NFkB and Bcl2 were screened.

Presence of apoptosis before and after bacterial protein application was determined by Annexin V. Before application of bacterial protein, Annexin V values were determined as 10,55 and 7,4 for CRL1790 and NCM460 cell lines, respectively. The result of the experiment showed that six bacterial strains including HIA, DE365, DE8, DE129, DE51 and DB7Y decreased annexin on either CRL1790 or NCM460 .

CD24 is a cell surface protein, which is expressed especially on premature lymphocytes, epithelial cells, and neural cells. It is a small, heavily glycosylated protein core that consists of 27 amino acids. It is effective in cell selection and maturation during hematopoiesis. It is expressed during the embryonic period on developing neural cells and pancreatic cells. CD24 is overexpressed in various malignant tissues, including B-cell lymphomas, gliomas, and small cell lung, hepatocellular, uterine, ovarian, breast, prostate and pancreatic carcinomas. Because it is the ligand of P-selectin and the adhesion receptor found in activated endothelial cells and platelets, CD24 is considered to be associated with tumor metastasis (Sagiv et al, 2006; Lim, 2005; Choi et al, 2006). Studies show that CD24 is overexpressed in the colonic mucosa at an early stage of carcinogenesis and overexpression of CD24 can be a specific marker of disease progression from the premalignant tumor phase to the development of carcinoma (Sagiv et al, 2006; Choi et al, 2006).

In our study, expression level of CD24 on CRL1790 and NCM460 before and after bacterial protein application was analysed. The results showed that there was no increase in CD24 level in NCM460 cell line. In fact, there was a decrease in most of the samples. However, CD24 level was not so affected after application of DE47 and DB7Y proteins on NCM460 cell line. Whereas in CRL1790, after treatment of the three strains coded as DE365, DE8 and HIA, an increase in CD24 level was observed compared with those before treatment. This difference may occur as a result of the differences between cell lines. CRL1790 is a colonic epithelial cell line driven from a 21 week gestation female fetus, whereas NCM 460 cell line is driven from normal

colonic mucosa of 68 year old male. (ATCC and in cell product sheet) Pathogenic effects on different cell lines may be related with different metabolites, which can be produced by various microorganisms, and pathogenic abilities can differ among bacterial strains. As a result of this, they can follow different pathways to cause diseases. As it was explained in the introduction part, colon has different parts called as ascending colon, transverse colon, descending colon and sigmoid colon. In different parts of the colon, different bacterial strains can colonize. The prevalence of bacteria in different parts of the gastrointestinal tract depends on several factors such as pH, peristalsis, redox potential, bacterial adhesion, bacterial cooperation, mucin secretion, nutrient availability, diet and bacterial antagonism. The stomach and the upper two-thirds of the small intestine (duodenum and jejunum) contain low numbers of microorganisms because of the low pH and the swift peristalsis through the stomach and the small bowel. In the distal part of the small intestine, which is called as the ileum, similar to the colon, there is high bacterial population and diverse microflora because of the decreased peristalsis, acidity and lower oxidation-reduction potential. Slow intestinal motility, and very low oxidation-reduction potential makes the colon the primary site of microbial colonization in humans (Hao and Lee, 2004). In a study that was performed to determine the bacterial populations in the distal small bowel and colon, it was found that *Bifidobacterial* numbers were significantly higher in the large bowel than in the terminal ileum whereas *lactobacilli* were more prominent in the distal large intestine. *Eubacterium rectale* and *Faecalibacterium prausnitzii* were dominant in the ascending and descending colon (Ahmed et al, 2007). Because the bacterial strains can exist in different parts of the colon, if the cell lines were not driven from the same part of the colon, the effect of bacterial proteins on those cell lines may also differ. Those properties may lead to the result, as a group of bacteria were found effective against NCM 460 cell line whereas another group was effective against CRL1790 in our study. Since all bacteria may differ based on their pathogenic abilities, some bacterial strains increased CD24 level and decreased apoptosis at the same time whereas in some only apoptosis was reduced without an alteration in CD24 level.

In our study, it was demonstrated that apoptosis decreased after bacterial protein application when compared with those before application. As a next step, to clarify the apoptosis reduction mechanism of those 6 effective bacterial strains, NFkB and Bcl2 expression of the cell lines before and after bacterial protein application were determined. When NFkB expression was tested before and after bacterial protein application, it was determined that the bacterial protein signed as DB7Y, increased NFkB expression on NCM460 cell line when compared with those before application. After statistical analysis, the increase that was observed in DB7Y was found as extremely significant ($p < 0,001$). DE129 also significantly increased NFkB on NCM460 ($p: 0,01-0,05$). In regards to the CRL1790 cell line, the strain coded as DE365 increased NFkB when compared with the one without application and similar to the DB7Y results, the increase in DE365 was found as extremely significant ($p < 0,001$). Also another *Enterobacter* strain, signed as DE8, significantly increased NFkB expression ($p: 0,01-0,05$). But the increase in DE365 was found higher than that of the increase in DE8.

NFkB (The nuclear factor KB) is a transcription factor, which is involved, in many biological pathways. Immune mediating genes, inflammatory genes, antiapoptotic genes, cell proliferation regulation genes are targets of NFkB. NFkB consists of a family of Rel-domain-containing proteins, which includes Rel A (also called p65), Rel B, c-Rel, p50 (also called NFkB1) and p52 (also called NFkB2). NFkB exists in the cytoplasm in an inactive state, which is inhibited by I κ B. In the presence of extracellular stimuli, such as cytokines, phosphorylation, ubiquitination, and proteolytic degradation occurs by either canonical I κ B kinase complex-dependent pathway or noncanonical NFkB inducing kinase pathway. Phosphorylation by casein kinase 2 may also lead to I κ B degradation. NFkB is released after I κ B degradation, and then it translocate to the nucleus. NFkB binds to the promoter regions of its target genes, which control immune system, growth and inflammation. Phosphorylation of NFkB is also required for activation (Lu et al, 2006; Shishodia, 2004).

NFkB is actually required for the normal functioning of immune system. Regulation of the expression of cytokine genes, functioning in hematopoiesis, antigen presentation, B cell development and proliferation, T cell development and proliferation are the beneficial activities of NFkB. In normal cells NFkB activation

occurs as a result of a stimuli, but in tumor cells different molecular alterations lead to impaired regulation of NF κ B activation, which results in constitutively activation. Therefore, deregulated expression is observed in genes, which are under NF κ B control. Genes that are involved in apoptosis regulation, cell cycle control, adhesion and migration are affected. Constitutively active NF κ B has been detected in many tumors such as multiple myeloma, acute myelogenous leukemia, acute lymphocyte leukemia, chronic myelogenous leukemia, prostate and breast cancers. It was shown that suppression of NF κ B in these tumors, inhibit proliferation, cause cell cycle arrest and lead to apoptosis (Dolcet et al, 2005; Shishodia, 2004).

It was determined that NF κ B is related to carcinogenesis by activating tumor-promoting cytokines or by activating NF κ B signaling in premalignant cells and immune/ inflammatory cells. In studies, it was demonstrated that, NF κ B was detected both in colorectal and colitis-associated tumors. The activation mechanism of NF κ B in tumorigenesis can be summarized as increasing cell proliferation and angiogenesis, inhibiting cell death, promoting cell invasion and metastasis (Terzic et al, 2010). In epithelial cells, NF κ B activation is involved mainly in the promotion and progression steps of colitis associated colorectal cancer (Wang et al, 2009).

Members of NF κ B family can be oncogenic. It was determined that *c-Rel* transforms cell in culture. *c-Rel* is activated in an avian B cell lymphoma and in human it is observed in Hodgkin's lymphoma. Some oncogenes are shown to activate NF κ B. Oncogenic Ras, that is active in many tumor types such as prostate and colon cancer, has been shown to activate NF κ B. Cytokines including IL-1, TNF and IL-6 which can be growth factors for tumor cells, are regulated by NF κ B. EGF, a growth factor in tumors activates NF κ B. Cytokines are either regulated by NF κ B or mediate proliferation by NF κ B activation. Cyclin D1, which is a cell cycle protein required for entry of cells from G1 to S phase is also regulated by NF κ B. Tumor invasion and metastasis processes, which are regulated by gene products such as matrix metalloproteinase, urinary plasminogen activator and interleukin-8, are regulated by NF κ B (Shishodia, 2004).

In a study performed, 28 resected colorectal carcinomas and colonic mucosa from healthy portions were tested for NF κ B activation and in tumors much greater activation was observed when compared with those in normal colonic mucosa. Researchers also indicate a relationship between NF κ B activation and cell

proliferation (Kojima et al, 2004). Angiogenesis defined, as blood vessel formation is an important process for solid tumors to grow. Production of angiogenic factors including TNF, VEGF, MCP-1 and IL-8 is regulated by NF κ B. In colorectal cancer, it was determined that NF κ B and VEGF was significantly overexpressed and associated with the increased microvessel density. It was suggested that increased expression of NF κ B in colorectal cancer, contributes to tumor angiogenesis (Shishodia, 2004).

NF κ B is required for neutrophil chemotaxis, it regulates inflammatory cell apoptosis and phagocytosis which shows the function of NF κ B in chronic inflammation. In connection to carcinogenesis, NF κ B suppresses apoptosis (Lu et al, 2006). The oncogenic role of NF κ B, related with its antiapoptotic function, is especially through Bcl2, Bcl-X_L and cFLIP activation (Karin, 2009, Terzic et al, 2010). NF κ B up regulates the expression of FLICE-like inhibitory protein (FLIP). FLIP is a homolog of caspase 8 but lacks protease activity. It competes with caspase 8 for the binding to the Death- Inducing Signaling Complex. High levels of FLIP, prevents binding of caspase 8. FLIP upregulation is observed in many tumors. The expression of Inhibitors of Apoptosis (IAPs), members of the Bcl2 family, is induced by NF κ B. IAPs suppress apoptosis by inhibiting caspases (caspases -3, -6, -7 and -9) PTEN, a tumor suppressor gene, is a negative regulator in P13K/Akt pathway. Studies show that NF κ B decreases PTEN, decreased PTEN increases Akt activity and suppresses apoptosis (Dolcet et al, 2005).

Expression of adhesion molecules such as ICAM -1, VCAM-1 and ELAM-1 which are active in metastasis are regulated by NF κ B. Inducible Nitric Oxide Synthase (iNOS), again related with tumor metastasis, is also regulated by NF κ B (Shishodia, 2004).

COX-2 is accepted as another marker, which is up regulated during colon cancer. (COX) Cyclooxygenase enzyme is required in prostaglandin biosynthesis. COX-2 was reported to modulate cell proliferation and apoptosis in many colorectal, breast, prostate cancers and also in hematological malignancies (Dixon et al, 2013; Sobolewski et al, 2010). The cell lines; CRL1790, and NCM460, that were used in this study were found COX-2 negative before and after bacterial protein application. This result indicates that the bacteria strains that we tested, used different pathways.

Bcl2 was the first protein that was identified in this family and derived its name from B cell lymphoma. Bcl2 members, which are located on the outer mitochondrial membrane, are functional in membrane permeability either by forming ion channels or creating pores. Bcl2 family is divided into 3 groups based on Bcl2 homology domains and their function. Antiapoptotic proteins such as; Bcl-2, Bcl-X_L, Bcl-W, A1/Bfl-1, Mcl-1 and Bcl-B/Bcl2L10 contain all four BH domains, is the first group. Second group; BH-3 only proteins, which is restricted to the BH3 domain, are initiators of apoptosis. This group includes; Bid, Bim, Puma, Noxa, Bad, Bmf, Hrk and Bik. Third group, which contains all four BH domains, is also proapoptotic. Examples can be given as; Bax, Bak and Bok/Mtd (Wong, 2011 ; Ouyang et al, 2012).

Bcl2 has no oncogenic potential as Myc or Ras, however it is oncogenic by enabling the cell survival in inappropriate conditions. Bcl2 performs its antiapoptotic functions based on the mitochondria. It could suppress the production of reactive oxygen species by the mitochondrion. It was also reported that antiapoptotic mechanism of Bcl2 is suppression of the release of cytochrome c and preventing caspase activation (Cotter, 2009).

Bcl2 was determined as an important factor in the development of B cell lymphomas. Increased Bcl2 expression was observed in many tumors such as lung cancers, renal, stomach and brain cancers and non-Hodgkin's lymphomas (Cotter, 2009). Bcl2 is also overexpressed in colorectal adenomas and carcinomas (Rupnarain et al, 2004; Sinicrope et al, 1995). In colon cancer, a gradient increase was demonstrated in Bcl2, during the tumor progression from adenoma to carcinoma. Expression increased in early stages but decreased in late stages of colon cancer (Huerta et al, 2006).

In the present study, two bacterial strains coded as DB7Y and DE51 increased expression of Bcl2 in NCM 460 cell line when compared with those before application. The increase of Bcl2 expression in DE129 was lower than that of the increase in DB7Y and DE51. These data confirmed Annexin V assay results on Table 2.1. DE365 application, extremely increased the expression of Bcl2 in CRL1790 cell line ($p < 0,001$). Bcl2 expression was not affected in CRL1790 cell lines after DE8 and HIA application.

Among thirteen bacterial strains that were tested in this study, six of them were defined as effective either on CRL1790 or NCM460 cell line. All effective strains increased the cell viability and proliferation at their optimum concentrations and decreased apoptosis. Also, they were determined as COX-2 negative. By molecular techniques based on 16S rDNA sequences, fatty acid compositions and metabolic activities, HIA and DE51 were identified as *Escherichia coli* and *Morganella morganii* respectively. It was found that the remaining four bacterial strains belonged to the *Enterobacter* spp. including DB7Y, DE129 and DE365 decreased apoptosis by increasing NF κ B and Bcl2 expression. DE365 also increased CD24 level in CRL1790. DE8, which was identified as *Enterobacter aerogenes*, increased CD24 level as well as NF κ B expression on CRL1790. However, it did not affect Bcl2 expression. In addition to the increase in NF κ B expression, these results indicate that DE8 may follow another pathway for apoptosis reduction. This suggestion was also supported by the phylogenetic tree of the effective *Enterobacter* strains. When the effective *Enterobacter* strains were examined in a phylogenetic tree, it was observed that DE8 was located far from the others.

Apoptosis inhibition can be observed in many bacterial strains. It is an important pathogenicity mechanism which enables the bacteria to replicate inside host cells. Some bacteria induce apoptosis but in that case they target immune cells like macrophages and neutrophils because otherwise these cells will kill them. Bacteria develop different strategies to inhibit apoptosis (Faherty and Maurelli, 2008).

It was determined that *Chlamydia trachomatis*, which is an obligate intracellular bacteria that causes urogenital and ocular infections, inhibits Bax and Bak proteins and prevents them from permeabilizing the mitochondrial membrane. In *Chlamydia* infected cells, cytochrome c release and caspase activation are inhibited. It was also determined that *Chlamydia* upregulates the inhibitor of apoptosis proteins (IAPs) when an inducer like tumor necrosis factor α (TNF- α) was used. IAPs are apoptosis regulators, which function at the level of caspases (Zhong et al, 2006; Rajalingam et al, 2006; Faherty and Maurelli, 2008).

By using the outer membrane porin protein PorB, *Neisseria meningitidis*, which is a gram-negative bacterium that causes bacterial meningitis and sepsis, stabilize the mitochondria and inhibits cytochrome c release. PorB also diminished DNA breakdown. As a result of immunoprecipitation experiments, researchers suggested

that Por B interacts with the mitochondrial porin VDAC (voltage dependent anion channel), which is a part of the permeability transition pore (PT) (Massari et al, 2000; Massari et al, 2003; Faherty and Maurelli, 2008).

Salmonella enterica serovar typhimurium is a common food-borne pathogen, causes gastroenteritis. By activating the PI3K/Akt pathway which prevents cytochrome c release and thus inhibits the activation of caspases *Salmonella enterica serovar typhimurium* inhibits apoptosis (Knodler et al, 2005; Faherty and Maurelli, 2008).

Anaplasma phagocytophilum, is an obligate intracellular bacterium that causes human granulocytic anaplasmosis, prevents apoptosis in neutrophils. It was demonstrated that *Anaplasma* infection upregulates antiapoptosis genes that control several pathways such as; p38MAPK, ERK, P13K and NFkB. Reduction was also observed in caspase 3 and caspase 8 activities (Choi et al, 2005; Lee and Goodman, 2006; Faherty and Maurelli, 2008).

Ehrlichia chaffeensis, is a gram negative, obligate intracellular bacterium, causes human monocytic ehrlichiosis, inhibits apoptosis in the human monocyte cell line THP1 by NFkB upregulation. Bcl2 is also induced during infection (Zhang et al, 2004; Faherty and Maurelli, 2008).

Another gram negative, obligate intracellular pathogen *Rickettsia rickettsii*, the agent of Rocky Mountain spotted fever, targets the vascular endothelium, prevents apoptosis in endothelial cells by NFkB pathway not only by upregulating the prosurvival proteins and downregulating the proapoptotic proteins, but also by inhibiting cytochrome c release and preventing activation of apical caspases -8, -9 and effector caspase -3 (Joshi et al, 2003; Joshi et al, 2004; Faherty and Maurelli, 2008).

Wolbachia, is a gram negative endosymbiotic bacteria of filarial nematode parasites, belonged to the *Anaplasmataceae* family. It is important during parasitic infections in humans. It was found that surface protein of *Wolbachia* inhibits apoptosis in human neutrophils by preventing caspase 3 activation (Bazzocchi et al, 2007; Faherty and Maurelli, 2008).

Bartonella henselae, a slow growing, fastidious, facultative intracellular bacterium which causes cat scratch disease, vasculoproliferative disorders, bacillary angiomatosis and peliosis, inhibits apoptosis by activating NF κ B, increasing expression of cIAP-1 and cIAP-2 and preventing caspase 3 activation (Kempf et al, 2005; Faherty and Maurelli, 2008).

Shigella, a gram negative pathogen that causes bacillary dysentery, can invade a variety of host cells such as, macrophages, dendritic cells and epithelial cells. It was demonstrated that, *Shigella flexneri* inhibits apoptosis in epithelial cells but causes cell death in macrophages. Apoptosis inhibition mechanism is preventing caspase 3 activation (Suzuki et al, 2005; Clark and Maurelli, 2007; Faherty and Maurelli, 2008).

Toxoplasma gondii, is an intracellular parasite. It also prevents apoptosis by inhibition of cytochrome c induced caspase activation. (Keller et al, 2006, Faherty and Maurelli, 2008).

Legionella pneumophila causes a life-threatening pneumonia called as Legionnaires disease, inhibits apoptosis through NF κ B activation (Abu-Zant et al, 2005; Abu-Zant et al, 2007; Faherty and Maurelli, 2008).

Helicobacter pylori, a gram-negative bacterium, causes gastritis and peptic ulcer. Studies also showed its association with gastric cancer and mucosa-associated lymphoid tissue (MALT) lymphoma. It inhibits apoptosis by NF κ B activation (Yanai et al, 2003).

As it was summarized above, many bacteria can reduce apoptosis. Our study was the first to demonstrate apoptosis can be inhibited by *Enterobacter* strains. Why is apoptosis inhibition so important? Apoptosis is a complex process that contains many pathways, at any point along these pathways defects can occur which lead to malignant transformation of the affected cells, tumor metastasis and resistance to anticancer drugs. In the previous studies, it was reported that the proto-oncogene Bcl-2, which inhibits apoptosis encourages tumor progression, the retinoblastoma protein that regulates cell cycle progression, bax, bcl-_{XL}, mcl-I, Fas receptor and Fas-ligand which regulate apoptosis, contribute to tumor progression. In addition to the genetic changes, a few studies showed that reduction of apoptosis is important for carcinogenesis (Wong, 2011; Rupnarain et al, 2004). Wright, 1994 tested, 10 known

or suspected tumor promoters and it was found that all of them inhibited DNA fragmentation and cell death of 7 different cell lines. In another study, it is shown that *Helicobacter pylori* and *Bartonella henselae* inhibit apoptosis and at the same time causes gastric carcinoma and bacillary angiomatosis, respectively (Faherty and Maurelli, 2008). Similarly some data in the previous works demonstrated that *Chlamydia* inhibits apoptosis, *Chlamydia pneumoniae* was found to be related with lung cancer (Mager, 2006; Zhong et al, 2006; Rajalingam et al, 2006).

In conclusion, the present study indicates that *Enterobacter* strains might promote colon cancer. This is the first study showing that *Enterobacter* spp. may be clinically important factor for colon cancer initiation and progression. Studies can be extended on animal models in order to develop new strategies for treatment.

REFERENCES

- Abu- Zant, A., Santic, M., Molmeret, M., Jones, S., Helbig, J. & Abu Kwaik, Y.** (2005). Incomplete activation of macrophage apoptosis during intracellular replication of *Legionella pneumophila*. *Infection and Immunity*, 73(9), 5339-5349.
- Abu- Zant, A., Jones, S., Asare, R., Suttles, J., Price, C., Graham, J. & Abu Kwaik, Y.** (2007). Anti apoptotic signalling by the Dot /Icm secretion system of *L.pneumophila*. *Cellular microbiology*, 9(1), 246-264.
- Ahmed, S., Macfarlane, T.G., Fite, A., McBain, J.A., Gilbert, P. & Macfarlane, S.** (2007). Mucosa Associated Bacterial Diversity in Relation to Human Terminal Ileum and colonic biopsy samples. *Applied and Environmental Microbiology*, 73(22), 7435-7442.
- Alberts, B., Johnson, A., Lewis, J., Raff, M., Roberts, K., Walter, P.** (2002). *Molecular biology of the cell* (4th ed.). USA: Garland Science Taylor and Francis Group.
- American Cancer Society.** (2011a). *Colorectal Cancer Facts and Figures 2011-2013*. Atlanta: American Cancer Society.
- American Cancer Society.** (2011b). *Global Cancer Facts and Figures* (2nd ed.). Atlanta: American Cancer Society.
- ATCC product sheet** (n.d). CCD 841 CoN (ATCC CRL1790) Retrieved from: www.atcc.org
- Bazzocchi, C., Comazzi, S., Santoni, R., Bandi, C., Genchi, C. & Mortarino, M.** (2007). Wolbachia surface protein (WSP) inhibits apoptosis in human neutrophils. *Parasite Immunology*, 29, 73-79.
- BD Technical Datasheet,** (n.d). FITC Annexin V Apoptosis Detection Kit 1 Retrieved from: www.bdbiosciences.com/
- Berridge, M.V. & Tan A.S.** (1993). Characterization of the cellular reduction of MTT: Subcellular localization, substrate dependence and involvement of mitochondrial electron transport in MTT reduction. *Arch. Biochem. Biophys*, 303, 477-482.
- Biarç, J., Nguyen, S. I., Pini, A., Gosse, F., Richert, S., Thierse, D., Schöller-Guinard, M.** (2004). Carcinogenic properties of proteins with pro-inflammatory activity from *Streptococcus infantarius* (formerly *S.bovis*). *Carcinogenesis*, 25(8), 1477-1484.
- Bilgehan, H.** (2000). *Özel Bakteriyoloji ve Bakteri Enfeksiyonları* (10.bs.). İzmir: Barış Yayınları Fakülteler Kitabevi.

- Breathnach, S. A., Riley, A.P., Shad, S., Jownally, M.S., Law, R., Chin, C.P., Smith, J.E.** (2006). An outbreak of wound infection in cardiac surgery patients caused by *Enterobacter cloacae* arising from cardioplegia ice. *Journal of Hospital Infection*, *64*, 124-128.
- Buyer, S. J.** (2002). Rapid sample processing and fast gas chromatography for identification of bacteria by fatty acid analysis. *Journal of Microbiological Methods*, *51*, 209-215.
- Choi, S. K., Tae Park, J. & Dumler, S. J.** (2005). *Anaplasma phagocytophilum* Delay of Neutrophil Apoptosis Through the p38 Mitogen-activated Protein Kinase Signal Pathway. *Infection and Immunity*, *73*(12), 8209-8218.
- Choi, Y., Xuan, H. Y., Lee, S., Park, M. S., Kim, J. W., Kim, H. & Kim, S.** (2006). Enhanced CD24 Expression in Colorectal Cancer Correlates With Prognostic Factors. *The Korean Journal of Pathology*, *40*, 103-111.
- Clark S. C. & Maurelli, T.A.** (2007). *Shigella flexneri* inhibits Staurospine-induced apoptosis in epithelial cells. *Infection and Immunity*, *75*(5), 2531-2539.
- Cotter, G. T.** (2009). Apoptosis and cancer: the genesis of a research field. *Nature Reviews*, *9*, 501-507.
- Cory, A.H., Owen, T. C., Barltrop, J. A. & Cory, J. G.** (1991). Use of an aqueous soluble tetrazolium/formazan assay for cell growth assays in culture. *Cancer Commun*, *3*, 207-212.
- Dillon, S. R., Mancini, M., Rosen, A. & Schlissel, M. S.** (2000). Annexin V binds to viable B cells and colocalizes with a marker of lipid rafts upon B cell receptor activation. *The Journal of Immunology*, *164*, 1322-1332.
- Dixon, A.D., Blanco, F. F., Bruno, A. & Patrignani, P.** (2013). Chapter 2: Mechanistic Aspects of COX-2 Expression in Colorectal Neoplasia. *Recent Results Cancer Res*, *191*, 7-37.
- Dolcet, X., Llobet, D., Pallares, J. & Matras-Guiu, X.** (2005). NF κ B in development and progression of human cancer. *Virchows Arch*, *446*, 475-482.
- Elmore, S.** (2007). Apoptosis: A review of Programmed Cell Death. *Toxicol Pathol*, *35*(4), 495-516.
- Faherty, S. C. & Maurelli, T. A.** (2008). Staying alive: bacterial inhibition of apoptosis during infection. *Trends in Microbiology*, *16* (4), 173-180.
- Felsenstein, J.** (1989). PHYLIP-Phylogeny Inference Package (Version 3.2). *Cladistics*, *5*, 164-166.
- Felsenstein, J.** (1993). (Version 3.5c) [PHYLIP-Phylogeny Inference Package]. Seattle, WA
- Guimaraes, A. C. & Linden, R.** (2004). Programmed cell death , Apoptosis and alternative deathstyles. *Eur J Biochem*, *271*, 1638-1650.
- Grimont, F. & Grimont P.** (2006). The Genus *Enterobacter*. *Prokaryotes*, *6*, 197-214.

- Han, S. J. & Nair, P. P.** (1995). Flow cytometric identification of cell surface markers on cultured human colonic cell lines using monoclonal antibodies. *Cancer*, 76(2), 195-200.
- Hao, L.W. & Lee, K.Y.** (2004). Microflora of the Gastrointestinal Tract, A review. In J. F. T. Spencer, A. L. Ragout de Spencer (Eds.), *Methods in Molecular Biology, Public Health Microbiology Methods and Protocols* (Vol. 268, pp. 491-502). Totowa: NJ.
- Higgins, D.G., Bleasby, A.J. & Fuchs, R.** (1992). CLUSTAL V: improved software for multiple sequence alignment. *Computer Applications in the Biosciences- CABIOS*, 8(2), 189-191.
- Huerta, S.; Goulet, J. & Livingston, H. E.** (2006). Colon cancer and apoptosis. *The American Journal of Surgery*, 191, 517-526.
- Huycke, M. M. & Gaskins, R. H.** (2004). Commensal Bacteria, Redox Stress, and Colorectal Cancer: Mechanisms and Models. *Exp Biol Med*, 229, 586-597.
- Incell Product sheet** (n.d). Normal-Derived Colon Mucosa (NCM460) Retrieved from: media.wix.com/ugd/463504_7934d0a2e95a933829a9239ec5610652.pdf
- Itzkowitz, H. S. & Yio, X.** (2004). Colorectal cancer in inflammatory bowel disease: the role of inflammation. *Am J Physiol Gastrointest Liver Physiol*, 287, G7-G17.
- Jin, Y. W., Jang, J. S., Lee, J. M., Park, G., Kim, J. M., Kook, K. J., Park, J. Y.** (2011). Evaluation of VITEK2, MicroScan and Phoenix for identification of clinical isolates and reference strains. *Diagnostic Microbiology and Infectious Disease*, 70, 442-447.
- Joshi, G. S., Francis, W. C., Silverman, J. D. & Sahni, K. S.** (2003). Nuclear factor KB Protects Against Host Cell Apoptosis during *Rickettsia rickettsii* Infection by Inhibiting Activation of Apical and Effector Caspases and Maintaining Mitochondrial Integrity. *Infection and Immunity*, 71(7), 4127-4136.
- Joshi, G. S., Francis, W. C., Silverman, J. D. & Sahni, K. S.** (2004). NFkB activation suppresses host cell apoptosis during *Rickettsia rickettsii* infection via regulatory effects on intracellular localization or levels of apoptogenic and antiapoptotic proteins. *FEMS Microbiology Letters*, 234, 333-341.
- Karin, M.** (2009). NFkB as a Critical Link Between Inflammation and Cancer. *Cold Spring Harb Perspect Biol.*, a000141
- Keller, P., Schaumburg, F., Fischer, F. S., Häcker, G., Groß, U. & Lüder, K. G. C.** (2006). Direct inhibition of cytochrome c induced caspase activation in vitro by *Toxoplasma gondii* reveals novel mechanisms of interference with host cell apoptosis. *FEMS Microbiol Lett*, 258, 312-319.

- Kempf, J.A.V., Schairer, A., Neumann, D., Grassl, A. G., Lauber, K., Lebiedziejewski, M., Autenrieth, B. I.** (2005). *Bartonella henselae* inhibits apoptosis in Mono Mac 6 cells. *Cellular Microbiology*, 7(1), 91-104.
- Kojima, M., Morisaki, T., Sasaki, N., Nakano, K., Mibu, R., Tanaka, M. & Katano, M.** (2004). Increased Nuclear Factor-KB Activation in Human Colorectal Carcinoma and its Correlation with Tumor Progression. *Anticancer Research*, 24, 675-682.
- Knodler A. L., Finlay B. B. & Steele-Mortimer O.** (2005). Mechanisms of Signal Transduction: The *Salmonella* Effector Protein SopB Protects Epithelial Cells from Apoptosis by Sustained Activation of Akt. *J Biol Chem*, 280, 9058-9064.
- Lax, J. A.** (2005). Bacterial toxins and cancer- a case to answer. *Nature Reviews*, 3, 343-349.
- Lax, J. A. & Thomas, W.** (2002). How bacteria could cause cancer: one step at a time. *Trends in Microbiology*, 10(6), 293-299.
- Lee, C. H. & Goodman, L. J.** (2006). *Anaplasma phagocytophilum* causes global induction of antiapoptosis in human neutrophils. *Genomics*, 88, 496-503.
- Levine, S. D. & Haggitt, C. R.** (1989). Normal Histology of the Colon. *The American Journal of Surgical Pathology*, 13(11), 966-984.
- Lim, C. S.** (2005). CD24 and human carcinoma: tumor biological aspects. *Biomedicine and Pharmacotherapy*, 59, 351-354.
- Lu, H., Ouyang, W. & Huang, C.** (2006). Inflammation, a Key Event in Cancer Development. *Mol Cancer Res*, 4(4), 221-233.
- Mager, L. D.** (2006). Bacteria and cancer: cause, coincidence or cure? A review. *Journal of Translational Medicine*, 4(14), 1-18.
- Massari, P., Ho, Y. & Wetzler, M. L.** (2000). *Neisseria meningitidis* porin PorB interacts with mitochondria and protects cells from apoptosis. *PNAS*.97(16), 9070-9075.
- Massari, P., King, A. C., Ho, Y. A. & Wetzler, M. L.** (2003). *Neisserial* PorB is translocated to the mitochondria of HeLa cells infected with *Neisseria meningitidis* and protects cells from apoptosis. *Cellular Microbiology*, 5(2), 99-109.
- MIDI (2005).** Sherlock MIS Operating Manual. Newark, DE: MIDI
- Niu G. & Chen X.** (2010). Apoptosis Imaging: Beyond Annexin V. *J Nucl Med*, 51, 1659-1662.
- Ouyang, L., Shi, Z., Zhao, S., Wang, T. F., Zhou, T. T., Liu, B. & Bao, K. J.** (2012). Programmed cell death pathways in cancer: a review of apoptosis, autophagy and programmed necrosis. *Cell Proliferation*, 1-12.
- Parsonnet, J.** (1995). Bacterial infection as a cause of cancer. *Environ Health Perspect*, 103(Suppl 8), 263-268.

- Perez - Vazquez, M., Oliver, A., Sanchez del Saz, B., Loza, E., Baquero, F. & Canton, R.** (2001). Performance of the VITEK2 system for identification and susceptibility testing of routine *Enterobacteriaceae* clinical isolates. *International Journal of Antimicrobial Agents*, 17, 371-376.
- Pincus, H.D.** (n.d). Microbial Identification Using the Biomerieux Vitek 2 System. Encyclopedia of Rapid Microbiological Methods, retrieved from www.pda.org/bookstore, date retrieved: 15.08.2013
- Rajalingam, K., Sharma, M., Paland, N., Hurwitz, R., Thieck, O., Oswald, M., Rudel, T.** (2006). IAP-IAP Complexes Required for Apoptosis Resistance of *C.trachomatis*- Infected Cells. *PLoS Pathogens*, 2(10) e114, 1013-1023.
- Rescher, U. & Gerke, V.** (2004). Annexins-unique membrane binding proteins with diverse functions. *Journal of Cell Science*, 117(13), 2631-2639.
- Riss, T. L. & Moravec, R. A.** (1992). Comparison of MTT, XTT and a novel tetrazolium compound for MTS for in vitro proliferation and chemosensitivity assays . *Mol Biol Cell Supp*, 184 a.
- Roncucci, L. & Ponz de Leon, M.** (2000). The cause of colorectal cancer. *Digest Liver Dis*, 32, 426-439.
- Rupnarain, C., Dlamini, Z., Naicker, S. & Bhoola, K.** (2004). Colon cancer: genomics and apoptotic events. *Biol Chem* 385, 449-464.
- Sagiv, E., Memeo, L., Karin, A., Kazanov, D., Jacob-Hirsch, J., Mansukhani, M., Arber, N.** (2006). CD24 is a new oncogene, early at the multistep process of colorectal cancer carcinogenesis. *Gastroenterology*, 131, 630-639.
- Şahin, F.** (2001). Computer-aided system for cellular fatty acid analysis in identification of microorganisms isolated from environmental, industrial and clinical samples. In Proceedings of the 1st. Eurasian Congress on Molecular Biotechnology : Vol.1.(pp. 253-257). Karadeniz Technical University, Trabzon, Turkey, 17-20 October, 2001
- Sanders, E. W. & Sanders, C. C.** (1997). *Enterobacter* spp.: Pathogens poised to flourish at the turn of the century. *Clinical Microbiology Reviews*, 220-241.
- Shishodia, S. & Aggarwal, B. B.** (2004). Nuclear factor- KB : a friend or a foe in cancer? *Biochemical Pharmacology*, 68, 1071-1080.
- Sinicrope F. A., Hart J., Michelassi F. & Lee, J. J.** (1995). Prognostic value of bcl2 oncoprotein expression in stage II colon carcinoma. *Clin Cancer Res*, 1, 1103-1110.
- Snustad, P. D., & Simmons, J. M.** (2006). Principles of genetics. (4th ed.). USA: John Wiley and Sons.
- Sobolewski, C., Cerella, C., Dicato, M., Ghibelli, L., Diederich, M.** (2010). The role of cyclooxygenase-2 in cell proliferation and cell death in human malignancies. *International Journal of Cell Biology*, Article ID 215158, 21 pages

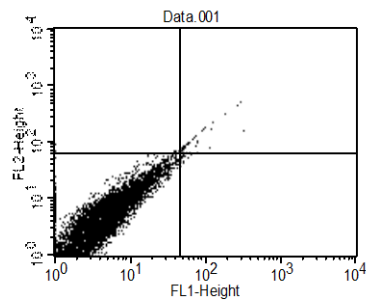
- Sohaily, S., Biankin, A., Leong R., Corish, M., & Warusavitarne, J.** (2012). Molecular pathways in colorectal cancer. *Journal of Gastroenterology and Hepatology*, 27, 1423-1431.
- Sun, Y., & Peng, L. Z** (2009). Programmed cell death cancer. *Postgrad Med J*, 85, 134-140.
- Suzuki, T., Nakanishi, K., Tsutsui, H., Iwai, H., Akira, S., Inohara, N., Sasakawa, C.** (2005). Mechanisms of Signal Transduction: A Novel Caspase 1/Toll-like Receptor 4- Independent Pathway of Cell Death Induced by Cytosolic *Shigella* in Infected Macrophages, *J Biol Chem*, 280, 14042-14050.
- Terzic, J., Grivennikov, S., Karin, E. & Karin, M.** (2010). Inflammation and colon cancer. *Gastroenterology*, 138, 2101-2114.
- Thompson J.D., Higgins D.G., & Gibson T.J.** (1994). "CLUSTAL W: improving the sensitivity of progressive multiple sequence alignment through sequence weighting, position-specific gap penalties and weight matrix choice." *Nucleic Acids Res.* 22:4673-4680
- Ullman, A. T. & Itzkowitz, H. S.** (2011). Intestinal Inflammation and cancer. *Gastroenterology*, 140, 1807-1816.
- Url-1** <<http://www.histol.chuvashia.com/atlas-en/digestive-02-en.htm>>, date retrieved 28.12.2012
- Url-2** <<http://www.lab.anhb.uwa.edu.au/mb140/CorePages/GIT/git.htm>>, date retrieved 28.12.2012
- Url-3** <<http://www.cancer.org/acs/groups/cid/documents/webcontent/003096-pdf.pdf>>, date retrieved 10.08.2013
- Url-4** <<http://www.metrohealth.org/body.cfm?id=1628>>, date retrieved 28.12.2012
- Wang, S., Liu, Z., Wang, L. & Zhang, X.** (2009). NFkB Signalling Pathway, Inflammation and Colorectal Cancer. *Cellular and Molecular Immunology*, 5(5), 327-334.
- Weisburg, G. W., Barns, M. S., Pelletier, A. D. & Lane, J. D.** (1991). 16S Ribosomal DNA Amplification for Phylogenetic Study. *Journal of Bacteriology*, 173 (2), 697-703.
- Willenbacher, F. R., Aust, E. D., Chang, G. C., Zelman, J. S., Ferrell, D. L., Moore, H. D. & Waldman, M. F.** (1999). Genomic instability is an early event during the progression pathway of ulcerative-colitis-related neoplasia. *Am J Pathol*, 154, 1825-1830.
- Wong Y. S. R.** (2011). Apoptosis in cancer: from pathogenesis to treatment. *Journal of Experimental and Clinical Cancer Research*, 30, 87
- Wright, C. S., Zhong, J. & Larrick, W. J.** (1994). Inhibition of apoptosis as a mechanism of tumor promotion. *The FASEB Journal*, 8, 654-660.
- Yanai, A., Hirata, Y., Mitsuno, Y., Maeda, S., Shibata, W., Akanuma, M., Omata, M.** (2003). *Helicobacter pylori* induces antiapoptosis through Nuclear Factor KB Activation. *The Journal of Infectious Diseases*, 188, 1741-1751.

- Zhang, J., Sinha, M., Luxon, A. B. & Yu, X.** (2004). Survival Strategy Of Obligately Intracellular *Ehrlichia chaffeensis*: Novel Modulation Of Immune Response and Host Cell Cycles. *Infection and Immunity*, 72(1), 498-507.
- Zhong, Y., Weininger, M., Pirbhai, M., Dong, F. & Zhong, G.** (2006). Inhibition of staurosporine-induced activation of the proapoptotic multidomain Bcl2 proteins Bax and Bak by three invasive chlamydial species. *Journal of Infection*, 53, 408-414.

APPENDICES

- APPENDIX A:** Detection of Apoptosis by Annexin in NCM460
- APPENDIX B :** Detection of Apoptosis by Annexin in CRL1790
- APPENDIX C:** CD24 Detection in CRL1790
- APPENDIX D:** CD24 Detection in NCM 460
- APPENDIX E:** MIS Results
- APPENDIX F :** Microbial Identification VITEK2 Results

APPENDIX A : Detection of Apoptosis by Annexin in NCM460

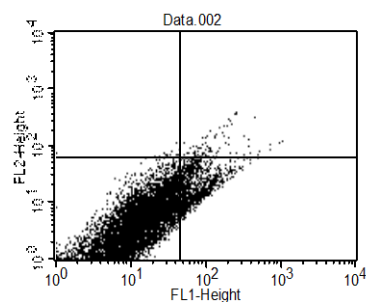


Quadrant Statistics

File: Data.001 Log Data Units: Linear Values
 Sample ID: Patient ID:
 Tube: nc Panel: Dilsad annexin
 Acquisition Date: 20-Dec-12 Gate: No Gate
 Gated Events: 10000 Total Events: 10000
 X Parameter: FL1-Height (Log) Y Parameter: FL2-Height (Log)
 Quad Location: 46, 62

Quad	Events	% Gated	% Total	X Mean	X Geo Mean	Y Mean	Y Geo Mean
UL	14	0.14	0.14	33.15	22.54	68.87	68.54
UF	45	0.45	0.45	85.31	73.73	129.88	112.63
LL	9929	99.29	99.29	4.43	2.59	5.28	2.73
LR	12	0.12	0.12	50.68	50.44	53.00	52.53

Figure A.1 : Detection of Apoptosis by Annexin in NCM460 (negative-cell without antibody).

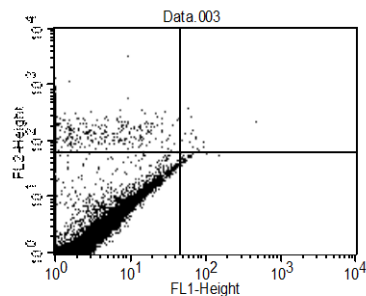


Quadrant Statistics

File: Data.002 Log Data Units: Linear Values
 Sample ID: Patient ID:
 Tube: annex Panel: Dilsad annexin
 Acquisition Date: 20-Dec-12 Gate: No Gate
 Gated Events: 10000 Total Events: 10000
 X Parameter: FL1-Height (Log) Y Parameter: FL2-Height (Log)
 Quad Location: 46, 62

Quad	Events	% Gated	% Total	X Mean	X Geo Mean	Y Mean	Y Geo Mean
UL	17	0.17	0.17	31.46	26.15	72.88	72.03
UF	94	0.94	0.94	174.25	130.72	113.35	99.67
LL	8848	88.48	88.48	13.37	8.89	5.89	3.62
LR	1041	10.41	10.41	80.25	73.27	22.74	19.33

Figure A.2 : Detection of Apoptosis by Annexin in NCM460 (only annexin).

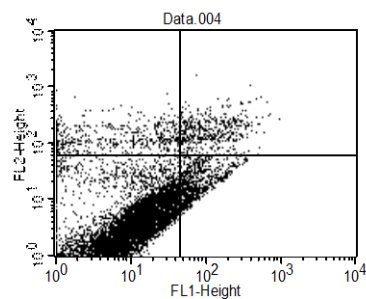


Quadrant Statistics

File: Data.003 Log Data Units: Linear Values
 Sample ID: Patient ID:
 Tube: pi Panel: Dilsad annexin
 Acquisition Date: 20-Dec-12 Gate: No Gate
 Gated Events: 10000 Total Events: 10000
 X Parameter: FL1-Height (Log) Y Parameter: FL2-Height (Log)
 Quad Location: 46, 62

Quad	Events	% Gated	% Total	X Mean	X Geo Mean	Y Mean	Y Geo Mean
UL	1251	12.51	12.51	2.42	1.38	166.36	143.31
UF	16	0.16	0.16	92.96	76.39	144.18	126.63
LL	8700	87.00	87.00	5.00	3.07	4.87	2.78
LR	33	0.33	0.33	56.97	55.05	49.60	49.18

Figure A.3 : Detection of Apoptosis by Annexin in NCM460 (only pi).

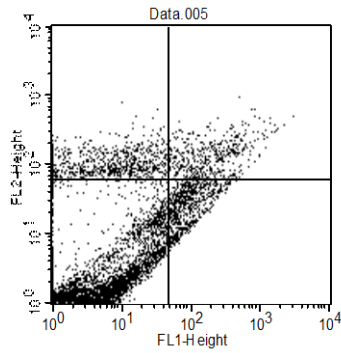


Quadrant Statistics

File: Data.004 Log Data Units: Linear Values
 Sample ID: Patient ID:
 Tube: ncm460 Panel: Dilsad annexin
 Acquisition Date: 20-Dec-12 Gate: No Gate
 Gated Events: 10000 Total Events: 10000
 X Parameter: FL1-Height (Log) Y Parameter: FL2-Height (Log)
 Quad Location: 46, 62

Quad	Events	% Gated	% Total	X Mean	X Geo Mean	Y Mean	Y Geo Mean
UL	653	6.53	6.53	11.55	4.69	142.35	127.04
UF	474	4.74	4.74	149.36	119.17	200.15	173.95
LL	8133	81.33	81.33	11.66	7.13	6.09	3.38
LR	740	7.40	7.40	87.04	77.11	23.75	20.17

Figure A.4 : Detection of Apoptosis by Annexin in NCM460 (cell before bacterial protein application).



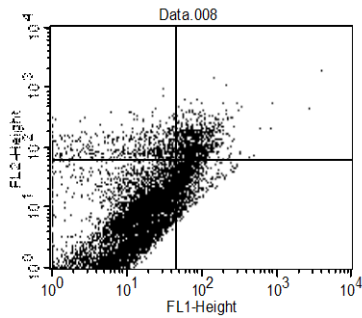
Quadrant Statistics

File: Data.005
 Sample ID:
 Tube: NCM460 3h
 Acquisition Date: 27-Dec-12
 Gated Events: 10000
 X Parameter: FL1-Height (Log)
 Quad Location: 46, 62

Log Data Units: Linear Values
 Patient ID:
 Panel: Dilsad annexin
 Gate: No Gate
 Total Events: 10000
 Y Parameter: FL2-Height (Log)

Quad	Events	% Gated	% Total	X Mean	X Geo Mean	Y Mean	Y Geo Mean
UL	862	8.62	8.62	10.07	4.98	116.76	107.37
UR	497	4.97	4.97	274.95	189.35	158.17	136.68
LL	7919	79.19	79.19	5.19	2.48	2.69	1.48
LR	722	7.22	7.22	99.12	86.47	29.09	24.47

Figure A.5 : Detection of Apoptosis by Annexin in NCM460 (after 3h protein application).



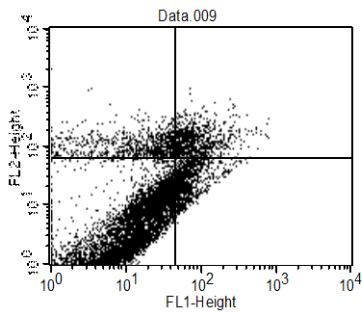
Quadrant Statistics

File: Data.008
 Sample ID:
 Tube: ncm460 HIA
 Acquisition Date: 20-Dec-12
 Gated Events: 10000
 X Parameter: FL1-Height (Log)
 Quad Location: 46, 62

Log Data Units: Linear Values
 Patient ID:
 Panel: Dilsad annexin
 Gate: No Gate
 Total Events: 10000
 Y Parameter: FL2-Height (Log)

Quad	Events	% Gated	% Total	X Mean	X Geo Mean	Y Mean	Y Geo Mean
UL	592	5.92	5.92	18.93	10.99	121.54	109.47
UR	876	8.76	8.76	100.82	85.02	146.99	127.13
LL	7570	75.70	75.70	14.02	8.68	8.53	4.53
LR	962	9.62	9.62	67.52	63.57	31.23	27.65

Figure A.6 : Detection of Apoptosis by Annexin in NCM460 (after HIA protein application).



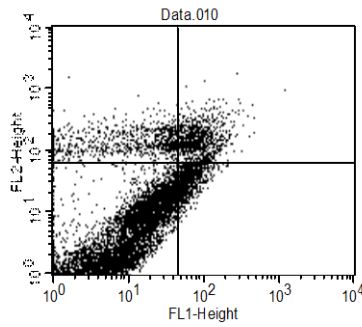
Quadrant Statistics

File: Data.009
 Sample ID:
 Tube: ncm460 huc
 Acquisition Date: 20-Dec-12
 Gated Events: 10000
 X Parameter: FL1-Height (Log)
 Quad Location: 46, 62

Log Data Units: Linear Values
 Patient ID:
 Panel: Dilsad annexin
 Gate: No Gate
 Total Events: 10000
 Y Parameter: FL2-Height (Log)

Quad	Events	% Gated	% Total	X Mean	X Geo Mean	Y Mean	Y Geo Mean
UL	915	9.15	9.15	20.12	13.16	119.56	108.05
UR	845	8.45	8.45	106.50	88.34	143.52	126.93
LL	7121	71.21	71.21	14.28	8.61	6.67	3.58
LR	1119	11.19	11.19	73.08	67.57	30.19	26.63

Figure A.7 : Detection of Apoptosis by Annexin in NCM460 (after huc2 protein application).



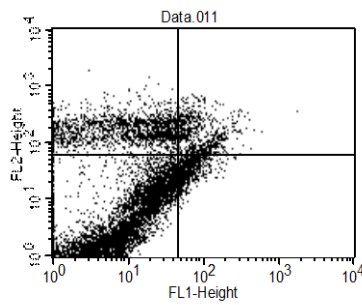
Quadrant Statistics

File: Data.010
 Sample ID:
 Tube: ncm460 de47
 Acquisition Date: 20-Dec-12
 Gated Events: 10000
 X Parameter: FL1-Height (Log)
 Quad Location: 46, 62

Log Data Units: Linear Values
 Patient ID:
 Panel: Dilsad annexin
 Gate: No Gate
 Total Events: 10000
 Y Parameter: FL2-Height (Log)

Quad	Events	% Gated	% Total	X Mean	X Geo Mean	Y Mean	Y Geo Mean
UL	850	8.50	8.50	16.60	8.69	153.55	139.17
UR	912	9.12	9.12	100.46	90.37	172.97	146.50
LL	7364	73.64	73.64	12.41	6.97	7.07	3.62
LR	874	8.74	8.74	66.50	64.07	35.01	32.10

Figure A.8 : Detection of Apoptosis by Annexin in NCM460 (after DE47 protein application).



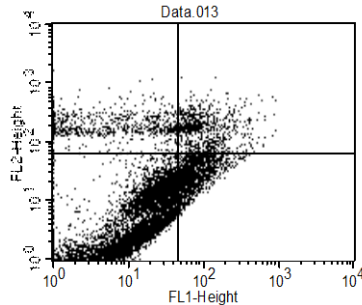
Quadrant Statistics

File: Data.011
 Sample ID:
 Tube: ncm460de256
 Acquisition Date: 20-Dec-12
 Gated Events: 10000
 X Parameter: FL1-Height (Log)
 Quad Location: 46, 62

Log Data Units: Linear Values
 Patient ID:
 Panel: Dilsad annexin
 Gate: No Gate
 Total Events: 10000
 Y Parameter: FL2-Height (Log)

Quad	Events	% Gated	% Total	X Mean	X Geo Mean	Y Mean	Y Geo Mean
UL	1726	17.26	17.26	14.93	8.12	192.01	171.11
UR	688	6.88	6.88	102.40	87.84	178.79	147.89
LL	6821	68.21	68.21	11.89	6.63	7.74	3.66
LR	765	7.65	7.65	68.34	64.91	36.75	34.17

Figure A.9 : Detection of Apoptosis by Annexin in NCM460 (after DE256 protein application).



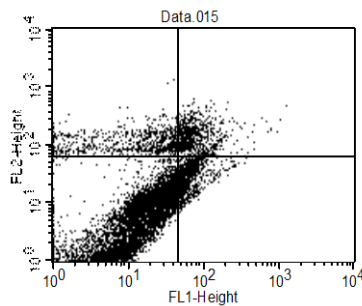
Quadrant Statistics

File: Data.013
 Sample ID:
 Tube: ncm460 de365
 Acquisition Date: 20-Dec-12
 Gated Events: 10000
 X Parameter: FL1-Height (Log)
 Quad Location: 46, 62

Log Data Units: Linear Values
 Patient ID:
 Panel: Dilsad annexin
 Gate: No Gate
 Total Events: 10000
 Y Parameter: FL2-Height (Log)

Quad	Events	% Gated	% Total	X Mean	X Geo Mean	Y Mean	Y Geo Mean
UL	783	7.83	7.83	12.71	5.98	212.87	191.16
UR	790	7.90	7.90	130.61	105.46	187.84	157.86
LL	6953	69.53	69.53	15.27	9.18	7.04	3.77
LR	1474	14.74	14.74	80.91	74.17	30.12	26.60

Figure A.10 : Detection of Apoptosis by Annexin in NCM460 (after DE365 protein application).



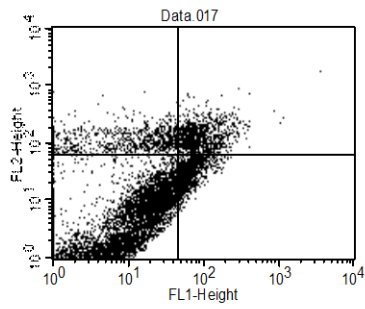
Quadrant Statistics

File: Data.015
 Sample ID:
 Tube: ncm460 de36
 Acquisition Date: 20-Dec-12
 Gated Events: 10000
 X Parameter: FL1-Height (Log)
 Quad Location: 46, 62

Log Data Units: Linear Values
 Patient ID:
 Panel: Dilsad annexin
 Gate: No Gate
 Total Events: 10000
 Y Parameter: FL2-Height (Log)

Quad	Events	% Gated	% Total	X Mean	X Geo Mean	Y Mean	Y Geo Mean
UL	854	8.54	8.54	21.34	13.27	126.51	116.16
UR	843	8.43	8.43	92.55	78.09	153.71	136.84
LL	7370	73.70	73.70	13.98	8.30	6.82	3.68
LR	933	9.33	9.33	69.78	65.60	31.33	28.10

Figure A.11 : Detection of Apoptosis by Annexin in NCM460 (after DE36 protein application).



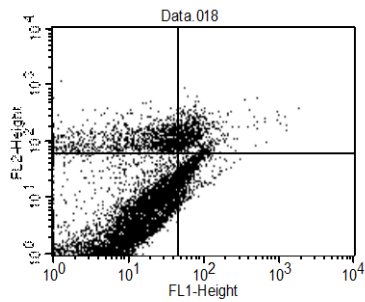
Quadrant Statistics

File: Data.017
 Sample ID:
 Tube: ncm460 de12
 Acquisition Date: 20-Dec-12
 Gated Events: 10000
 X Parameter: FL1-Height (Log)
 Quad Location: 46, 62

Log Data Units: Linear Values
 Patient ID:
 Panel: Dilsad annexin
 Gate: No Gate
 Total Events: 10000
 Y Parameter: FL2-Height (Log)

Quad	Events	% Gated	% Total	X Mean	X Geo Mean	Y Mean	Y Geo Mean
UL	896	8.96	8.96	18.08	10.69	127.86	117.32
UR	1048	10.48	10.48	108.83	92.23	150.63	133.32
LL	6862	68.62	68.62	13.12	7.14	7.15	3.54
LR	1194	11.94	11.94	70.29	67.15	33.49	30.49

Figure A.12 : Detection of Apoptosis by Annexin in NCM460 (after DE12 protein application).



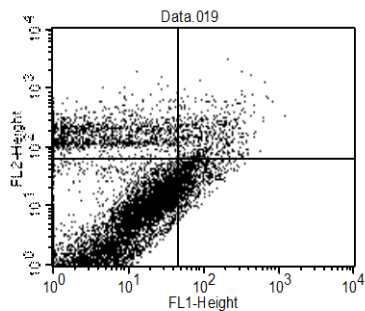
Quadrant Statistics

File: Data.018
 Sample ID:
 Tube: ncm460 de8
 Acquisition Date: 20-Dec-12
 Gated Events: 10000
 X Parameter: FL1-Height (Log)
 Quad Location: 46, 62

Log Data Units: Linear Values
 Patient ID:
 Panel: Dilsad annexin
 Gate: No Gate
 Total Events: 10000
 Y Parameter: FL2-Height (Log)

Quad	Events	% Gated	% Total	X Mean	X Geo Mean	Y Mean	Y Geo Mean
UL	1121	11.21	11.21	19.50	12.02	120.97	110.95
UR	708	7.08	7.08	99.21	78.48	151.91	134.43
LL	7403	74.03	74.03	12.98	7.84	6.02	3.23
LR	768	7.68	7.68	66.94	64.04	31.29	28.05

Figure A.13 : Detection of Apoptosis by Annexin in NCM460 (after DE8 protein application).



Quadrant Statistics

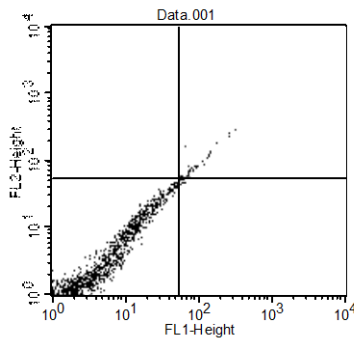
File: Data.019
 Sample ID:
 Tube: ncm460 de103
 Acquisition Date: 20-Dec-12
 Gated Events: 10000
 X Parameter: FL1-Height (Log)
 Quad Location: 46, 62

Log Data Units: Linear Values
 Patient ID:
 Panel: Dilsad annexin
 Gate: No Gate
 Total Events: 10000
 Y Parameter: FL2-Height (Log)

Quad	Events	% Gated	% Total	X Mean	X Geo Mean	Y Mean	Y Geo Mean
UL	1493	14.93	14.93	8.45	3.99	184.89	163.01
UR	532	5.32	5.32	146.88	118.14	217.89	164.94
LL	7118	71.18	71.18	12.16	6.81	8.23	4.15
LR	857	8.57	8.57	74.85	68.94	32.84	29.32

Figure A.14 : Detection of Apoptosis by Annexin in NCM460 (after DE103 protein application).

APPENDIX B : Detection of Apoptosis by Annexin in CRL1790



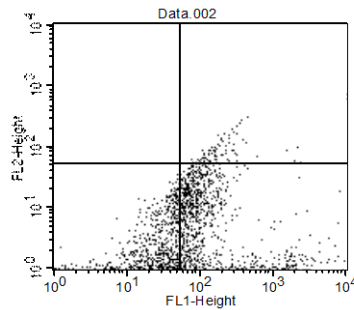
Quadrant Statistics

File: Data.001
 Sample ID:
 Tube: nc
 Acquisition Date: 21-Dec-12
 Gated Events: 10000
 X Parameter: FL1-Height (Log)
 Quad Location: 53, 53

Log Data Units: Linear Values
 Patient ID:
 Panel: Dilsad annexin
 Gate: No Gate
 Total Events: 10000
 Y Parameter: FL2-Height (Log)

Quad	Events	% Gated	% Total	X Mean	X Geo Mean	Y Mean	Y Geo Mean
UL	1	0.01	0.01	52.33	52.33	56.74	56.74
UF	43	0.43	0.43	99.24	89.81	96.40	86.45
LL	9945	99.45	99.45	1.91	1.21	1.71	1.16
LR	11	0.11	0.11	57.57	57.49	48.65	48.58

Figure B.1 : Detection of Apoptosis by Annexin in CRL1790 (negative- cell without antibody).



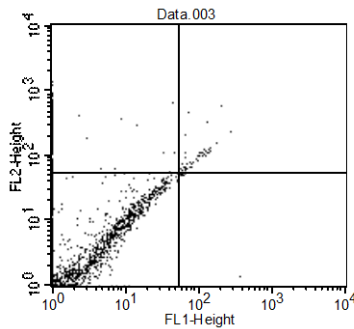
Quadrant Statistics

File: Data.002
 Sample ID:
 Tube: annex
 Acquisition Date: 21-Dec-12
 Gated Events: 10000
 X Parameter: FL1-Height (Log)
 Quad Location: 53, 53

Log Data Units: Linear Values
 Patient ID:
 Panel: Dilsad annexin
 Gate: No Gate
 Total Events: 10000
 Y Parameter: FL2-Height (Log)

Quad	Events	% Gated	% Total	X Mean	X Geo Mean	Y Mean	Y Geo Mean
UL	0	0.00	0.00	***	***	***	***
UR	87	0.87	0.87	492.75	210.51	109.22	91.50
LL	8330	83.30	83.30	8.62	3.49	1.26	1.08
LR	1583	15.83	15.83	316.07	142.33	6.85	2.61

Figure B.2 : Detection of Apoptosis by Annexin in CRL1790 (only annexin).



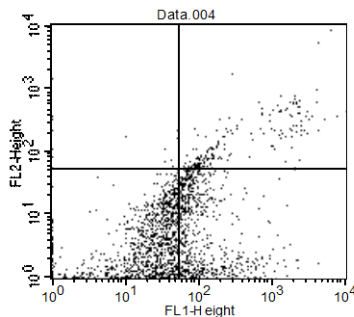
Quadrant Statistics

File: Data.003
 Sample ID:
 Tube: pi
 Acquisition Date: 21-Dec-12
 Gated Events: 10000
 X Parameter: FL1-Height (Log)
 Quad Location: 53, 53

Log Data Units: Linear Values
 Patient ID:
 Panel: Dilsad annexin
 Gate: No Gate
 Total Events: 10000
 Y Parameter: FL2-Height (Log)

Quad	Events	% Gated	% Total	X Mean	X Geo Mean	Y Mean	Y Geo Mean
UL	207	2.07	2.07	2.01	1.14	336.02	259.46
UR	43	0.43	0.43	96.60	89.66	121.40	100.55
LL	9744	97.44	97.44	1.65	1.16	2.02	1.25
LR	6	0.06	0.06	106.48	77.50	43.24	28.30

Figure B.3 : Detection of Apoptosis by Annexin in CRL1790 (only pi).



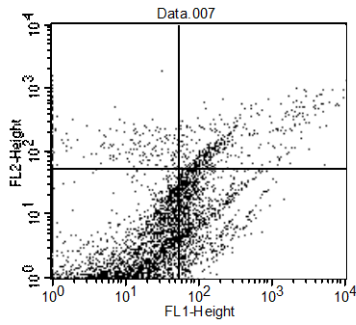
Quadrant Statistics

File: Data.004
 Sample ID:
 Tube: CRL1790
 Acquisition Date: 21-Dec-12
 Gated Events: 10000
 X Parameter: FL1-Height (Log)
 Quad Location: 53, 53

Log Data Units: Linear Values
 Patient ID:
 Panel: Dilsad annexin
 Gate: No Gate
 Total Events: 10000
 Y Parameter: FL2-Height (Log)

Quad	Events	% Gated	% Total	X Mean	X Geo Mean	Y Mean	Y Geo Mean
UL	14	0.14	0.14	19.43	5.84	247.85	154.69
UR	180	1.80	1.80	931.73	364.94	284.22	153.00
LL	8751	87.51	87.51	7.89	3.06	1.63	1.16
LR	1055	10.55	10.55	166.30	115.11	7.73	2.76

Figure B.4 : Detection of Apoptosis by Annexin in CRL1790 (cell before bacterial protein application).



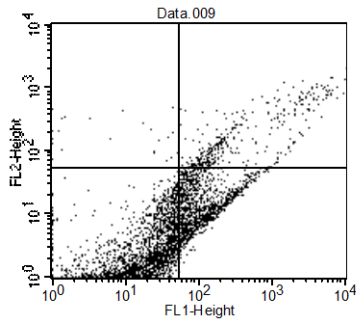
Quadrant Statistics

File: Data.007
 Sample ID:
 Tube: CRL1790 3h
 Acquisition Date: 21-Dec-12
 Gated Events: 10000
 X Parameter: FL1-Height (Log)
 Quad Location: 53, 53

Log Data Units: Linear Values
 Patient ID:
 Panel: Dilsad annexin
 Gate: No Gate
 Total Events: 10000
 Y Parameter: FL2-Height (Log)

Quad	Events	% Gated	% Total	X Mean	X Geo Mean	Y Mean	Y Geo Mean
UL	226	2.26	2.26	13.74	5.62	212.29	153.19
UF	437	4.37	4.37	708.94	255.77	192.45	139.91
LL	8253	82.53	82.53	7.52	2.91	2.40	1.38
LR	1084	10.84	10.84	124.77	97.80	16.60	10.69

Figure B.5 : Detection of Apoptosis by Annexin in CRL1790 (after 3h protein application).



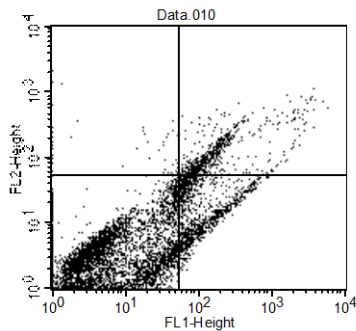
Quadrant Statistics

File: Data.009
 Sample ID:
 Tube: CRL1790 huc
 Acquisition Date: 21-Dec-12
 Gated Events: 10000
 X Parameter: FL1-Height (Log)
 Quad Location: 53, 53

Log Data Units: Linear Values
 Patient ID:
 Panel: Dilsad annexin
 Gate: No Gate
 Total Events: 10000
 Y Parameter: FL2-Height (Log)

Quad	Events	% Gated	% Total	X Mean	X Geo Mean	Y Mean	Y Geo Mean
UL	23	0.23	0.23	17.11	6.87	212.87	178.59
UF	351	3.51	3.51	1059.60	389.00	270.55	165.34
LL	8510	85.10	85.10	7.38	2.90	1.82	1.27
LR	1116	11.16	11.16	132.93	106.52	17.48	13.39

Figure B.6 : Detection of Apoptosis by Annexin in CRL1790 (after huc2 protein application).



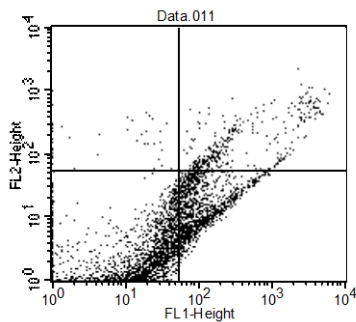
Quadrant Statistics

File: Data.010
 Sample ID:
 Tube: CRL1790 de47
 Acquisition Date: 21-Dec-12
 Gated Events: 10000
 X Parameter: FL1-Height (Log)
 Quad Location: 53, 53

Log Data Units: Linear Values
 Patient ID:
 Panel: Dilsad annexin
 Gate: No Gate
 Total Events: 10000
 Y Parameter: FL2-Height (Log)

Quad	Events	% Gated	% Total	X Mean	X Geo Mean	Y Mean	Y Geo Mean
UL	53	0.53	0.53	26.44	12.23	230.30	134.47
UF	659	6.59	6.59	349.76	179.70	153.12	119.01
LL	8227	82.27	82.27	7.45	3.35	3.06	1.78
LR	1061	10.61	10.61	126.08	99.81	21.16	15.50

Figure B.7 : Detection of Apoptosis by Annexin in CRL1790 (after DE47 protein application).



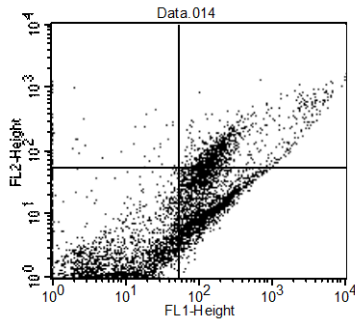
Quadrant Statistics

File: Data.011
 Sample ID:
 Tube: CRL1790 DE256
 Acquisition Date: 21-Dec-12
 Gated Events: 10000
 X Parameter: FL1-Height (Log)
 Quad Location: 53, 53

Log Data Units: Linear Values
 Patient ID:
 Panel: Dilsad annexin
 Gate: No Gate
 Total Events: 10000
 Y Parameter: FL2-Height (Log)

Quad	Events	% Gated	% Total	X Mean	X Geo Mean	Y Mean	Y Geo Mean
UL	41	0.41	0.41	13.01	5.43	219.12	172.34
UF	357	3.57	3.57	883.52	374.81	235.40	156.92
LL	8422	84.22	84.22	7.19	2.86	1.78	1.26
LR	1180	11.80	11.80	132.20	104.99	17.65	13.41

Figure B.8 : Detection of Apoptosis by Annexin in CRL1790 (after DE256 protein application).



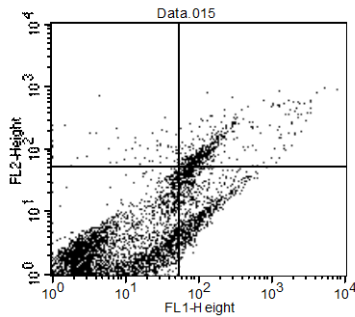
Quadrant Statistics

File: Data.014
 Sample ID:
 Tube: CRL1790 de129
 Acquisition Date: 21-Dec-12
 Gated Events: 10000
 X Parameter: FL1-Height (Log)
 Quad Location: 53, 53

Log Data Units: Linear Values
 Patient ID:
 Panel: Dilsad annexin
 Gate: No Gate
 Total Events: 10000
 Y Parameter: FL2-Height (Log)

Quad	Events	% Gated	% Total	X Mean	X Geo Mean	Y Mean	Y Geo Mean
UL	65	0.65	0.65	8.64	2.87	255.95	170.86
UF	945	9.45	9.45	648.67	273.33	172.98	122.46
LL	6837	68.37	68.37	7.48	3.74	1.89	1.31
LR	2153	21.53	21.53	139.65	116.32	20.51	15.65

Figure B.9 : Detection of Apoptosis by Annexin in CRL1790 (after DE129 protein application).



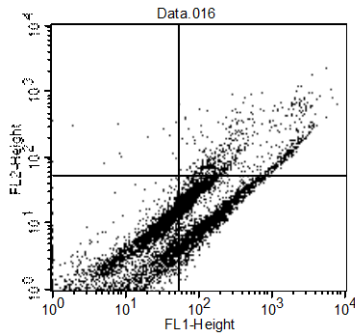
Quadrant Statistics

File: Data.015
 Sample ID:
 Tube: CRL1790 de36
 Acquisition Date: 21-Dec-12
 Gated Events: 10000
 X Parameter: FL1-Height (Log)
 Quad Location: 53, 53

Log Data Units: Linear Values
 Patient ID:
 Panel: Dilsad annexin
 Gate: No Gate
 Total Events: 10000
 Y Parameter: FL2-Height (Log)

Quad	Events	% Gated	% Total	X Mean	X Geo Mean	Y Mean	Y Geo Mean
UL	60	0.60	0.60	23.36	13.16	126.71	108.30
UR	454	4.54	4.54	347.13	163.89	145.08	111.84
LL	8659	86.59	86.59	6.15	2.58	2.28	1.45
LR	827	8.27	8.27	108.99	92.11	19.11	13.32

Figure B.10 : Detection of Apoptosis by Annexin in CRL1790 (after DE36 protein application).



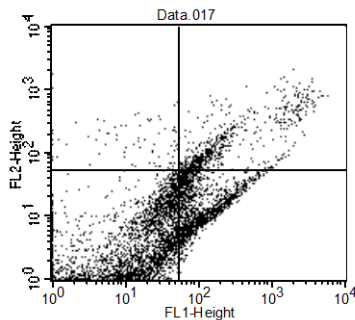
Quadrant Statistics

File: Data.016
 Sample ID:
 Tube: CRL1790 de51
 Acquisition Date: 21-Dec-12
 Gated Events: 10000
 X Parameter: FL1-Height (Log)
 Quad Location: 53, 53

Log Data Units: Linear Values
 Patient ID:
 Panel: Dilsad annexin
 Gate: No Gate
 Total Events: 10000
 Y Parameter: FL2-Height (Log)

Quad	Events	% Gated	% Total	X Mean	X Geo Mean	Y Mean	Y Geo Mean
UL	15	0.15	0.15	24.48	12.63	223.52	178.36
UF	697	6.97	6.97	876.03	468.20	184.91	129.07
LL	5840	58.40	58.40	16.75	7.96	4.73	2.64
LR	3448	34.48	34.48	132.66	107.27	21.64	17.42

Figure B.11 : Detection of Apoptosis by Annexin in CRL1790 (after DE51 protein application).



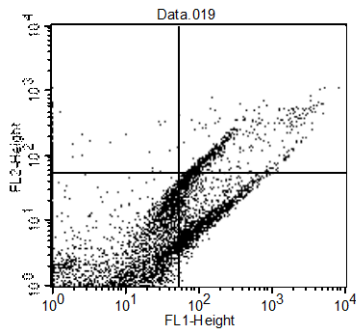
Quadrant Statistics

File: Data.017
 Sample ID:
 Tube: CRL1790 de12
 Acquisition Date: 21-Dec-12
 Gated Events: 10000
 X Parameter: FL1-Height (Log)
 Quad Location: 53, 53

Log Data Units: Linear Values
 Patient ID:
 Panel: Dilsad annexin
 Gate: No Gate
 Total Events: 10000
 Y Parameter: FL2-Height (Log)

Quad	Events	% Gated	% Total	X Mean	X Geo Mean	Y Mean	Y Geo Mean
UL	84	0.84	0.84	21.51	12.04	225.53	156.44
UF	626	6.26	6.26	618.20	259.35	236.97	150.46
LL	7802	78.02	78.02	9.06	3.48	3.18	1.60
LR	1488	14.88	14.88	128.69	102.64	19.54	15.07

Figure B.12 : Detection of Apoptosis by Annexin in CRL1790 (after DE12 protein application).



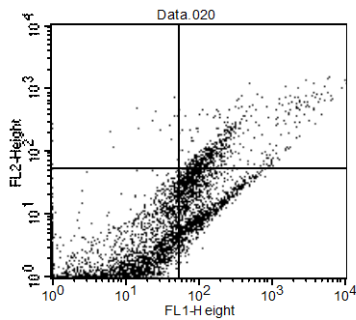
Quadrant Statistics

File: Data.019
 Sample ID:
 Tube: CRL1790 de103
 Acquisition Date: 21-Dec-12
 Gated Events: 10000
 X Parameter: FL1-Height (Log)
 Quad Location: 53, 53

Log Data Units: Linear Values
 Patient ID:
 Panel: Dilsad annexin
 Gate: No Gate
 Total Events: 10000
 Y Parameter: FL2-Height (Log)

Quad	Events	% Gated	% Total	X Mean	X Geo Mean	Y Mean	Y Geo Mean
UL	120	1.20	1.20	3.84	1.44	166.41	126.27
UR	603	6.03	6.03	569.59	251.85	170.23	126.29
LL	7797	77.97	77.97	8.96	3.20	3.68	1.81
LR	1480	14.80	14.80	134.74	106.56	18.79	14.06

Figure B.13 : Detection of Apoptosis by Annexin in CRL1790 (after DE103 protein application).



Quadrant Statistics

File: Data.020
 Sample ID:
 Tube: CRL1790 db7y
 Acquisition Date: 21-Dec-12
 Gated Events: 10000
 X Parameter: FL1-Height (Log)
 Quad Location: 53, 53

Log Data Units: Linear Values
 Patient ID:
 Panel: Dilsad annexin
 Gate: No Gate
 Total Events: 10000
 Y Parameter: FL2-Height (Log)

Quad	Events	% Gated	% Total	X Mean	X Geo Mean	Y Mean	Y Geo Mean
UL	20	0.20	0.20	25.07	11.93	246.88	193.17
UR	574	5.74	5.74	583.33	240.72	192.51	129.00
LL	7983	79.83	79.83	7.12	2.97	2.05	1.32
LR	1423	14.23	14.23	118.60	99.15	21.26	16.36

Figure B.14 : Detection of Apoptosis by Annexin in CRL1790 (after DB7Y protein application).

APPENDIX C: CD24 Detection in CRL1790

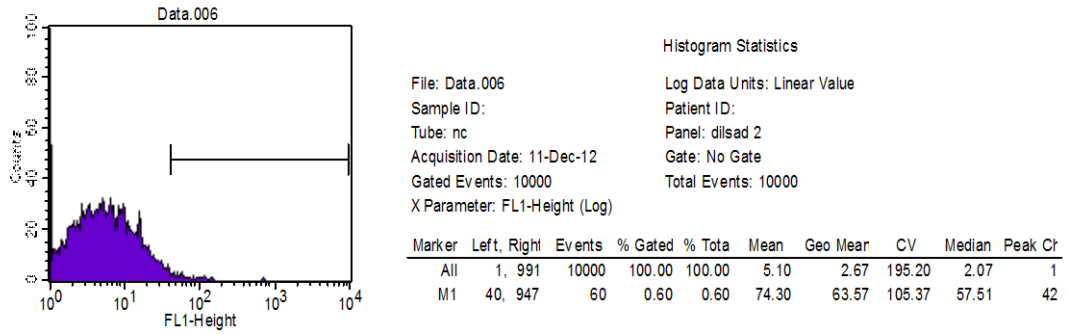


Figure C.1: CD24 Detection in CRL1790 cell line - negative (cell without antibody).

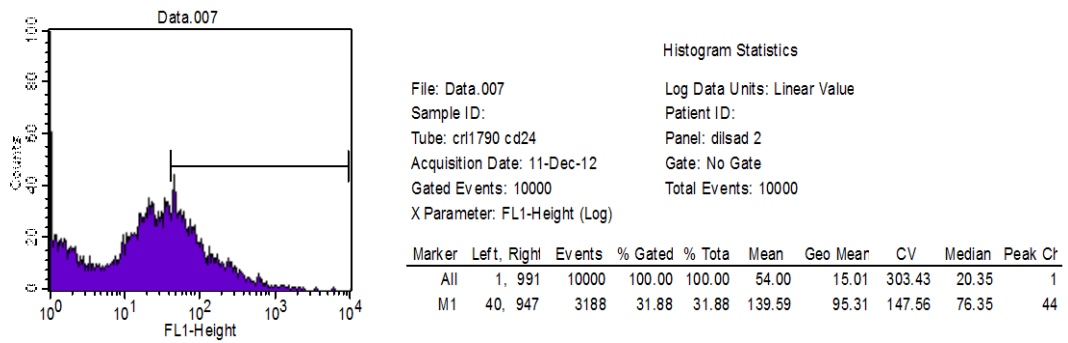


Figure C.2: CD24 Detection in CRL1790 cell line – (cell before bacterial protein application).

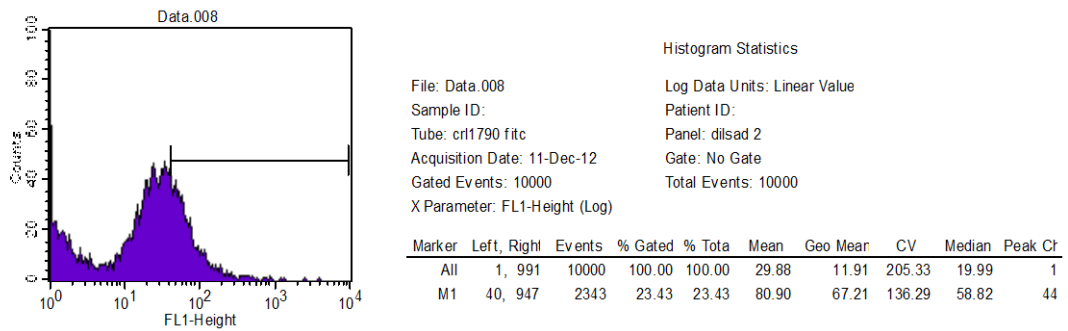
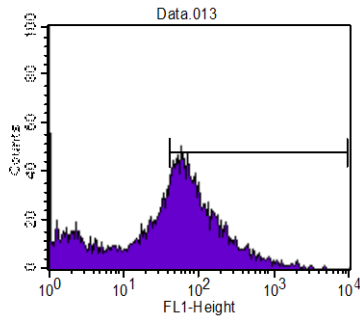


Figure C.3: CD24 Detection in CRL1790 cell line – (isotype, before bacterial protein application).

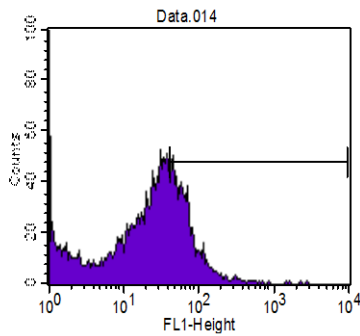


File: Data.013
 Sample ID:
 Tube: crl1790 3h cd24
 Acquisition Date: 11-Dec-12
 Gated Events: 10000
 X Parameter: FL1-Height (Log)

Histogram Statistics
 Log Data Units: Linear Value
 Patient ID:
 Panel: dilsad 2
 Gate: No Gate
 Total Events: 10000

Marker	Left, Right	Events	% Gated	% Tot	Mean	Geo Mean	CV	Median	Peak Ct
All	1, 991	10000	100.00	100.00	87.65	30.49	239.76	46.98	1
M1	40, 947	5591	55.91	55.91	142.39	99.77	135.15	82.79	53

Figure C.4: CD24 Detection in CRL1790 cell line – (after 3h bacterial protein application).

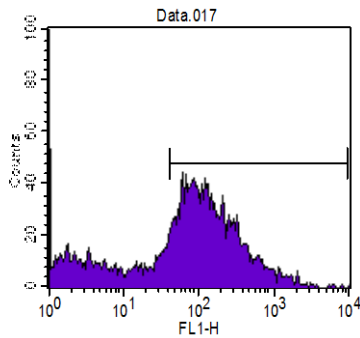


File: Data.014
 Sample ID:
 Tube: crl1790 3h fitc
 Acquisition Date: 11-Dec-12
 Gated Events: 10000
 X Parameter: FL1-Height (Log)

Histogram Statistics
 Log Data Units: Linear Value
 Patient ID:
 Panel: dilsad 2
 Gate: No Gate
 Total Events: 10000

Marker	Left, Right	Events	% Gated	% Tot	Mean	Geo Mean	CV	Median	Peak Ct
All	1, 991	10000	100.00	100.00	31.59	14.49	167.44	22.88	1
M1	40, 947	2782	27.82	27.82	74.33	64.66	113.54	58.29	43

Figure C.5: CD24 Detection in CRL1790 cell line – (isotype after 3h bacterial protein application).

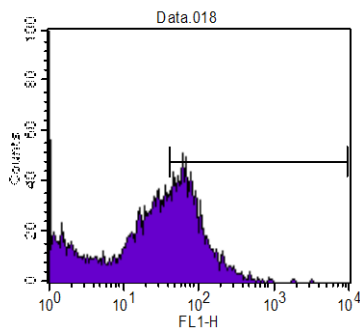


File: Data.017
 Sample ID:
 Tube: crl1790 huc cd24
 Acquisition Date: 11-Dec-12
 Gated Events: 10000
 X Parameter: FL1-H (Log)

Histogram Statistics
 Log Data Units: Linear Value
 Patient ID:
 Panel: dilsad 2
 Gate: No Gate
 Total Events: 10000

Marker	Left, Right	Events	% Gated	% Tot	Mean	Geo Mean	CV	Median	Peak Ct
All	1, 991	10000	100.00	100.00	158.39	52.79	207.72	79.15	1
M1	40, 947	6990	69.90	69.90	217.71	141.82	146.73	122.98	58

Figure C.6: CD24 Detection in CRL1790 cell line – (after huc2 bacterial protein application).

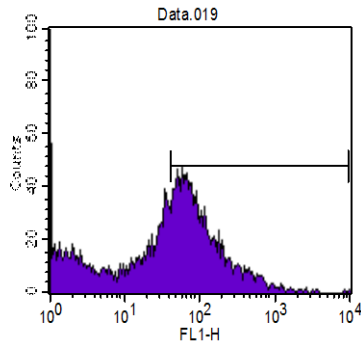


File: Data.018
 Sample ID:
 Tube: crl1790 huc fitc
 Acquisition Date: 11-Dec-12
 Gated Events: 10000
 X Parameter: FL1-H (Log)

Histogram Statistics
 Log Data Units: Linear Value
 Patient ID:
 Panel: dilsad 2
 Gate: No Gate
 Total Events: 10000

Marker	Left, Right	Events	% Gated	% Tot	Mean	Geo Mean	CV	Median	Peak Ct
All	1, 991	10000	100.00	100.00	44.46	19.26	149.98	28.39	1
M1	40, 947	3931	39.31	39.31	90.82	77.18	95.63	69.16	57

Figure C.7: CD24 Detection in CRL1790 cell line – (isotype after huc bacterial protein application)

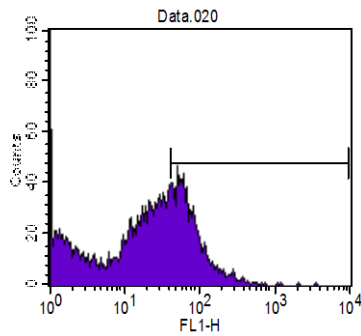


File: Data.019
 Sample ID:
 Tube: crl1790 de256 cd24
 Acquisition Date: 11-Dec-12
 Gated Events: 10000
 X Parameter: FL1-H (Log)

Log Data Units: Linear Value
 Patient ID:
 Panel: dilsad 2
 Gate: No Gate
 Total Events: 10000

Marker	Left, Right	Events	% Gated	% Tot	Mean	Geo Mean	CV	Median	Peak Cr
All	1, 991	10000	100.00	100.00	83.11	27.21	259.80	44.11	1
M1	40, 947	5299	52.99	52.99	143.16	98.56	173.49	80.58	54

Figure C.8: CD24 Detection in CRL1790 cell line – (after DE256 bacterial protein application).

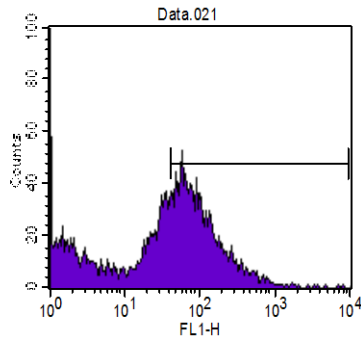


File: Data.020
 Sample ID:
 Tube: crl1790 de256 fitc
 Acquisition Date: 11-Dec-12
 Gated Events: 10000
 X Parameter: FL1-H (Log)

Log Data Units: Linear Value
 Patient ID:
 Panel: dilsad 2
 Gate: No Gate
 Total Events: 10000

Marker	Left, Right	Events	% Gated	% Tot	Mean	Geo Mean	CV	Median	Peak Cr
All	1, 991	10000	100.00	100.00	34.41	13.39	170.87	21.19	1
M1	40, 947	3108	31.08	31.08	81.96	70.27	105.73	62.64	48

Figure C.9: CD24 Detection in CRL1790 cell line – (isotype after DE256 bacterial protein application).

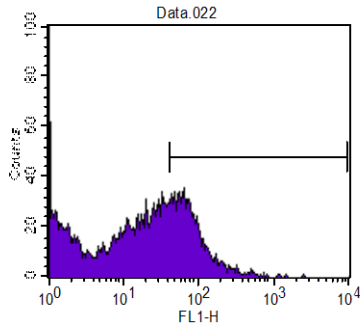


File: Data.021
 Sample ID:
 Tube: crl1790 de36 cd24
 Acquisition Date: 11-Dec-12
 Gated Events: 10000
 X Parameter: FL1-H (Log)

Log Data Units: Linear Value
 Patient ID:
 Panel: dilsad 2
 Gate: No Gate
 Total Events: 10000

Marker	Left, Right	Events	% Gated	% Tot	Mean	Geo Mean	CV	Median	Peak Cr
All	1, 991	10000	100.00	100.00	76.33	25.75	279.26	41.42	1
M1	40, 947	5097	50.97	50.97	132.52	96.53	158.50	83.54	55

Figure C.10: CD24 Detection in CRL1790 cell line – (after DE36 bacterial protein application).

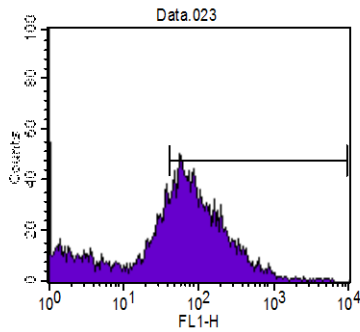


File: Data.022
 Sample ID:
 Tube: cri1790 de36 fitc
 Acquisition Date: 11-Dec-12
 Gated Events: 10000
 X Parameter: FL1-H (Log)

Log Data Units: Linear Value
 Patient ID:
 Panel: dilsad 2
 Gate: No Gate
 Total Events: 10000

Marker	Left, Right	Events	% Gated	% Tota	Mean	Geo Mear	CV	Median	Peak Ct
All	1, 991	10000	100.00	100.00	34.05	11.34	333.89	16.25	1
M1	40, 947	2872	28.72	28.72	87.15	74.18	93.18	66.12	59

Figure C.11: CD24 Detection in CRL1790 cell line – (isotype after DE36 bacterial protein application).

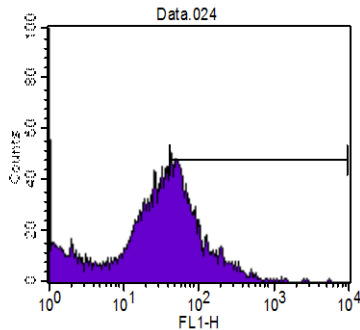


File: Data.023
 Sample ID:
 Tube: cri1790 de51 cd24
 Acquisition Date: 11-Dec-12
 Gated Events: 10000
 X Parameter: FL1-H (Log)

Log Data Units: Linear Value
 Patient ID:
 Panel: dilsad 2
 Gate: No Gate
 Total Events: 10000

Marker	Left, Right	Events	% Gated	% Tota	Mean	Geo Mear	CV	Median	Peak Ct
All	1, 991	10000	100.00	100.00	105.33	37.77	221.13	55.23	1
M1	40, 947	6138	61.38	61.38	160.90	109.19	157.61	92.22	51

Figure C.12: CD24 Detection in CRL1790 cell line – (after DE51 bacterial protein application).

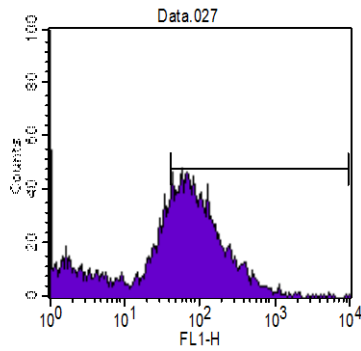


File: Data.024
 Sample ID:
 Tube: cri1790 de51 fitc
 Acquisition Date: 11-Dec-12
 Gated Events: 10000
 X Parameter: FL1-H (Log)

Log Data Units: Linear Value
 Patient ID:
 Panel: dilsad 2
 Gate: No Gate
 Total Events: 10000

Marker	Left, Right	Events	% Gated	% Tota	Mean	Geo Mear	CV	Median	Peak Ct
All	1, 991	10000	100.00	100.00	48.10	21.04	192.21	29.96	1
M1	40, 947	3831	38.31	38.31	99.10	77.81	134.79	64.94	40

Figure C.13: CD24 Detection in CRL1790 cell line – (isotype after DE51 bacterial protein application).

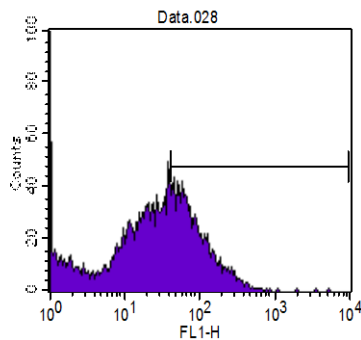


File: Data.027
 Sample ID:
 Tube: cr1790 de103 cd24
 Acquisition Date: 11-Dec-12
 Gated Events: 10000
 X Parameter: FL1-H (Log)

Log Data Units: Linear Value
 Patient ID:
 Panel: dilsad 2
 Gate: No Gate
 Total Events: 10000

Marker	Left, Right	Events	% Gated	% Tot	Mean	Geo Mean	CV	Median	Peak Ct
All	1, 991	10000	100.00	100.00	100.52	37.62	261.85	54.74	1
M1	40, 947	6201	62.01	62.01	149.83	103.95	181.79	88.17	55

Figure C.14: CD24 Detection in CRL1790 cell line – (after DE103 bacterial protein application)

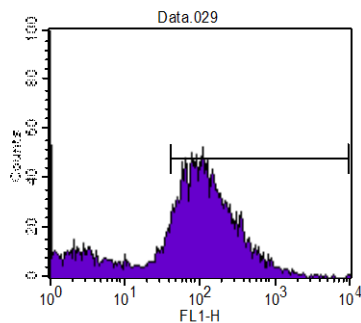


File: Data.028
 Sample ID:
 Tube: cr1790 de103 fitc
 Acquisition Date: 11-Dec-12
 Gated Events: 10000
 X Parameter: FL1-H (Log)

Log Data Units: Linear Value
 Patient ID:
 Panel: dilsad 2
 Gate: No Gate
 Total Events: 10000

Marker	Left, Right	Events	% Gated	% Tot	Mean	Geo Mean	CV	Median	Peak Ct
All	1, 991	10000	100.00	100.00	44.96	19.17	181.90	25.95	1
M1	40, 947	3666	36.66	36.66	97.29	79.96	120.20	69.16	42

Figure C.15: CD24 Detection in CRL1790 cell line – (isotype after DE103 bacterial protein application).

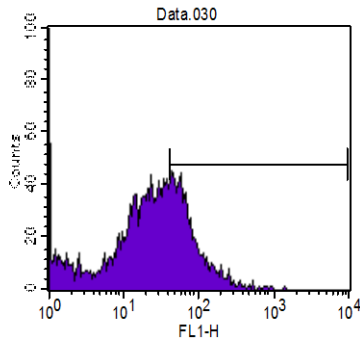


File: Data.029
 Sample ID:
 Tube: cr1790 de129 cd24
 Acquisition Date: 11-Dec-12
 Gated Events: 10000
 X Parameter: FL1-H (Log)

Log Data Units: Linear Value
 Patient ID:
 Panel: dilsad 2
 Gate: No Gate
 Total Events: 10000

Marker	Left, Right	Events	% Gated	% Tot	Mean	Geo Mean	CV	Median	Peak Ct
All	1, 991	10000	100.00	100.00	146.79	57.99	221.44	83.54	1
M1	40, 947	7461	74.61	74.61	187.60	129.68	153.98	114.44	104

Figure C.16: CD24 Detection in CRL1790 cell line – (after DE129 bacterial protein application).

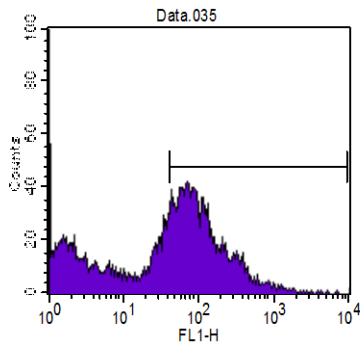


File: Data.030
 Sample ID:
 Tube: cri1790 de129 fitc
 Acquisition Date: 11-Dec-12
 Gated Events: 10000
 X Parameter: FL1-H (Log)

Log Data Units: Linear Value
 Patient ID:
 Panel: dilsad 2
 Gate: No Gate
 Total Events: 10000

Marker	Left, Right	Events	% Gated	% Tota	Mean	Geo Mear	CV	Median	Peak Ct
All	1, 991	10000	100.00	100.00	34.48	16.51	133.22	22.88	1
M1	40, 947	3005	30.05	30.05	78.98	68.47	78.76	59.89	41

Figure C.17: CD24 Detection in CRL1790 cell line – (isotype after DE129 bacterial protein application).

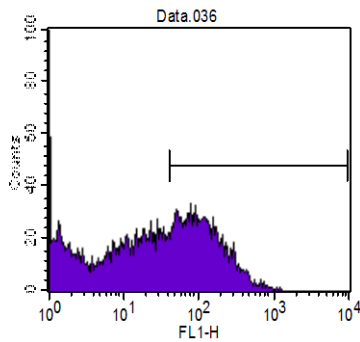


File: Data.035
 Sample ID:
 Tube: cri1790 de12 cd24
 Acquisition Date: 11-Dec-12
 Gated Events: 10000
 X Parameter: FL1-H (Log)

Log Data Units: Linear Value
 Patient ID:
 Panel: dilsad 2
 Gate: No Gate
 Total Events: 10000

Marker	Left, Right	Events	% Gated	% Tota	Mean	Geo Mear	CV	Median	Peak Ct
All	1, 991	10000	100.00	100.00	91.39	26.06	289.62	46.98	1
M1	40, 947	5465	54.65	54.65	150.92	105.86	146.05	89.77	66

Figure C.18: CD24 Detection in CRL1790 cell line – (after DE12 bacterial protein application).

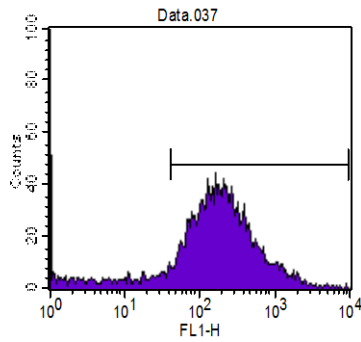


File: Data.036
 Sample ID:
 Tube: cri1790 de12 fitc
 Acquisition Date: 11-Dec-12
 Gated Events: 10000
 X Parameter: FL1-H (Log)

Log Data Units: Linear Value
 Patient ID:
 Panel: dilsad 2
 Gate: No Gate
 Total Events: 10000

Marker	Left, Right	Events	% Gated	% Tota	Mean	Geo Mear	CV	Median	Peak Ct
All	1, 991	10000	100.00	100.00	61.12	19.00	146.28	25.37	1
M1	40, 947	4174	41.74	41.74	131.40	105.96	78.01	99.55	72

Figure C.19: CD24 Detection in CRL1790 cell line – (isotype after DE12 bacterial protein application).

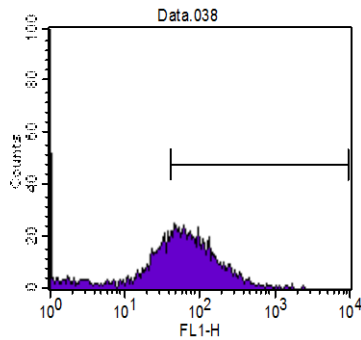


File: Data.037
Sample ID:
Tube: crl1790 de47 cd24
Acquisition Date: 11-Dec-12
Gated Events: 7980
X Parameter: FL1-H (Log)

Log Data Units: Linear Value
Patient ID:
Panel: dilsad 2
Gate: No Gate
Total Events: 7980

Marker	Left, Right	Events	% Gated	% Total	Mean	Geo Mean	CV	Median	Peak Ct
All	1, 991	7980	100.00	100.00	279.65	133.68	162.40	161.08	1
M1	40, 947	7072	88.62	88.62	311.33	201.31	142.63	184.34	151

Figure C.20: CD24 Detection in CRL1790 cell line – (after DE47 bacterial protein application)

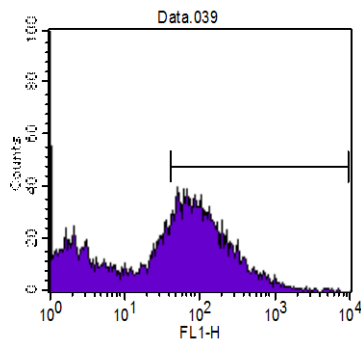


File: Data.038
Sample ID:
Tube: crl1790 de47 fitc
Acquisition Date: 11-Dec-12
Gated Events: 4155
X Parameter: FL1-H (Log)

Log Data Units: Linear Value
Patient ID:
Panel: dilsad 2
Gate: No Gate
Total Events: 4155

Marker	Left, Right	Events	% Gated	% Total	Mean	Geo Mean	CV	Median	Peak Ct
All	1, 991	4155	100.00	100.00	80.26	44.53	124.44	53.76	1
M1	40, 947	2613	62.89	62.89	115.59	92.49	96.35	82.05	43

Figure C.21: CD24 Detection in CRL1790 cell line – (isotype after DE47 bacterial protein application)

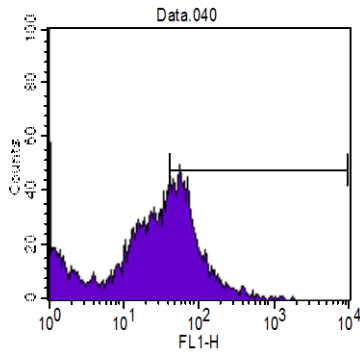


File: Data.039
Sample ID:
Tube: crl1790 db7y cd24
Acquisition Date: 11-Dec-12
Gated Events: 10000
X Parameter: FL1-H (Log)

Log Data Units: Linear Value
Patient ID:
Panel: dilsad 2
Gate: No Gate
Total Events: 10000

Marker	Left, Right	Events	% Gated	% Total	Mean	Geo Mean	CV	Median	Peak Ct
All	1, 991	10000	100.00	100.00	103.33	29.62	233.06	49.14	1
M1	40, 947	5603	56.03	56.03	173.93	116.28	157.01	100.00	47

Figure C.22: CD24 Detection in CRL1790 cell line – (after DB7Y bacterial protein application).



File: Data.040
 Sample ID:
 Tube: cr1790 db7y fitc
 Acquisition Date: 11-Dec-12
 Gated Events: 10000
 X Parameter: FL1-H (Log)

Histogram Statistics
 Log Data Units: Linear Value
 Patient ID:
 Panel: dilsad 2
 Gate: No Gate
 Total Events: 10000

Marker	Left, Right	Events	% Gated	% Tota	Mean	Geo Mear	CV	Median	Peak Ct
All	1, 991	10000	100.00	100.00	40.13	16.56	148.57	25.71	1
M1	40, 947	3594	35.94	35.94	86.44	73.01	91.59	64.36	51

Figure C.23: CD24 Detection in CRL1790 cell line – (isotype after DB7Y bacterial protein application).

APPENDIX D: CD24 Detection in NCM460

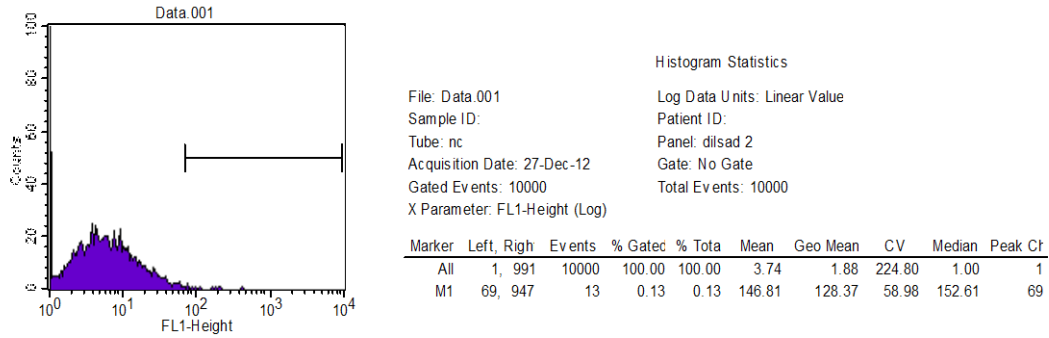


Figure D.1: CD24 Detection in NCM 460 cell line (negative : cell without antibody).

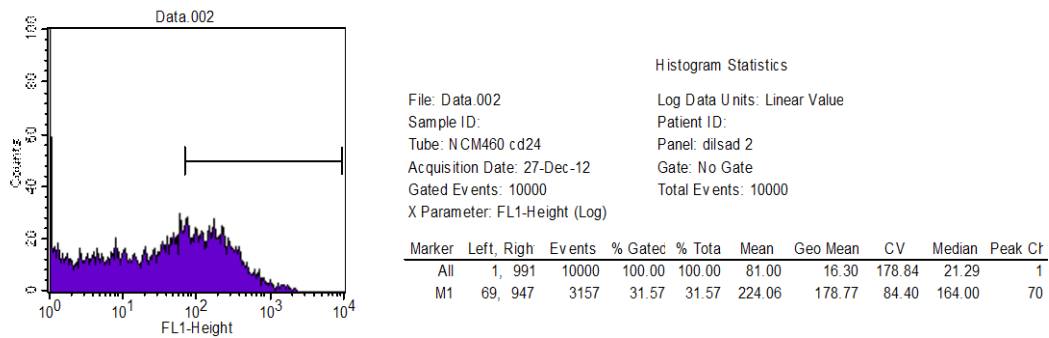


Figure D.2: CD24 Detection in NCM 460 cell line – (cell before bacterial protein application).

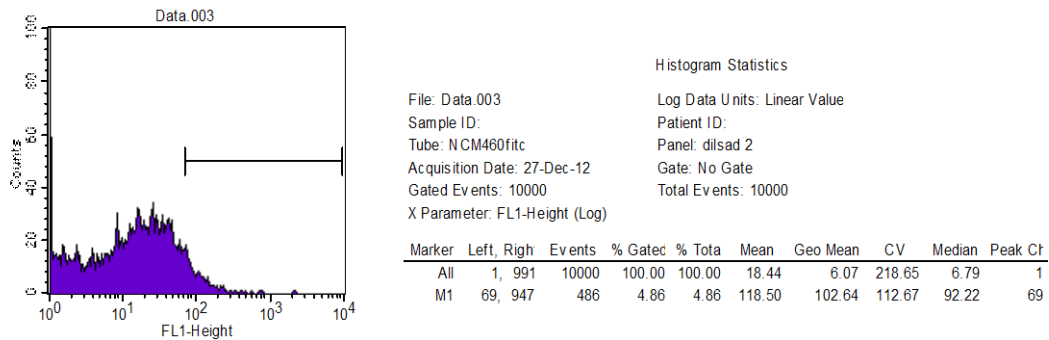
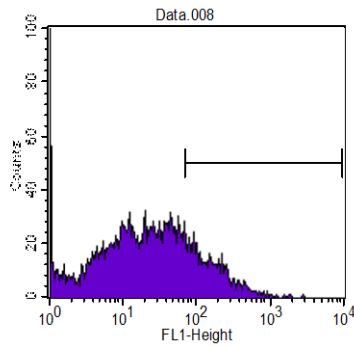


Figure D.3: CD24 Detection in NCM 460 cell line (isotype, before bacterial protein application).

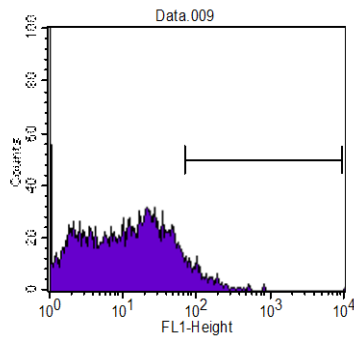


File: Data.008
 Sample ID:
 Tube: NCM460 3h cd24
 Acquisition Date: 27-Dec-12
 Gated Events: 10000
 X Parameter: FL1-Height (Log)

Log Data Units: Linear Value
 Patient ID:
 Panel: dilsad 2
 Gate: No Gate
 Total Events: 10000

Marker	Left, Right	Events	% Gatec	% Tota	Mean	Geo Mean	CV	Median	Peak Ct
All	1, 991	10000	100.00	100.00	42.93	12.39	195.55	14.46	1
M1	69, 947	1694	16.94	16.94	171.30	142.72	82.99	130.97	85

Figure D.4: CD24 Detection in NCM 460 cell line (after 3h bacterial protein application).

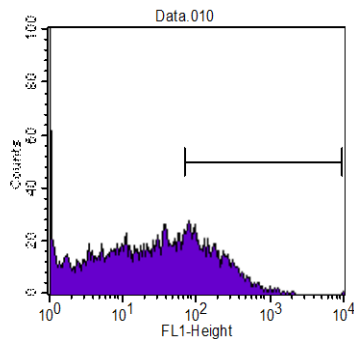


File: Data.009
 Sample ID:
 Tube: NCM460 3h fitc
 Acquisition Date: 27-Dec-12
 Gated Events: 10000
 X Parameter: FL1-Height (Log)

Log Data Units: Linear Value
 Patient ID:
 Panel: dilsad 2
 Gate: No Gate
 Total Events: 10000

Marker	Left, Right	Events	% Gatec	% Tota	Mean	Geo Mean	CV	Median	Peak Ct
All	1, 991	10000	100.00	100.00	18.78	6.37	519.75	6.26	1
M1	69, 947	478	4.78	4.78	142.21	111.40	297.50	97.34	94

Figure D.5: CD24 Detection in NCM 460 cell line (isotype after 3h bacterial protein application).

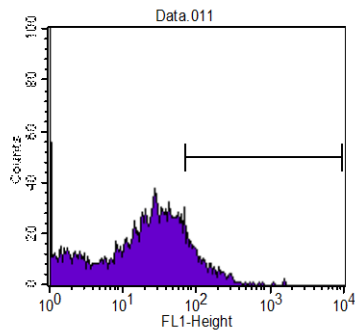


File: Data.010
 Sample ID:
 Tube: NCM460 HIA cd24
 Acquisition Date: 27-Dec-12
 Gated Events: 10000
 X Parameter: FL1-Height (Log)

Log Data Units: Linear Value
 Patient ID:
 Panel: dilsad 2
 Gate: No Gate
 Total Events: 10000

Marker	Left, Right	Events	% Gatec	% Tota	Mean	Geo Mean	CV	Median	Peak Ct
All	1, 991	10000	100.00	100.00	60.08	13.22	238.01	15.12	1
M1	69, 947	2449	24.49	24.49	199.16	158.33	119.74	144.60	72

Figure D.6: CD24 Detection in NCM 460 cell line (after HIA bacterial protein application).

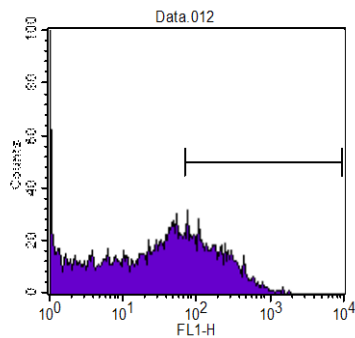


File: Data.011
 Sample ID:
 Tube: NCM460 HIA fitc
 Acquisition Date: 27-Dec-12
 Gated Events: 10000
 X Parameter: FL1-Height (Log)

Log Data Units: Linear Value
 Patient ID:
 Panel: dilsad 2
 Gate: No Gate
 Total Events: 10000

Marker	Left, Right	Events	% Gated	% Tota	Mean	Geo Mean	CV	Median	Peak Ct
All	1, 991	10000	100.00	100.00	25.66	7.53	179.68	10.09	1
M1	69, 947	931	9.31	9.31	125.66	111.51	74.10	99.10	70

Figure D.7: CD24 Detection in NCM 460 cell line (isotype after HIA bacterial protein application).

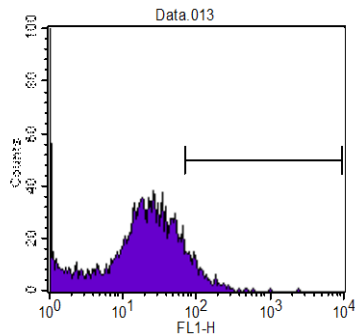


File: Data.012
 Sample ID:
 Tube: NCM460 huc c d24
 Acquisition Date: 27-Dec-12
 Gated Events: 10000
 X Parameter: FL1-H (Log)

Log Data Units: Linear Value
 Patient ID:
 Panel: dilsad 2
 Gate: No Gate
 Total Events: 10000

Marker	Left, Right	Events	% Gated	% Tota	Mean	Geo Mean	CV	Median	Peak Ct
All	1, 991	10000	100.00	100.00	62.55	12.92	180.83	16.55	1
M1	69, 947	2605	26.05	26.05	197.52	161.20	77.56	147.22	71

Figure D.8: CD24 Detection in NCM 460 cell line (after huc2 bacterial protein application).

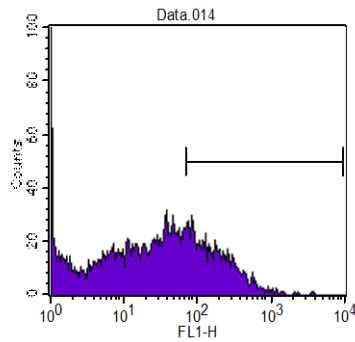


File: Data.013
 Sample ID:
 Tube: NCM460huc fitc
 Acquisition Date: 27-Dec-12
 Gated Events: 10000
 X Parameter: FL1-H (Log)

Log Data Units: Linear Value
 Patient ID:
 Panel: dilsad 2
 Gate: No Gate
 Total Events: 10000

Marker	Left, Right	Events	% Gated	% Tota	Mean	Geo Mean	CV	Median	Peak Ct
All	1, 991	10000	100.00	100.00	19.94	6.51	187.16	9.82	1
M1	69, 947	588	5.88	5.88	111.54	100.96	91.66	91.81	72

Figure D.9: CD24 Detection in NCM 460 cell line (isotype, after huc2 bacterial protein application).

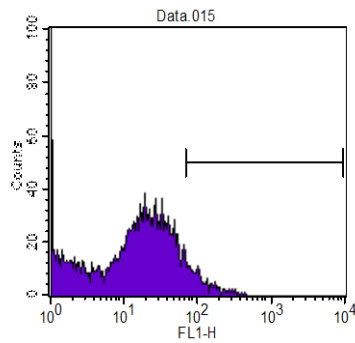


File: Data.014
 Sample ID:
 Tube: NCM460 de256 cd24
 Acquisition Date: 27-Dec-12
 Gated Events: 10000
 X Parameter: FL1-H (Log)

Log Data Units: Linear Value
 Patient ID:
 Panel: dilsad 2
 Gate: No Gate
 Total Events: 10000

Marker	Left	Right	Events	% Gated	% Tota	Mean	Geo Mean	CV	Median	Peak Ct
All	1	991	10000	100.00	100.00	58.16	13.61	197.06	17.00	1
M1	69	947	2373	23.73	23.73	193.48	156.72	89.89	143.30	78

Figure D.10: CD24 Detection in NCM 460 cell line (after DE256 bacterial protein application).

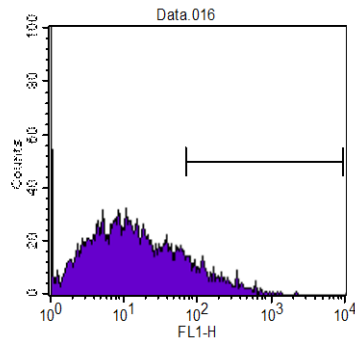


File: Data.015
 Sample ID:
 Tube: NCM460 de256 fitc
 Acquisition Date: 27-Dec-12
 Gated Events: 10000
 X Parameter: FL1-H (Log)

Log Data Units: Linear Value
 Patient ID:
 Panel: dilsad 2
 Gate: No Gate
 Total Events: 10000

Marker	Left	Right	Events	% Gated	% Tota	Mean	Geo Mean	CV	Median	Peak Ct
All	1	991	10000	100.00	100.00	17.94	6.00	155.88	7.67	1
M1	69	947	471	4.71	4.71	110.57	102.88	44.86	92.22	70

Figure D.11: CD24 Detection in NCM 460 cell line (isotype after DE256 bacterial protein application).

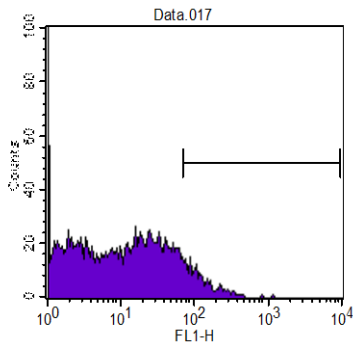


File: Data.016
 Sample ID:
 Tube: NCM460 de36 cd24
 Acquisition Date: 27-Dec-12
 Gated Events: 10000
 X Parameter: FL1-H (Log)

Log Data Units: Linear Value
 Patient ID:
 Panel: dilsad 2
 Gate: No Gate
 Total Events: 10000

Marker	Left	Right	Events	% Gated	% Tota	Mean	Geo Mean	CV	Median	Peak Ct
All	1	991	10000	100.00	100.00	27.43	7.24	432.07	6.98	1
M1	69	947	902	9.02	9.02	173.31	142.58	84.60	123.54	69

Figure D.12: CD24 Detection in NCM 460 cell line (after DE36 bacterial protein application).

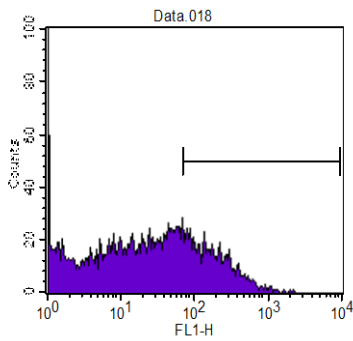


File: Data.017
 Sample ID:
 Tube: NCM460 de36 fitc
 Acquisition Date: 27-Dec-12
 Gated Events: 10000
 X Parameter: FL1-H (Log)

Log Data Units: Linear Value
 Patient ID:
 Panel: dilsad 2
 Gate: No Gate
 Total Events: 10000

Marker	Left, Right	Events	% Gated	% Total	Mean	Geo Mean	CV	Median	Peak Ct
All	1, 991	10000	100.00	100.00	17.94	5.39	192.61	4.00	1
M1	69, 947	597	5.97	5.97	120.13	109.16	59.58	99.10	79

Figure D.13: CD24 Detection in NCM 460 cell line (isotype, after DE36 bacterial protein application).

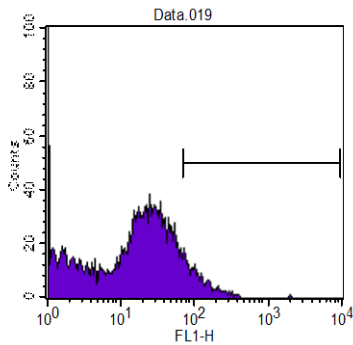


File: Data.018
 Sample ID:
 Tube: NCM460 de51 cd24
 Acquisition Date: 27-Dec-12
 Gated Events: 10000
 X Parameter: FL1-H (Log)

Log Data Units: Linear Value
 Patient ID:
 Panel: dilsad 2
 Gate: No Gate
 Total Events: 10000

Marker	Left, Right	Events	% Gated	% Total	Mean	Geo Mean	CV	Median	Peak Ct
All	1, 991	10000	100.00	100.00	56.45	13.41	185.75	16.11	1
M1	69, 947	2323	23.23	23.23	190.49	155.82	79.25	142.02	73

Figure D.14: CD24 Detection in NCM 460 cell line (after DE51 bacterial protein application).

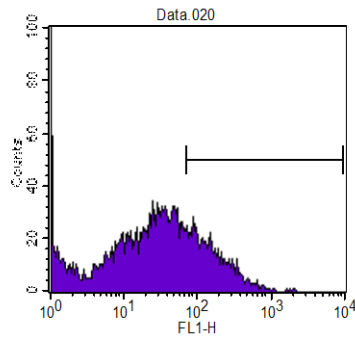


File: Data.019
 Sample ID:
 Tube: NCM460 de51 fitc
 Acquisition Date: 27-Dec-12
 Gated Events: 10000
 X Parameter: FL1-H (Log)

Log Data Units: Linear Value
 Patient ID:
 Panel: dilsad 2
 Gate: No Gate
 Total Events: 10000

Marker	Left, Right	Events	% Gated	% Total	Mean	Geo Mean	CV	Median	Peak Ct
All	1, 991	10000	100.00	100.00	20.66	6.88	171.00	9.73	1
M1	69, 947	597	5.97	5.97	115.31	105.43	72.35	94.75	69

Figure D.15: CD24 Detection in NCM 460 cell line (isotype, after DE51 bacterial protein application).

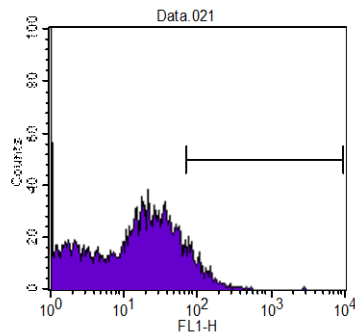


File: Data.020
 Sample ID:
 Tube: NCM460 de365 cd24
 Acquisition Date: 27-Dec-12
 Gated Events: 10000
 X Parameter: FL1-H (Log)

Log Data Units: Linear Value
 Patient ID:
 Panel: dilsad 2
 Gate: No Gate
 Total Events: 10000

Marker	Left, Right	Events	% Gated	% Tota	Mean	Geo Mean	CV	Median	Peak Ct
All	1, 991	10000	100.00	100.00	49.08	14.33	176.69	19.99	1
M1	69, 947	2068	20.68	20.68	167.69	140.95	78.42	128.64	79

Figure D.16: CD24 Detection in NCM 460 cell line (after DE365 bacterial protein application).

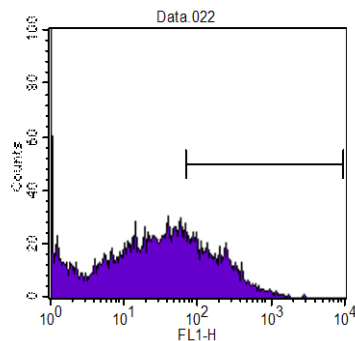


File: Data.021
 Sample ID:
 Tube: NCM460 de365 fitc
 Acquisition Date: 27-Dec-12
 Gated Events: 10000
 X Parameter: FL1-H (Log)

Log Data Units: Linear Value
 Patient ID:
 Panel: dilsad 2
 Gate: No Gate
 Total Events: 10000

Marker	Left, Right	Events	% Gated	% Tota	Mean	Geo Mean	CV	Median	Peak Ct
All	1, 991	10000	100.00	100.00	19.81	6.65	198.20	7.70	1
M1	69, 947	593	5.93	5.93	114.67	103.27	96.42	93.06	69

Figure D.17: CD24 Detection in NCM 460 cell line (isotype, after DE365 bacterial protein application).

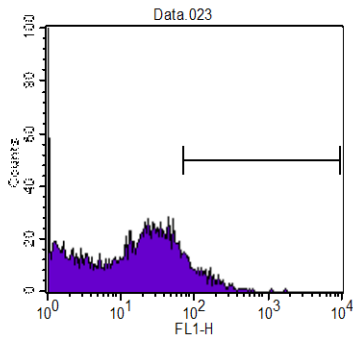


File: Data.022
 Sample ID:
 Tube: NCM460 de103 cd24
 Acquisition Date: 27-Dec-12
 Gated Events: 10000
 X Parameter: FL1-H (Log)

Log Data Units: Linear Value
 Patient ID:
 Panel: dilsad 2
 Gate: No Gate
 Total Events: 10000

Marker	Left, Right	Events	% Gated	% Tota	Mean	Geo Mean	CV	Median	Peak Ct
All	1, 991	10000	100.00	100.00	59.62	14.30	188.60	17.78	1
M1	69, 947	2368	23.68	23.68	198.63	160.26	82.67	144.60	82

Figure D.18: CD24 Detection in NCM 460 cell line (after DE103 bacterial protein application).

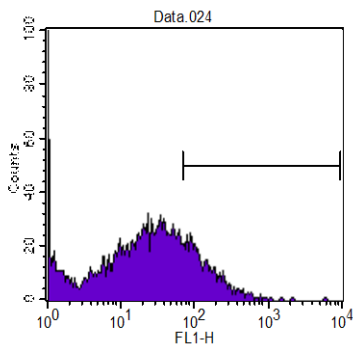


File: Data.023
 Sample ID:
 Tube: NCM460 de103 fitc
 Acquisition Date: 27-Dec-12
 Gated Events: 10000
 X Parameter: FL1-H (Log)

Log Data Units: Linear Value
 Patient ID:
 Panel: dilsad 2
 Gate: No Gate
 Total Events: 10000

Marker	Left, Right	Events	% Gated	% Total	Mean	Geo Mean	CV	Median	Peak Ct
All	1, 991	10000	100.00	100.00	18.87	4.94	208.76	2.57	1
M1	69, 947	622	6.22	6.22	126.08	111.74	74.25	100.90	71

Figure D.19: CD24 Detection in NCM 460 cell line (isotype, after DE103 bacterial protein application).

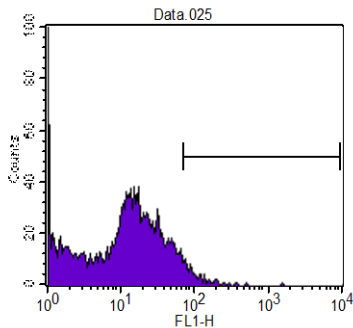


File: Data.024
 Sample ID:
 Tube: NCM460 de129 cd24
 Acquisition Date: 27-Dec-12
 Gated Events: 10000
 X Parameter: FL1-H (Log)

Log Data Units: Linear Value
 Patient ID:
 Panel: dilsad 2
 Gate: No Gate
 Total Events: 10000

Marker	Left, Right	Events	% Gated	% Total	Mean	Geo Mean	CV	Median	Peak Ct
All	1, 991	10000	100.00	100.00	38.99	10.64	265.52	14.46	1
M1	69, 947	1560	15.60	15.60	160.85	131.41	138.10	115.48	82

Figure D.20: CD24 Detection in NCM 460 cell line (after DE129 bacterial protein application).

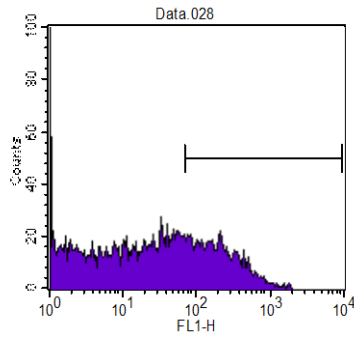


File: Data.025
 Sample ID:
 Tube: NCM460 de129 fitc
 Acquisition Date: 27-Dec-12
 Gated Events: 10000
 X Parameter: FL1-H (Log)

Log Data Units: Linear Value
 Patient ID:
 Panel: dilsad 2
 Gate: No Gate
 Total Events: 10000

Marker	Left, Right	Events	% Gated	% Total	Mean	Geo Mean	CV	Median	Peak Ct
All	1, 991	10000	100.00	100.00	14.27	4.82	715.25	4.76	1
M1	69, 947	240	2.40	2.40	106.34	95.75	90.45	85.44	69

Figure D.21: CD24 Detection in NCM 460 cell line (isotype, after DE129 bacterial protein application).

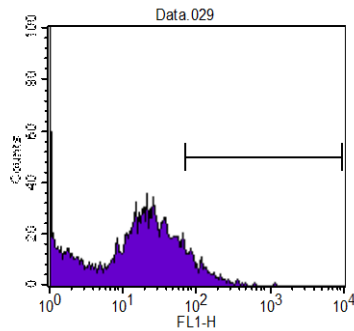


File: Data.028
 Sample ID:
 Tube: NCM460 de8 cd24
 Acquisition Date: 27-Dec-12
 Gated Events: 10000
 X Parameter: FL1-H (Log)

Log Data Units: Linear Value
 Patient ID:
 Panel: dilsad 2
 Gate: No Gate
 Total Events: 10000

Marker	Left, Right	Events	% Gatec	% Tota	Mean	Geo Mean	CV	Median	Peak Ct
All	1, 991	10000	100.00	100.00	69.82	13.99	187.17	15.12	1
M1	69, 947	2667	26.67	26.67	222.01	177.36	80.00	166.98	189

Figure D.22: CD24 Detection in NCM 460 cell line (after DE8 bacterial protein application).

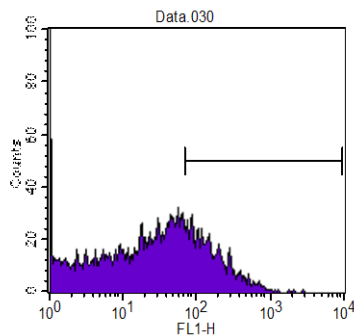


File: Data.029
 Sample ID:
 Tube: NCM460 de8 fitc
 Acquisition Date: 27-Dec-12
 Gated Events: 10000
 X Parameter: FL1-H (Log)

Log Data Units: Linear Value
 Patient ID:
 Panel: dilsad 2
 Gate: No Gate
 Total Events: 10000

Marker	Left, Right	Events	% Gatec	% Tota	Mean	Geo Mean	CV	Median	Peak Ct
All	1, 991	10000	100.00	100.00	18.40	5.41	175.03	4.41	1
M1	69, 947	570	5.70	5.70	114.49	105.62	56.05	96.47	77

Figure D.23: CD24 Detection in NCM 460 cell line (isotype, after DE8 bacterial protein application).

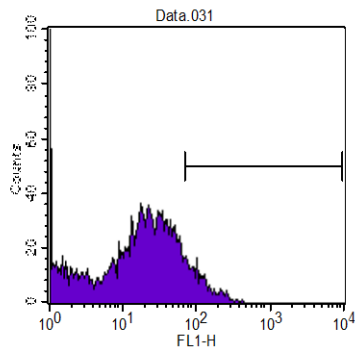


File: Data.030
 Sample ID:
 Tube: NCM460 de12 cd24
 Acquisition Date: 27-Dec-12
 Gated Events: 10000
 X Parameter: FL1-H (Log)

Log Data Units: Linear Value
 Patient ID:
 Panel: dilsad 2
 Gate: No Gate
 Total Events: 10000

Marker	Left, Right	Events	% Gatec	% Tota	Mean	Geo Mean	CV	Median	Peak Ct
All	1, 991	10000	100.00	100.00	53.12	13.56	177.68	19.11	1
M1	69, 947	2284	22.84	22.84	174.21	145.54	78.51	129.80	81

Figure D.24: CD24 Detection in NCM 460 cell line (after DE12 bacterial protein application).

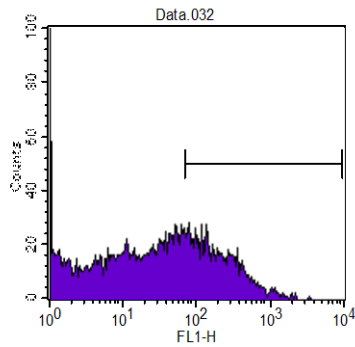


File: Data.031
 Sample ID:
 Tube: NCM460 de12 fitc
 Acquisition Date: 27-Dec-12
 Gated Events: 10000
 X Parameter: FL1-H (Log)

Log Data Units: Linear Value
 Patient ID:
 Panel: dilsad 2
 Gate: No Gate
 Total Events: 10000

Marker	Left, Right	Events	% Gated	% Total	Mean	Geo Mean	CV	Median	Peak Ct
All	1, 991	10000	100.00	100.00	21.64	7.36	147.75	10.94	1
M1	69, 947	668	6.68	6.68	113.84	106.35	41.76	97.34	95

Figure D.25: CD24 Detection in NCM 460 cell line (isotype, after DE12 bacterial protein application).

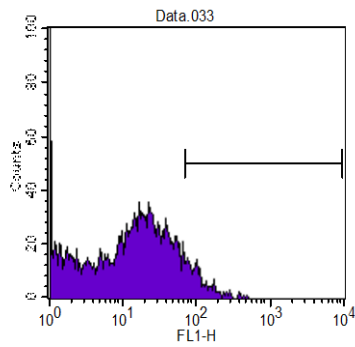


File: Data.032
 Sample ID:
 Tube: NCM460 de47 cd24
 Acquisition Date: 27-Dec-12
 Gated Events: 10000
 X Parameter: FL1-H (Log)

Log Data Units: Linear Value
 Patient ID:
 Panel: dilsad 2
 Gate: No Gate
 Total Events: 10000

Marker	Left, Right	Events	% Gated	% Total	Mean	Geo Mean	CV	Median	Peak Ct
All	1, 991	10000	100.00	100.00	78.91	18.02	187.70	23.29	1
M1	69, 947	2911	29.11	29.11	229.74	178.37	89.60	164.00	72

Figure D.26: CD24 Detection in NCM 460 cell line (after DE47 bacterial protein application).

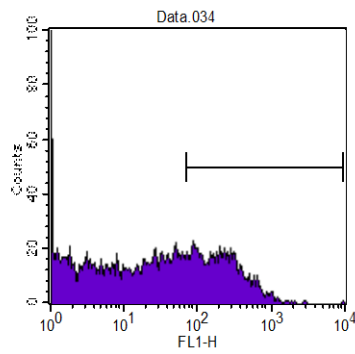


File: Data.033
 Sample ID:
 Tube: NCM460 de47 fitc
 Acquisition Date: 27-Dec-12
 Gated Events: 10000
 X Parameter: FL1-H (Log)

Log Data Units: Linear Value
 Patient ID:
 Panel: dilsad 2
 Gate: No Gate
 Total Events: 10000

Marker	Left, Right	Events	% Gated	% Total	Mean	Geo Mean	CV	Median	Peak Ct
All	1, 991	10000	100.00	100.00	17.65	6.22	154.47	7.70	1
M1	69, 947	488	4.88	4.88	106.34	99.66	44.16	91.40	71

Figure D.27: CD24 Detection in NCM 460 cell line (isotype, after DE47 bacterial protein application).

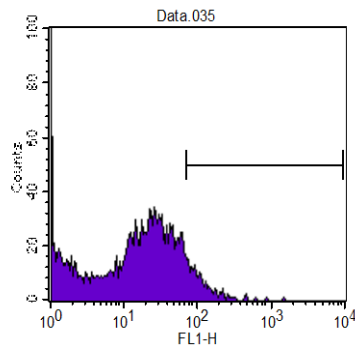


File: Data.034
 Sample ID:
 Tube: NCM460 db7y cd24
 Acquisition Date: 27-Dec-12
 Gated Events: 10000
 X Parameter: FL1-H (Log)

Log Data Units: Linear Value
 Patient ID:
 Panel: dilsad 2
 Gate: No Gate
 Total Events: 10000

Marker	Left, Right	Events	% Gatec	% Tota	Mean	Geo Mean	CV	Median	Peak Ct
All	1, 991	10000	100.00	100.00	77.31	13.36	217.04	13.70	1
M1	69, 947	2799	27.99	27.99	242.41	190.46	102.67	182.69	79

Figure D.28: CD24 Detection in NCM 460 cell line (after DB7Y bacterial protein application).



File: Data.035
 Sample ID:
 Tube: NCM460 db7y fitc
 Acquisition Date: 27-Dec-12
 Gated Events: 10000
 X Parameter: FL1-H (Log)

Log Data Units: Linear Value
 Patient ID:
 Panel: dilsad 2
 Gate: No Gate
 Total Events: 10000

Marker	Left, Right	Events	% Gatec	% Tota	Mean	Geo Mean	CV	Median	Peak Ct
All	1, 991	10000	100.00	100.00	18.84	5.84	174.42	6.21	1
M1	69, 947	523	5.23	5.23	111.85	102.00	71.04	93.06	69

Figure D.29: CD24 Detection in NCM 460 cell line (isotype, after DB7Y bacterial protein application).

APPENDIX E : MIS Results

E.1: MIS Result of 3h

Volume: DATA File: E131045.99A Samp Ctr: 12 ID Number: 8489
 Type: Samp Bottle: 11 Method: RCLIN6
 Created: 1/4/2013 3:55:36 PM
 Sample ID: 3h

RT	Response	Ar/Ht	RFact	ECL	Peak Name	Percent	Comment1	Comment2
0.6919	273101	0.004	----	6.6791		----	< min rt	
0.7003	9.835E+8	0.016	----	6.7415	SOLVENT	----	< min rt	
1.5261	2257	0.008	1.045	11.9998	12:0	2.09	ECL deviates	Reference -0.004
1.7772	1161	0.009	0.998	13.0009	13:0	1.02	ECL deviates	Reference -0.003
2.0571	7430	0.009	0.965	13.9991	14:0	6.34	ECL deviates	Reference -0.005
2.2084	2468	0.010	0.953	14.5050	Sum In Feature 1	2.08	ECL deviates	13:0 3OH/15:1 iso
2.3007	367	0.008	0.947	14.8137	15:1 w8c	0.31	ECL deviates	
2.3569	9478	0.009	0.944	15.0016	15:0	----	ECL deviates	
2.4122	462	0.009	----	15.1791		----		
2.4292	1049	0.008	0.940	15.2336	14:0 2OH	0.87	ECL deviates	
2.5174	10052	0.008	0.937	15.5166	Sum In Feature 2	8.32	ECL deviates	14:0 3OH/16:1 iso
2.6167	7044	0.009	0.933	15.8354	Sum In Feature 3	5.81	ECL deviates	16:1 w7c/16:1 w6c
2.6463	326	0.009	0.932	15.9303	16:1 w5c	0.27	ECL deviates	
2.6677	31805	0.009	0.931	15.9990	16:0	26.19	ECL deviates	Reference -0.007
2.6974	1164	0.012	----	16.0941		----		
2.8340	618	0.010	0.927	16.5307	15:0 3OH	0.51	ECL deviates	
2.9236	476	0.009	0.926	16.8171	17:1 w8c	0.39	ECL deviates	
2.9539	23125	0.009	0.925	16.9139	17:0 cyclo	18.91	ECL deviates	
2.9815	8389	0.009	0.925	17.0022	17:0	6.86	ECL deviates	Reference -0.004
3.2172	1073	0.010	0.922	17.7545	Sum In Feature 5	0.87	ECL deviates	18:2 w6,9c/18:0
3.2447	15736	0.009	0.922	17.8423	Sum In Feature 8	12.82	ECL deviates	18:1 w7c
3.2626	1120	0.012	0.922	17.8996	Sum In Feature 8	0.91	ECL deviates	18:1 w6c
3.2938	1233	0.010	0.921	17.9990	18:0	1.00	ECL deviates	Reference -0.008
3.4381	1487	0.012	----	18.4698		----		
3.5050	791	0.010	----	18.6883		----		
3.5779	4221	0.010	0.918	18.9262	19:0 cyclo w8c	3.42	ECL deviates	
3.5981	654	0.010	0.917	18.9922	19:0	0.53	ECL deviates	
3.6456	581	0.010	0.917	19.1502	18:1 2OH	0.47	ECL deviates	
----	2468	---	----	----	Summed Feature	2.08	15:1 iso H/13:0	13:0 3OH/15:1 iso
----	10052	---	----	----	Summed Feature	8.32	12:0 aldehyde ?	unknown 10.9525
----	----	---	----	----	----	----	16:1 iso I/14:0	14:0 3OH/16:1 iso
----	7044	---	----	----	Summed Feature	5.81	16:1 w7c/16:1 w6c	16:1 w6c/16:1 w7c
----	1073	---	----	----	Summed Feature	0.87	18:0 ante/18:2	18:2 w6,9c/18:0
----	16856	---	----	----	Summed Feature	13.73	18:1 w7c	18:1 w6c

ECL Deviation: 0.003
 Total Response: 125090
 Percent Named: 96.88%

Reference ECL Shift: 0.005 Number Reference Peaks: 6
 Total Named: 121185
 Total Amount: 122068

Matches:

Library	Sim Index	Entry Name
RCLIN6 6.00	0.507	Enterobacter-cloacae-GC subgroup B
	0.487	Kluyvera-cryocrescens
	0.481	Klebsiella-pneumoniae-pneumoniae-GC subgroup C
	0.478	Escherichia-coli-GC subgroup A (high DNA homol. with Shigella)
	0.381	Escherichia-coli-O157:H7-GC subgroup A
	0.347	Enterobacter-aerogenes-GC subgroup B
	0.347	Enterobacter-aerogenes-GC subgroup A
	0.340	Shigella-boydii-GC subgroup A (high DNA homol. with E. coli)
	0.336	Escherichia-coli-GC subgroup B1 (high DNA homol. with Shigella)
	0.325	Salmonella-typhimurium

E.2: MIS Result of huc2

Volume: DATA File: E118255.87A Samp Ctr: 13 ID Number: 7407
 Type: Samp Bottle: 12 Method: RTSBA6 Calc. Method: RCLIN6
 Created: 8/25/2011 3:47:01 PM
 Sample ID: huc2

RT	Response	Ar/Ht	RFact	ECL	Peak Name	Percent	Comment1	Comment2
0.6916	428489	0.004	----	6.6653		----	< min rt	
0.7007	1.226E+9	0.015	----	6.7332	SOLVENT	----	< min rt	
1.1684	1878	0.009	----	10.1505		----		
1.3069	926	0.013	1.069	10.9491	Sum In Feature 2	0.32	ECL deviates -	unknown 10.9525
1.5320	10022	0.008	1.022	12.0009	12:0	3.34	ECL deviates	Reference -0.001
1.7839	3539	0.008	0.989	13.0004	13:0	1.14	ECL deviates	Reference -0.001
1.9257	521	0.011	----	13.5045		----		
2.0179	573	0.010	----	13.8322		----		
2.0644	23034	0.009	0.967	13.9975	14:0	7.27	ECL deviates -	Reference -0.003
2.2162	4952	0.011	0.959	14.5037	Sum In Feature 1	1.55	ECL deviates	13:0 3OH/15:1 iso
2.3089	714	0.009	0.955	14.8127	15:1 w8c	0.22	ECL deviates -	
2.3648	22213	0.008	0.953	14.9990	15:0	----	ECL deviates -	
2.4202	794	0.009	----	15.1772		----		
2.5257	24900	0.008	0.948	15.5164	Sum In Feature 2	7.71	ECL deviates	14:0 3OH/16:1 iso
2.6248	33165	0.009	0.946	15.8348	Sum In Feature 3	10.25	ECL deviates -	16:1 w7c/16:1 w6c
2.6541	743	0.010	0.946	15.9291	16:1 w5c	0.23	ECL deviates	
2.6760	96098	0.008	0.946	15.9997	16:0	29.67	ECL deviates	Reference -0.003
2.7066	1249	0.012	----	16.0975		----		
2.8423	840	0.011	0.944	16.5309	15:0 3OH	0.26	ECL deviates -	
2.9310	1321	0.010	0.944	16.8142	17:1 w8c	0.41	ECL deviates -	
2.9623	52040	0.009	0.944	16.9141	17:0 cyclo	16.03	ECL deviates -	
2.9896	13355	0.009	0.944	17.0014	17:0	4.11	ECL deviates	Reference -0.003
3.2249	1009	0.010	0.945	17.7559	Sum In Feature 5	0.31	ECL deviates	18:2 w6,9c/18:0
3.2531	41729	0.010	0.945	17.8462	Sum In Feature 8	12.87	ECL deviates -	18:1 w7c
3.2712	1920	0.009	0.945	17.9044	Sum In Feature 8	0.59	ECL deviates	18:1 w6c
3.2863	631	0.008	----	17.9528		----		
3.3017	1263	0.010	0.945	18.0019	18:0	0.39	ECL deviates	Reference -0.005
3.4471	1066	0.012	----	18.4782		----		
3.5131	751	0.010	----	18.6944		----		
3.5863	10319	0.009	0.948	18.9340	19:0 cyclo w8c	3.19	ECL deviates	
3.6058	389	0.010	0.948	18.9981	19:0	0.12	ECL deviates -	Reference -0.012
----	4952	---	----	----	Summed Feature	1.55	15:1 iso H/13:0	13:0 3OH/15:1 iso
----	25826	---	----	----	Summed Feature	8.03	12:0 aldehyde ?	unknown 10.9525
----	-----	---	----	----		----	16:1 iso I/14:0	14:0 3OH/16:1 iso
----	33165	---	----	----	Summed Feature	10.25	16:1 w7c/16:1 w6c	16:1 w6c/16:1 w7c
----	1009	---	----	----	Summed Feature	0.31	18:0 ante/18:2	18:2 w6,9c/18:0
----	43649	---	----	----	Summed Feature	13.46	18:1 w7c	18:1 w6c

ECL Deviation: 0.002
 Total Response: 329739
 Percent Named: 97.74%

Reference ECL Shift: 0.005 Number Reference Peaks: 7
 Total Named: 322277
 Total Amount: 327468

Matches:

Library	Sim Index	Entry Name
RCLIN6 6.00	0.821	Enterobacter-cloacae-GC subgroup B
	0.746	Escherichia-coli-GC subgroup A (high DNA homol. with Shigella)
	0.733	Klebsiella-oxytoca
	0.716	Kluyvera-cryocrescens
	0.680	Enterobacter-cancerogenus
	0.662	Enterobacter-aerogenes-GC subgroup B
	0.615	Klebsiella-pneumoniae-pneumoniae-GC subgroup C
	0.603	Shigella-sonnei-GC subgroup B (high DNA homol. with E. coli)
	0.593	Kluyvera-ascorbata
	0.561	Enterobacter-asburiae

E.3: MIS Result of DE8

Volume: DATA File: E131045.99A Samp Ctr: 5 ID Number: 8482
 Type: Samp Bottle: 4 Method: RCLIN6
 Created: 1/4/2013 2:55:44 PM
 Sample ID: DE 8

RT	Response	Ar/Ht	RFact	ECL	Peak Name	Percent	Comment1	Comment2
0.6916	307960	0.004	----	6.6769		----	< min rt	
0.6998	9.868E+8	0.016	----	6.7383	SOLVENT	----	< min rt	
1.3013	365	0.008	1.114	10.9415	Sum In Feature 2	0.22	ECL deviates -	unknown 10.9525
1.5260	1456	0.008	1.045	12.0000	12:0	0.81	ECL deviates	Reference -0.004
1.7770	807	0.010	0.998	13.0005	13:0	0.43	ECL deviates	Reference -0.004
1.9286	383	0.008	----	13.5414		----		
2.0570	21007	0.008	0.965	13.9993	14:0	10.82	ECL deviates -	Reference -0.006
2.2087	2551	0.012	0.953	14.5065	Sum In Feature 1	1.30	ECL deviates	13:0 3OH/15:1 iso
2.3568	8894	0.008	0.944	15.0019	15:0	----	ECL deviates	
2.4125	556	0.009	----	15.1806		----		
2.4289	1826	0.009	0.940	15.2333	14:0 2OH	0.92	ECL deviates	
2.5173	15986	0.009	0.937	15.5170	Sum In Feature 2	7.99	ECL deviates	14:0 3OH/16:1 iso
2.6167	15395	0.009	0.933	15.8360	Sum In Feature 3	7.67	ECL deviates -	16:1 w7c/16:1 w6c
2.6443	338	0.009	0.932	15.9245	16:1 w5c	0.17	ECL deviates -	
2.6676	62092	0.009	0.931	15.9993	16:0	30.87	ECL deviates -	Reference -0.007
2.6971	625	0.010	----	16.0938		----		
2.7463	318	0.010	0.929	16.2508	15:0 2OH	0.16	ECL deviates -	
2.8340	406	0.009	0.927	16.5312	15:0 3OH	0.20	ECL deviates -	
2.9227	537	0.010	0.926	16.8149	17:1 w8c	0.27	ECL deviates	
2.9533	31448	0.009	0.925	16.9125	17:0 cyclo	15.53	ECL deviates -	
2.9812	7247	0.009	0.925	17.0018	17:0	3.58	ECL deviates	Reference -0.005
3.2169	538	0.010	0.922	17.7542	Sum In Feature 5	0.26	ECL deviates -	18:2 w6,9c/18:0
3.2446	23292	0.009	0.922	17.8427	Sum In Feature 8	11.46	ECL deviates -	18:1 w7c
3.2626	1376	0.009	0.922	17.9001	Sum In Feature 8	0.68	ECL deviates -	18:1 w6c
3.2772	361	0.007	0.921	17.9466	18:1 w5c	0.18	ECL deviates	
3.2936	1866	0.009	0.921	17.9991	18:0	0.92	ECL deviates -	Reference -0.009
3.4380	701	0.009	----	18.4703		----		
3.5049	546	0.011	----	18.6887		----		
3.5778	10577	0.010	0.918	18.9266	19:0 cyclo w8c	5.18	ECL deviates -	
3.5970	383	0.011	0.917	18.9893	19:0	0.19	ECL deviates -	
3.6451	447	0.011	0.917	19.1491	18:1 2OH	0.22	ECL deviates	
4.2573	384	0.010	----	21.1896		----	> max rt	
----	2551	---	----	----	Summed Feature	1.30	15:1 iso H/13:0	13:0 3OH/15:1 iso
----	16351	---	----	----	Summed Feature	8.21	12:0 aldehyde ?	unknown 10.9525
----	-----	---	----	----		----	16:1 iso I/14:0	14:0 3OH/16:1 iso
----	15395	---	----	----	Summed Feature	7.67	16:1 w7c/16:1 w6c	16:1 w6c/16:1 w7c
----	538	---	----	----	Summed Feature	0.26	18:0 ante/18:2	18:2 w6,9c/18:0
----	24668	---	----	----	Summed Feature	12.14	18:1 w7c	18:1 w6c

ECL Deviation: 0.004 Reference ECL Shift: 0.006 Number Reference Peaks: 6
 Total Response: 203430 Total Named: 200619
 Percent Named: 98.62% Total Amount: 195750

Matches:

Library	Sim Index	Entry Name
RCLIN6 6.00	0.826	Enterobacter-aerogenes-GC subgroup A
	0.806	Enterobacter-cloacae-GC subgroup C
	0.795	Klebsiella-pneumoniae-pneumoniae-GC subgroup C
	0.791	Enterobacter-aerogenes-GC subgroup B
	0.704	Enterobacter-cloacae-GC subgroup B
	0.676	Proteus-mirabilis-GC subgroup A
	0.625	Escherichia-coli-GC subgroup A (high DNA homol. with Shigella)
	0.579	Klebsiella-pneumoniae-pneumoniae-GC subgroup A
	0.577	Mannheimia-haemolytica-GC subgroup B (Pasteurella)
	0.575	Klebsiella-oxytoca

E.4: MIS Result of DB7Y

Volume: DATA File: E131084.18A Samp Ctr: 4 ID Number: 8497
 Type: Samp Bottle: 3 Method: RCLIN6 Calc. Method: RTSBA6
 Created: 1/8/2013 10:26:54 AM
 Sample ID: DB7Y

RT	Response	Ar/Ht	RFact	ECL	Peak Name	Percent	Comment1	Comment2
0.6917	276247	0.004	----	6.6820		----	< min rt	
0.7000	9.751E+8	0.016	----	6.7436	SOLVENT	----	< min rt	
1.3021	321	0.008	1.104	10.9449	Sum In Feature 2	0.24	ECL deviates -	unknown 10.9525
1.5261	5888	0.008	1.039	11.9995	12:0	4.09	ECL deviates	Reference -0.004
1.7772	2781	0.009	0.994	13.0013	13:0	1.85	ECL deviates	Reference -0.003
1.9190	469	0.012	----	13.5064		----		
2.0459	1015	0.007	0.965	13.9585	unknown 13.951	----	ECL deviates	
2.0573	9455	0.008	0.964	13.9991	14:0	6.10	ECL deviates -	Reference -0.006
2.2078	3978	0.010	0.953	14.5020	Sum In Feature 1	2.54	ECL deviates -	13:0 3OH/15:1 iso
2.3007	560	0.009	0.948	14.8122	15:1 w8c	0.36	ECL deviates -	
2.3570	17333	0.009	0.945	15.0003	15:0	----	ECL deviates	
2.4121	711	0.010	----	15.1774		----		
2.5179	15177	0.009	0.939	15.5172	Sum In Feature 2	9.53	ECL deviates	14:0 3OH/16:1 iso
2.6174	18865	0.009	0.936	15.8367	Sum In Feature 3	11.81	ECL deviates -	16:1 w7c/16:1 w6c
2.6460	473	0.009	0.935	15.9288	16:1 w5c	0.30	ECL deviates	
2.6680	38356	0.008	0.934	15.9994	16:0	23.98	ECL deviates -	Reference -0.006
2.6988	807	0.011	----	16.0976		----		
2.8347	837	0.010	0.931	16.5312	15:0 3OH	0.52	ECL deviates -	
2.9233	584	0.010	0.930	16.8139	17:1 w8c	0.36	ECL deviates -	
2.9542	26348	0.009	0.930	16.9125	17:0 cyclo	16.39	ECL deviates -	
2.9819	7704	0.009	0.930	17.0010	17:0	4.79	ECL deviates	Reference -0.005
3.2174	787	0.010	0.928	17.7541	Sum In Feature 5	0.49	ECL deviates -	18:2 w6,9c/18:0
3.2453	21193	0.009	0.928	17.8432	Sum In Feature 8	13.16	ECL deviates -	18:1 w7c
3.2635	1118	0.010	0.928	17.9015	Sum In Feature 8	0.69	ECL deviates -	18:1 w6c
3.2942	965	0.009	0.927	17.9996	18:0	0.60	ECL deviates	Reference -0.007
3.4389	1090	0.012	----	18.4724		----		
3.5053	611	0.011	----	18.6893		----		
3.5788	2365	0.009	0.925	18.9297	19:0 cyclo w8c	1.46	ECL deviates -	
3.5977	464	0.009	0.925	18.9914	19:0	0.29	ECL deviates -	
3.6452	742	0.011	0.924	19.1486	18:1 2OH	0.46	ECL deviates	
----	3978	---	----	----	Summed Feature	2.54	15:1 iso H/13:0	13:0 3OH/15:1 iso
----	15498	---	----	----	Summed Feature	9.77	12:0 aldehyde ?	unknown 10.9525
----	-----	---	----	----		----	16:1 iso I/14:0	14:0 3OH/16:1 iso
----	18865	---	----	----	Summed Feature	11.81	16:1 w7c/16:1 w6c	16:1 w6c/16:1 w7c
----	787	---	----	----	Summed Feature	0.49	18:0 ante/18:2	18:2 w6,9c/18:0
----	22311	---	----	----	Summed Feature	13.85	18:1 w7c	18:1 w6c

ECL Deviation: 0.003
 Total Response: 162647
 Percent Named: 97.73%

Reference ECL Shift: 0.005 Number Reference Peaks: 6
 Total Named: 158960
 Total Amount: 166817

Matches:

Library	Sim Index	Entry Name
RTSBA6 6.00	0.380	Enterobacter-cancerogenus (Erwinia cancerogena)
	0.349	Enterobacter-hormaechei
	0.286	Escherichia-fergusonii-GC subgroup A

E.5: MIS Result of DE12

Volume: DATA File: E131045.99A Samp Ctr: 17 ID Number: 8493
 Type: Samp Bottle: 15 Method: RCLIN6
 Created: 1/4/2013 4:38:07 PM
 Sample ID: DE 12

RT	Response	Ar/Ht	RFact	ECL	Peak Name	Percent	Comment1	Comment2
0.6919	278168	0.004	----	6.6745		----	< min rt	
0.7002	9.762E+8	0.016	----	6.7362	SOLVENT	----	< min rt	
1.3021	491	0.012	1.105	10.9478	Sum In Feature 2	0.35	ECL deviates -	unknown 10.9525
1.5265	5798	0.008	1.039	12.0007	12:0	3.89	ECL deviates	Reference -0.001
1.7777	794	0.012	0.994	13.0008	13:0	0.51	ECL deviates	Reference 0.000
1.9293	532	0.013	----	13.5403		----		
2.0576	10489	0.009	0.964	13.9973	14:0	6.53	ECL deviates -	Reference -0.002
2.2113	1890	0.011	0.953	14.5108	unknown 14.502	----	ECL deviates -	
2.3576	4333	0.008	0.945	14.9993	15:0	----	ECL deviates -	
2.4126	650	0.009	----	15.1761		----		
2.5180	14563	0.009	0.938	15.5154	Sum In Feature 2	8.82	ECL deviates	14:0 3OH/16:1 iso
2.6175	18086	0.009	0.935	15.8356	Sum In Feature 3	10.92	ECL deviates -	16:1 w7c/16:1 w6c
2.6685	52994	0.009	0.934	15.9998	16:0	31.95	ECL deviates	Reference 0.000
2.6979	1380	0.012	----	16.0937		----		
2.9321	340	0.007	0.930	16.8426	17:1 w7c	0.20	ECL deviates	
2.9546	29492	0.009	0.929	16.9145	17:0 cyclo	17.69	ECL deviates -	
2.9817	3271	0.009	0.929	17.0012	17:0	1.96	ECL deviates	Reference 0.000
3.2173	1149	0.009	0.927	17.7551	Sum In Feature 5	0.69	ECL deviates -	18:2 w6,9c/18:0
3.2452	23082	0.010	0.927	17.8447	Sum In Feature 8	13.81	ECL deviates -	18:1 w7c
3.2944	1480	0.009	0.927	18.0021	18:0	0.89	ECL deviates	Reference -0.002
3.4382	1643	0.012	----	18.4735		----		
3.5057	899	0.011	----	18.6949		----		
3.5785	1873	0.010	0.924	18.9338	19:0 cyclo w8c	1.12	ECL deviates	
3.5981	587	0.009	0.924	18.9981	19:0	0.35	ECL deviates -	Reference -0.009
3.6463	535	0.012	0.924	19.1587	18:1 2OH	0.32	ECL deviates	
----	15054	---	----	----	Summed Feature	9.17	12:0 aldehyde ?	unknown 10.9525
----	-----	---	----	----	----	----	16:1 iso I/14:0	14:0 3OH/16:1 iso
----	18086	---	----	----	Summed Feature	10.92	16:1 w7c/16:1 w6c	16:1 w6c/16:1 w7c
----	1149	---	----	----	Summed Feature	0.69	18:0 ante/18:2	18:2 w6,9c/18:0
----	23082	---	----	----	Summed Feature	13.81	18:1 w7c	18:1 w6c

ECL Deviation: 0.004 Reference ECL Shift: 0.003 Number Reference Peaks: 7
 Total Response: 170128 Total Named: 165025
 Percent Named: 97.00% Total Amount: 160817

Matches:

Library	Sim Index	Entry Name
RCLIN6 6.00	0.833	Enterobacter-cancerogenus
	0.833	Enterobacter-cloacae-GC subgroup B
	0.824	Klebsiella-pneumoniae-rhinoscleromatis-GC subgroup B
	0.820	Klebsiella-oxytoca
	0.783	Enterobacter-cloacae-GC subgroup D
	0.758	Kluyvera-ascorbata
	0.649	Enterobacter-asburiae
	0.636	Shigella-boydii-GC subgroup A (high DNA homol. with E. coli)
	0.609	Escherichia-coli-GC subgroup A (high DNA homol. with Shigella)
	0.582	Kluyvera-cryocrescens

E.6: MIS Result of DE256

Volume: DATA File: E131045.99A Samp Ctr: 16 ID Number: 8492
 Type: Samp Bottle: 14 Method: RCLIN6
 Created: 1/4/2013 4:29:40 PM
 Sample ID: DE 256

RT	Response	Ar/Ht	RFact	ECL	Peak Name	Percent	Comment1	Comment2
0.6919	291290	0.004	----	6.6770		----	< min rt	
0.7003	9.711E+8	0.016	----	6.7394	SOLVENT	----	< min rt	
1.5260	3422	0.008	1.039	12.0003	12:0	2.45	ECL deviates	Reference -0.003
1.7774	1146	0.010	0.994	13.0012	13:0	0.79	ECL deviates	Reference -0.001
2.0572	11489	0.009	0.964	13.9976	14:0	7.64	ECL deviates -	Reference -0.004
2.2091	2294	0.011	0.953	14.5051	Sum In Feature 1	1.51	ECL deviates	13:0 3OH/15:1 iso
2.3570	8641	0.009	0.945	14.9987	15:0	----	ECL deviates -	
2.4119	592	0.009	----	15.1755		----		
2.5174	13169	0.009	0.938	15.5151	Sum In Feature 2	8.53	ECL deviates	14:0 3OH/16:1 iso
2.6170	11464	0.009	0.935	15.8355	Sum In Feature 3	7.40	ECL deviates -	16:1 w7c/16:1 w6c
2.6679	45790	0.009	0.934	15.9992	16:0	29.51	ECL deviates -	Reference -0.002
2.6976	1260	0.012	----	16.0944		----		
2.8331	409	0.010	----	16.5275		----		
2.9312	617	0.014	0.930	16.8412	17:1 w7c	0.40	ECL deviates	
2.9538	29163	0.009	0.929	16.9135	17:0 cyclo	18.70	ECL deviates -	
2.9816	6243	0.009	0.929	17.0022	17:0	4.00	ECL deviates	Reference -0.001
3.2170	1069	0.010	0.927	17.7555	Sum In Feature 5	0.68	ECL deviates -	18:2 w6,9c/18:0
3.2446	20668	0.009	0.927	17.8438	Sum In Feature 8	13.22	ECL deviates -	18:1 w7c
3.2633	710	0.010	0.927	17.9038	Sum In Feature 8	0.45	ECL deviates	18:1 w6c
3.2937	1687	0.010	0.927	18.0008	18:0	1.08	ECL deviates	Reference -0.004
3.4378	1433	0.011	----	18.4734		----		
3.5051	762	0.010	----	18.6940		----		
3.5777	5174	0.009	0.924	18.9322	19:0 cyclo w8c	3.30	ECL deviates	
3.5980	561	0.008	0.924	18.9987	19:0	0.36	ECL deviates -	Reference -0.009
3.6462	589	0.010	----	19.1592		----		
----	2294	---	----	----	Summed Feature	1.51	15:1 iso H/13:0	13:0 3OH/15:1 iso
----	13169	---	----	----	Summed Feature	8.53	12:0 aldehyde ?	unknown 10.9525
----	-----	---	----	----	----	----	16:1 iso I/14:0	14:0 3OH/16:1 iso
----	11464	---	----	----	Summed Feature	7.40	16:1 w7c/16:1 w6c	16:1 w6c/16:1 w7c
----	1069	---	----	----	Summed Feature	0.68	18:0 ante/18:2	18:2 w6,9c/18:0
----	21377	---	----	----	Summed Feature	13.67	18:1 w7c	18:1 w6c

ECL Deviation: 0.002
 Total Response: 159710
 Percent Named: 96.84%

Reference ECL Shift: 0.004 Number Reference Peaks: 7
 Total Named: 154665
 Total Amount: 153125

Matches:

Library	Sim Index	Entry Name
RCLIN6 6.00	0.781	Enterobacter-cloacae-GC subgroup B
	0.759	Escherichia-coli-GC subgroup A (high DNA homol. with Shigella)
	0.680	Shigella-boydii-GC subgroup A (high DNA homol. with E. coli)
	0.637	Klebsiella-oxytoca
	0.598	Enterobacter-cloacae-GC subgroup C
	0.573	Klebsiella-pneumoniae-pneumoniae-GC subgroup C
	0.573	Enterobacter-aerogenes-GC subgroup A
	0.569	Salmonella-typhimurium
	0.568	Kluyvera-cryocrescens
	0.558	Enterobacter-cancerogenus

E.7: MIS Result of DE103

Volume: DATA File: E131045.99A Samp Ctr: 15 ID Number: 8491
 Type: Samp Bottle: 13 Method: RCLIN6
 Created: 1/4/2013 4:21:05 PM
 Sample ID: DE 103

RT	Response	Ar/Ht	RFact	ECL	Peak Name	Percent	Comment1	Comment2
0.6918	259891	0.004	----	6.6764		----	< min rt	
0.7002	9.734E+8	0.016	----	6.7391	SOLVENT	----	< min rt	
1.3021	638	0.013	1.105	10.9492	Sum In Feature 2	0.42	ECL deviates -	unknown 10.9525
1.5261	1837	0.009	1.039	12.0001	12:0	1.12	ECL deviates	Reference -0.003
1.7776	919	0.013	0.994	13.0015	13:0	0.54	ECL deviates	Reference 0.000
2.0574	16890	0.009	0.964	13.9976	14:0	9.58	ECL deviates -	Reference -0.003
2.2107	2430	0.011	----	14.5095		----		
2.3572	6672	0.009	0.945	14.9984	15:0	----	ECL deviates -	
2.4123	731	0.009	----	15.1759		----		
2.5173	15292	0.009	0.938	15.5137	Sum In Feature 2	8.45	ECL deviates -	14:0 3OH/16:1 iso
2.6171	16455	0.008	0.935	15.8349	Sum In Feature 3	9.06	ECL deviates -	16:1 w7c/16:1 w6c
2.6681	55475	0.009	0.934	15.9990	16:0	30.51	ECL deviates -	Reference -0.002
2.6980	1177	0.012	----	16.0945		----		
2.9250	335	0.009	0.930	16.8199	17:1 w8c	0.18	ECL deviates	
2.9540	28135	0.009	0.929	16.9127	17:0 cyclo	15.39	ECL deviates -	
2.9822	6048	0.009	0.929	17.0028	17:0	3.31	ECL deviates	Reference 0.001
3.2174	1058	0.010	0.927	17.7555	Sum In Feature 5	0.58	ECL deviates -	18:2 w6,9c/18:0
3.2449	27570	0.010	0.927	17.8436	Sum In Feature 8	15.05	ECL deviates -	18:1 w7c
3.2634	661	0.011	0.927	17.9027	Sum In Feature 8	0.36	ECL deviates	18:1 w6c
3.2938	1785	0.009	0.927	17.9999	18:0	0.97	ECL deviates	Reference -0.004
3.4387	1410	0.012	----	18.4747		----		
3.5050	754	0.010	----	18.6922		----		
3.5783	7141	0.009	0.924	18.9327	19:0 cyclo w8c	3.89	ECL deviates	
3.5986	552	0.009	0.924	18.9992	19:0	0.30	ECL deviates -	Reference -0.007
3.6451	529	0.010	0.924	19.1540	18:1 2OH	0.29	ECL deviates	
----	15929	---	----	----	Summed Feature	8.86	12:0 aldehyde ?	unknown 10.9525
----	----	---	----	----	----	----	16:1 iso I/14:0	14:0 3OH/16:1 iso
----	16455	---	----	----	Summed Feature	9.06	16:1 w7c/16:1 w6c	16:1 w6c/16:1 w7c
----	1058	---	----	----	Summed Feature	0.58	18:0 ante/18:2	18:2 w6,9c/18:0
----	28231	---	----	----	Summed Feature	15.41	18:1 w7c	18:1 w6c

ECL Deviation: 0.003
 Total Response: 187821
 Percent Named: 96.54%

Reference ECL Shift: 0.003 Number Reference Peaks: 7
 Total Named: 181319
 Total Amount: 176158

Matches:

Library	Sim Index	Entry Name
RCLIN6 6.00	0.897	Enterobacter-cloacae-GC subgroup B
	0.788	Escherichia-coli-GC subgroup A (high DNA homol. with Shigella)
	0.779	Enterobacter-aerogenes-GC subgroup B
	0.723	Klebsiella-pneumoniae-pneumoniae-GC subgroup C
	0.668	Shigella-boydii-GC subgroup A (high DNA homol. with E. coli)
	0.659	Proteus-mirabilis-GC subgroup A
	0.656	Enterobacter-cloacae-GC subgroup C
	0.635	Klebsiella-pneumoniae-pneumoniae-GC subgroup B
	0.619	Kluyvera-ascorbata
	0.604	Klebsiella-pneumoniae-ozaenae-type 6

APPENDIX F : Microbial Identification VITEK2 Results

İzolat Grubu: de-36

Biyonumara: 0627634453572010

Seçilen Organizma: Enterobacter cloacae ssp cloacae

Yorumlar:	Oksidaz (-)

İdentifikasyon Bilgileri	Kart: GN	Lot No: 241247640	Son Kullanım Tarihi: 24.Eyl.2013 13:00 EEST
	Tamamlandı: 24.Nis.2013 19:18 EEST	Durum: Son	Analiz Zamanı: 5,00 saat
Seçilen Organizma	99% Olasılık Enterobacter cloacae ssp cloacae		
	Biyonumara: 0627634453572010	Uyum:	Mükemmel identifikasyon
SRF Organizması			
Ayrılacak Analiz Organizmaları ve Testler:			
Enterobacter cloacae complex			
Enterobacter kobei	UREASE(83),LACTOSE(88),MOB(82),dSORBITOL(94),		
Enterobacter hormaechei	UREASE(87),MOB(52),dSORBITOL(0),		
Enterobacter cloacae ssp cloacae	UREASE(100),LACTOSE(30),MOB(99),dSORBITOL(100),		
Enterobacter cloacae ssp dissolvens	UREASE(100),MOB(0),dSORBITOL(100),		
Enterobacter ludwigii	UREASE(0),LACTOSE(60),MOB(100),dSORBITOL(100),		
Analiz Mesajları:			

Figure F.1: VITEK2 Result of DE36.

İzolat Grubu: de129-1

Biyonumara: 2625634453472210

Seçilen Organizma: Enterobacter cloacae ssp dissolvens

Yorumlar:	Oksidaz (-)

İdentifikasyon Bilgileri	Kart: GN	Lot No: 241247640	Son Kullanım Tarihi: 24.Eyl.2013 13:00 EEST
	Tamamlandı: 24.Nis.2013 19:18 EEST	Durum: Son	Analiz Zamanı: 5,00 saat
Seçilen Organizma	98% Olasılık Enterobacter cloacae ssp dissolvens		
	Biyonumara: 2625634453472210	Uyum:	Mükemmel identifikasyon
SRF Organizması			
Ayrılacak Analiz Organizmaları ve Testler:			
Enterobacter cloacae complex			
Enterobacter kobei	UREASE(83),LACTOSE(88),MOB(82),dSORBITOL(94),		
Enterobacter hormaechei	UREASE(87),MOB(52),dSORBITOL(0),		
Enterobacter cloacae ssp cloacae	UREASE(100),LACTOSE(30),MOB(99),dSORBITOL(100),		
Enterobacter cloacae ssp dissolvens	UREASE(100),MOB(0),dSORBITOL(100),		
Enterobacter ludwigii	UREASE(0),LACTOSE(60),MOB(100),dSORBITOL(100),		
Analiz Mesajları:			

Figure F.2: VITEK2 Result of DE129.

Izolot Grubu: de-47

Biyonumara: 0605614453432210
Seçilen Organizma: Enterobacter hormaechei

Yorumlar:	Oksidaz (-)

Identifikasyon Bilgileri	Kart: GN	Lot No: 241247640	Son Kullanım Tarihi: 24.Eyl.2013 13:00 EEST
	Tamamlandı: 24.Nis.2013 19:17 EEST	Durum: Son	Analiz Zamanı: 5,00 saat
Seçilen Organizma	93% Olasılık	Enterobacter hormaechei	
	Biyonumara: 0605614453432210	Uyum:	Çok iyi identifikasyon
SRF Organizması			
Ayrılabak Analiz Organizmaları ve Testler:			
Enterobacter cloacae complex			
Enterobacter kobei	UREASE(83),LACTOSE(88),MOB(82),dSORBITOL(94),		
Enterobacter hormaechei	UREASE(87),MOB(52),dSORBITOL(0),		
Enterobacter cloacae ssp cloacae	UREASE(100),LACTOSE(30),MOB(99),dSORBITOL(100),		
Enterobacter cloacae ssp dissolvens	UREASE(100),MOB(0),dSORBITOL(100),		
Enterobacter ludwigii	UREASE(0),LACTOSE(60),MOB(100),dSORBITOL(100),		
Analiz Mesajları:			

Figure F.3: VITEK2 Result of DE47.

Izolot Grubu: de-51

Biyonumara: 0003010240040211
Seçilen Organizma: Morganella morganii ssp sibirii

Yorumlar:	Oksidaz (-)

Identifikasyon Bilgileri	Kart: GN	Lot No: 241247640	Son Kullanım Tarihi: 24.Eyl.2013 13:00 EEST
	Tamamlandı: 24.Nis.2013 20:17 EEST	Durum: Son	Analiz Zamanı: 6,00 saat
Seçilen Organizma	99% Olasılık	Morganella morganii ssp sibirii	
	Biyonumara: 0003010240040211	Uyum:	Mükemmel identifikasyon
SRF Organizması			
Ayrılabak Analiz Organizmaları ve Testler:			
Analiz Mesajları:			
Uyumsuz Olan Tipik Biopattern(ler)			

Figure F.4: VITEK2 Result of DE51.

İzolat Grubu: 365-1

Biyonumara: 6627734453056210

Seçilen Organizma: Enterobacter aerogenes

Yorumlar:	Oksidaz (-)

İdentifikasyon Bilgileri	Kart: GN	Lot No: 241247640	Son Kullanım Tarihi: 24.Eyl.2013 13:00 EEST
	Tamamlandı: 24.Nis.2013 18:17 EEST	Durum: Son	Analiz Zamanı: 4,00 saat
Seçilen Organizma	99% Olasılık Biyonumara: 6627734453056210	Enterobacter aerogenes	Uyum: Mükemmel identifikasyon
SRF Organizması			
Ayrılabilecek Analiz Organizmaları ve Testler:			
Analiz Mesajları:			
Uyumsuz Olan Tipik Biopattern(ler)			

Figure F.5: VITEK2 Result of DE365.

CURRICULUM VITAE

Name Surname: Dilşad Yurdakul

Place and Date of Birth: Istanbul- 30.04.1978

Address: Adatepe Süreyyapaşa Street 13/14 Maltepe / Istanbul

E-Mail: yurdakuldilsad@gmail.com

B.Sc.: Istanbul University, Biology Department - 2003

M.Sc. : Marmara University, Pharmaceutical Microbiology Department - 2006

Professional Experience: Research and Teaching assistant at Yeditepe University, Genetics and Bioengineering Department

List of Publications:

- **Yurdakul D.**, Gürer S. Ü., Rayaman E., Erçağ E., Haklar G.,Çevikbaş A., Gönentür G. A. : The effects of antidepressant drugs on polymorphonuclear leukocyte functions and levels of folic acid, vitamin B12, zinc and copper in Major Depression , Nobel Medicus, 2013, Volume 9, Numer 1, 81-88
- Çıkla P., Tatar E., Küçükgüzel İ., Şahin F., **Yurdakul D.**, Basu A., Krishnan R., Nichols B.D., Basu K .N., Küçükgüzel G.Ş.: Synthesis and Characterization of Flurbiprofen Hydrazone Derivatives as potential anti HCV, anticancer, antimicrobial agents , 2013, Medicinal Chemistry Research
- Mete E., Ozengul C., Kazaz C., **Yurdakul D.**, Şahin F., Gul I.H. : Synthesis and Antifungal Activity of 1-Aryl-3-phenethylamino-1-propanone Hydrochlorides and 3-Aroyl-4-aryl-1-phenethyl-4-piperidinols, Archiv der Pharmazie Chemistry in Life Sciences, 2010, 343, 291-300
- Sayın I., Kahraman M., Şahin F., **Yurdakul D.**, Çulha M.: Characterization of Yeast Species Using Surface Enhanced Raman Scattering, Applied Spectroscopy, 2009, Volume 63, Number 11

Conference Publications:

- **Yurdakul D.**, Sahin F.: Antibacterial Effect of Secondary Metabolites of *Bacillus* species against Quinolone Resistant Bacteria, Current Opinion in Biotechnology, S124, Istanbul, Turkey (Abstract, EUROBIOTECH 2011 Oral Presentation)

- **Yurdakul D.**, Şahin F.: Degredation of *microcystin* by *Bacillus* spp. strains, III. International Entomopathogens and Microbial Control Symposium, Şile, Istanbul, Turkey, 18-22 September, 2011 (Oral Presentation)

- **Yurdakul D.**, Ağuş S., Şahin F. : *Bacillus cereus* and *Bacillus subtilis* strains can prevent *Microcystis* Bloom, 11th World Congress on Environmental Health, Vancouver, BC, Canada, September 5- 10, 2010 (Oral Presentation)

- **Yurdakul D.**, Şahin F., Ağuş S., Karaltı İ., Görmez Ala A.: New Bacterial Strains for Fungi Control. PP87, IMPPS-3 Third International Meeting on Pharmacy and Pharmaceutical Sciences, İstanbul, Turkey, June 9-12, 2010 (Poster Presentation)

- **Yurdakul D.**, Gürer Soyoğul Ü., Rayaman E., Erçağ E., Haklar G., Çevikbaş A., Gönentür Gimzal A. : The Effects of Antidepressant Drugs on Polymorphonuclear Leukocyte Functions and Levels of Folic Acid, Vitamin B12, Zinc and Copper in Major Depression PP 137, IMPPS-3 Third International Meeting on Pharmacy and Pharmaceutical Sciences, İstanbul, Turkey, June 9-12, 2010 (Poster Presentation)

- Tatar E., Çıkla P., Küçükgüzel G.Ş., Küçükgüzel İ., Şahin F., **Yurdakul D.**, Kaushik-basu N., Krishnan R. Synthesis and biological activity of (±)-2-(2-Fluoro-4-Biphenyl) Propanoic acid Hydrazide Derivatives. PP8, IMPPS-3 Third International Meeting on Pharmacy and Pharmaceutical Sciences, İstanbul, Turkey, June 9-12, 2010 (Poster Presentation)

- Duman G., Taralp A., Şahin F., **Yurdakul D.**, Yıldız B., Robinson R.J. : Pluronic F 127 Dental Formulation Containing Hen Egg White Lysozyme and Lactoferrin Demonstrates Antibacterial Activity, AAPS Conference, The Impact Of Pharmacokinetics In Modern Drug Development 10 Years Later, San Francisco, November 16-17, 2007 (Poster Presentation)

- Tatar E., Çıkla P., Küçükgüzel G. Ş., Küçükgüzel İ., Şahin F., **Yurdakul D.:** Synthesis and Biological Activity Of Flurbiprofen Hydrazide Derivatives 5th International Symposium On Pharmaceutical Chemistry, September 5-7 (2007) İstanbul, Turkey

- Gul H.I., Ozelgul C., Mete E., Şahin F., **Yurdakul D.:** Antifungal Activities Of 3-Phenethylamino-1-Aryl-1-Propanone Hydrochlorides and 3-aroyl-4-Aryl-1-Phenethyl-4-Piperidinols Against Some Plant And Human Pathogenic Fungi (Poster 23) International Symposium On Drug Research And Development From ‘ Chemistry To Medicine’, DRD 2007, Antalya, Turkey, May 17-20, 2007

PUBLICATIONS/PRESENTATIONS ON THE THESIS

- **Yurdakul D.,** Karatas A., Sahin F. : *Enterobacter* spp. strains stimulate NFκB and Bcl2 in NCM460 cell lines, EMBO/EMBL Symposium: New Approaches and Concepts in Microbiology, October 14-16, 2013, Heidelberg, Germany (Poster Presentation)
- **Yurdakul D.,** Karatas Y.A., Şahin F. : *Enterobacter aerogenes* Strains Might Cause Colon Cancer, (ICCMB 2013) International Conference on Cellular and Molecular Biology (World Academy of Science, Engineering and Technology), June 20-21, 2013 Istanbul (Oral presentation)

